# Interactions between primary cilia length and hedgehog signalling in response to mechanical and thermal stress.

Thompson, Clare

# INTERACTIONS BETWEEN PRIMARY CILIA LENGTH AND HEDGEHOG SIGNALLING IN RESPONSE TO MECHANICAL AND THERMAL STRESS

Clare Thompson

A thesis submitted to Queen Mary, University of London for the degree of Doctor of Philosophy

June 2013

Queen Mary University of London

Mile End Road

E1 4NS

London

UK

# Abstract

The primary cilium is a microtubule-based organelle present on the majority of interphase cells where it functions as a hub for numerous signalling pathways including hedgehog signalling. Chondrocytes, the unique cellular component of articular cartilage, possess primary cilia which are required for mechanotransduction and maintenance of a healthy extracellular matrix. However in osteoarthritis there is an increase in primary cilia length and prevalence associated with aberrant activation of hedgehog signalling which promotes cartilage degradation. The aim of this thesis was therefore to examine the influence of biophysical stimuli on chondrocyte primary cilia structure and function, relating changes in ciliary length to perturbations in hedgehog signalling.

An *in vitro* mechanical loading model was established to study the influence of cyclic tensile strain on chondrocyte primary cilia. Loading at 10% strain activated hedgehog signalling measured by expression of Gli1 and Ptch1. Cilia progressively disassembled in response to increasing levels of mechanical strain in a manner dependent upon tubulin deacetylation. Cilia disassembly at 20% strain was associated with the loss of mechanosensitive hedgehog signalling despite continued expression of hedgehog ligand (Ihh). Therefore this behaviour may function as a protective mechanism limiting hedgehog-mediated cartilage degradation in response to high levels of mechanical strain.

To further understand the influence the extracellular environment exerts over ciliary function, a second *in vitro* model was developed investigating the effects of thermal stress. In chondrocytes and fibroblasts, primary cilia underwent rapid resorption in response to elevated temperature and ligand mediated hedgehog signalling was inhibited.

These studies demonstrate that regulated disassembly of the cilium in response to physical stress modulates both cilia size and function. In particular, the findings suggest that changes in the chondrocyte physical environment affect cilia structure and function and may therefore be an important factor in the aetiology of cartilage disease.

# Acknowledgements

I would like to take this opportunity to thank the Biotechnology and Biological Sciences Research Council (BBSRC) for funding this work.

I would like thank my supervisors Dr Paul Chapple and Prof Martin Knight for their support, advice and guidance during the course of my PhD. I count myself especially lucky to have had not one but two excellent supervisors during my PhD. My gratitude also extends to my panel of advisors, Dr Peter King and Prof Maurice Elphick for their valuable suggestions about the project.

I would like to express my gratitude to all members of the Knight and Chapple labs, past and present, for making QM a fun and enjoyable place to work. In particular I would like to thank Dr Natasha Prodromou for her contribution to the heat shock work and Dr Angus Wann for his insightful discussions and invaluable support throughout the project.

I would also like to thank my friends and family, especially my parents, for their support and patience over the years. And finally I would like to give extra special thanks to David Thompson for his support and constant encouragement which makes all things possible.

# Table of contents

# Table of figures

# Table of tables

# List of abbreviations

| | |
|---|---|
| ADAMTS-5 | A disintegrin and metalloproteinase with thrombospondin motifs 5 |
| AER | Apical ectodermal ridge |
| ATP | Adenosine triphosphate |
| AURA | Aurora A kinase |
| BBS | Bardet Biedel syndrome |
| BSA | Bovine serum albumin |
| cAMP | Cyclic adenosine monphosphate |
| cDNA | Complementary deoxyribonucleic acid |
| COX-2 | Cyclo-oxygenase-2 |
| CTTN | Cortactin |
| DAPI | 4',6-Diamidino-2-Phenylindole, Dihydrochloride |
| Dhh | Desert hedgehog |
| DISP | Dispatched |
| DMEM | Dulbeccos modified eagles medium |
| DMM | Destabilisation of the medial meniscus |
| DMMB | 1,9-Dimethyl-methylene blue |
| dsDNA | Double stranded deoxyribonucleic acid |
| ECM | Extracellular matrix |
| EGTA | Ethylene glycol tetraacetic acid |
| EthD-1 | Ethidium homodimer |
| EVC | Ellis van Creveld |
| FCS | Fetal calf serum |
| GLI | Glioma associated-oncogene |
| GPCR | G-protein coupled receptor |
| GTP | Guanidine triphosphate |
| HDAC | Histone deacetylase |
| HEPES | *4-(2-hydroxyethyl)-1-piperazineethanesulfonic acid* |
| HHAT | Hedgehog acetyltransferase |
| HIF | Hypoxia inducible factor |
| HPF | Hurs post fertilisation |
| IFT | Intraflagellar transport |
| IGF-1 | Insulin growth factor-1 |
| IGF-1R | Insulin growth factor-1 receptor |
| Ihh | Indian hedgehog |
| IMS | Industrial methylated spirit |
| MAPK | Mitogen activated protein kinase |
| MIM | Missing-in-metastasis |
| MMP | Matrix metalloproteinase |
| OA | Osteoarthritis |
| OPG | Osteoprotegrin |
| PC-1 | Polycystin-1 |

| | |
|---|---|
| PC-2 | Polycystin-2 |
| PCR | Polymerase chain reaction |
| PDGF | Platelet derived growth factor |
| PDGFR | Platelet derived growth factor receptor |
| PFA | Paraformaldehyde |
| PKA | Protein kinase A |
| PKC | Protein kinase C |
| PTCH1 | Patched1 |
| PTHrP | Parathyroid hormone related peptide |
| PTHrPR | Parathyroid hormone related peptide receptor |
| qRT-PCR | Quantitative reverse transcription polymerase chain reaction |
| RNA | Ribonucleic acid |
| RT-PCR | Reverse transcriptase polymerase chain reaction |
| RUNX-2 | Runt-related transcription factor 2 |
| RUNX-2 | Runt related transcription factor-2 |
| SDS-PAGE | sodium dodecyl sulfate polyacrylamide gel electrophoresis |
| sGAG | Sulphated glycosaminoglycan |
| Shh | Sonic hedgehog |
| SIRT | Sirtuin |
| SKI | Skinny hedgehog |
| SMO | Smoothened |
| SuFu | Suppressor of fused |
| TRPV4 | Transient receptor potential cation channel subfamily V member 4 |
| ZPA | Zone of polarising activity |
| αTAT1 | Alpha tubulin acetyltransferase |

# CHAPTER 1

# The structure and function of the primary cilium

## 1.1 The primary cilium

The primary cilium is a solitary cytoplasmic organelle present on nearly every cell-type in the mammalian body (Wheatley et al. 1996). It consists of a microtubule based axoneme which is anchored to the cell through the basal body, a centriole derived microtubule organising centre, and is enveloped by a highly specialised extension of the cell membrane (Rohatgi and Snell 2010). The axoneme is commonly described to project into the extracellular space; however this concept is constantly challenged by reports of cilia closely positioned alongside the cell body and within invaginated cell pockets which may enclose just the base of the cilium or in some instances the entire axoneme (Figure 1.1).

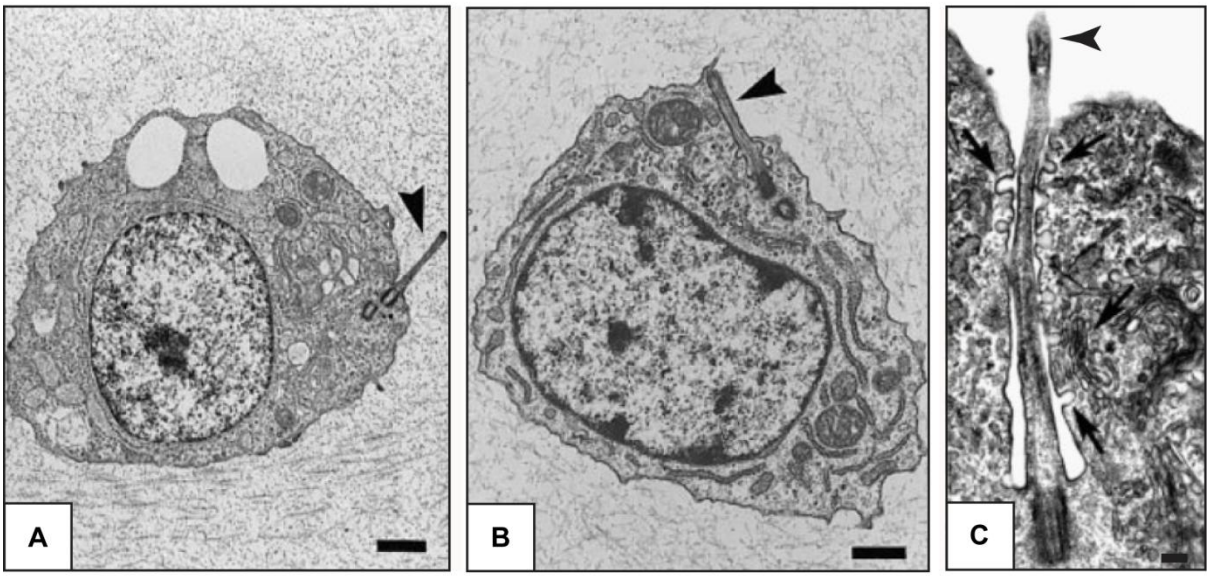


**Figure 1.1 The primary cilium**
Electron micrographs of chondrocytes from embryonic chick sterna **(A and B)** and human synoviocytes **(C)** demonstrating the variations observed in axoneme positioning, arrow heads show cilia. In image **(A)** the chondrocyte primary cilium is shown projecting out into the extracellular space, in image **(B)** the cilium is 'reclining' against the cell membrane (Poole et al. 2001). Scale bar represents 1µm. Image **(C)** shows an invaginated cilium, arrows in this image indicate sites of endocytosis and prominent Golgi complexes that line this ciliary pit (taken from (Moser et al. 2010)). Scale bar represents 0.1µm.

For many years the primary cilium was ignored by biologists and considered to be a vestigial remnant of evolution, however a recent explosion of data has linked the cilium to several key cellular processes and signalling pathways such as wnt (Ross et al. 2005), PDGFα

(Schneider et al. 2005), Polycystin (Nauli et al. 2003) and Hedgehog signalling (Huangfu et al. 2003; Corbit et al. 2005; Rohatgi et al. 2007). Consequently abnormalities in primary cilia have been linked to a plethora of phenotypically and genetically overlapping diseases collectively named 'ciliopathies'. These include polycystic kidney disease (PKD), Bardet Beidel syndrome (BBS) and Joubert syndrome (JKS) (for review see (Waters and Beales 2011)).

### 1.1.1 Ciliogenesis

Ciliogenesis, the formation of a primary cilium, is intrinsically linked to centriole duplication and the cell cycle (Sorokin 1962; Ishikawa and Marshall 2011). Cilium formation typically occurs during G1/G0 while cilium resorption occurs before mitotic entry. The exact point of ciliary resorption during the cell cycle depends on the cell type, with some cells initiating cilia resorption in S-phase, and others at the G2/M transition (Rieder et al. 1979; Jensen et al. 1987).

The ciliary axoneme is assembled onto the more mature of the cells two centrioles, the mother centriole. Upon entry into $G_1$, the mother centriole dissociates from the core of the mitotic spindle and migrates to an actin rich assembly site at the cell surface. En route to this assembly site the centriole associates with several Golgi-derived vesicles to become the basal body. Upon docking at the assembly site, these membranous vesicles fuse with the plasma membrane and the axoneme extends out from the distal end of the basal body whilst remaining sheathed in the ciliary membrane (Sorokin 1962). While contiguous with the plasma membrane, the two membrane compartments are separated by a region called the ciliary necklace (Johnson and Rosenbaum 1992). The positioning and orientation of the basal body at the assembly site is important and dictates the alignment of the resulting cilium (Nonaka et al. 2005). As protein synthesis does not occur within the cilium, the continued elongation of the ciliary axoneme becomes dependent on the selective import and transport of ciliary proteins by a process called intraflagellar transport (IFT) (Rosenbaum and Witman 2002), discussed in section 1.3. In the absence of IFT only a stunted cilium is able to form and ciliary signalling is disrupted (Pazour et al. 2000). A schematic depicting the major steps involved in ciliogenesis is presented in Figure 1.2.

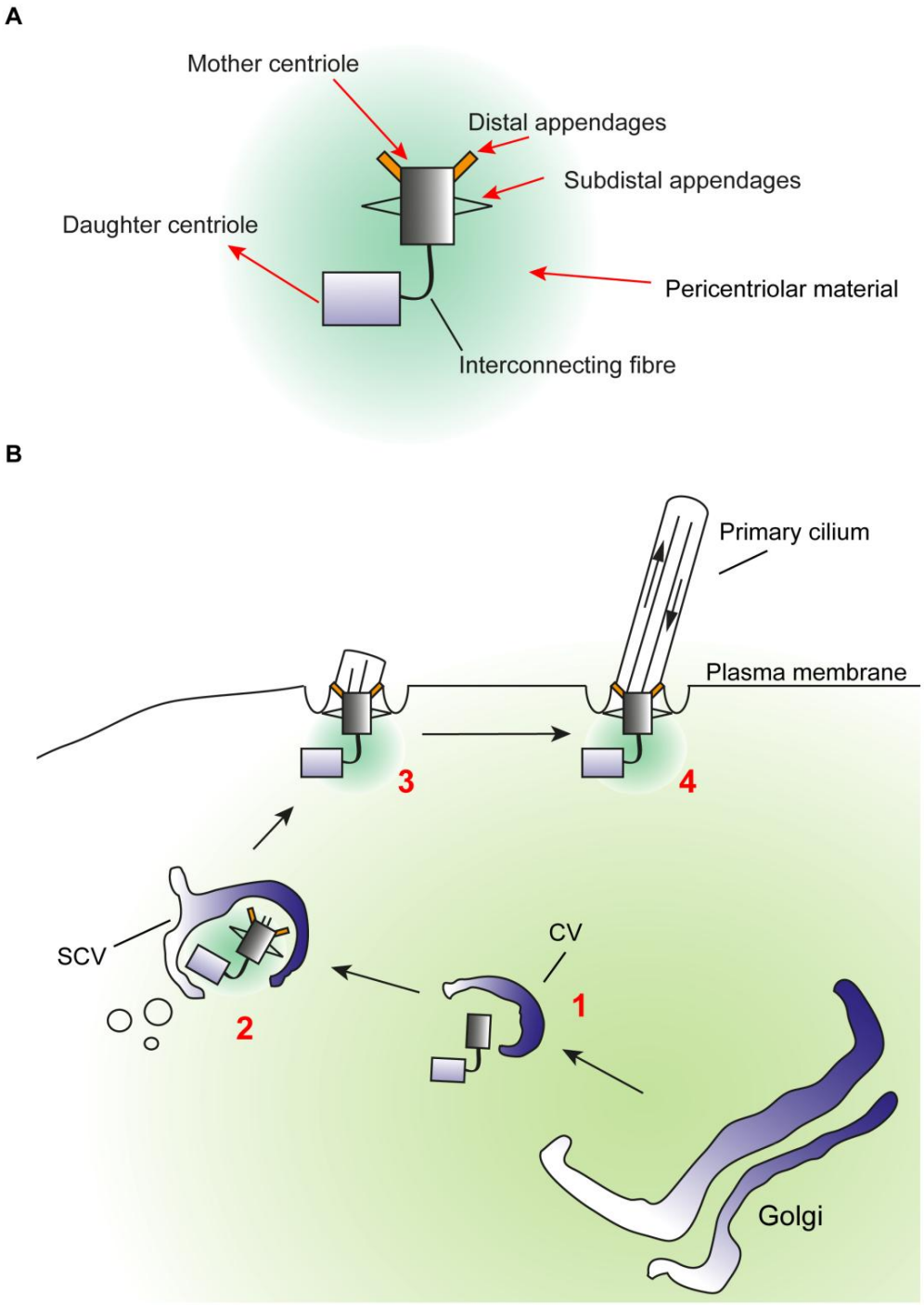


**Figure 1.2 Primary cilia formation**
**(A)** A schematic detailing the structure of the basal body**. (B)** A schematic model of cilium formation (adapted from (Pedersen and Rosenbaum 2008): 1) The Golgi-derived centriolar vesicle (CV) forms at the distal end of the mother centriole. 2) The centriole migrates towards the plasma membrane and en route the CV fuses with secondary CVs (SCV). 3) The centriole docks and fuses with the plasma membrane becoming the basal body. 4) The ciliary axoneme elongates via intraflagellar transport forming the primary cilium.

Of note, primary cilia formation has been shown to be asynchronous in a given sister pair following cell division (Anderson and Stearns 2009). Ciliogenesis typically occurs first in the sister cell receiving the oldest mother centriole (Anderson and Stearns 2009). Intriguingly, asynchronous recruitment of ciliary signalling proteins has also been observed suggesting the segregation of differently aged mother centrioles may be an important mechanism influencing the ability of sister cells to respond to different environmental signals during development (Anderson and Stearns 2009; Piotrowska-Nitsche and Caspary 2012).

## 1.2 Primary cilia structure

### 1.2.1 The ciliary axoneme

Primary cilia, motile cilia and flagella are evolutionarily related organelles that share a similar microtubule structure (Figure 1.3). However, the primary cilium is distinct from flagella and motile cilia for several reasons, firstly only a single primary cilium is found per cell and this is present on almost every eukaryotic cell type. Secondly, the primary cilium is immotile. This is due to key differences in the microtubule structure of this organelle. Primary cilia exhibit 9-fold symmetry and have what is called a '9+0' microtubule structure. The axoneme contains 9 outer doublet microtubules which surround a central core and extend out from the basal body. Motile cilia have what is called a '9+2' structure which comprises the same 9 doublet microtubules but with an additional central pair which, in conjunction with accessory structures such as inner and outer dynein arms, confers motility on these cilia (Figure 1.3). As with most phenomena in biology there are exceptions to this rule. The sensory kino-cilium of the hair cells in the inner ear, while classified as non-motile, exhibit the '9+2' structure of motile cilia (Dabdoub and Kelley 2005). Likewise, nodal cells in the developing embryo have been shown to exhibit motile '9+0' cilia and are essential for left-right patterning (Hirokawa et al. 2006). Finally, primary cilia have key roles in sensing physical and biochemical extracellular signals to bring about changes in gene expression.

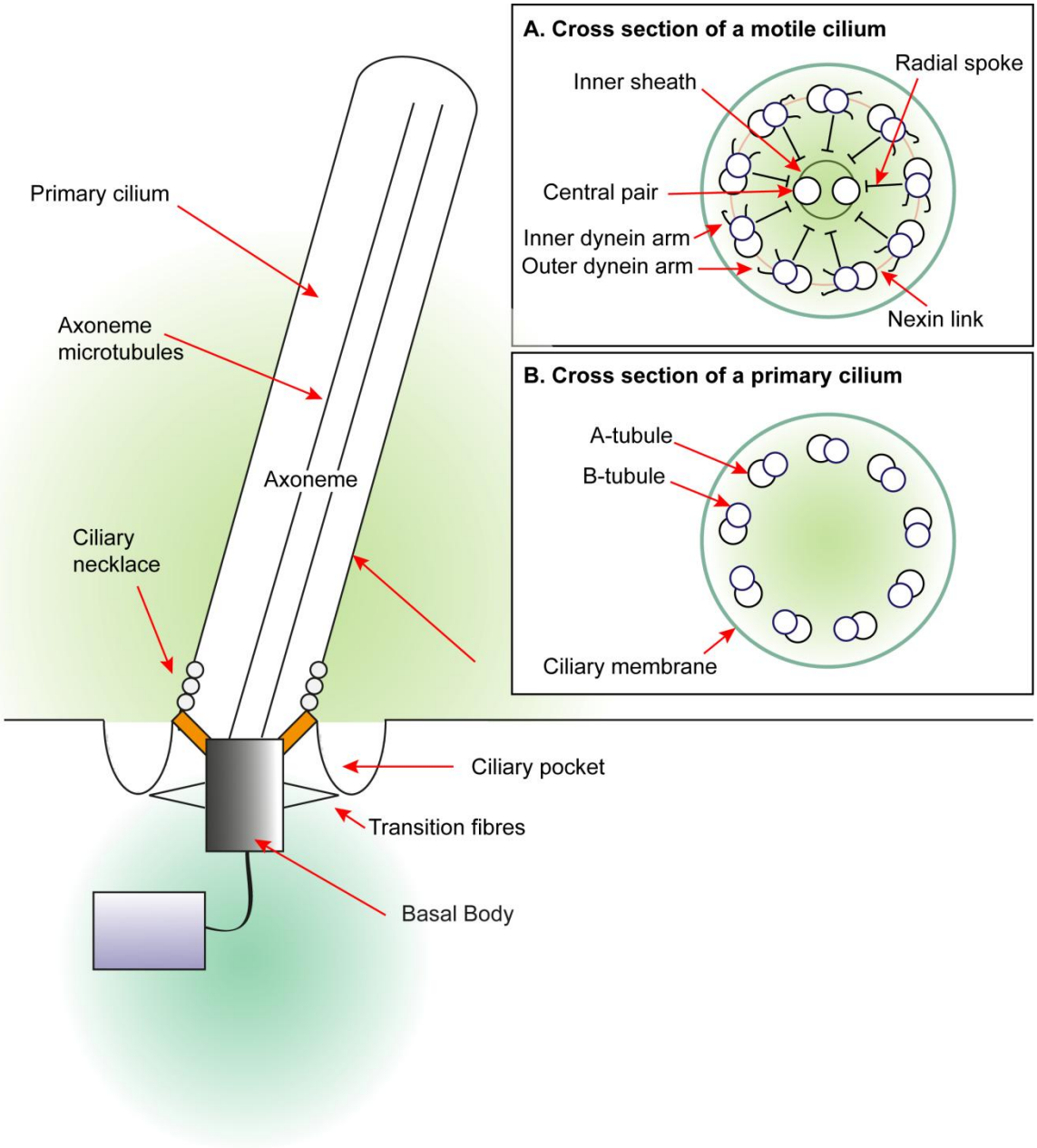


**Figure 1.3 The structure of the primary cilium**
Schematic of a primary cilium showing the major structural features of this organelle. Inset, schematic illustrating the differences in the microtubule structure of **(A)** motile '9+2' cilia and **(B)** primary '9+0' cilia. Figure adapted from (Ishikawa and Marshall 2011).

### 1.2.2 The basal body

In vertebrates, only the eldest of the cells two centrioles, the mother centriole, can function as a basal body and nucleate cilia formation hence there can only ever be one cilium per cell. Aberrant centriole numbers are seen in many cancers and in some ciliopathies (Fukasawa 2007; Kinzel et al. 2010) giving rise to cells with multiple primary cilia which compromises ciliary signalling pathways (Mahjoub and Stearns 2012).

The basal body, like the centriole, is a cylindrical structure of 9 triplet microtubule 'blades' arranged in a barrel. Each blade is arranged parallel to the long axis of the cylinder and is composed of a single complete microtubule and two partial microtubules. These tubules are named A, B and C respectively (Ringo 1967). The doublet microtubules of the ciliary axoneme are contiguous with the A and B tubules of the basal body (Ringo 1967). In addition to providing a template for ciliogenesis, the basal body also functions to anchor the cilium to the cell membrane and cytoskeleton. A number of fibrous structures such as the striated rootlet, basal foot and distal and sub-distal appendages assist in this function and form a link between the basal body and the cytoskeleton (Yang et al. 2002; Reiter et al. 2012) (Figure 1.2A). The point at which the triplet microtubules of the basal body transition to the doublet microtubules of the axoneme is called the transition zone. This is an evolutionarily conserved ciliary sub-domain which is characterised by distinctive Y-shaped fibres connecting the axonemal doublets to the ciliary membrane the composition of which is unknown (Reiter et al. 2012). There is some ambiguity concerning the boundaries of the transition zone with respect to the basal body and ciliary axoneme.

The import and export of ciliary proteins is regulated at the basal body [for review see (Reiter et al. 2012)]. Microtubule based extensions called transition fibres appear to serve as docking sites for intraflagellar transport particles (Deane et al. 2001; Williams et al. 2011). These fibres most likely originate from the distal appendages that mark the mother centriole prior to cilia formation (Reiter et al. 2012). The localisation of proteins such as importin-β1, importin-β2/transportin, RanBP1 and several nucleoporins to cilia suggest a ciliary pore complex, analogous to the nuclear pore complex, may also regulate cilia composition at the base of the axoneme (Fan et al. 2007; Dishinger et al. 2010; Fan et al.

2011; Hurd et al. 2011; Kee et al. 2012). Additional protein complexes for the selective transport and retention of proteins in cilia have been identified (Garcia-Gonzalo et al. 2011; Chih et al. 2012). Much still remains to be understood regarding the mechanisms by which the basal body functions as gate-keeper for protein transport however it is clear that this function is essential for the generation of cell-type specific primary cilia that can be tailored to a specific signalling niche [For review see (Hu and Nelson 2011)].

### 1.2.3 The ciliary membrane

The ciliary axoneme is sheathed in a lipid bilayer, the ciliary membrane, which while contiguous with the plasma membrane has a distinct protein composition (Ostrowski et al. 2002; Teilmann et al. 2005; Teilmann and Christensen 2005). Two distinct membrane structures at the base of the cilium separate the ciliary compartment from the cell body, the ciliary necklace and the ciliary pocket which are sites of membrane/basal body interactions that form a functional barrier (Gilula and Satir 1972; Molla-Herman et al. 2010). The ciliary necklace is located at the level of the transition zone (Figure 1.3). Freeze-fracture electron microscopy shows that it is formed by multiple circumferential rows of intra-membranous particles which sit adjacent to the Y-shaped fibres of the transition zone (Gilula and Satir 1972; Reiter et al. 2012). The Y-fibres appear to terminate within this region and may contribute to the organisation of this structure (Gilula and Satir 1972). While this zone may function as a barrier, physically preventing transport vesicles from entering the cilium, it is also suggested to be required for the insertion of ciliary membrane components (Deane et al. 2001).

The ciliary pocket is an invagination of the plasma membrane at the base of the cilium and is found on some types of mammalian cells and trypanosomatids (Molla-Herman et al. 2010). In some instances this invagination will envelop a substantial fraction of the axoneme surrounding it in a double membrane called the ciliary sheath (Figure 1.1C). This sheath has been observed to completely surround the axoneme in some cells resulting in formation of a non-emergent cilium (Rohatgi and Snell 2010). The ciliary pocket interacts extensively with the basal body through the transition fibres (Reiter et al. 2012).

The ciliary membrane adheres closely to the axoneme in most cases, giving the cilium its cylindrical shape with a diameter of approximately 200nm (Rohatgi and Snell 2010). However, the membrane can be expanded to carry out sensory functions as in the photoreceptor cells of the retina. The ciliary membrane in these cells forms a structure called the outer segment and is modified to form elaborate stacks of membrane which are filled with the photoreceptor protein opsin facilitating the function of these cells as light sensors (Liu et al. 2010).

The lipid composition of the ciliary membrane also differs from the plasma membrane. Studies so far have found ciliary membranes to be higher in sterols relative to phospholipid content (Chailley and Boisvieux-Ulrich 1985; Simons and Toomre 2000). This will arguably have consequences for transmembrane proteins within the cilium as the stiffness of the ciliary membrane will be increased. This altered stiffness is hypothesised to facilitate the function of the cilium as a signalling platform for organising the transduction machinery.

### 1.2.4 Ciliary tubulin

Microtubules are cytoskeletal filaments that play essential roles in structural support, intracellular trafficking and mitosis. Like all microtubules, ciliary microtubules are formed by the polymerisation of α/β tubulin dimers. This is a GTP dependent process which results in formation of polarised tubulin filaments which have a fast growing plus end and a slow growing minus end. Within the cilium the plus ends are directed towards the distal tip and it is here that new tubulin is incorporated into the axoneme as it lengthens (Johnson and Rosenbaum 1992). Ciliary tubulin is highly heterogeneous due to extensive post translational modifications which occur shortly after axoneme assembly. Such modifications include; detyrosination, glutamylation, glycylation, phosphorylation and acetylation and are hypothesised to dictate the recruitment of protein complexes and increase microtubule stability (Reed et al. 2006; Gaertig and Wloga 2008). While these modifications are not restricted to ciliary tubulin they are particularly concentrated within the axoneme and have been used as cytological markers of the cilium and basal body.

Tubulin acetylation is highly enriched in axonemal microtubules. Acetylation occurs at Lysine-40 on α-tubulin. This residue is located within the N-terminal domain of α-tubulin which projects into the microtubule lumen (Nogales et al. 1999). The acetyl transferase enzyme responsible for tubulin acetylation has only recently been identified as α-tubulin K40 acetyltransferase/MEC-17 (αTAT1/MEC-17) (Shida et al. 2010). Tubulin acetylation is proposed to stabilise microtubules and reportedly increases with microtubule age (Piperno et al. 1987). Moreover, treatment with the microtubule stabilising agent paclitaxel increases tubulin acetylation (Piperno et al. 1987). Two conserved tubulin deacetylase's have been identified in mammals, histone deacetylase 6 (HDAC6) and sirtuin type 2 (SIRT2) (Hubbert et al. 2002; North et al. 2003; Verhey and Gaertig 2007). HDAC6 activation has been implicated in ciliary resorption which suggests tubulin deacetylation may be required for axoneme disassembly (Pugacheva et al. 2007).

In addition to increased microtubule stability, tubulin modifications have also been reported to influence kinesin motor function and alter transport processes (Reed et al. 2006; Hammond et al. 2010).

## 1.3 Intraflagellar transport

Primary cilia do not possess the machinery for protein synthesis; as a result cilia are both assembled and maintained by intraflagellar transport (IFT). IFT is the selective, bidirectional, microtubule-based transport of protein transport modules, IFT particles or IFT trains, along the ciliary axoneme (for review see (Pedersen and Rosenbaum 2008)). IFT was first discovered in the laboratory of Joel Rosenbaum in 1993, where the movement of granule-like particles along *Chlamydomonas Rheindharti* flagella was observed using differential interference contrast microscopy (DIC) (Kozminski et al. 1993). Since this discovery IFT was found to be conserved in other ciliated eukaryotes and is essential for ciliary function (Pazour and Witman 2003; Huangfu and Anderson 2005; Haycraft et al. 2007; Berbari et al. 2009).

The assembly of IFT particles occurs at the base of the cilium. In *Chlamydomonas*, concentrations of IFT particle polypeptides, molecular motors and flagella precursors can be

observed at the point at which the transition fibres contact the flagella membrane (Pazour et al. 1999; Deane et al. 2001). These IFT particles contain numerous protein cargos and partially assembled protein complexes that are transported in the antereograde direction, from the base to the tip, by the Kinesin-2 motor complex (Iomini et al. 2001; Qin et al. 2004). At the tip of the cilium Kinesin-2 is inactivated facilitating both cargo release and the return of the raft to the base of the cilium by cytoplasmic dynein 2 (Pazour et al. 1999). Antereograde particle movement has been reported to occur at speeds of ~2µm/s and at ~3.5µm/s for retrograde transport (Kozminski et al. 1993). A schematic illustrating this process can be found in Figure 1.4.

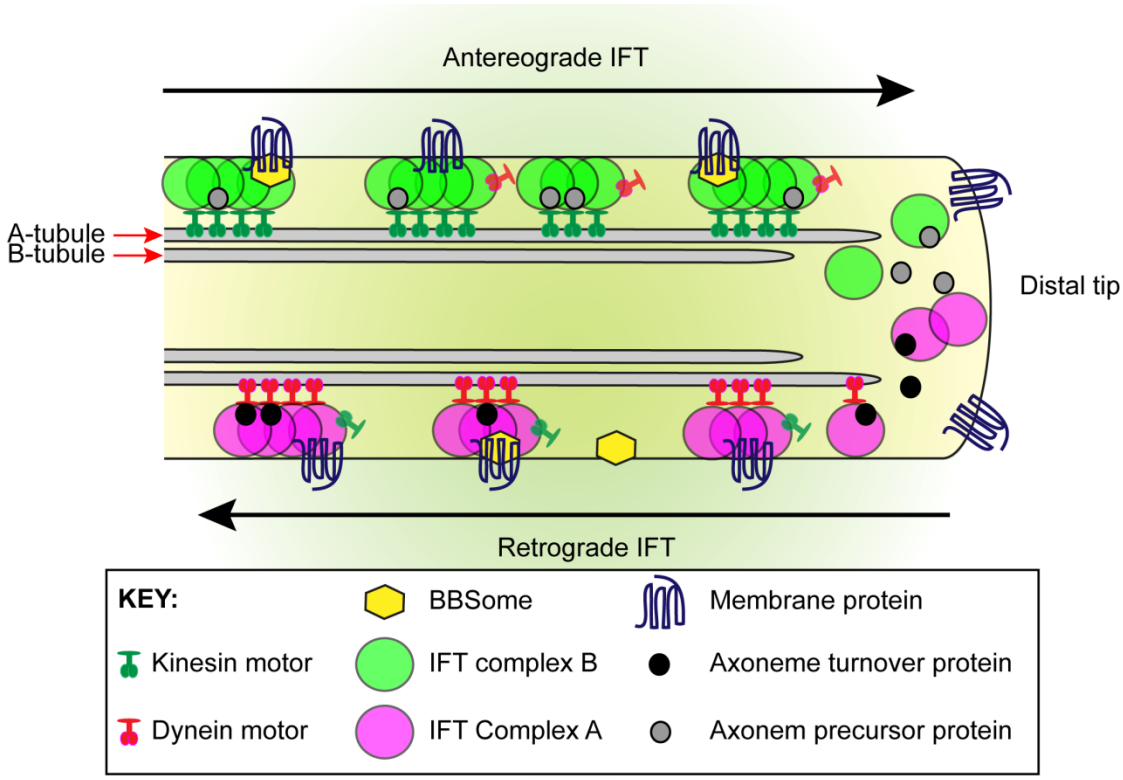


**Figure 1.4 Intraflagellar transport**
Schematic illustrating the process of intraflagellar transport (IFT) occurring within the cilium (adapted from (Ishikawa and Marshall 2011)). The Kinesin-2 motor transports IFT complexes, axonemal precursor proteins and inactive dynein 2 in the antereograde direction to the ciliary tip. At the ciliary tip, antereograde IFT trains release their cargoes and rearrange their conformation for retrograde IFT. Kinesin 2 is inactivated, and cytoplasmic dynein 2 becomes activated promoting the retrograde transport of Kinesin-2, axonemal turnover products and other unwanted material to the cell body. Typically Complex A proteins are associated with retrograde transport while complex B proteins are associated with antereograde transport. Subsets of IFT trains are involved in transporting membrane proteins and the BBSome.

The canonical antereograde IFT motor heterotrimeric Kinesin-2 consists of two heterodimerized Kinesin-2 motor subunits, (KIF3A and KIF3B) and an accessory subunit, kinesin-associated protein (KAP) (Cole 1999). This motor complex is essential for the assembly and maintenance of cilia and flagella in most ciliated organisms such that mutation or deletion of one of the motor subunits inhibits cilia formation (Morris and Scholey 1997; Nonaka et al. 1998; Cole 1999; Huangfu et al. 2003). Cytoplasmic dynein 2 is a multi-protein complex that regulates retrograde transport. When this complex is disrupted, cilia assembly still occurs however the cilia/flagella that form are stumpy and swollen with accumulated proteins and cannot function correctly (Pazour et al. 1998; Pazour et al. 1999; Signor et al. 1999; Hou et al. 2004; Huangfu and Anderson 2005).

Analysis of the *Chlamydomonas* genome revealed there to be around 20 proteins involved in IFT, these proteins become associated to form two large, biochemically distinct complexes; complex A and complex B (Cole et al. 1998; Qin et al. 2004). IFT complex A contains six known proteins, listed in Table 1.1, while IFT complex B contains 14 known proteins (Ishikawa and Marshall 2011). Typically complex B has been associated with antereograde transport and complex A with retrograde transport. The complete loss of any one complex B protein inhibits cilia assembly resulting in either absent or severely truncated cilia (Pazour et al. 2000; Huangfu et al. 2003; Hou et al. 2007). In contrast, complex A proteins are not always required for ciliary assembly, however these mutants do exhibit malformed cilia with prominent bulges (Piperno et al. 1998; Iomini et al. 2009). These phenotypes resemble mutations in Kinesin-2 and cytoplasmic dynein 2 respectively (Pazour et al. 1999; Matsuura et al. 2002).

In addition to IFT complexes another large protein complex has been identified in cilia, namely the BBSome (Nachury et al. 2007). The BBSome is a protein complex of at least 7 highly conserved core proteins; BBS1, BBS2, BBS4, BBS5, BBS7, BBS8 and BBS9 and has been implicated in the trafficking of membrane proteins to the cilium (Handel et al. 1999; Berbari et al. 2008).

| IFT system component | General protein name | *Chlamydomonas reinhardtii* | *Caenorhabditis elegans* | *Homo sapiens* | Other |
|---|---|---|---|---|---|
| Kinesin-2 | Heterotrimeric | FLA10 | KLP-20 | KIF3A | |
| | | FLA8 | KLP-11 | KIF3B | |
| | | FLA3 | KAP-1 | KAP3, KIFAP3 | |
| Kinesin-2 | Homodimeric | – | OSM-3, KLP-2 | KIF17 | Kin5 |
| Cytoplasmic dynein 2‡ | Heavy chain | DHC1B | CHE-3 | DYNC2H1 | |
| | Intermediate chain | FAP133 | DYCI-1 | WDR34 | |
| | Light intermediate chain | D1BLIC | D2LIC, XBX-1 | DYNC2LI1 | |
| | Light chain | LC8, FLA14 | DLC-1 | DYNLL1 | |
| IFT complex A | IFT144 | IFT144 | DYF-2 | WDR19 | |
| | IFT140 | IFT140 | CHE-11 | IFT140 | |
| | IFT139 | IFT139 | ZK328.7 | THM1, TTC21B | |
| | IFT122, IFT122A | IFT122, FAP80 | DAF-10 | IFT122, WDR10 | |
| | IFT121, IFT122B | IFT121 | IFTA-1 | WDR35 | |
| | IFT43 | IFT43 | – | IFT43, C14orf179 | |
| IFT complex B | IFT172 | IFT172 | OSM-1 | IFT172 | |
| | IFT88 | IFT88 | OSM-5 | IFT88 | Tg737, Polaris |
| | IFT81 | IFT81 | IFT-81 | IFT81 | |
| | IFT80 | IFT80 | CHE-2 | IFT80, WDR56 | |
| | IFT74, IFT72 | IFT74, IFT72 | IFT-74 | IFT74, IFT72 | |
| | IFT70 | IFT70, FAP259 | DYF-1 | TTC30A, TTC30B | Fleer |
| | IFT57 | IFT57 | CHE-13 | IFT57 | Hippi |
| | IFT54 | IFT54, FAP116 | DYF-11 | IFT54, TRAF3IP1, MIPT3 | Elipsa |
| | IFT52 | IFT52, BLD1 | OSM-6 | IFT52, NGD5 | |
| | IFT46 | IFT46 | DYF-6 | IFT46, C11orf60 | |
| | IFT27 | IFT27 | – | IFT27, RABL4 | |
| | IFT25 | IFT25, FAP232 | – | IFT25, HSPB11 | |
| | IFT22 | IFT22, FAP9 | IFTA-2 | RABL5 | |
| | IFT20 | IFT20 | Y110A7A.20 | IFT20 | |
| IFT complex A accessory | | TLP1 | TUB-1 | TULP3 | |
| IFT complex B accessory | | FAP22 | DYF-3 | CLUAP1 | Qilin |
| | | DYF13 | DYF-13 | TTC26 | |
| BBSome | BBS1 | BBS1 | BBS-1 | BBS1 | |
| | BBS2 | – | BBS-2 | BBS2 | |
| | BBS4 | BBS4 | F58A4.14 | BBS4 | |
| | BBS5 | BBS5 | BBS-5 | BBS5 | |
| | BBS7 | BBS7 | BBS-7 | BBS7 | |
| | BBS8 | BBS8 | BBS-8 | BBS8 | |
| | BBS9 | BBS9 | BBS-9 | BBS9 | |
| | BBIP10 | – | – | BBIP10 | |

**Table 1.1 Components of the intraflagellar transport system**

This table lists all known components of the IFT complexes A and B and their accessory proteins, the molecular motors required for IFT and all components of the BBSome required for trafficking of G-protein coupled receptors (GPCR). In this table, the nomenclature is listed for each protein across core species in which IFT is studied. This table was taken from (Ishikawa and Marshall 2011).

## 1.4 Ciliary length control

The ability of the cilium to modulate its size in response to environmental cues is proposed to function as a mechanism by which the cell can modulate cilia mediated signalling. Although ciliary tubulin is stabilised by acetylation, the primary cilium remains a dynamic structure as microtubule turnover continually occurs at the distal tip of the axoneme. However, the cilium is maintained at a set length as disassembly at the ciliary tip is balanced by the continual delivery and assembly of ciliary precursors from the cell body. When this balance is disrupted cilia growth, or cilia resorption will occur (Kozminski et al. 1993; Brown et al. 1999; Marshall and Rosenbaum 2001; Marshall et al. 2005). Thus the structural components of the cilium are dependent on the same transport processes that regulate cilia mediated signalling pathways, a change in cilia length is therefore considered to be indicative of a change in antereograde or retrograde IFT.

In *c.reinhardtii*, several studies have examined IFT during flagella growth and length maintenance. These studies support a 'balance point' length control model (Marshall and Rosenbaum 2001; Marshall et al. 2005). They demonstrate that as newly forming and full-length flagella possess the same amount of IFT proteins it is the rate of arrival of these particles, the velocity of antereograde IFT, at the flagella tip that regulates flagella growth. An increased delivery rate would favour axoneme construction and an increase in length, while a reduced delivery rate would favour disassembly as the retrieval rate appears to remain constant (Marshall and Rosenbaum 2001; Marshall et al. 2005). The *c.reinhardtii Fla10-1* mutant provides further support for this model. *Fla10-1* harbours a temperature sensitive mutation in the gene encoding the antereograde motor Kinesin-2. When *Fla10-1* mutants are cultured at 32$^{o}$C antereograde IFT is inhibited and flagella progressively shorten at the basal rate of retrograde IFT (Marshall and Rosenbaum 2001). Interestingly flagella disassembly in this mutant can be enhanced further by extracellular stimuli that increase the rate of retrograde IFT such as sodium pyrophosphate (Pan and Snell 2005).

Studies in mammalian cells show that changes in the rate of antereograde IFT can also influence primary cilia length. Increased cellular levels of cAMP and subsequent PKA activation result in a faster rate of antereograde IFT in mammalian epithelial and

mesenchymal cells and triggers significant cilia lengthening (Besschetnova et al. 2010). The application of shear stress reduces cAMP levels in these cells and is accompanied by significant ciliary shortening (Besschetnova et al. 2010). However this mechanism is not fully understood, and is likely to be cell-type dependent as the inhibition of adenylate cyclase, which reduces cAMP levels, produces significant increases in cilia length in both chondrocytes and synovial fibroblasts (Ou et al. 2009; Wann and Knight 2012).

On the whole, the 'balance point' length control model is over simplified and likely to be far more complex. For example, Pan et al. made the surprising observation that flagella shortening in *Chlamydomonas* in response to sodium pyrophosphate is actually accompanied by significant increases in the rate of antereograde IFT as well as retrograde IFT (Pan and Snell 2005). However, the antereograde particles entering the flagellum lacked cargo, indicating cargo loading at the base of the cilium was disrupted. This results in the increased transport of cargo-less rafts into the flagellum and facilitates disassembly by increasing the availability of empty cargo binding sites at the ciliary tip for the retrieval of disassembly products (Pan and Snell 2005). The mechanisms regulating cargo loading at the base of the cilium/flagellum are not well understood.

Importantly, these studies identify two key regulatory points in the maintenance of cilia and flagella length firstly in the regulation of the velocity of antereograde and retrograde IFT and secondly in cargo binding at the base of the cilium. A wide range of possible signalling pathways that regulate cilia length have been identified including the cAMP-PKA system, the PKC- Mitogen-activated (MAP) Protein Kinases, a large range of actin and tubulin related proteins, many cell-cycle related proteins, Galectins, FGF signalling, and Hypoxia-inducible factors (HIFs) and appear to function in a cell type and context specific manner (Pugacheva et al. 2007; Neugebauer et al. 2009; Ou et al. 2009; Verghese et al. 2009; Besschetnova et al. 2010; Cruz et al. 2010; Kim et al. 2010; Kinzel et al. 2010; Lopes et al. 2010; May-Simera et al. 2010; Abdul-Majeed et al. 2011; Li et al. 2011; Massinen et al. 2011; Miyoshi et al. 2011; Palmer et al. 2011; Rondanino et al. 2011; Sharma et al. 2011; Thiel et al. 2011; Verghese et al. 2011).

Prominent roles for tubulin de-acetylases and cell cycle related kinases such as Aurora A have been identified in cilia disassembly and will be discussed in the following section (Hubbert et al. 2002; Pugacheva et al. 2007; Gradilone et al. 2013).

### 1.4.1 AurA/HDAC6 mediated cilium resorption

Primary cilia are regulated dynamically through the cell cycle. Although there is evidence that primary cilia are present on some proliferating cells, cilia resorption generally occurs upon mitotic entry and is followed by re-emergence after cell division (Seeley and Nachury 2010). In serum starved, cultured mammalian cells, cell cycle re-entry and cilia resorption can be induced by the addition of serum. In mammalian cells resorption in response to serum occurs via an Aurora A (AurA) kinase dependent pathway (Pugacheva et al. 2007).

AurA kinase and the pro-metastatic scaffolding protein HEF-1/Cas-L/NEDD9 co-localise at the basal body of the cilium. In response to serum addition, AurA becomes activated through its interaction with HEF1 which stabilises the kinase and is required for its full activation. AurA induces rapid ciliary resorption by the phosphorylation and consequent activation of histone deacetylase 6 (HDAC6). HDAC6 is an important cytoplasmic tubulin deacetylase and has been shown to influence processes like mitosis and chemotaxis, both of which have been linked to ciliary function (Hubbert et al. 2002). While HDAC6 is mainly cytoplasmic, localisation to the ciliary axoneme has been reported (Pugacheva et al. 2007). Following AurA-dependent activation, HDAC6 deacetylates ciliary tubulin and destabilises the axonemal microtubules resulting in cilia disassembly (Pugacheva et al. 2007) (Figure 1.5).

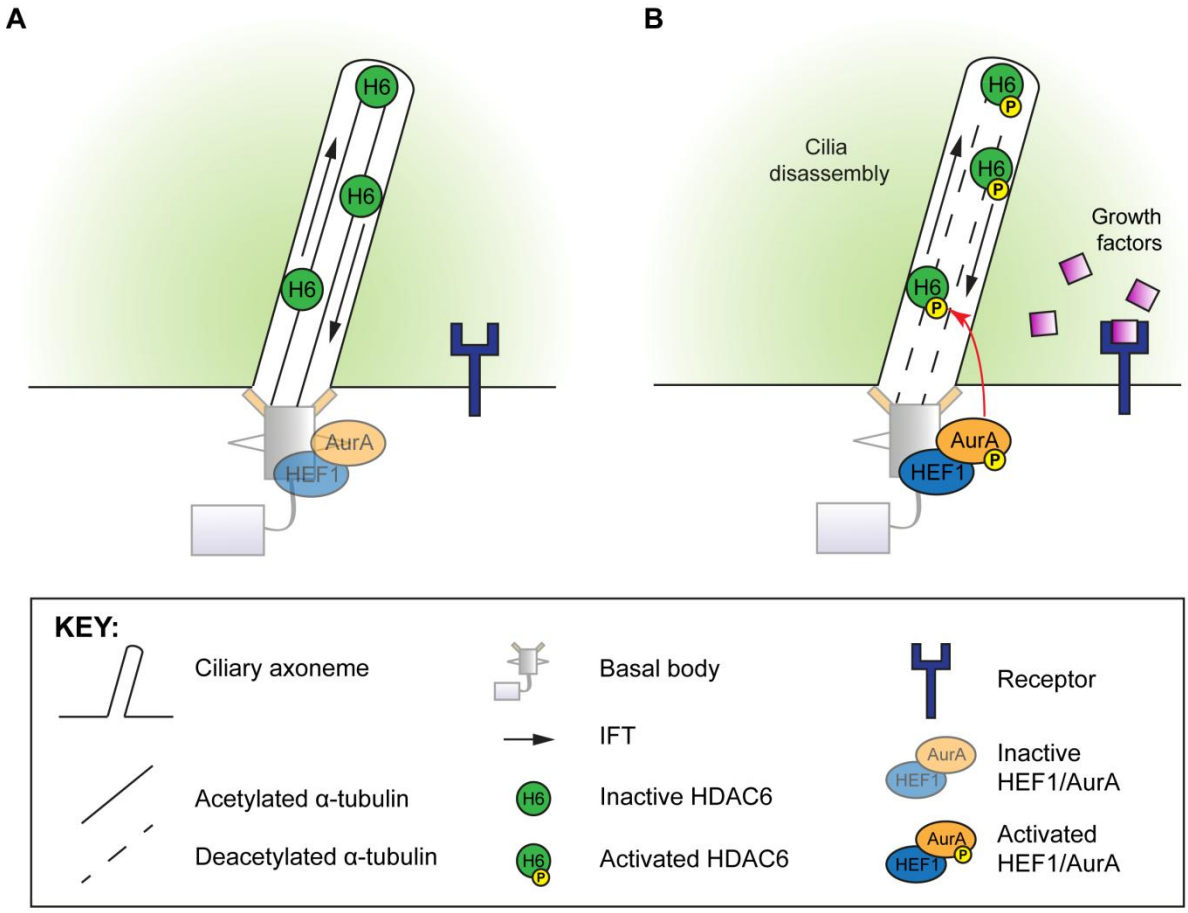


**Figure 1.5 AurA/HDAC6 disassembly pathway**
**(A)** Aurora A (AurA) and HEF1 are localised to the basal body of quiescent, ciliated cells (Pan and Snell 2007). **(B)** Growth factors contained within serum induce HEF1 expression and promote HEF1-dependent activation of AurA. AurA phosphorylates and activates ciliary HDAC6 6 (H6). HDAC6 de-acetylates α-tubulin within the cilium destabilising the ciliary microtubules and inducing ciliary resorption. This schematic was adapted from (Pugacheva et al. 2007).

## 1.5 Cilia mediated signalling pathways

Since the discovery of a role for the primary cilium as a mechanosensor in kidney epithelia, numerous extracellular signalling pathways have been shown to require ciliary function. These include the PDGFRα (Schneider et al. 2005; Schneider et al. 2010), IGF-1R (Zhu et al. 2009), Wnt (Ross et al. 2005; Gerdes and Katsanis 2008; Lancaster et al. 2011) and Hedgehog (Huangfu et al. 2003; Corbit et al. 2005; Rohatgi et al. 2007) signalling pathways which utilise a number of mechanisms involving the cilium to control signal transduction.

Hedgehog signalling is perhaps the best characterised of these pathways. However its relationship with the cilium is complex as this organelle is required for both the negative and positive regulation of this pathway. As the focus of much of this thesis, hedgehog signalling and its dependence on the primary cilium will be discussed in more detail in section 1.6.

### 1.5.1 Mechanotransduction

In the renal epithelium the cilium functions as a mechanosensor; urinary flow through the renal tubules deflects the cilium and this deflection is sensed by a heterodimeric complex at the base of the cilium comprised of the integral membrane proteins polycystin-1 (PC-1) and polycystin-2 (PC-2) (Nauli et al. 2003). PC-1 and PC-2 are encoded by *Pkd1* and *Pkd2* respectively, the disease genes mutated in autosomal dominant polycystic kidney disease (ADPKD) (Calvet and Grantham 2001). In response to ciliary deflection, the large extracellular domain of PC-1 undergoes a conformational change and activates PC-2, a $Ca^{2+}$ permeable cation channel of the TRP family (Gonzalez-Perrett et al. 2001; Joly et al. 2003; Nauli et al. 2003; Berbari et al. 2009). PC-2 activation triggers local increases in $Ca^{2+}$ concentrations which stimulate intra-organellar $Ca^{2+}$ release activating a signalling cascade that regulates cell proliferation, adhesion, differentiation and morphology (Praetorius and Spring 2001; Nauli et al. 2003; Praetorius et al. 2003; Chauvet et al. 2004; Nauli and Zhou 2004).

While this signalling cascade was initially identified in kidney epithelial cells it has since been demonstrated to exist in cholangiocytes (Masyuk et al. 2006). However it does not function

in all mechanosensitive cells. While PC-1 localises to the stereo-cilia of the inner ear hair cells it is not required for mechanoelectrical transduction (MET) (Steigelman et al. 2011). In these cells PC-1 co-localises with F-actin *in vivo* and is essential for cilia structure and maintenance (Steigelman et al. 2011).

PC-1 also contains a G-protein receptor proteolytic site in its extracellular N-terminal region (Parnell et al. 1998; Nauli et al. 2003). When this site is cleaved it produces an intracellular C-terminal fragment that is reported to interact with STAT6 and its co-activator P100 stimulating STAT6-dependent gene expression (Low et al. 2006). PC-1 cleavage is triggered upon the cessation of luminal fluid flow in kidney epithelia (Weimbs 2007).

Mechanical stimulation of the skeleton is an important anabolic signal in bone leading to increased osteoblastic proliferation and matrix deposition, conversely the absence of mechanical stimuli is associated with bone loss (You et al. 2001; Reilly et al. 2003; Kim et al. 2006). In bone, osteocytes are housed within fluid filled lacunae that are connected to each other, and to matrix forming osteoblasts at the bone surface, through channels called canaliculae. Osteoblasts and osteocytes respond to dynamic fluid flow through these channels with characteristic increases in gene expression and cytokine release. *In vitro* studies have demonstrated that primary cilia are essential for mechanotransduction in bone cells and are deflected by fluid flow (Malone et al. 2007). In the absence of cilia, the mechanosensitive induction of osteoprotegrin (OPG) and cyclo-oxygenase-2 (COX-2) is abrogated and the mechanical regulation of the OPG/receptor activator of NF-κB ligand (RANKL) signalling system disrupted (Malone et al. 2007). In contrast to kidney epithelial cells, flow induced $Ca^{2+}$ signalling does not require PC-2 or the primary cilium in bone cells indicating mechanotransduction in these cells occurs via a different mechanism (Malone et al. 2007). One candidate protein for this is PC-1 as *Pkd1* mutant's exhibit disrupted skeletal development and bone formation (Xiao et al. 2006; Kolpakova-Hart et al. 2008). Xiao et al showed that the PC-1 c-terminal tail regulates the expression of Runt-related transcription factor 2 (RUNX-2) in a gene dose-dependent manner *in vivo* and thus regulates the expression of osteogenic genes (Xiao et al. 2006). Over expression of the PC-1 c-terminal tail resulted in an increase in RUNX-2 promoter activity in osteoblast cell lines, as well as an increase in the expression of genes downstream of this transcription factor, namely

osteocalcin, osterix and OPG (Xiao et al. 2006). While it has yet to be demonstrated, the mechanical regulation of PC-1 cleavage may therefore represent an important component of mechanotransduction in bone cells.

In articular chondrocytes, the cilium is required for mechanotransduction however the evidence suggests that, unlike in bone, it does not function as the mechanosensor in this response but rather as a transducer downstream of mechanosensitive ATP release (Wann et al. 2012). This pathway will be discussed further in chapter 2.

### 1.5.2 Platelet derived growth factor receptor α (PDGFRα) signalling

Independent of its roles in mechanotransduction, the cilium also provides an isolated compartment for other signalling pathways. The enrichment of signalling components within this compartment facilitates reaction kinetics and promotes signal transduction.

PDGFRα is widely expressed in human tissues controlling migration, proliferation, and apoptosis and has been implicated in numerous types of cancer (Heldin and Westermark 1999). PDGFRα homodimers (PDGFRαα) localise to the plasma membrane in proliferating NIH3T3 fibroblasts. Upon serum starvation the expression of PDGFRα is increased and PDGFRαα progressively localises to the newly formed primary cilium with time (Schneider et al. 2005). In response to ligand stimulation, PDGFRαα is activated within the cilium where it triggers the Raf-dependent activation of Mek1/2 at the basal body controlling cell growth and proliferation (Schneider et al. 2005). In fibroblasts derived from *IFT88* mutant mice, MEK1/2 signalling is not activated and cells exhibit defects in cell cycle regulation and chemotaxis (Schneider et al. 2005; Schneider et al. 2010).

### 1.5.3 Insulin-like growth factor receptor (IGFR) signalling

The first key step in adipocyte differentiation is the differentiation of dividing pre-adipocytes to growth arrested adipocytes highlighting a potential role for the cilium in this process (Tucker et al. 1979; Johnson 2005). Zhu et al. reported IGF-1 receptors to localise to the primary cilium of pre-adipocytes, however, in contrast to PDGFRα signalling, the authors did not find ciliary localisation of IGF-1R to be essential for receptor activity (Zhu et al. 2009).

Receptor compartmentalisation in this case is used to increase ligand sensitivity within the ciliary compartment. Ciliated cells exhibit enhanced Akt activation in response to insulin and were more responsive to lower concentrations of insulin than cycling cells. Receptor activation occurred more rapidly within the cilium than in other plasma membrane areas potentially due to the recruitment of the downstream signalling components to the basal body (Zhu et al. 2009).

### 1.5.4 Canonical Wnt signalling

Compartmentalisation can also play a negative role in signalling, as seen for the canonical Wnt pathway (Simons et al. 2005; Corbit et al. 2008; Lancaster et al. 2011). Wnt signalling regulates the degradation of β-catenin. In the presence of Wnt, the protein Dishevelled promotes the accumulation of β-catenin which translocates to the nucleus and promotes gene transcription through an interaction with the TCF/LEF1 transcription complex [for review see (Logan and Nusse 2004)].

The ciliary protein Inversin is proposed to function as a molecular switch between the canonical and non-canonical pathways (Simons et al. 2005). Inversin inhibits canonical Wnt signalling by binding Dishevelled and targeting it for degradation thus preventing β-catenin accumulation. Concomitant with this degradation, Inversin promotes convergent extension movements in gastrulating *Xenopus laevis* embryos, a process which is regulated by non-canonical Wnt signalling (Simons et al. 2005). More recently Lancaster et al. have shown that the primary cilium further dampens canonical Wnt signalling through a unique spatial mechanism involving the ciliopathy protein Jouberin (Lancaster et al. 2011). Jouberin binds β-catenin and promotes its nuclear accumulation, however in ciliated cells Jouberin is sequestered to the basal body and ciliary axoneme and canonical Wnt signalling is inhibited (Lancaster et al. 2011).

## 1.6 Hedgehog Signalling

Hedgehog proteins constitute a family of morphogenic proteins that control cell growth, survival and fate and are responsible for patterning tissues during both vertebrate and invertebrate development. Hedgehog was initially identified in *Drosophila melanogaster* by Nussein-Volhard and Wieschaus during a systematic screen for larval segmentation defects (Nusslein-Volhard and Wieschaus 1980). It was subsequently discovered in a range of invertebrate and vertebrate organisms and while many of the key components of the hedgehog pathway are conserved there are several differences that suggest the pathways have evolved differently after separation of the vertebrate and invertebrate lineages. Perhaps one of the most striking differences is the requirement for the primary cilium in vertebrate hedgehog signalling (for review see (Goetz and Anderson 2010)).

### 1.6.1 Mammalian Hedgehog proteins

Mammals possess three hedgehog homolog's; Sonic (Shh), Indian (Ihh) and Desert (Dhh) hedgehog all of which share the same signal transduction machinery. The activity of these three proteins is believed to be similar as they can often act redundantly within the same tissue; the differences in their developmental roles arise due to their different spatial and temporal expression patterns (Stone et al. 1996; Vortkamp et al. 1996; Varjosalo and Taipale 2008). Shh is expressed in mid-line tissues such as the node, notochord and floor plate where it controls the patterning of both the left-right and dorsal-ventral axes (Wilson et al. 2009). In later development Shh is expressed in most epithelial tissues where it effects tissue development and organogenesis. Shh and Ihh act in concert to regulate skeletogenesis, Shh is expressed early in the limb bud where it controls the patterning of the anterior-posterior axis (Tickle 2006). Ihh is expressed later in the growth plate and regulates chondrocyte hypertrophy and proliferation and is essential for the process of endochondral ossification (Vortkamp et al. 1996; Varjosalo and Taipale 2008). Dhh expression is largely restricted to the gonads where it regulates spermatogenesis (Bitgood and McMahon 1995).

#### 1.6.1.1 Hedgehog protein processing and secretion

All members of the hedgehog protein family undergo a unique series of post-translational processing events that result in dual lipidation and efficient secretion. These processing events have been studied extensively for Shh (for review see (Ryan and Chiang 2012)). Shh is initially synthesised as a precursor protein approximately 45kDa in size and contains an N-terminal signal sequence that promotes entry into the secretory pathway. In the endoplasmic reticulum, this signal sequence is cleaved resulting in the activation of an intein-like domain in the C-terminus. This domain catalyzes an auto-cleavage reaction which produces a 25kDa C-terminal fragment (ShhC) and a 19-kDa N-terminal fragment (ShhN) (Porter et al. 1996). The signalling capabilities of hedgehog ligands reside within ShhN, therefore ShhC undergoes endoplasmic reticulum-associated degradation (Chen et al. 2011).

ShhN is modified covalently with two lipids, cholesterol and palmitate. The cholesterol modification occurs concomitant with auto-cleavage and is added to the C-terminus of ShhN (Porter et al. 1996). The palmitate residue is attached to the N-terminus via amide linkage to an N-terminal cysteine in a reaction that is catalyzed by Hedgehog acyltransferase/Skinny hedgehog (Hhat/Ski) (Chamoun et al. 2001). This Hhat/Ski mediated ShhN palmitoylation can occur independent of auto-cleavage and cholesterol modification; however both modifications are required for normal Shh function (Chamoun et al. 2001; Traiffort et al. 2004).

Hedgehog ligands can function at both short and long range, this is largely due to the C-terminal cholesterol moiety which not only functions to anchor hedgehog ligands to the plasma membrane but is required for the formation of soluble multimeric forms of hedgehog and for the active release of hedgehog monomers by the transmembrane protein Dispatched (Disp). Disp is a 12-pass transmembrane protein required for the release of cholesterol modified hedgehog and thus long range signalling (Burke et al. 1999; Ma et al. 2002; Nakano et al. 2004). Disp belongs to the RND family of transporters and contains a sterol sensing domain (SSD) (Kuwabara and Labouesse 2002). It was recently discovered that Disp co-operates with a member of the Scube family of secreted proteins, Scube2, to

dramatically enhance the solubility and secretion of cholesterol modified hedgehog ligands (Creanga et al. 2012; Tukachinsky et al. 2012). The vertebrate homolog Dispatched A (DispA) binds to membrane associated Shh in a cholesterol dependent manner. Shh is then transferred to Scube2 via a mechanism reminiscent of the transfer of free cholesterol by the Niemann-Pick disease proteins NPC-1 and NPC-2 (Infante et al. 2008; Tukachinsky et al. 2012). Scube2 and DispA recognise different features of the Shh cholesterol moiety, ensuring this region is never exposed to the aqueous environment and remains soluble. While the two groups that discovered this mechanism did not agree upon the role of ShhN palmitoylation in ShhN release, both studies showed that in the absence of this modification scube2-released Shh is not active (Creanga et al. 2012; Tukachinsky et al. 2012).

### 1.6.2 Vertebrate hedgehog signalling requires the primary cilium

In the absence of ligand, the hedgehog receptor Patched-1 (Ptch1) functions to inhibit a second transmembrane protein Smoothened (Smo) (Rohatgi et al. 2007). This interaction regulates the activity of a family of bi-functional transcription factors the Glioma associated oncogene homolog (Gli) proteins (Haycraft et al. 2005; Milenkovic et al. 2009). Three Gli genes have been identified in mammals, Gli1, Gli2 and Gli3 (Ingham and McMahon 2001). In their full length forms Gli2 and Gli3 function as transcriptional activators. However, in the absence of hedgehog ligands these proteins are targeted for proteasomal cleavage and a truncated repressor protein is produced (Dai et al. 1999; Sasaki et al. 1999). Biochemical and genetic evidence indicates that Gli3 predominantly acts as a repressor and Gli2 predominantly as an activator (Ding et al. 1998). The function of Gli2 is amplified by the inducible expression of Gli1 which lacks the N-terminal repressor domain (Dai et al. 1999; Bai et al. 2004). Interestingly, Gli1 induces the expression of Ptch1, indicating that the major function of this transcription factor might be to establish a negative feedback mechanism (Buttitta et al. 2003).

In vertebrates, Ptch1 localises to the primary cilium, binding of one of the three mammalian hedgehog ligands triggers Ptch1 internalisation and degradation releasing Smo inhibition (Rohatgi et al. 2007). Consequently, Smo traffics into the cilium and is activated (Corbit et al. 2005). Within the cilium, Smo inhibits Gli processing and promotes formation of

transcriptional activators resulting in hedgehog pathway activation (Corbit et al. 2005; Haycraft et al. 2005; Milenkovic et al. 2009). See Figure 1.6 for a schematic diagram representing this pathway.

The first evidence that intraflagellar transport/cilia are required for hedgehog signalling was provided by two mouse mutants, wimple and flexo. These mice were identified in a screen for embryonic patterning mutations and displayed defects in neural tube formation and exhibited pre-axial polydactyly, classic indications of disrupted Shh signalling (Huangfu et al. 2003). The causative mutations for these phenotypes were subsequently identified as *Ift88* (flexo) and *Ift172* (wimple). Huangfu et al demonstrated that in addition to Ift88 and Ift172, Kif3a and dnchc2, components of the antereograde and retrograde motors, are required for hedgehog signalling (Huangfu et al. 2003; Huangfu and Anderson 2005). Interestingly, these studies showed that in addition to the formation of Gli activators, the cilium is also required for the formation of the Gli3 repressor (Gli3R). Cilia disruption results in a reduction in the levels of Gli3R such that the de-repression of hedgehog target genes occurs and the pathway becomes activated in the absence of ligand.

In addition to Ptch1 and Smo, several key components of this signal transduction pathway have been identified. The protein suppressor of fused (SuFu) forms inhibitory complexes with Gli proteins in the absence of ligand (Ding et al. 1999; Barnfield et al. 2005). These protein complexes transit through the cilium and are phosphorylated by protein kinase A (PKA) at the ciliary base targeting full length Gli proteins for proteosome-dependent processing and repressor formation (Tuson et al. 2011). When activated Smo is present in the cilium, these SuFu-Gli complexes dissociate and full length Gli activators exit the cilium, translocate to the nucleus and promote gene transcription.

The Kinesin family member Kif7 plays a central role in mammalian hedgehog signalling. KIF7 localises to the base of the cilium in unstimulated cells and functions as a ciliary motor, transporting Gli complexes to the ciliary tip when the pathway is activated (Liem et al. 2009). Kif7 interacts directly with Gli proteins and has dual positive and negative roles as it is also required for the correct processing of Gli3 to its repressor form. Hsu et al report that in *Kif7* deficient chondrocytes the ciliary localisation of Gli2/3 and Sufu is increased suggesting

that Kif7 might function to restrain Gli proteins from entering the cilium and trafficking to the ciliary tip in the absence of ligand (Hsu et al. 2011).

Until recently the mechanism by which Smo ciliary accumulation results in the dissociation of Sufu/Gli complexes and altered Gli processing has remained a mystery. This was until the discovery of an interaction between Smo and the cilium associated protein Ellis van Creveld (Evc) 2 (Dorn et al. 2012; Yang et al. 2012). Evc2 forms a complex with a second protein, Evc that localises to the base of the primary cilium (Blair et al. 2011; Dorn et al. 2012; Yang et al. 2012). This complex identifies a new ciliary region called the Evc zone which lies just distal to the transition zone (Dorn et al. 2012). The Evc/Evc2 complex acts downstream of Smo, yet upstream of suppressor of fused (sufu) and promotes the formation of Gli activators. In response to hedgehog stimulation, Evc2 binds to the intracellular tail of Smo (Dorn et al. 2012; Yang et al. 2012). While activated Smo localises along the full length of the cilium, the Smo-Evc2 complex is restricted to the Evc zone and is proposed to modify Gli-Sufu complexes as they transit through this region promoting complex dissociation (Dorn et al. 2012; Caparros-Martin et al. 2013).

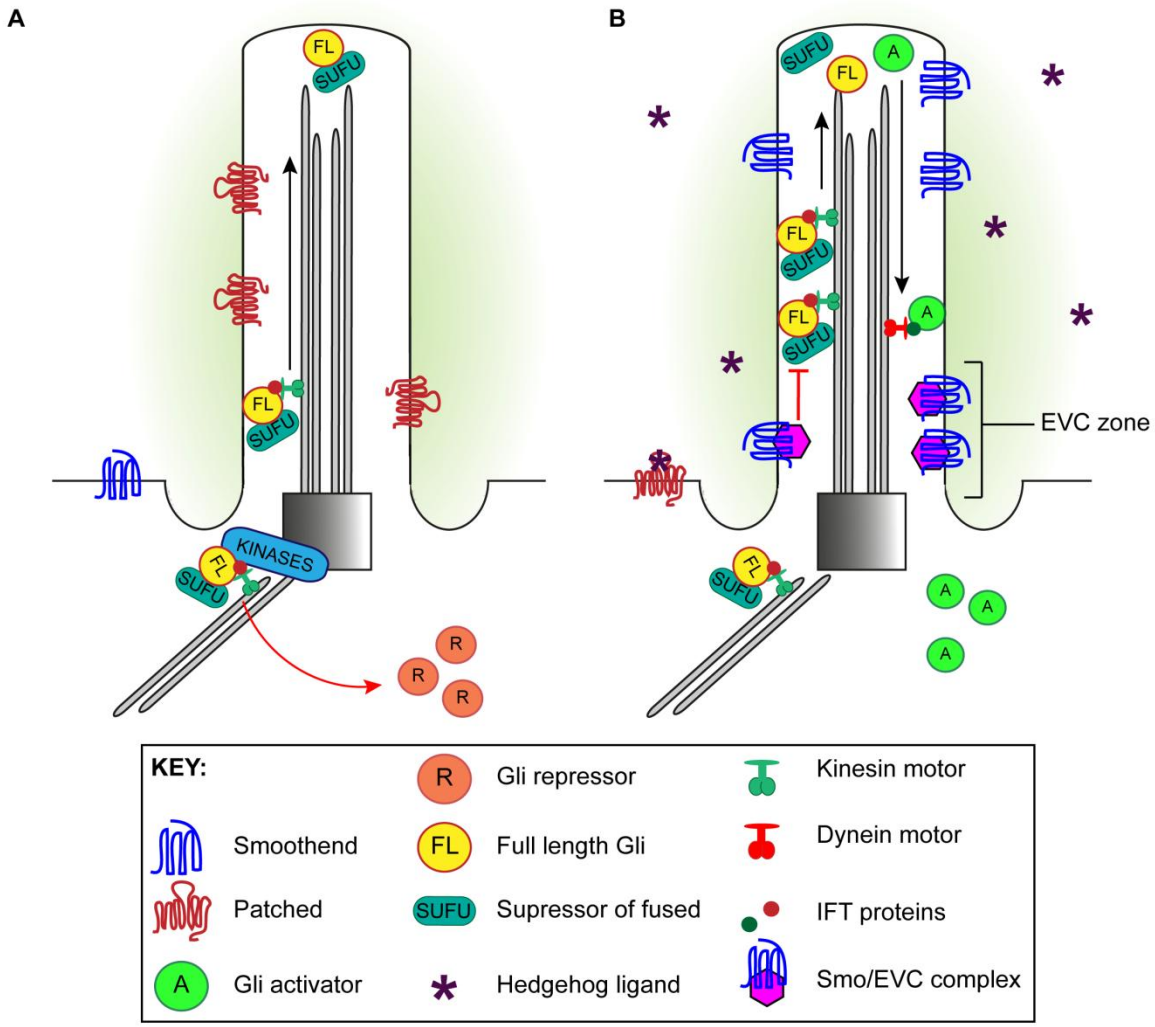


**Figure 1.6 Vertebrate hedgehog signalling requires the primary cilium**
**(A)** In the absence of hedgehog ligands, the hedgehog receptor Patched (Ptch) inhibits the ciliary localisation of Smoothened (Smo). The kinesin motor KIF7 forms a complex with Gli proteins and suppressor of fused (SUFU) at the base of the cilium and prevents Gli enrichment within the cilium. Gli proteins are phosphorylated by kinases such as PKA and targeted for proteasomal degradation or GliR formation. **(B)** Hedgehog binding to Ptch releases the inhibition on Smo, which binds to the EVC complex and traffics into the cilium. KIF7 moves into the cilium thereby promoting the accumulation of Gli proteins and activated Smo promotes the dissociation of inhibitory SUFU/Gli complexes and formation of Gli activators. Gli activators are transported out of the cilium by the dynein motor and intraflagellar transport (IFT) particles.

# CHAPTER 2

# Articular cartilage

## 2.1 Articular cartilage structure and function

Articular cartilage is an aneural, avasuclar connective tissue that covers the surfaces of the bones in diarthrodial joints such as the knee. It provides a smooth, frictionless surface that functions to resist and distribute compressive forces protecting the underlying bone from damage during normal joint articulation. Articular cartilage has a limited capacity for repair and failure of this tissue results in the development of the chronic degenerative disease osteoarthritis (OA) which affects over 200 million people world-wide (Lin et al. 2009).

### 2.1.1 Extracellular matrix

Articular cartilage comprises an expansive extracellular matrix (ECM) that is synthesised and maintained by a small number of chondrocytes. Chondrocytes are the only cell type present in this tissue and constitute 1-10% of the tissue volume (Mow et al. 1999; Kim et al. 2008). The major components of the cartilage ECM are collagens, proteoglycans and water. Collagen type II is by far the most abundant protein in the ECM at 60% of the tissue dry weight and forms a highly organised fibrillar network, which imparts strength to the tissue to withstand compressive and tensile strain. The most predominant proteoglycan in the ECM is aggrecan. The aggrecan core protein is modified by numerous sulphated glycosaminoglycans (sGAG) and thus has a high negative charge which promotes ionic interactions with water molecules. Thus it forms highly hydrated, high molecular weight aggregates in association with hyaluronan and Link protein (Figure 2.1A). These aggregates are immobilised within the collagen network (Figure 2.1B), their extreme hydration coupled with the resistance of the collagen network to expansion is what gives articular cartilage its unique load bearing capabilities (Poole 1997; Dudhia 2005; Chen et al. 2006). Additional small proteoglycans and non-collagenous proteins are also present in the cartilage ECM such as biglycan, decorin, perlecan and fibronectin amongst others (for review see (Velleman 2000; Knudson and Knudson 2001)). At the articular surface, a boundary layer of hyaluronic acid and lubricin provides a smooth surface with a low coefficient of friction which permits efficient gliding motion during joint movement (Greene et al. 2011).

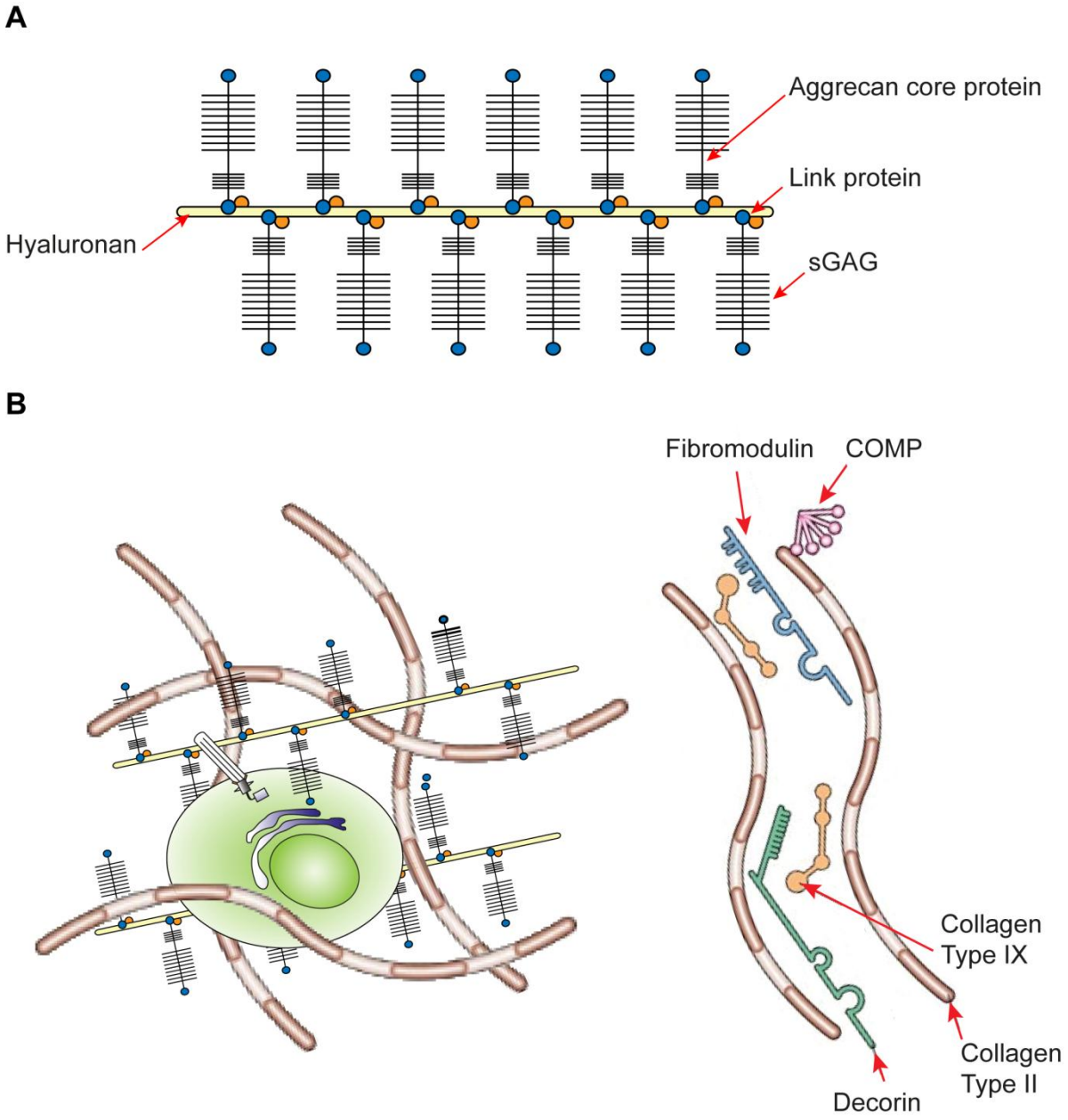


**Figure 2.1 The extracellular matrix of cartilage**
**A)** Schematic representation of the extracellular matrix protein aggrecan. **B)** Simplified schematic of the cartilage extracellular matrix showing the three classes of proteins that exist in articular cartilage: collagens (mostly type II); proteoglycans (mostly aggrecan, but also the smaller proteoglycans biglycan, decorin and fibromodulin); and other non-collagenous proteins (including link protein, fibronectin and cartilage oligomeric matrix protein (COMP)). Adapted from (Chen et al. 2006).

## 2.1.2 Structural organisation

Articular cartilage is heterogeneous in structure and thus divisible in to four major zones: superficial, middle, deep and a layer of calcified cartilage (Figure 2.2A). The superficial layer is characterised by its low proteoglycan content and layers of densely packed collagen II fibrils in which flattened disc-shaped chondrocytes reside. The chondrocytes in this zone are responsible for synthesising proteins that have lubricating and protective functions and produce very little proteoglycan (Wong et al. 1996). The chondrocytes within the middle zone are much rounder and the proteoglycan content in this zone is higher. In the middle zone the collagen fibrils are arranged in an intersecting transitional network that is intermediate between the tangential arrangement observed in the superficial zone and the radial network that is found in the deep zone. Proteoglycan content is further increased in the deep zone and the rounded chondrocytes are arranged in columns perpendicular to the articular surface. The deep zone transitions into a layer of calcified cartilage which interfaces with the sub-chondral bone, the junction between these two zones is defined by an undulating tidemark (Poole 1997; Mow et al. 1999; Pearle et al. 2005).

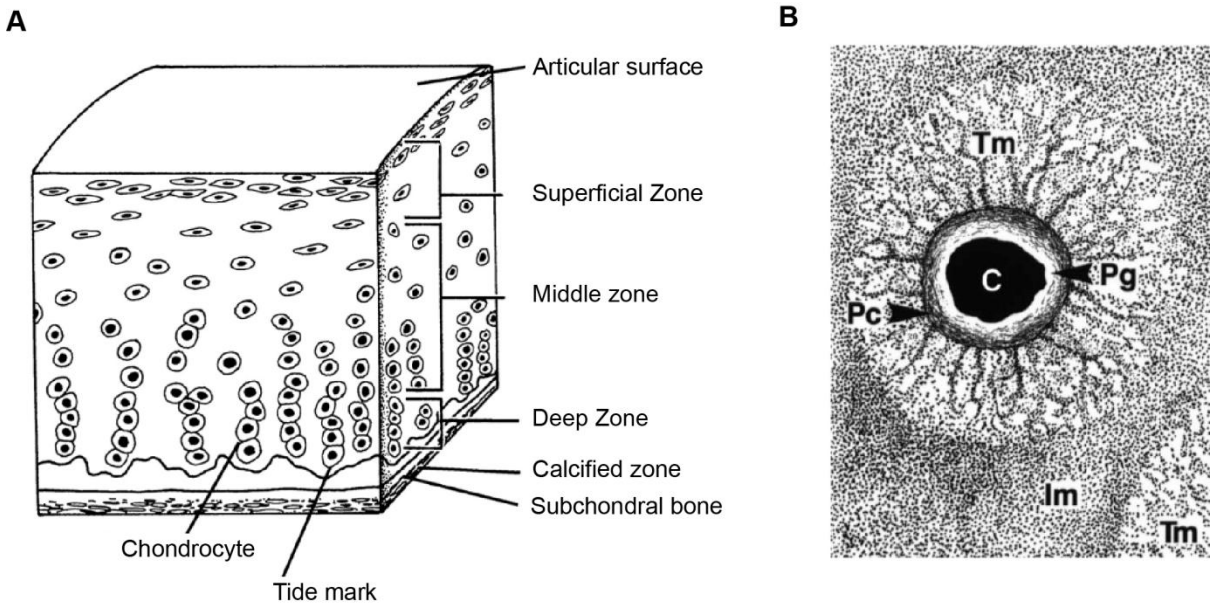


**Figure 2.2 Articular cartilage structural organisation**
**(A)** Schematic illustrating the zonal organisation of the articular cartilage adapted from (Newman 1998). **(B)** Schematic illustrating the circumferential collagen organisation in the deep layer showing a single chondrocyte **(C)**, pericellular glycocalyx (Pg), pericellular capsule (Pc), territorial matrix (Tm) and inter-territorial matrix (Im) taken from (Poole et al. 1984).

In addition to this zonal architecture, the cartilage ECM also exhibits circumferential variations based upon the distance from the chondrocyte. These variations can be classified into distinct regions named pericellular, territorial and inter-territorial matrix (Figure 2.2B). Proteoglycan content varies within these concentric subdivisions. The inter-territorial matrix is enriched with keratan sulphate rich proteoglycans whereas chondroitin sulphate rich proteoglycans are more concentrated in the territorial matrix (Poole 1997). The pericellular matrix forms a narrow region of tightly woven collagen fibres around the chondrocyte that has a high collagen type VI content (Poole et al. 1988). This matrix completely encloses the chondrocyte forming a structure called the chondron, considered to be the basic metabolic unit of cartilage (Poole et al. 1988). The collagen fibre size increases with distance from the cell so that the largest fibres predominate in the inter-territorial matrix where they form a radial network (Poole 1997).

Contained within the fluid filled fibrillar capsule of the chondron, the chondrocyte interacts with the pericellular matrix via integrins expressed at the cell surface and through a pericellular glycocalyx (Poole 1997). A chondron may contain a single chondrocyte, however single, double and linear columns of chondrons have been identified. Significant variations in chondron shape, size, volume and orientation occur within the different zones of the articular cartilage (Youn et al. 2006). Consistent with the variations observed for chondrocyte morphology, more flattened discoidal chondrons occur in the superficial zone, these chondrons are oriented parallel to the articular surface. In the middle and deep zones chondrons are oriented perpendicular to the articular surface and contain more rounded chondrocytes. Multi-cellular chondrons are more frequent in the deep zone (Youn et al. 2006).

## 2.2 Mechanical loading regulates cartilage health and maintenance

During physical activity, the articular cartilage is subjected to dynamic mechanical loading which is essential for the health and homeostasis of the tissue. Joint loading alters the extracellular environment of the chondrocyte such that the cells are subjected to compressive tensile and shear strain, fluid flow and changes in hydrostatic pressure, pH and osmolarity (Figure 2.3).

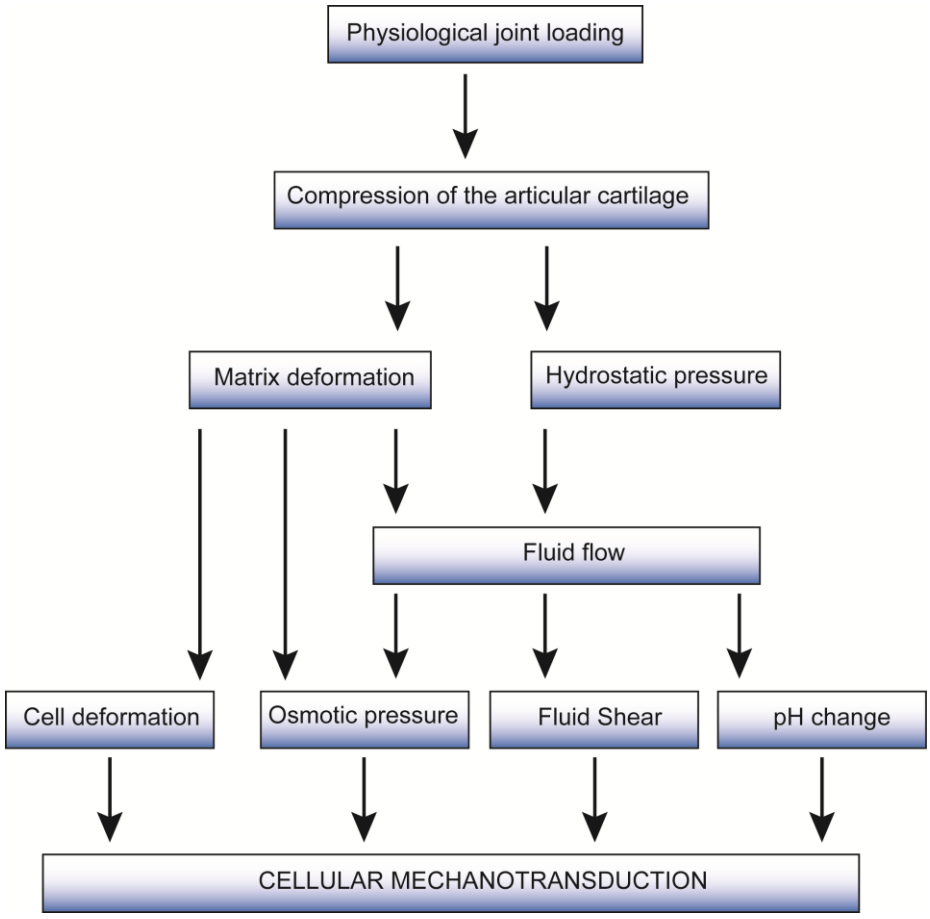


**Figure 2.3 Mechanotransduction events in cartilage**
Schematic flow chart indicating the mechanotransduction events associated with physiological joint loading adapted from (Pingguan-Murphy and Knight 2008). Physiological joint loading compresses the articular cartilage leading to increases in hydrostatic pressure and deformation of the cartilage matrix. Consequently cells experience increases in compressive/tensile strain, osmotic pressure, fluid shear and changes in pH due to solute movement. Chondrocytes sense these changes in the extracellular environment and convert mechanical signals to chemical signals that alter cell metabolism. Catabolic or anabolic processes become activated depending upon the type, duration and frequency of the applied load.

Chondrocytes are specially adapted to sense and respond to mechanical stimuli and regulate their metabolic profile according to the frequency and amplitude of the load applied [for review see (Urban 1994)]. Physiological loading promotes cartilage matrix production and joint maintenance. Consistent with this concept, regions of cartilage that experience high levels of mechanical stress during joint loading have been found to have the highest proteoglycan content relative to regions where lower stresses are experienced (Kempson et al. 1971; Kiviranta et al. 1987). By contrast insufficient, excessive or traumatic loading promotes cartilage degradation and leads to OA (for review see (Goldring and Goldring 2007; Goldring and Goldring 2010; Sun 2010)). In line with this, *in vivo* joint immobilization produces a reversible reduction in the proteoglycan content of canine cartilage (Palmoski and Brandt 1982; Behrens et al. 1989; Saamanen et al. 1990). While an increase in cartilage thickness and proteoglycan content occurs in the contra-lateral limb as a consequence of the increased weight bearing (Behrens et al. 1989).

A number of *in vitro* models have been developed to study the effects of mechanical stimuli on cellular function. For example, compressive loading of cartilage explants *in situ* modulates chondrocyte viability, gene expression and the synthesis and break down of extracellular matrix macromolecules (Steinmeyer and Knue 1997; Ragan et al. 1999; Loening et al. 2000; Blain et al. 2001; Fitzgerald et al. 2004; Torzilli et al. 2006). The application of physiological levels of mechanical stress (0.5 – 1.0MPa) to full thickness cartilage explants resulted in the synthesis and release of sulphated proteoglycan in a strain dependent manner (Steinmeyer and Knue 1997). By contrast, Ragan et al showed that static loading down regulates the mRNA levels of aggrecan and type II collagen in a dose dependent manner (Ragan et al. 1999). The expression of catabolic enzymes, such as a disintegrin and metalloproteinase with thrombospondin motif-5 (ADAMTS-5) and the matrix metalloproteinases (MMP) MMP-3 and MMP-13, are increased following injurious loading of explants *in* situ and promote cartilage degradation (Lee et al. 2005). ADAMTS-5 is the predominant enzyme responsible for aggrecan cleavage during OA (Majumdar et al. 2007), while MMPs target collagen and other matrix components (for review see (Goldring and Goldring 2007)). In addition, injurious mechanical compression can lead to cell death by both apoptosis and necrosis (Torzilli et al. 1997; Chen et al. 2001).

Due to the heterogeneous structure of cartilage, compression at the articular surface results in zonal variations in local tissue strain. Typically, strain is amplified in the superficial zone, while in the deep zone local tissue strain is much lower (Choi et al. 2007). Therefore in addition to explant studies, many *in vitro s*ystems involve the isolation of chondrocytes from the extracellular matrix. The cells can then be placed in an inert 3D matrix such as agarose or alginate, or cultured in a 2D monolayer. Isolated from the matrix, chondrocytes can then be subjected to a uniform strain of known amount and the frequency, amplitude and type of loading applied varied in a controlled manner. Moreover, distinct cell population's (e.g. surface or deep zone chondrocytes) can be studied in isolation.

Buschmann et al first demonstrated that chondrocytes cultured in 3D agarose constructs increase proteoglycan synthesis by 6 - 25% in response to dynamic compression (3% strain, 0.01 – 1 Hz) over 10 hours (Buschmann et al. 1995). Similarly, Lee et al also showed that dynamic compression (15% strain, 1 Hz) over 48 hrs increases sGAG synthesis by almost 50% (Lee and Bader 1997). As in explants, this response is dependent on the magnitude, duration and frequency of the load applied and is not observed in response to static compression where sGAG synthesis is reduced (Lee and Bader 1997).

Chondrocytes also exhibit mechanosensitive changes in the expression of collagen type II and aggrecan in response to tensile strain, applied to the cells in monolayer (Millward-Sadler et al. 2000; Huang et al. 2007; Doi et al. 2008). Huang et al demonstrated that the expression of these genes is upregulated early on during the first 12 hrs of loading (10% strain, 0.5Hz). However, after 12 hrs the expression returned to the level observed in the control and a catabolic response involving MMP-1 was initiated. In contrast, other groups have observed ADAMTS-5 expression to be upregulated following short periods of mechanical strain (10%, 0.5Hz, 30 min) (Tetsunaga et al. 2011; Saito et al. 2013).

### 2.2.1 Mechanisms of chondrocyte mechanotransduction

The mechanisms by which chondrocytes convert mechanical signals into intracellular responses that modulate cell behaviour are not well understood. Numerous pathways involving the cellular cytoskeleton, integrins mechanosensitive ion channels and primary

cilium have been identified in the process of chondrocyte mechanotransduction and will be discussed in the following sections. Given the variety of mechanical stimuli the chondrocyte experiences (Urban 1994), it is unlikely that any one mechanism will prove to be wholly responsible for the multitude of responses that have been observed upon loading (for review see (Ramage et al. 2009)).

#### 2.2.1.1 Cytoskeleton

The chondrocyte cytoskeleton is comprised of actin microfilaments, vimentin intermediate filaments and tubulin microtubules which form a highly organised 3D network throughout the cell. This network provides the cell with the mechanical integrity required to withstand the compressive forces that occur in the joint. Furthermore it is vital for the maintenance of the chondrocyte phenotype and is an essential component of the mechanotransduction response providing a means by which the cell can reversibly adapt to external mechanical stimuli [for review see (Blain 2009)].

Within the cartilage matrix, the chondrocyte has a rounded morphology; the actin filaments exhibit a cortical localisation and are typically distributed towards the periphery of the cell in close association with the chondrocyte membrane (Idowu et al. 2000; Knight et al. 2001; Trickey et al. 2004). Vimentin intermediate filaments form a highly organised fibrillar network throughout the cell, while the tubulin microtubules form a loose basket-like mesh that is similarly distributed (Idowu et al. 2000; Langelier et al. 2000; Trickey et al. 2004; Blain et al. 2006). Actin remodelling has been observed in response to both static and dynamic compression in agarose culture (Knight et al. 2006), increased hydrostatic pressure (Parkkinen et al. 1995; Knight et al. 2006) and changes in osmolarity (Erickson et al. 2003; Chao et al. 2006). Localised changes in actin have also been observed in response to micropipette aspiration (Horoyan et al. 1990).

In 3D culture, the actin cytoskeleton is reversibly altered by static and dynamic compressive loading (Knight et al. 2006). Cortical actin staining at the periphery of the cell becomes more pronounced following compressive loading and has a more punctate appearance but fully recovers after 1 hr (Knight et al. 2006). However, while static hydrostatic loading produces a similarly reversible change in actin organisation, the changes observed in response to

cyclical hydrostatic loading are retained after the same recovery period (Knight et al. 2006). By contrast, the reduction in the number of cells with F-actin microfilaments that occurs in response to cyclic hydrostatic loading of cells in monolayer is reversible (Parkkinen et al. 1995). Intriguingly, the response in this study was shown to be proportional to the magnitude of the load applied as there was near total disappearance of F-actin following 30MPa compared with 15MPa (Parkkinen et al. 1995). A progressive disorganisation of F-actin was observed in response to static osmotic loading which eventually became detached from the cell cortex and exhibited a more central, nuclear localisation (Erickson et al. 2003; Chao et al. 2006). In contrast, dynamic osmotic loading resulted in a more uniform actin distribution throughout the cell (Chao et al. 2006). Interestingly, while dynamic osmotic loading resulted in an increase in aggrecan gene expression, static loading for the same duration reduced the expression of this gene (Chao et al. 2006).

Mechanical loading regulates the expression of numerous actin accessory proteins (Blain et al. 2002, 2003; Campbell et al. 2007; Wan et al. 2013). For example, studies in the Knight lab have observed a significant increase in the gene expression of cofilin, an actin depolymerising and severing protein, in response to cyclic mechanical loading (Campbell et al. 2007).

#### 2.2.1.2 Integrins

Integrins are heterodimeric transmembrane glycoprotein's consisting of α-subunits and β-subunits that function to connect the ECM with the cytoskeleton. Integrin receptors have a large extracellular domain which forms the ligand-binding region and interacts with the cell matrix. It is the combination of α-subunits and β-subunits which determine integrin ligand specificity (Hynes 1992). A smaller cytoplasmic domain is associated with both the actin cytoskeleton (Shyy and Chien 1997) and intracellular signalling molecules such as paxillin (Burridge et al. 1992), tensin (Bockholt and Burridge 1993) and FAK (focal adhesion kinase) (Schaller et al. 1995) which transduce mechanical signals to biochemical responses. These intracellular proteins are recruited to the receptor upon ligand binding and receptor clustering. They promote association of the receptor with the actin cytoskeleton; intimately connecting it to the ECM which ultimately leads to the formation of actin stress fibres and

focal adhesions (Otey and Burridge 1990; Hildebrand et al. 1995; Millward-Sadler and Salter 2004). Actin remodelling promotes further integrin clustering and protein recruitment facilitating intracellular signalling by concentrating signalling molecules in one place and improving reaction kinetics (Millward-Sadler and Salter 2004).

Articular chondrocytes express several different integrin isoforms, the most notable of which is α5β1 which is extensively expressed in the chondrocyte plasma membrane and primary cilium (Wright et al. 1997; McGlashan et al. 2006). Disruption of α5β1 signalling with specific function blocking antibodies, or RGD (Arg-Gly-Asp) containing peptides blocks chondrocyte membrane hyperpolarisation in response to cyclic strain and inhibits the mechanical induction of proteoglycan synthesis (Wright et al. 1997; Holledge et al. 2008).

#### 2.2.1.3 Mechanosensitive ion channels

Intracellular $Ca^{2+}$ is a ubiquitous second messenger that triggers changes in cell metabolism, proliferation and differentiation in response to a plethora of different intra and extracellular signals (for review see (Bootman et al. 2001)). The versatility in the spatial and temporal characteristics of $Ca^{2+}$ signalling and the variations that can occur in signal amplitude are vital to the ability of this messenger to regulate diverse cellular processes.

The induction of $Ca^{2+}$ signalling in chondrocytes has been reported in response to numerous types of mechanical stimuli which include compression (Roberts et al. 2001; Fitzgerald et al. 2004; Pingguan-Murphy et al. 2005; Tanaka et al. 2005; Pingguan-Murphy et al. 2006), fluid flow (Yellowley et al. 1997; Edlich et al. 2001; Degala et al. 2012), cyclic tensile strain (Wright et al. 1996; Tanaka et al. 2005), hydrostatic loading (Browning et al. 2004; Mizuno 2005) and osmotic loading (Erickson et al. 2003; Chao et al. 2006).

In agarose culture where approximately 50% of chondrocytes exhibit $Ca^{2+}$ transients in the absence of loading (Pingguan-Murphy et al. 2005), mechanical compression has been shown to produce transient increases in intracellular $Ca^{2+}$. These transients are dependent on both the activation of $Ca^{2+}$ channels in the cell membrane and the release of $Ca^{2+}$ from intracellular stores. Both static and dynamic compression of chondrocytes in agarose culture increase the number of cells exhibiting $Ca^{2+}$ transients (Roberts et al. 2001; Pingguan-

Murphy et al. 2005; Pingguan-Murphy et al. 2006). These responses are inhibited by EGTA, an extracellular $Ca^{2+}$ chelator, and thapsigargin, which depletes $Ca^{2+}$ from intracellular stores (Roberts et al. 2001; Pingguan-Murphy et al. 2006). In these studies, the response maxima observed on static compression exhibited a highly reproducible delay, suggesting that this $Ca^{2+}$ response may not represent the initial mechanotransduction event, but rather occurs after the mechanosensitive action of stretch activated cation (SA-cat) channels or $K^{+}$ channels. Consistent with this, the $Ca^{2+}$ response was inhibited by gadolinium ($Gd^{3+}$), an SA-cat channel blocker, which has also been shown to block the mechanosensitive upregulation of proteoglycan synthesis and mechanosensitive changes in gene expression (Bavington et al. 1995; Tanaka et al. 2005).

Changes in the electrophysiology of the chondrocyte membrane have also been investigated in response to cyclic tensile strain in chondrocytes cultured in monolayer. Wright et al showed that the chondrocyte membrane becomes hyperpolarised following 20 min cyclic loading at 0.33Hz. This hyperpolarisation is frequency-dependent and is blocked by amiloride indicating it is dependent on the activation of small conductance, apamin-sensitive $Ca^{2+}$-dependent $K^{+}$ (SK) channels that trigger the efflux of $K^{+}$ ions from the cell (Wright et al. 1996). These SK channels are likely activated by a signalling cascade that begins with voltage-gated and/or SA-cat channels as hyperpolarisation could also be blocked by $Gd^{3+}$ (Wright et al. 1996). These channels have been reported to associate with integrin receptors within the plasma membrane (Wiesner et al. 2005). Consistent with a role for these receptors in mechanotransduction, the hyperpolarisation response can be blocked by cytochalsin D and RGD-containing peptides (Wright et al. 1996). Thus loading of the tissue, and the associated cell deformation would result in the influx of Na+ ions through SA-cat channels triggering an initial membrane depolarisation that leads to the activation of mechanosensitive $Ca^{2+}$ signalling.

The osmotic environment in articular cartilage is unique due to the high fixed charge density associated with the large concentration of proteoglycan in the matrix (Oswald et al. 2008). This environment can be altered by both mechanical loading and cartilage degeneration. Chondrocytes respond to changes in osmotic stress by initiating a $Ca^{2+}$ signalling cascade that results in changes in cell volume and actin organisation and alters the expression of

matrix genes such as aggrecan (Chao et al. 2006). The non-specific cation channel transient receptor potential vanilloid 4 (TRPV4) functions as an osmotic sensor in chondrocytes, inhibition or knock out of this channel abolishes these transients both *in vitro* and *in situ* (Clark et al. 2010; Hung 2010).

In chondrocytes, although TRPV4 can be found throughout the cell, it is also found within the primary cilium (Phan et al. 2009). Ciliary localisation is essential for TRPV4 function, possibly due to the distinct membrane environment in this organelle, and chemical disruption of primary cilia abolishes TRPV4 mediated $Ca^{2+}$ signalling in response to osmotic stress (Phan et al. 2009).

#### 2.2.1.4 Purinergic $Ca^{2+}$ signalling

The addition of endogenous adenosine triphosphate (ATP) to articular chondrocytes in 2D culture increases proteoglycan synthesis and stimulates the production of $Ca^{2+}$ transients similar to those observed during mechanical loading (D'Andrea and Vittur 1996; Graff et al. 2000). Several studies have reported that chondrocytes release ATP in response to mechanical loading (Millward-Sadler et al. 2004; Pingguan-Murphy et al. 2006). ATP receptors can be classified into two distinct groups, P1 and P2 which are sensitive to adenosine and ATP respectively. In agarose culture, pre-incubation with the P2 blockers suramin and basilen blue completely inhibited the increase in $Ca^{2+}$ signalling observed in response to cyclic compression identifying mechanosensitive ATP release as an important component of chondrocyte mechanotransduction (Pingguan-Murphy et al. 2006).

Three major mechanisms exist for the mechanosensitive release of ATP: (1) connexin hemi-channels (unopposed halves of gap junctions), (2) anion channels and (3) the exocytosis of ATP-filled vesicles. In astrocytes, ATP release occurs through connexin-43 (Cx43) hemi-channels in response to electrical and mechanical stimuli activating a $Ca^{2+}$ signalling response (Stout et al. 2002). Studies in the Knight lab have shown that articular chondrocytes express Cx43 channels throughout their membrane (Knight et al. 2009). Cyclic compression of chondrocytes in agarose results in hemi-channel activation and compression-induced ATP release can be inhibited by the hemi-channel blocker flufenamic

acid (Garcia and Knight 2010). These data suggest that the predominant route for mechanosensitive ATP release in articular chondrocytes is through Cx43 hemi-channels.

#### 2.2.1.5 The primary cilium

*In vivo* studies suggest a role for the primary cilium in articular cartilage maintenance. The Tg737$^{ORPK}$ mouse possesses a hypomorphic mutation in the *Ift88* gene; as a consequence of this mutation primary cilia are absent or severely truncated. In this mutant, the cellularity of the articular cartilage is increased and exhibits altered expression and distribution of collagen II (McGlashan et al. 2007). In mice harbouring mutations in several of the Bardet Biedel syndrome (BBS) proteins , the proteoglycan content of the cartilage matrix was reported to be lower and had a reduced thickness relative to wild type mice (Kaushik et al. 2009). More recently, Chang et al reported that in *Col2a-Cre;Ift88*$^{loxP/loxP}$ mice both the thickness and cellularity of the articular cartilage were higher and the expression of collagen II and aggrecan were increased in the pericellular region (Chang et al. 2012). In this study, the authors used micro-indentation to demonstrate that the mechanical properties of the cartilage formed by these mice were inferior.

Wann et al provided the first direct evidence supporting a role for the primary cilium in chondrocyte mechanotransduction (Wann et al. 2012). This study used a mutant cell line generated from the Tg737$^{ORPK}$ mouse. In wild type (WT) cells, cyclic mechanical compression triggered ATP release and activated a $Ca^{2+}$ signalling cascade which culminated in the upregulation of aggrecan gene expression and proteoglycan synthesis. However, in mutant (ORPK) chondrocytes no significant changes in aggrecan expression were observed in response to mechanical loading and proteoglycan production was not altered (Wann et al. 2012). Surprisingly, the mechanosensitive release of ATP was observed in both WT and ORPK chondrocytes, however the $Ca^{2+}$ signalling downstream of this event was disrupted in ORPK cells. This study indicated that in contrast to the role of the cilium in the kidney, the chondrocyte primary cilium does not function as a mechanosensor, but rather is essential component of the mechanotransduction response downstream of this event (Wann et al. 2012).

Intriguingly, cleavage of the PC-1 C-terminal tail is increased in IFT88$^{ORPK}$ chondrocytes lacking cilia suggesting PC-1 may have a novel function in this mechanosensory response (Wann et al. 2012).

### 2.2.2 Osteoarthritis

Osteoarthritis (OA) is a chronic degenerative disease that results in destruction of the articular cartilage and the loss of joint function. It is considered a 'whole joint' disease as multiple components of the joint are affected. In addition to cartilage degeneration, the pathological features of OA include synovial inflammation, sub-chondral bone thickening, osteophyte formation and the degeneration of ligaments in the knee and menisci. While the primary risk factor for OA is ageing, other risk factors include gender, obesity, genetic predisposition, prior joint injury and mechanical factors such as mal-alignment and abnormal joint shape.

The earliest changes in OA occur in the superficial zone of the articular cartilage, closest to the joint surface. It is here that mechanical forces are highest and where proteoglycan loss and type II collagen cleavage are first observed (Wu et al. 2002). Degradation in the deeper zones occurs as the disease progresses. During OA chondrocytes undergo a shift to a more activated phenotype in which the proliferation rate is higher resulting in chondrocyte clustering. The balance between matrix production and catabolism is disrupted and both are increased. Increased expression of catabolic enzymes, such as MMP-13 and ADAMTS-5 leads to cartilage softening and fibrillation with the eventual loss of the functional cartilage and exposure of the sub-chondral bone (Figure 2.4).

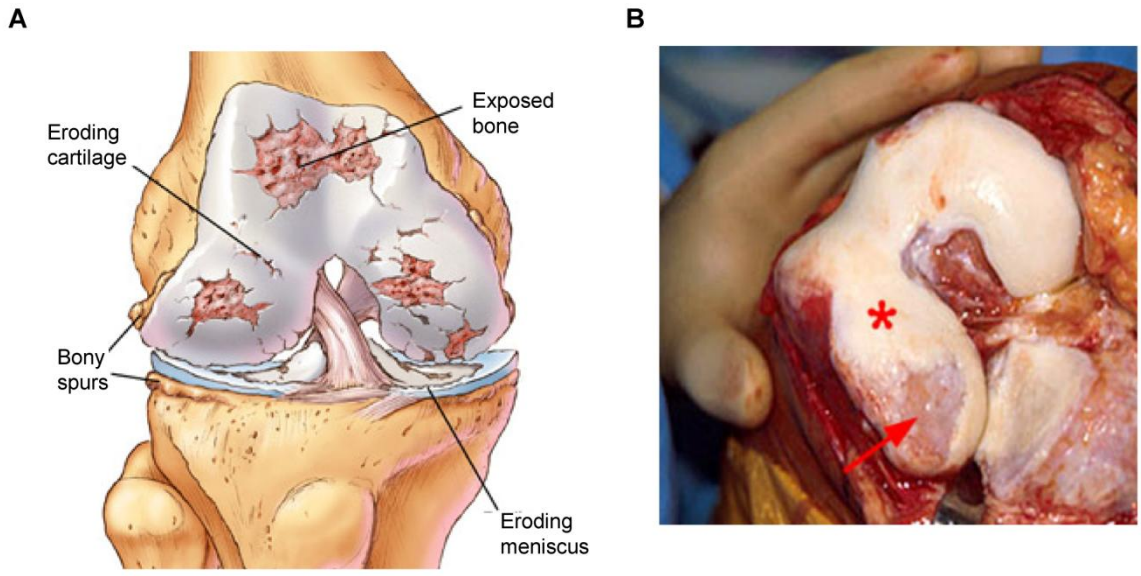


**Figure 2.4 Cartilage degeneration in OA**
**(A)** Schematic of the human knee depicting the joint damage observed in OA (taken from http://www.osteoarthritisblog.com/category/about-knee-osteoarthritis/). **(B)** Photograph of a full thickness defect in the medial compartment of the knee of a patient with OA. Pink, vascularised bone (arrow) has become exposed due to cartilage loss and is surrounded by normal cartilage (asterix). This image was taken from http://www.radsource.us/clinic/1011

The molecular mechanisms regulating the pathogenesis and progression of OA, are poorly understood, as a result there are currently no pharmacological agents that can completely prevent this disease. The discovery that isolated OA chondrocytes are unable to respond to mechanical signals in the same way as normal chondrocytes implies a defect exists in the ability of these cells to either sense mechanical signals or transduce them to a functional response (Poole 1997; Millward-Sadler et al. 2000; Millward-Sadler et al. 2004; Holledge et al. 2008; McGlashan et al. 2008; Chang et al. 2009; Lin et al. 2009). Such changes are likely to be important for the aetiology of the disease.

## 2.3 Primary cilia in articular cartilage

The majority of articular chondrocytes exhibit a primary cilium (Wislman and Fletcher 1978; Meier-Vismara et al. 1979; Poole et al. 1985; Poole et al. 2001; McGlashan et al. 2007; McGlashan et al. 2008; McGlashan et al. 2010; Wann et al. 2012). The cilium is found in a juxta-nuclear position in close association with the trans-face of the Golgi apparatus (Figure 2.5). This has led to the suggestion that a potential relationship exists between the cilium and the direction of cellular secretion of ECM components and/or the maintenance of cellular shape through the regulation of cytoskeletal microtubules (Poole et al. 1985; Poole et al. 1997).

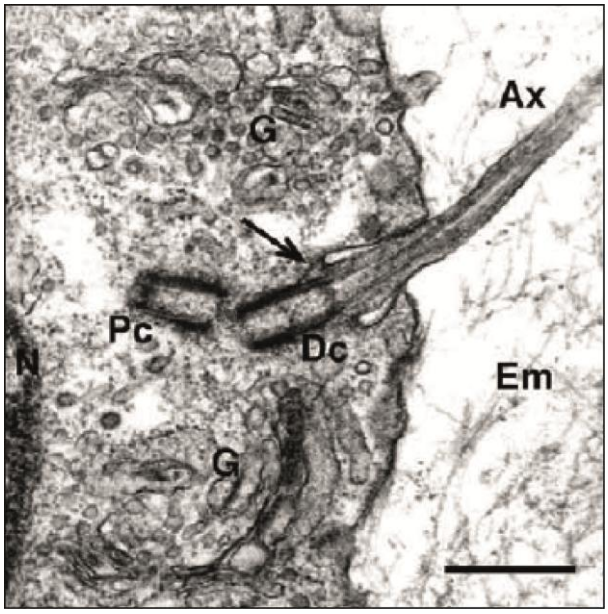


**Figure 2.5 The Golgi-cilium continuum**
Electron micrograph of chondrocyte primary cilium in chick sterna cartilage demonstrating the structural relationship between the extracellular matrix (Em), the ciliary axoneme (Ax), the distal (Dc) and proximal (Pc) centrioles, the Golgi apparatus (G) and the nucleus (N). The distal centriole acts as the basal body of the cilium. Arrow=transitional fibre. Bar=500 nm. Image taken from (Jensen et al. 2004).

The prevalence and length of chondrocyte primary cilia varies with cartilage depth (McGlashan et al. 2008). In bovine patellae, less than 40% of cells in the superficial zone exhibit a primary cilium with a mean length of 1.1µm (McGlashan et al. 2008). This increases to 65% in the deep zone and mean cilia length in this zone is 1.5µm (McGlashan et al. 2008). In the mouse femoral head, cilia length has also been reported to vary between condyles such that primary cilia are longer on the medial than the lateral condyle (Rich and Clark 2012). Subtle variations across the surface of a condyle were also reported in this study as cilia length was typically greatest on the medial surface of each individual condyle (Rich and

Clark 2012). That cilia length is lowest in the superficial zone where cells experience the greatest levels of compressive strain (Guilak et al. 1995) suggests a relationship exists between cilium length and mechanical loading. In line with this, prolonged cyclic compression of chondrocytes *in vitro* has been shown to trigger dramatic cilium disassembly (McGlashan et al. 2010).

Furthermore, several studies have also reported zonal variations in cilia orientation and positioning (Wilsman 1978; Poole et al. 1985; McGlashan et al. 2007; McGlashan et al. 2008; Farnum and Wilsman 2011). Primary cilia in the middle and deep zones are frequently found on the medial or lateral surface of the cell, with respect to the articular surface, or between two cells in a chondron (McGlashan et al. 2008; Farnum and Wilsman 2011). While in the superficial zone cilia are almost exclusively found pointing away from the articular surface (McGlashan et al. 2008; Farnum and Wilsman 2011). Orienting the cilium in this way is proposed to shield it from the compressive forces applied to the articular surface on joint loading. Consistent with this theory, these trends in cilia orientation were shown to be more pronounced in load bearing regions compared with regions that experience little to no mechanical load. Moreover, in osteoarthritic cartilage, where the mechanical environment of the chondrocyte is disrupted, primary cilia within cell clusters will orient toward the centre of the cluster (McGlashan et al. 2008).

Chondrocyte primary cilia are often at least partially invaginated within a ciliary pocket (Farnum and Wilsman 2011; Rich and Clark 2012). However, the region that does project out from the cell has been observed to interact intimately with the collagen fibres and proteoglycan aggregates of the ECM (Jensen et al. 2004; McGlashan et al. 2006). A number of ultra structural studies in cartilage have shown the axoneme is deformed through a range of angles *in situ* when it is surrounded by matrix (Wilsman 1978; Poole et al. 1985; Poole et al. 2001; Jensen et al. 2004) and several ECM receptors have been shown to localise to the ciliary membrane, namely α2, α3 and β1 integrins and NG2 (McGlashan et al. 2006).

## 2.4 Hedgehog signalling and primary cilia in cartilage development and disease

Hedgehog signalling plays an essential role in the patterning and development of the skeleton. While Shh functions in the early stages of skeletal patterning, Ihh acts somewhat later and is an essential regulator of endochondral bone formation. Consequently, many ciliopathies are characterised by skeletal abnormalities such as polydactyly, cleft lip/palate and skeletal dysplasia (Badano et al. 2006; Tobin and Beales 2009; Waters and Beales 2011; Bergmann 2012).

### 2.4.1 Hedgehog proteins in skeletal development

Limb development begins with a structure called the limb bud which occurs at a discrete position within the embryo called the limb field. The limb bud is formed by mesenchymal cells from the somatic layer of the lateral plate mesoderm which proliferate and accumulate beneath the ectodermal tissue (Figure 2.6) (Gilbert 2006). The ectodermal tissue over the limb bud forms a structure called the apical ectodermal ridge (AER). This is a major signalling centre for the developing limb (Figure 2.6B). It maintains the cells beneath it in a state of mitotic proliferation, establishing the proximal-distal axis and allowing proper outgrowth of the limb (Gilbert 2006; Haycraft et al. 2007). The patterning of the anterior-posterior axis (from thumb to little finger) is defined by a region of Shh expressing mesodermal tissue called the Zone of Polarising Activity (ZPA) (Figure 2.6B). Shh is released from the cells of the ZPA and forms a protein gradient along the anterior-posterior axis. This patterns the development of the five digits by inhibiting the processing of the Gli3 transcription factor to its repressor form leading to the de-repression of hedgehog target genes such as the BMP-antagonist gremlin (Litingtung et al. 2002). Digit specification is dependent on the length of exposure to Shh, shorter periods of exposure dictate formation of anterior digits whilst longer exposure formation of posterior digits (Gilbert 2006).

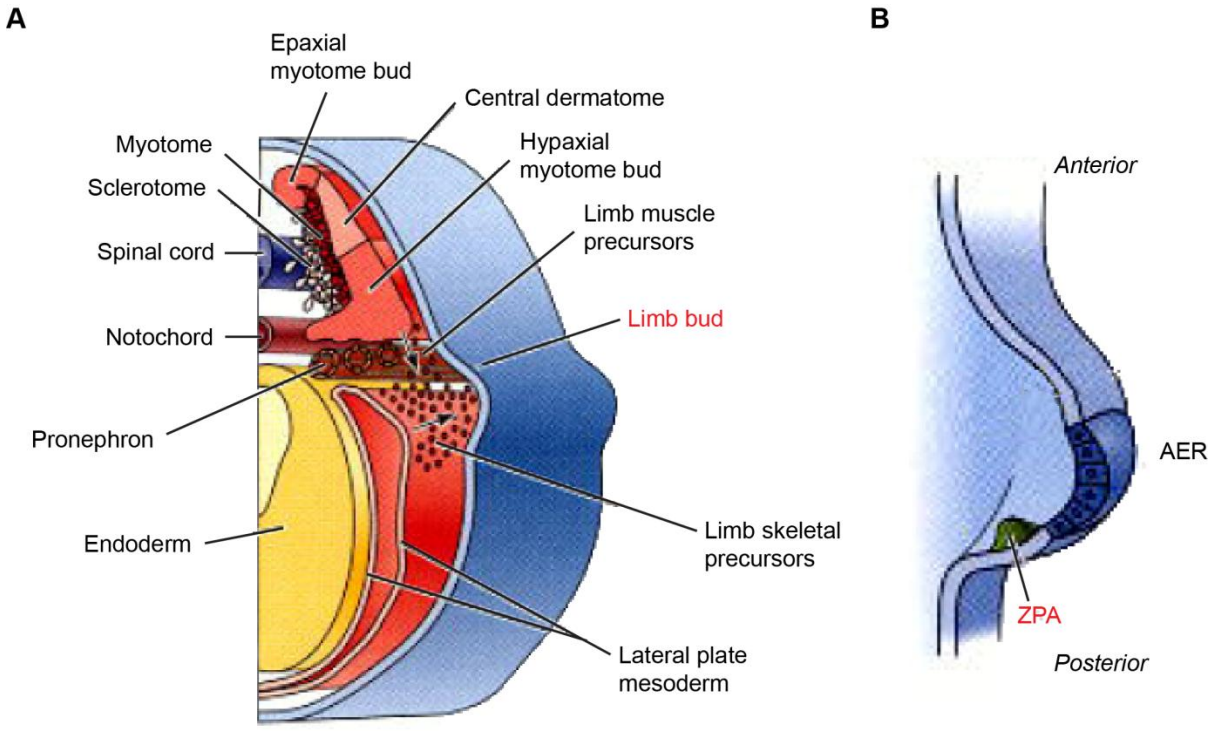


**Figure 2.6 Development of the limb bud**
**(A)** Mesenchymal stem cells from the lateral plate mesoderm proliferate causing the limb bud to bulge outwards. **(B)** The overlying ectoderm of the limb bud forms a structure called the AER which runs along the distal margin of the limb and regulates proximal-distal patterning. The ZPA is formed by a population of Shh-secreting cells at the posterior junction (figure adapted from (Gilbert 2006)).

Hedgehog signalling is also required for proper formation of the appendicular skeleton which occurs via a process called endochondral ossification (Vortkamp et al. 1996; St-Jacques et al. 1999; Razzaque et al. 2005). This process begins with the condensation of mesenchymal precursor cells which differentiate into chondrocytes forming a cartilage anlagen, or template for the future bone (see Figure 2.7 for an overview of this process). Within the cartilage anlagen there are two distinct chondrocyte subpopulations, the distal chondrocytes at the epiphyses of the skeletal elements and the columnar, proliferating chondrocytes at the centre. At the periphery, the developing cartilage is surrounded by a thin layer of fibroblastic cells called the perichondrium. When the developing skeletal element reaches a certain size the columnar chondrocytes at the centre of the anlagen exit the cell cycle and undergo terminal differentiation first becoming pre-hypertrophic then hypertrophic. These hypertrophic cells secrete a distinct matrix that becomes progressively

calcified. Coincident with chondrocyte differentiation, the perichondrial cells flanking this region differentiate into osteoblasts and form the bone collar, or periost. Vascular invasion occurs in response to factors secreted by the hypertrophic cells and consequently osteoblasts migrate into the calcified matrix and replace the cartilage template with bone thus forming the primary ossification centre. Proliferating chondrocytes become increasingly restricted to the epiphyses of the developing skeletal elements as longitudinal growth occurs such that when secondary ossification centres form during post natal development the region of growth becomes confined to the epiphyseal, or growth plate [For review see (Olsen et al. 2000; Lai and Mitchell 2005)].

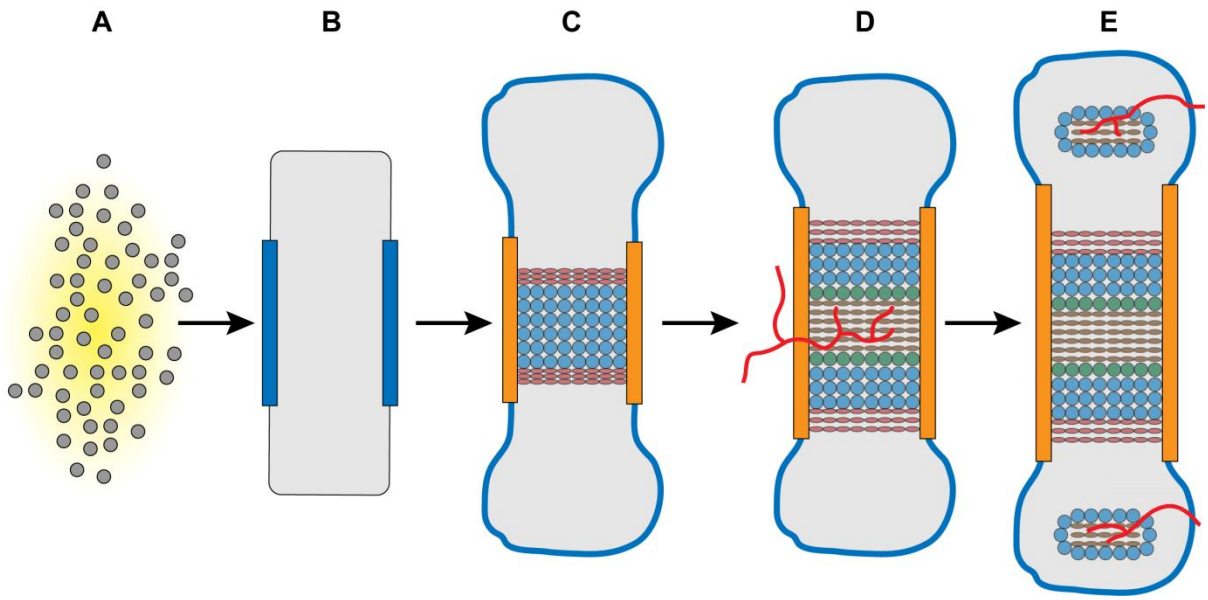


**Figure 2.7 Endochondral ossification**
**(A)** Mesenchymal precursors condense and differentiate into chondrocytes. **(B)** A cartilage template is formed surrounded by the perichondrium. **(C)** The cells at the centre of the template differentiate to pre-hypertrophic chondrocytes (red) and hypertrophic chondrocytes (blue) and form a calcified matrix. These cells release factors that trigger osteoblastic differentiation in the perichondrium and the formation of the bone collar (orange). **(D)** Hypertrophic cells undergo apoptosis and blood vessels invade the calcified matrix and initiate formation of the primary ossification centre. **(E)** Secondary ossification centres form within the zone of the distal chondrocytes during post natal development restricting chondrocyte proliferation and differentiation to the epiphyseal growth plates. Figure adapted from (Wuelling and Vortkamp 2010).

Ihh plays a key role in endochondral bone formation; it coordinates both chondrocyte proliferation and differentiation but is also required for osteoblast differentiation in the perichondrium (Vortkamp et al. 1996; St-Jacques et al. 1999). Mutations in the *Ihh* gene have been linked to two inherited skeletal disorders: brachydactyly type A-1 (Gao et al. 2001) and acrocapitofemoral dysplasia (Hellemans et al. 2003).

Ihh is produced by pre-hypertrophic and early hypertrophic chondrocytes. It regulates hypertrophic differentiation through the formation of a negative feedback loop with parathyroid hormone related peptide (PTHrP; Figure 2.8). Ihh induces the expression of PTHrP in the peri-articular perichondrium which inhibits hypertrophic differentiation (Vortkamp et al. 1996; Razzaque et al. 2005). The highest levels of the PTH/PTHrP receptor are found in proliferating chondrocytes thus PTHrP maintains these cells in a proliferative state. Loss of PTHrP, or the PTH/PTHrP receptor, results in premature differentiation in the growth plate (Karaplis et al. 1994; St-Jacques et al. 1999; Maeda et al. 2009). Conversely, PTHrP over expression delays hypertrophy and bone formation to such an extent that mutant mice are born with a completely cartilaginous skeleton (Weir et al. 1996; St-Jacques et al. 1999). The level of Ihh and PTHrP signalling determines the distance from the joint at which hypertrophic differentiation takes place. When pre-hypertrophic cells commit to the hypertrophic state, Ihh expression is switched off. Consequently, PTHrP levels are reduced and another layer of proliferating chondrocytes will commit to differentiation. This process occurs in a cyclical manner maintaining the balance between growth and ossification in the developing bone (Figure 2.8). It continues in the cartilage growth plates during postnatal development until growth plate closure at skeletal maturity (Vortkamp et al. 1998).

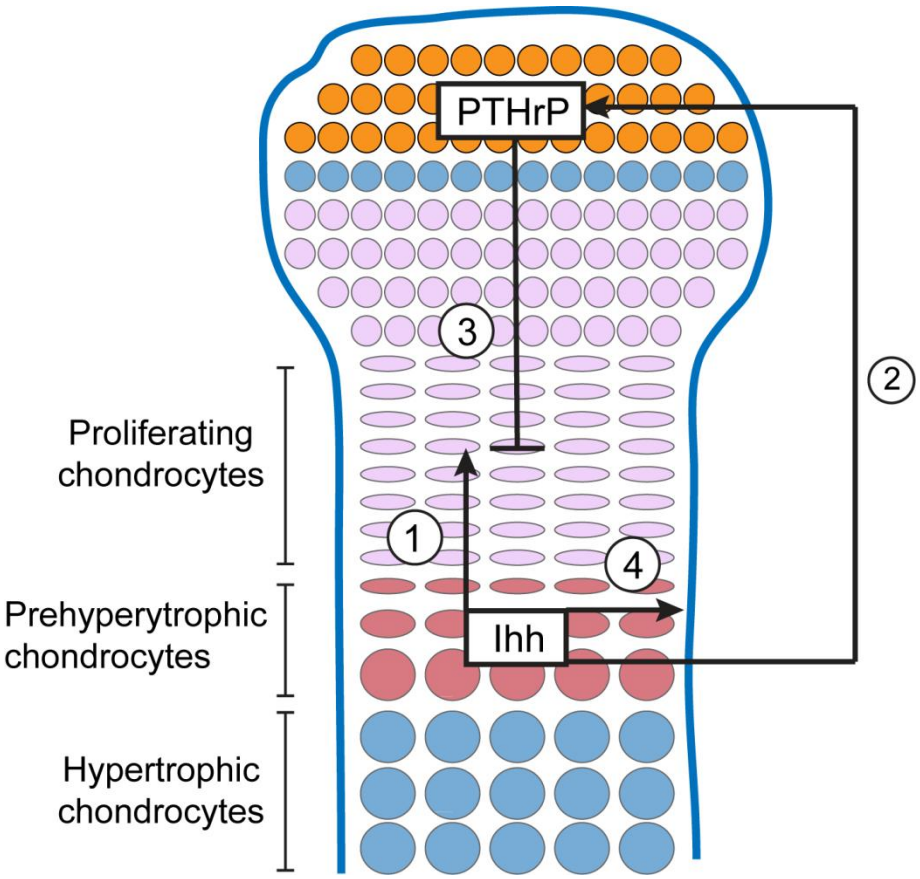


**Figure 2.8 The Ihh/PTHrP feedback loop**
Pre-hypertrophic chondrocytes secrete Ihh which acts on chondrocytes directly to promote proliferation and differentiation (1). Furthermore it stimulates cells in the peri-articular region to secrete PTHrP (2), however the mechanism for this is poorly understood. PTHrP acts on cells in the proliferating zone to inhibit differentiation (3). When the source of PTHrP is sufficiently distant, the cells of the proliferative zone initiate the differentiation process first becoming pre-hypertrophic cells that secrete Ihh. Additionally, Ihh acts on perichondrial cells to promote their differentiation and formation of the bone collar (4). Adapted from (Kronenberg 2003).

### 2.4.2 Evidence supporting a role for the cilium in cartilage development

A role for the cilium in limb patterning was first demonstrated in mice harbouring a hypomorphic mutation in the *Ift88*/polaris/Tg737 gene ($Tg737^{ORPK}$). Null mutations in *Ift88* result in mid-gestation lethality, these mice exhibit early neural tube closure and patterning defects such as randomisation of the left-right body axis and polydactyly (Pazour et al. 2000). Due to the lethal nature of cilia disruption, hypomorphic $Tg737^{ORPK}$ mutant mice

were generated. These mice are viable and exhibit hydrocephalus, cyst formation in the liver, pancreas and kidneys and similarly have skeletal patterning defects that include extra molar teeth, cleft palate, and preaxial polydactyly (Moyer et al. 1994; Pazour et al. 2000; Yoder et al. 2002; Zhang et al. 2003).

To further investigate the role of the cilium in skeletal development, Haycraft et al used Cre-mediated deletion of *Ift88* to disrupt primary cilia in the limb mesenchyme using the *Prx1* promoter to drive Cre expression. Consequently primary cilia were lost from the developing cartilage and perichondrium. *Prx1-Cre;Ift88*$^{loxP/loxP}$ mice exhibit extensive polydactyly with the formation of up to 8 un-patterned digits (Haycraft et al. 2007). By contrast, *Shh*-null mice exhibit syndactyly (Chiang et al. 2001). Polydactyly arises in this mutant as the processing of the Gli3 repressor is disrupted leading to the aberrant de-repression of gene expression (Haycraft et al. 2005; Liu et al. 2005). Interestingly, conditional deletion of *Ift88* in the ectoderm using *Msx1*-Cre had no overt effects on skeletal patterning and limb outgrowth suggesting that cilia function is only required to direct proper antero-posterior patterning (Haycraft et al. 2007).

In addition to limb patterning defects, *Prx1-Cre;Ift88*$^{loxP/loxP}$ and *Prx1-Cre;Kif3a*$^{loxP/loxP}$ mice exhibit defects in embryonic endochondral bone formation as the length of the developing long bones is dramatically reduced (Haycraft et al. 2007). This phenotype occurs due to accelerated chondrocyte hypertrophy and a delay in the formation of the primary ossification centre and is reminiscent of germ line *Ihh*-deletion (St-Jacques et al. 1999; Haycraft et al. 2007). Consistent with the disruption of hedgehog signalling, the expression of Ptc1 and Gli1 was reduced in both chondrocytes and perichondrial cells in these mice (Haycraft et al. 2007). By contrast, *Col2a-Cre;Ift88*$^{loxP/loxP}$ and *Col2a-Cre;Kif3a*$^{loxP/loxP}$ mutants develop normally and do not exhibit alterations in embryonic bone formation despite the fact that the number of ciliated cells in the developing cartilage is dramatically reduced as early as embryonic day 15.5 (Song et al. 2007). This difference is accounted for by the inability of Col2a-Cre to efficiently target the perichondrium, thus the Ihh-PTHrP feedback loop remains intact. However, alterations in the organisation of the growth plate were observed 7-10 days after birth in *Col2a-Cre; Ift88*$^{loxP/loxP}$ mutants indicating a role for the cilium in post-natal development. Chondrocyte proliferation was reduced and the columnar

organisation of the growth plate disrupted. Moreover, chondrocyte hypertrophy was accelerated resulting in early growth plate closure and severe post-natal dwarfism (Song et al. 2007). Intriguingly it is at this time that the mice are becoming active and their joints subjected to significant mechanical load.

The function of the cilium in post natal cartilage is complex. McGlashan et al have shown that at post natal day 4 (P4), the *Tg737*$^{ORPK}$ hypomorphs have shortened limbs due to a *delay* in hypertrophic differentiation (McGlashan et al. 2007). While this difference might reflect the differences between hypomorphic and null alleles, it could also be due to the systemic effects of the germ line *Ift88* mutation.

### 2.4.3 Hedgehog signalling in osteoarthritis

The development of osteoarthritis is associated with a recapitulation of the events that occur during endochondral ossification suggestive of a role for hedgehog signalling in the aetiology of this disease. Chondrocytes start to proliferate and form clusters; they change their expression profile and begin expressing hypertrophic markers such as collagen type X, ADAMTS-5 and MMP-13. Moreover, an increase in calcification is observed throughout the joint while the tissue surface becomes fibrillated and cracked as it is degraded until eventually the cartilage is completely lost and the subchondral bone exposed [for review see (Dreier 2010)].

Several *in vitro* and *in vivo* studies have shown that the expression of Ihh is regulated by mechanical stimuli during skeletal development (Wu et al. 2001; Ng et al. 2006; Nowlan et al. 2008; Shao et al. 2011). However, the mechanosensitivity of this pathway has not been examined in adult chondrocytes. In osteoarthritic cartilage, the mechanical environment of the chondrocyte is altered (Braman et al. 2005; Gratz et al. 2008) and an increase in Ihh expression has been observed in early cartilage lesions (Tchetina et al. 2005). One suggestion therefore is that hedgehog signalling is mechanosensitive in articular cartilage such that signalling is increased in OA.

In 2009, Lin et al provided the first evidence that hedgehog signalling is activated in OA and promotes cartilage degeneration (Lin et al. 2009). This study, published in Nature Medicine,

examined the expression of downstream hedgehog markers in cartilage samples from patients undergoing total knee arthroplasty. Significant pathway activation was observed and correlated with the severity of the disease phenotype. In this seminal paper, the authors showed that activated hedgehog signalling drives the expression of ADAMTS-5, and thus cartilage degradation, through the regulation of the RUNX-2 transcription factor (Lin et al. 2009). Remarkably, both pharmacological and genetic inhibition of hedgehog signalling attenuated disease severity in the destabilisation of the medial meniscus (DMM) mouse model highlighting the potential of this pathway as a therapeutic target (Lin et al. 2009). Subsequent studies have found that the expression of Indian hedgehog is increased in human OA by almost 3-fold, with a 37% increase in protein content reported in the synovial fluid (Wei et al. 2012). This study showed that hedgehog signalling promotes chondrocyte hypertrophy and the expression of MMP-13 (Wei et al. 2012). More recently, Ruiz-Heiland et al identified a role for hedgehog signalling in osteophyte formation, a common component of rheumatoid arthritis suggesting a link between hedgehog and inflammatory signalling (Ruiz-Heiland et al. 2012).

A growing number of studies have implicated cilia dysfunction in cartilage degeneration and the development of OA (McGlashan et al. 2008; Kaushik et al. 2009; Chang et al. 2012; Wann and Knight 2012). McGlashan et al first reported that the incidence and length of primary cilia increased at the articular surface in osteoarthritic cartilage. The proportion of ciliated cells was increased from 38% in healthy tissue to 68% in severely diseased samples. Additionally cilia on osteoarthritic chondrocytes had a mean axoneme length of 1.4 µm compared to 1.1 µm in healthy cells, an increase of 21% (McGlashan et al. 2008). This was suggested to result from a change in the mechanical properties of the cartilage as previous studies had shown that mechanical stimuli could modulate cilia length in other cell types (Iomini et al. 2004; Resnick and Hopfer 2008). Later reports that pathological stimuli including mechanics and inflammatory cytokines influence cilia length support the hypothesis that it is the changes in a chondrocytes cellular microenvironment that influence this organelle (McGlashan et al. 2010; Wann and Knight 2012). However, as discussed in section 2.3, cilia prevalence and length increase with cartilage depth therefore the changes observed in OA could also be caused by a loss of the superficial zone tissue rather than an

active lengthening. Whether an active increase in ciliation or not, the net effect on cell signalling will likely be the same.

Given the importance of the primary cilium in hedgehog signalling, one might hypothesise that the increased pathway activity observed in this disease is linked to changes in primary cilia structure. Kaushik et al provided the first tangible link between alterations in ciliary structure and cartilage degeneration in OA when they reported cartilage abnormalities in the joints of BBS mutant mice (Kaushik et al. 2009). However, this observation was confounded by the fact that these mice were obese therefore it was unclear whether cartilage defects resulted from the increased mechanical load associated with this pathology. The subsequent discovery that the cilium is required for chondrocyte mechanotransduction (see section 2.2.1.5), indicates that both these factors are likely to contribute to the abnormalities reported in this study.

More recently, Chang et al have used Col2aCre;Ift88$^{fl/fl}$ transgenic mice to study the relationship between ciliary structure and function (Chang et al. 2012). They showed that articular chondrocytes in these mice do not form primary cilia which results in aberrant hedgehog pathway activation due to the loss of the Gli3 repressor and the development of symptoms of early arthritis. Although cilia are longer in OA, this study provides a proof of principle that structural changes in cilia can affect cartilage health through the regulation of hedgehog signalling.

## 2.5 Thesis aims and objectives

Alterations in primary cilia structure have been reported for a number of pathologies and are hypothesised to influence cilia mediated signalling pathways such as hedgehog. Within the last decade a handful of studies have linked the aberrant activation of hedgehog signalling to the development and progression of OA. Most recently Chang et al have demonstrated that the modulation of ciliary structure increases the susceptibility of articular cartilage to damage. The aim of this thesis was to investigate the effects of biophysical stimuli on chondrocyte primary cilia structure and function with a particular focus on hedgehog signalling. To complete this work, I have developed various tools to influence cilium length and examined the effects that cilia disassembly has on this signalling pathway. Moreover, I have explored the mechanisms of ciliary resorption in response to extracellular stress in the form of mechanics and temperature.

Studies have shown that hedgehog signalling is mechanosensitive during skeletal development (Wu et al. 2001; Ng et al. 2006; Nowlan et al. 2008). However there is a lack of evidence to support a role for this signalling pathway in adult cells. Therefore the first objective of this thesis was to examine the responsiveness of articular chondrocytes isolated from healthy adult tissues to hedgehog ligand stimulation. The second objective was to develop a mechanical loading model which was used to explore the effect of mechanical strain on this pathway.

The majority of chondrocytes exhibit a cilium the length and prevalence of which is influenced by mechanical stimuli. Moreover, primary cilia length and prevalence is lowest in the superficial zone where chondrocytes are subjected to the highest levels of mechanical stress. Therefore the third objective of this thesis was to investigate the relationship between mechanical loading and changes in ciliary structure.

Cilia disassembly in response to environmental cues is hypothesised to function as a negative feedback mechanism to modulate cilia mediated signalling. The fourth objective of this thesis was therefore to investigate the relationship between cilia structure and function

by examining how ciliary resorption in response to mechanical strain and elevated temperature influences hedgehog signalling.

# CHAPTER 3

# Materials and methods

# 3.1 Cell culture models

## 3.1.1 Isolation and culture of primary bovine chondrocytes

Bovine metacarpalphalangeal joints from adult steers (18-24 months) were obtained from an abbatoir (Humprheys, Chelmsford) within six hours of slaughter. On arrival joints were thoroughly washed to remove any attached debris and immersed in disinfectant (Virkon) for 5min, followed by 15min in 70% industrial methylated spirits (IMS). The joint was opened under sterile conditions and the cartilage removed (Figure 3.1).

To open the joint; a transverse cut was made along the fetlock from the start of the hide along the length of the foot using a no.20 scalpel blade. This was followed by a second longitudinal cut made below the joint near the hoof, which allows the hide to be peeled back exposing the joint capsule. A no.11 scalpel blade was then inserted into the joint and used to cut across the ligaments freeing the joint and exposing the cartilage (Figure 3.1A). Full-depth slices of articular cartilage were dissected from the proximal surface of the joint and finely diced (Figure 3.1B). The tissue was then incubated on rollers for 1 hour at 37°C in 10ml pronase solution (type E, 700 units/ml). Following pronase treatment, the cartilage was incubated with 30 ml of collagenase (type IX, 100 units/ml) for up to 16 hours at 37°C. Both enzyme solutions were prepared in low glucose Dulbecco's Modified Eagles Medium (DMEM) supplemented with 10% (v/v) fetal calf serum (FCS), 1.92mM L-glutamine, 96µg/ml penicillin, 96U/ml streptomycin, 19.2 mM HEPES buffer, and 0.76µM L-ascorbic acid (hereafter referred to as DMEM + 10% FCS). The resulting cellular digest was passed through a 70-µm filter then centrifuged at 733xg for 5min on an ALC multispeed PK131 centrifuge and the cell pellet re-suspended in 20ml DMEM + 10% FCS. Cell viability and concentration were subsequently assessed using a Trypan Blue dye exclusion assay (see section 3.3.1).

The cell suspension was plated onto either glass coverslips coated for 3hr with FCS at 37°C, or onto elastic membranes (Dunnlab, Germany) coated with collagen type I (100µg/ml; Sigma, UK). Cultures were maintained at 37$^{o}$C in a humidified atmosphere with 5% $CO_2$ for 6 days prior to further experiments and culture medium was changed every 2-3 days (Figure 3.1C).

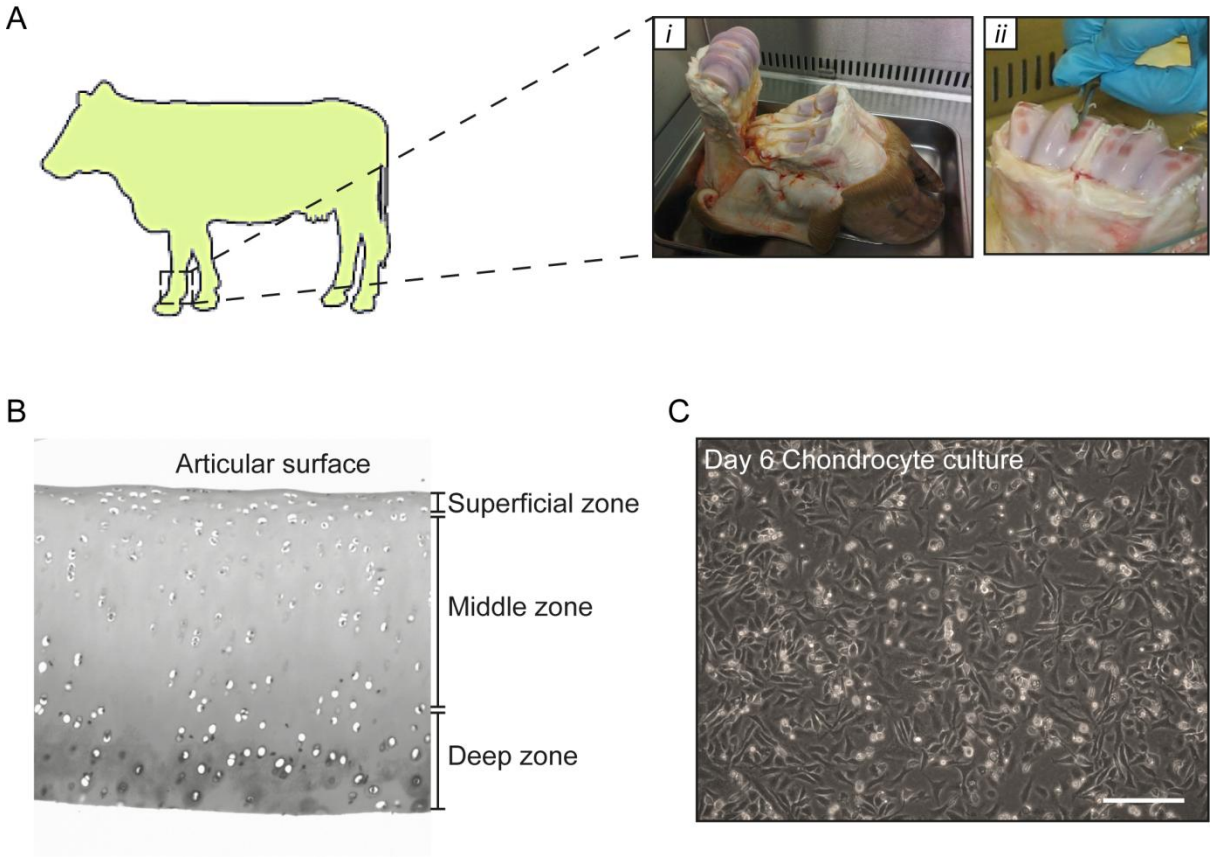


**Figure 3.1 Isolation and culture of primary bovine chondrocytes**
**(A)** Articular cartilage was dissected from the proximal surface of the bovine metacarpal phalangeal joint (red box). The joint was opened under sterile conditions **(i)** and full depth slices of cartilage removed for digestion **(ii)**. **(B)** Image of full depth cartilage stained with saffranin O showing all three zones collected during isolation. **(C)** 2D-culture of bovine articular chondrocytes (6 days in culture). Scale bar=200µm.

### 3.1.2 Tg737$^{ORPK}$ mouse immortalised chondrocyte cell line culture

An immortalised Tg737$^{ORPK}$ mouse chondrocyte cell line was used to study the loss of cilia function. These cells possess a hypomorphic mutation in the *Ift88* gene, encoding IFT88/Polaris, a complex B protein and a key component of the IFT machinery. As a consequence of this mutation, cilia are either absent or severely truncated in these cells (Wann et al. 2012).

Homozygous *Tg737$^{ORPK}$* mutant mouse lines were a gift from Courtney Haycraft and were generated as described previously (Moyer et al. 1994; Yoder et al. 1997). Briefly, heterozygous Oak Ridge polycystic kidney (ORPK) mice were bred with heterozygous

immortomouse mice (H-2Kb-tsA58), which harbour a temperature-sensitive SV40 large T-antigen transgene under the control of an interferon-ɣ-inducible H-2Kb promoter (H-2Kb-tsA58) generating *orpk/immortomouse* compound heterozygous mice (Jat et al. 1991). Heterozygous ORPK females were bred with heterozygous *orpk/immortomouse* males. Mice were maintained on a mixed genetic background according to approved protocols at the Medical University of South Carolina. All mice were genotyped by PCR from tail biopsy DNA.

Chondrocytes were isolated from the sterna of 4 day old mice by digestion with collagenase type II (2 mg/ml) at 37°C for 4 hours. Isolated chondrocytes were cultured under permissive conditions in DMEM supplemented with 10% FCS, 96µg/ml penicillin, 96U/ml streptomycin, 2.5mM L-glutamine and 10ng/ml INF-ɣ (Invitrogen) and maintained at 33°C. Western blot analysis was conducted to confirm the expression of SV40 large T antigen in chondrocytes (Wann et al. 2012).

For experiments, chondrocytes were trypsinised then plated at 50,000cells/$cm^2$ onto serum coated glass coverslips or elastic membranes and cultured at 33°C for 24hrs. They were then washed and cultured for 4 days under non-permissive condition in the absence of IFN-ɣ at 37°C ensuring expression of the SV40 antigen is switched off prior to experimentation.

### 3.1.3 NIH3T3 mouse fibroblast culture

NIH3T3 mouse fibroblasts (American Type Culture Collection) were cultured in high glucose DMEM supplemented with 10% (v/v) FCS and 96µg/ml penicillin, 96U/ml streptomycin at 37°C, 5% $CO_2$. Cells were seeded at a density of 30,000 cells/$cm^2$ onto serum coated glass coverslips or plastic culture dishes and cultured for 24 hours until approximately 70-80% confluency, they were then transferred to serum free medium for a further 20-24 hours to induce growth arrest and promote ciliation prior to experimentation.

## 3.2 Tissue/animal models

### 3.2.1 Cartilage explant isolation and culture

Bovine metacarpal phalangeal joints were obtained, and dissected under sterile conditions as described in section 3.1.1. Full-depth tissue explants were taken from the proximal surface of the metacarpal phalangeal joint using a circular dermal punch with a 5mm diameter (Miltex, York, PA, USA). The circular explants were cut out by slowly rotating the dermal punch down through to the subchondral bone then removed with a no.11 scalpel blade. Explants were immediately placed into serum free DMEM and incubated at 37°C in 5% $CO_2$. After 48 hours, explants were weighed and placed in 1 ml of fresh DMEM in separate wells prior to experiments.

### 3.2.2 Zebrafish Care and maintenance

Zebrafish (*Danio rerio*) were bred and raised in-house at the zebrafish facility of Queen Mary, University of London, UK. Embryos were collected by natural spawning and staged according to Kimmel and colleagues (Kimmel et al. 1995) given in the text as hours post fertilisation (hpf), the standard developmental time at 28.5°C. Embryos were maintained in embryo medium (13.7 mM NaCl, 0.54mM KCl, 25.2µM $Na_2HPO_4$, 44.1µM $KH_2PO_4$, 1.3mM $CaCl_2$, 1mM $MgSO_4$, 10mM HEPES, 4–5 drops Methylene Blue, pH 7.2) and all subsequent manipulations were performed in embryo medium unless stated otherwise.

Work on zebrafish embryos (prior to independent feeding) is exempt under the U.K. Animals (Scientific Procedures) Act 1986 and does not require ethical approval.

## 3.3 General methods

### 3.3.1 Trypan Blue dye exclusion assay

Following isolation/passage cells were thoroughly mixed by pipetting, a 20μl aliquot was removed and mixed with an equal volume of trypan blue (Sigma Aldrich) to assess viability. The mixture was applied to a haemocytometer and the cells were counted and visually examined at x10 magnification to determine whether cells take up or exclude the dye. Trypan blue dye cannot traverse the membrane of live cells, therefore a viable cell will have a clear cytoplasm whereas a non-viable cell will have a blue cytoplasm. Viability was expressed as the % of trypan blue negative cells and typically ranged between 95-100% for a healthy cell suspension.

### 3.3.2 DNA quantification

DNA was quantified using Hoechst 33342 fluorescence primarily as a means to assess cell proliferation (Kim et al. 1988). Hoescht 33342 is cell-permeable fluorescent dye used to stain DNA, it has an excitation/emission spectra of 350/460nm (Figure 3.2A) It binds to the minor groove of double stranded DNA with a preference for sequences rich in adenine and thymine and can be used to measure changes in total cell number.

Culture media and cellular digests were assayed with 1μg/ml Hoechst 33342 prepared in phosphate buffered saline (PBS). A DNA standard was prepared from calf thymus Type XV DNA (Sigma-Aldrich) in the appropriate medium for the sample being assayed and ranged from 0 to 20μg/ml. Briefly, 100μl of sample/standard was pipetted into a 96-well plate (Nunc Maxisorp® flat bottom, Fisher Scientific), mixed with an equal volume of Hoechst 33342 and the fluorescence at 460nm read on a Fluostar Galaxy spectrophotometer (BMG Labtech, UK).

In addition to measuring changes in cell proliferation, this assay was also used to normalise sGAG release and to monitor cell detachment following the application of cyclic tensile strain (see section 3.6).

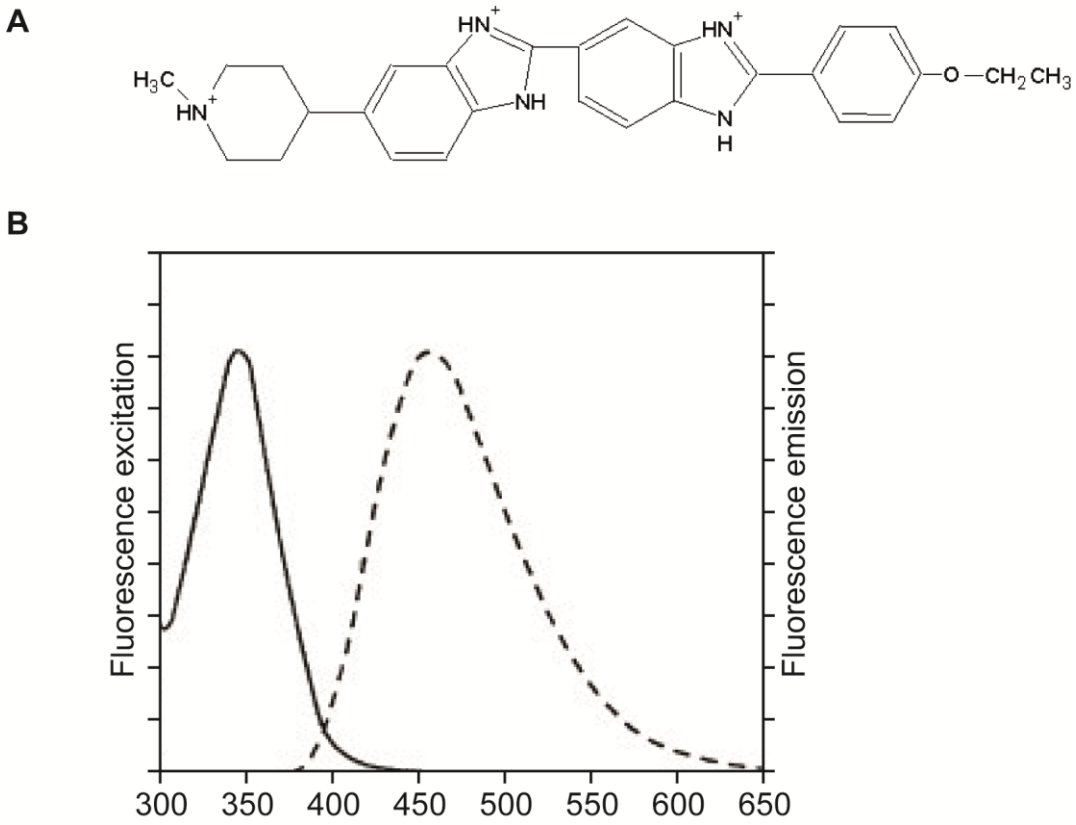


**Figure 3.2 Hoescht 33342 structure and excitation/emission spectrum**
**(A)** Schematic of Hoescht 33342 chemical structure. **(B)** Excitation (solid line)/emission (dashed line) spectrum of Hoescht 33342.

### 3.3.3 Quantification of sulphated glycosaminoglycan (sGAG) production

The proteoglycan aggrecan is one of the major matrix components of the cartilage extracellular matrix, it is crucial for the proper functioning of articular cartilage. This molecule comprises the aggrecan core protein, a 210-250kDa multi-domain globular protein, to which numerous sulphated glycosaminoglycans (sGAG), namely chondroitin sulphate and keratan sulphate, are attached (see Figure 2.1A) (Kiani et al. 2002).

Aggrecan gene expression and proteoglycan synthesis are increased by mechanical loading (see chapter 2). In cell culture models, this proteoglycan is released into the extracellular milieu and the level of matrix production can be assessed by assaying the sGAG content of the culture medium. Some of this sGAG remains bound up with the cells therefore cellular

content is also examined. In cartilage explants, newly synthesised proteoglycan is not released and is instead incorporated into the extracellular matrix. Therefore matrix production cannot be assessed in this way. In explant culture, sGAG is released into the culture medium as a result of cartilage degradation in response to damaging stimuli such as IL-1 treatment (Wann et al. 2010), therefore this same assay can be used to monitor cartilage degradation in this instance.

The dimethylmethylene blue (DMMB), assay was used to measure the sGAG content of both cells and culture medium (Farndale et al. 1982). This spectroscopic assay is based on the ability of sGAGs to bind the cationic dye 1,9-dimethylmethylene blue and produce a change in its absorption spectrum. Uncomplexed DMMB has a peak absorbance at 595nm which is shifted to 525nm on formation of the sGAG-DMMB complex. The reduction in absorbance is measured and used to determine the concentration of sGAG in the sample using a chondroitin sulphate calibration curve.

In this thesis, DMMB was used at a final concentration of 16 µg/ml; 1,9-DMMB powder (Sigma-Aldrich) was first reconstituted in ethanol and then in 29 mM sodium formate. The final pH was adjusted to 3 using formic acid. Chondroitin sulphate (6-sulphate:4-sulphate; 0.33:1) standards (Sigma-Aldrich) were prepared in the appropriate treatment medium for the sample being assayed and ranged from 0-50µg/ml. In all cases there was a linear relationship between standard concentration and absorbance ($r^2$ >0.99). Experimental samples not in this range were diluted in the appropriate medium prior to assay.

For 2D culture models, attached cells were briefly washed with sterile PBS then removed from the elastic membranes by trypsinisation. For assay, cell suspensions were digested for 4hrs at 60$^{o}$C with 2.8 U/ml papain (Sigma Aldrich) then homogenised with a 20-gauge needle. Culture media and cellular digests were assayed with DMMB reagent and the absorbance at 595nm read on an *Ascent* microplate reader. In cell culture studies sGAG was normalised to DNA and expressed as sGAG (µg)/DNA (µg) to account for differences in cell number (see section 3.3.2), while in explant studies sGAG was normalised to the pre-treatment explant weight and expressed as sGAG (µg)/mg tissue. This value was further normalised to the mean of the control group with values expressed as a fold change.

## 3.3.4 Western Blotting

### 3.3.4.1 Tissue/cell lysate preparation

Cells were cultured in 6-well plastic/bioflex dishes (surface area 9.6 $cm^2$/well) or 35mm culture dishes (surface area 9.6 $cm^2$) until 70-80% confluent. Prior to lysis cells were washed twice in 2ml ice-cold PBS. Cells were then lysed in 200µl 2X Laemelli buffer and the culture surfaces repeatedly scraped with a plastic cell scraper. The lysate was collected and homogenised by passing it through a 21G needle 10 times. The samples were then boiled for 5min at 100$^o$C and either immediately subjected to SDS polyacrylamide gel electrophoresis (SDS-PAGE) or stored at -20$^o$C for later use.

### 3.3.4.2 SDS PAGE

Cell lysates were run on precast 4-12% or 10% polyacrylamide NuPage BisTris gels, depending on the protein under examination. The Novex® Sharp molecular weight marker (Life Technologies) for SDS PAGE consisting of 12 pre-stained protein bands in the range of 3.5-260kDa was run alongside samples.

Gels were loaded with 15µl/well and were run at 150V for 1-2hrs, depending on the protein under examination.

### 3.3.4.3 Immunoblotting and band quantification

Following electrophoresis, the samples were transferred to nitrocellulose membrane by semi-dry transfer using a Trans-Blot SD semi-dry transfer cell (Biorad). The transfer buffer used comprised: 20mM Tris, 120mM glycine and 10% methanol. Proteins were transferred for 45mins at 15V at room temperature for 1 gel, when two gels were transferred this time was extended to 1hr.

Following transfer, membranes were cut to size and blocked in 20ml 5% non-fat milk in PBS with 0.1% tween20 (PBST) for 1 hr at room temperature. After blocking membranes were incubated with the appropriate primary antibodies overnight at 4$^o$C (see Table 3.1). Following this, membranes were washed three times for 10 min in PBST then incubated with the appropriate species-specific infra-red secondary antibodies (see Table 3.2) in 5% non fat

milk in PBST for 1 hr at room temperature. This was followed by two 5 min washes in PBST and a single, final wash in PBS. Membranes were imaged using the Licor Odyssey infra red scanner and densitometry was performed using the Odyssey software to quantify band intensity.

**Table 3.1 Primary antibodies used in this thesis**

| Target | Species | Supplier | Use | Titration |
|---|---|---|---|---|
| Acetylated alpha tubulin (clone 611b-1) | Mouse | Sigma Aldrich | ICC | 1:2000 |
| Acetylated alpha tubulin (clone C3B1) | Mouse | A generous gift from C.A. Poole | IHC | 1:10 |
| Arl13b | Rabbit | Protientech | ICC/IHC | 1:500 |
| Pericentrin | Rabbit | Abcam | ICC | 1:1000 |
| β-tubulin | Rabbit | Abcam | WB | 1:10,000 |
| β-tubulin | Mouse | Sigma Aldrich | WB | 1:10,000 |
| Ki-67 | Mouse | Sigma Aldrich | ICC | 1:1000 |
| HDAC-6 (L-18) | Goat | Santa Cruz biotechnology | ICC | 1:50 |
| HDAC6 (S22) | Rabbit | Abcam | ICC | 1:500 |
| HDAC-6 | Rabbit | Abcam | ICC | 1:250 |
| Hsp90 | Rabbit | Abcam | ICC/IP | 1:500 |
| Indian Hedgehog | Rabbit | Abcam | IHC/ICC/WB | 1:1000 |
| GAPDH | Rabbit | Santa Cruz | WB | 1:5000 |

*ICC=Immunocytochemistry, IHC=Immunohistochemistry, WB=Western blot, IP=Immunoprecipitation

**Table 3.2. Fluorescent molecules and secondary antibodies used in this thesis**

| Target | Supplier | Use | Titration |
|---|---|---|---|
| IRDye® 800CW Donkey anti-goat | Licor, Cambridge, UK | WB | 1:15000 |
| IRDye® 680LT Goat anti-mouse | Licor, Cambridge, UK | WB | 1:15000 |
| IRDye® 800CW Donkey anti-rabbit | Licor, Cambridge, UK | WB | 1:15000 |
| AlexaFluor594-conjugated goat anti-rabbit secondary | Life Technologies, UK | IHC/ICC | 1:1000 |
| AlexaFluor594-conjugated goat anti-mouse secondary | Life Technologies, UK | IHC/ICC | 1:1000 |
| AlexaFluor488-conjugated goat anti-rabbit secondary | Life Technologies, UK | IHC/ICC | 1:1000 |
| AlexaFluor488-conjugated goat anti-mouse secondary | Life Technologies, UK | IHC/ICC | 1:1000 |
| 4',6-diamidino-2-phenylindole 5mg/ml (DAPI) | Sigma Aldrich, UK | IHC/ICC | 1:5000 |
| AlexaFluor55-conjugated Phalloidin | Life Technologies, UK | IHC/ICC | 1U/$cm^2$ |

*ICC=Immunocytochemistry, IHC=Immunohistochemistry, WB=Western blot

## 3.4 Immunofluorescence methods

### 3.4.1 Immunofluorescence in isolated cells

NIH3T3 cells were cultured on 15mm glass coverslips while chondrocytes were cultured both on coverslips and on Bioflex membranes. Both membranes and coverslips were treated identically following fixation after which membranes were excised from the culture plates.

Prior to fixation the culture medium was removed and the cells briefly washed with warm phosphate buffered saline (PBS) then immediately fixed in 4% (w/v) formaldehyde at room temperature for 10min. The cells were then washed three times for 5min in PBS then permeabilised with 0.25% (v/v) triton-X 100 for 5min. Triton-X 100 was removed then cells were blocked in 5% (v/v) goat serum for 1 hour to reduce non-specific antibody interactions. The steps described above were all conducted at room temperature.

Samples were incubated with primary antibody at 4$^{o}$C overnight in 0.1% (w/v) bovine serum albumin (BSA) in PBS hereafter referred to as 0.1%BSA/PBS at suitable titres as determined by antibody optimisation (Table 3.1). Cells were then washed three times for 10 min in 0.1%BSA/PBS then incubated for 1hr with species-specific fluorescent secondary antibodies at room temperature (Table 3.2). Following this samples were incubated with 1µg/ml 4',6-diamidino-2-phenylindole (DAPI) at room temperature for 1min to label cell nuclei then washed three times for 5 min in 0.1%BSA/PBS and mounted with ProLong® Gold antifade reagent (Life Technologies).

In studies examining changes to the actin cytoskeleton, actin was labelled with Alexa Fluor555 conjugated phalloidin, which was included in the secondary antibody step at a concentration of 1U/cm$^2$. Membranes and coverslips were sealed using nail varnish to prevent drying out.

### 3.4.2 Immunofluorescence in Zebrafish

Zebrafish (*Danio rerio*) embryos at the 24 hpf stage were fixed at 4$^{o}$C overnight in BT Fix (4% (w/v) PFA, 0.15mM $CaCl_2$, 4% sucrose in phosphate buffer (PB) (0.1M $Na_2HPO_4$, 0.1M

$NaH_2PO_4$)). Embryos were then washed three times for 10min in PB on a shaker then incubated for 1hr at room temperature in 0.8% Triton X-100 in PB (PBT) containing 10% goat serum. Following blocking embryos were incubated with primary antibody in PBT containing 1% goat serum at 4$^{o}$C overnight then washed five times for 30 min in PBT. Appropriate secondary antibodies were made up in PBT containing 1% goat serum and incubated at room temperature for 3hrs. Embryos were then incubated with 1µg/ml DAPI for 1hr to label nuclei and washed five times for 10min in PBT and either mounted in 100% glycerol or stored at 4$^{o}$C in 70% glycerol in PBS.

## 3.5 Microscopy techniques

### 3.5.1 Monitoring changes in actin organisation in 2D-cell culture

To monitor changes in the organisation of the actin cytoskeleton cells were labelled with Alexa-Fluor594 conjugated phalloidin. A Leica DMI4000 epifluorescent microscope with a x63/1.4-NA objective was used for imaging cells in at least 5 representative fields of view for each experimental condition. A small proportion of cells exhibited a rounded morphology typically with more intensely stained cortical actin. Others showed a flattened, or spread, morphology, these typically exhibited diffuse cytoplasmic staining while others exhibited either mild or more prominent stress fibre formation. To quantify changes in actin organisation following strain, cells were grouped into four classifications; cortical, diffuse, mild and prominent (Figure 3.3). Experiments were conducted in duplicate and statistical significant changes in the proportionate size of these groups assessed using a $Chi^2$ test ($p<0.05$).

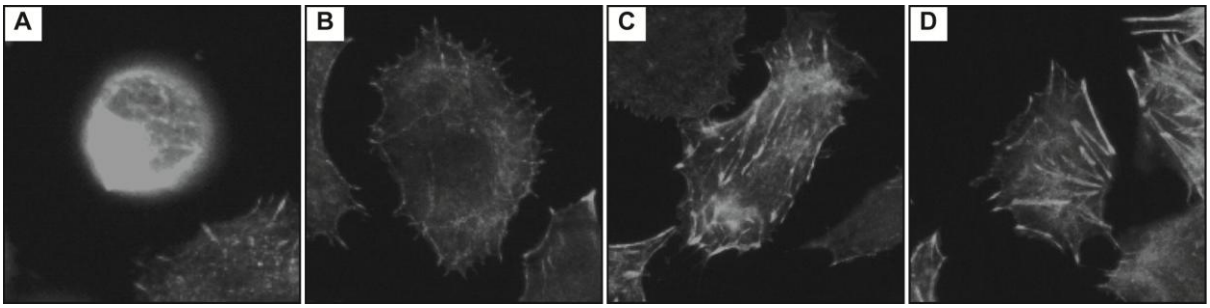


**Figure 3.3 Classification of actin organisation**
Representative images of cells exhibiting typical phalloidin staining for the four classifications of actin organisation: in 2D-culture **(A)** Cortical **(B)** Diffuse **(C)** Mild and **(D)** prominent stress fibre formation.

### 3.5.2 Quantification of percentage Ki-67 positive cells in 2D-cell culture

Cell cycle status was assessed by immunofluorescent labelling of the Ki-67 antigen. Ki-67 labels the nuclei of cells at all stages of the cell cycle except $G_0$. A Leica DMI4000 epifluorescent microscope with a x63/1.4-NA objective was used for imaging and the proportion of Ki-67 positive cells in a given field determined. Ki-67 labelling was quantified

in 10 representative fields of view for each experimental condition and expressed as a fold change relative to control to reduce inter-experimental variability. Experiments were conducted in triplicate and statistical significance determined using a student's T-test ($p<0.05$).

### 3.5.3 Measurement of primary cilia prevalence in 2D-cell culture

Primary cilia prevalence was quantified using a Leica DMI4000B epifluorescent microscope with a x63/1.4-NA objective. Primary cilia were immunofluorescently labelled with antibodies directed against acetylated α-tubulin, and nuclei were counterstained with DAPI. Both cell number and the proportion of cells exhibiting primary cilia were determined in 10 representative fields of view for each experimental condition. Each field was approximately 200µm x 150µm in size and contained 30-50 cells for a typical monolayer culture. Mean cilia prevalence was expressed as the % ciliated cells. Experiments were conducted in triplicate and significance assessed using a student's T-test ($p<0.05$).

### 3.5.4 Measurement of primary cilia length in 2D-cell culture

Imaging and quantification of cilia length was performed on a Leica TCS SP2 confocal microscope using an x63/1.4-NA lens (Leica Microsystems, Wetzlar, Germany). Primary cilia were immunofluorescently labelled with antibodies directed against acetylated α-tubulin and/or Arl13b, and nuclei were counterstained with DAPI. Full depth sequential z-stacked sections were imaged through the entirety of the cellular profile and subsequently used to create 2D maximum intensity projections (MIPs). Section thickness was set to 0.5µm so that approximately 20 sections were imaged for each field. Image format was set to 1024x1024 pixels with a zoom of 1 yielding a pixel size of 0.232µm. Line averaging (x4) was performed on each slice.

Image J software was used to trace and measure the length of cilia in captured images (Figure 3.4). Only cilia that were approximately 90° to the incident light (at least 95% of cilia in a given field) were selected for measurement. Vertical cilia were excluded from analyses as their length cannot reliably be measured due to the decreased resolution of the microscope in the z-dimension. This is typically half that of the x and y planes due to the

blurring effect of the point spread function (Pawley 2006). Careful examination of z-stacks prior to length analyses ensured vertical cilia were not included. At least 30 cilia (NIH 3T3 cells) or 100 cilia (primary bovine chondrocytes) were measured from 5 representative fields for each experimental condition. Experiments were conducted in triplicate giving a final n of 90-300 cilia, depending on the cell type under examination. Cilia length measurements were not always normally distributed, particularly for chondrocytes where the spread of cilium lengths were greater, therefore statistical significance was assessed using the non-parametric Mann Whitney *U* test ($p<0.05$).

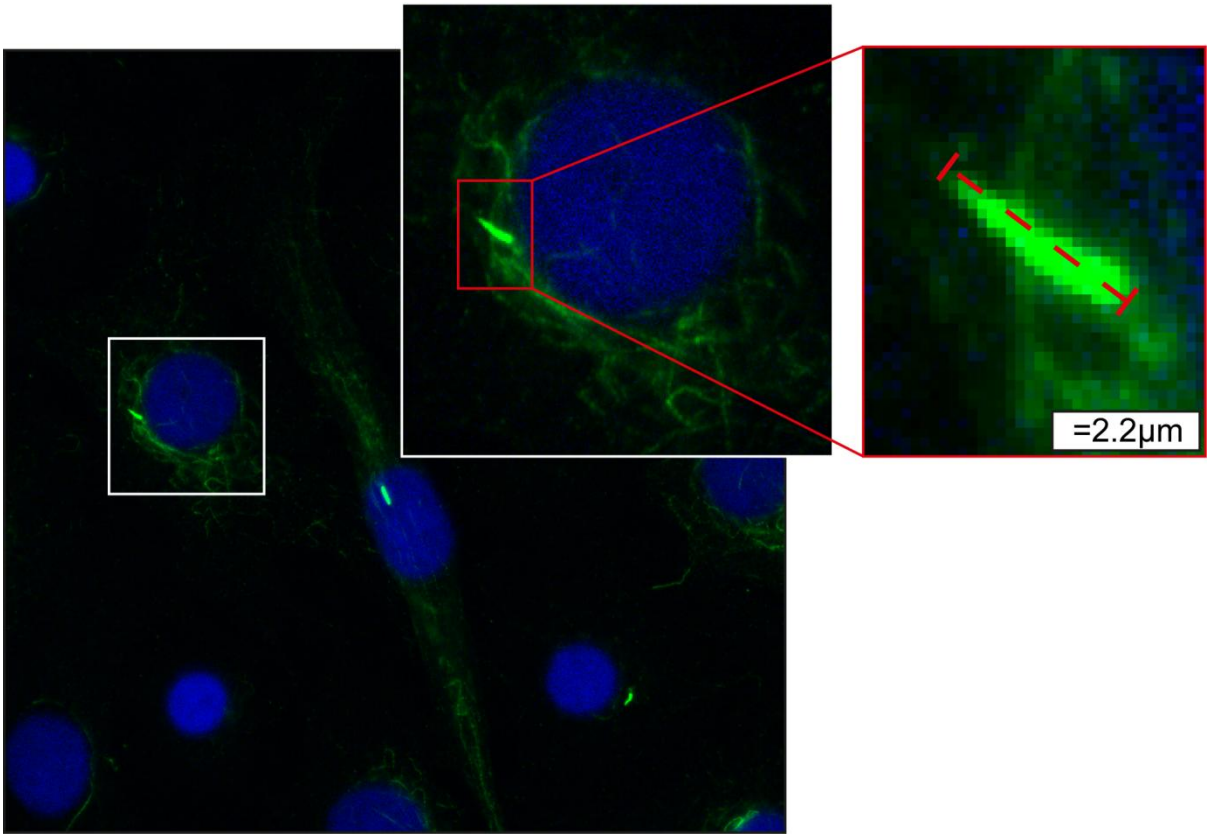


**Figure 3.4 Confocal analyses and measurement of primary cilia length in Image J**
Primary cilia length was measured using image J software. Z stacks were flattened to created 2D maximum intensity projections and the distance from the base to the tip of the cilium measured manually by tracing along the length of the cilium.

### 3.5.5 Measurement of primary cilia length and prevalence in 24hpf Zebrafish embryos

Imaging and quantification of cilia length in Zebrafish was performed on a Zeiss LSM510 laser scanning confocal microscope with a x63/1.4NA objective. Primary cilia were immunofluorescently labelled for acetylated α-tubulin and nuclei were counterstained with DAPI. Sequential 0.5µm thick z-stacked sections were imaged through the full thickness of the tail in a region up to 100µm from the tip (Figure 3.5) and subsequently used to create 2D maximum intensity projections (MIPs). The image format was set to 1024x1024 pixels with a zoom of 1 yielding a pixel size of 0.232µm. Line averaging (x2) was performed on each slice. Zen analysis software (Zeiss) was used to trace and measure the length of cilia in captured images. Z-stacks were generated from five embryos for each treatment and the lengths of 30 randomly selected cilia were quantified for each embryo. Cilia length measurements were not normally distributed therefore statistical significance was assessed using the non-parametric Mann Whitney *U* test ($p<0.05$).

Primary cilia prevalence was also quantified from MIPs within the same region. Nuclei and cilia were counted within this region and mean cilia prevalence was expressed as % ciliated cells. Statistical significance was assessed using a Student's T- test ($p<0.05$).

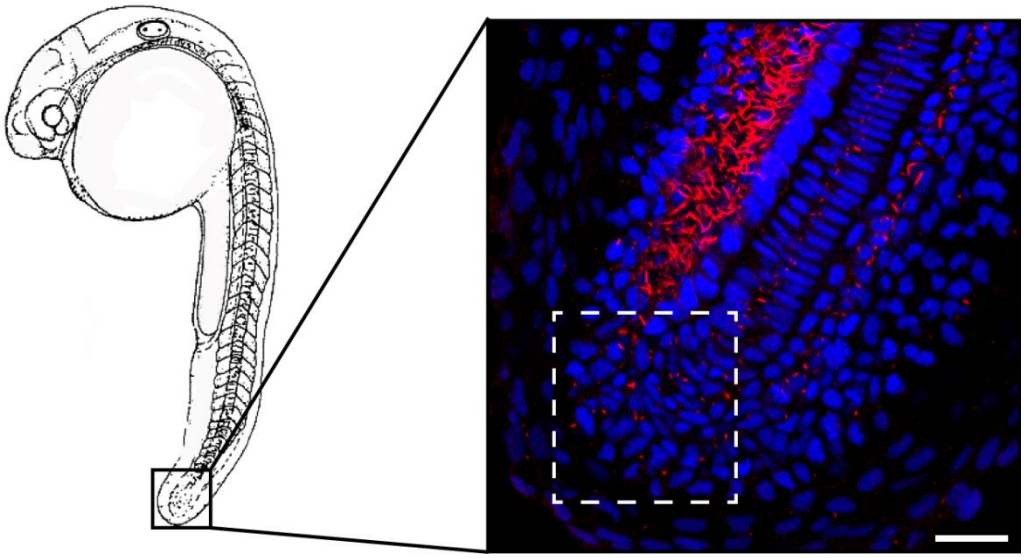

**Figure 3.5 Primary cilia length and prevalence were measured in 24hpf Zebrafish embryos** Schematic highlighting the tip of the Zebrafish tail, the region within which cilia length and prevalence were quantified by confocal microscopy. The image shows a confocal slice through the tail region of a 24hpf zebrafish embryo highlighting cilia, labelled with acetylated α-tubulin (red), in this region. Cell nuclei were counterstained with DAPI (blue). The white box in this image demarcates the region in which cilia length was quantified. Scale bar represents 20μm.

### 3.5.6 Assessment of Zebrafish morphology and development

As with all organisms, zebrafish development occurs according to a specific program, the timings of which have been carefully mapped out. Several simple measurements can be used to determine whether development is occurring in a timely and correct fashion. In this thesis head/trunk and somite angles were measured to assess the effects of heat shock on Zebrafish gross morphology and developmental progression (Figure 3.6A).

Dechorionated Zebrafish were imaged on a Leica DMI 4000 microscope (Leica) using a x10/0.3-NA objective. For head trunk angles, the angle made between a line drawn through the middle of the ear and eye, and a second line parallel to the notochord in the mid-trunk region (myotomes 5-10) was measured using image J software (Figure 3.6B). The head/trunk angle increases from 20hpf as a consequence of embryo straightening (Kimmel et al. 1995). Zebrafish development can also be tracked by counting the formation of somites (Kimmel et al. 1995) which occurs at a rate of approximately 2 per hr between

12hpf and 22hpf. Somites form chevron shapes in Zebrafish and the angles formed by these chevrons can be measured (Figure 3.6B). Comparisons between control and experimental embryos can be used to identify defects in somite formation and changes in body curvature. Somite angles were measured using Image J software.

Head/trunk measurements were taken for at least 10 embryos per experiment and 2 somite angle measurements were taken for each embryo. Somites were counted over a 12hr period between 12 and 24hpf for at least 10 embryos per time point. Experiments were conducted in duplicate and statistical significance was determined using a Student's T-test ($p<0.05$).

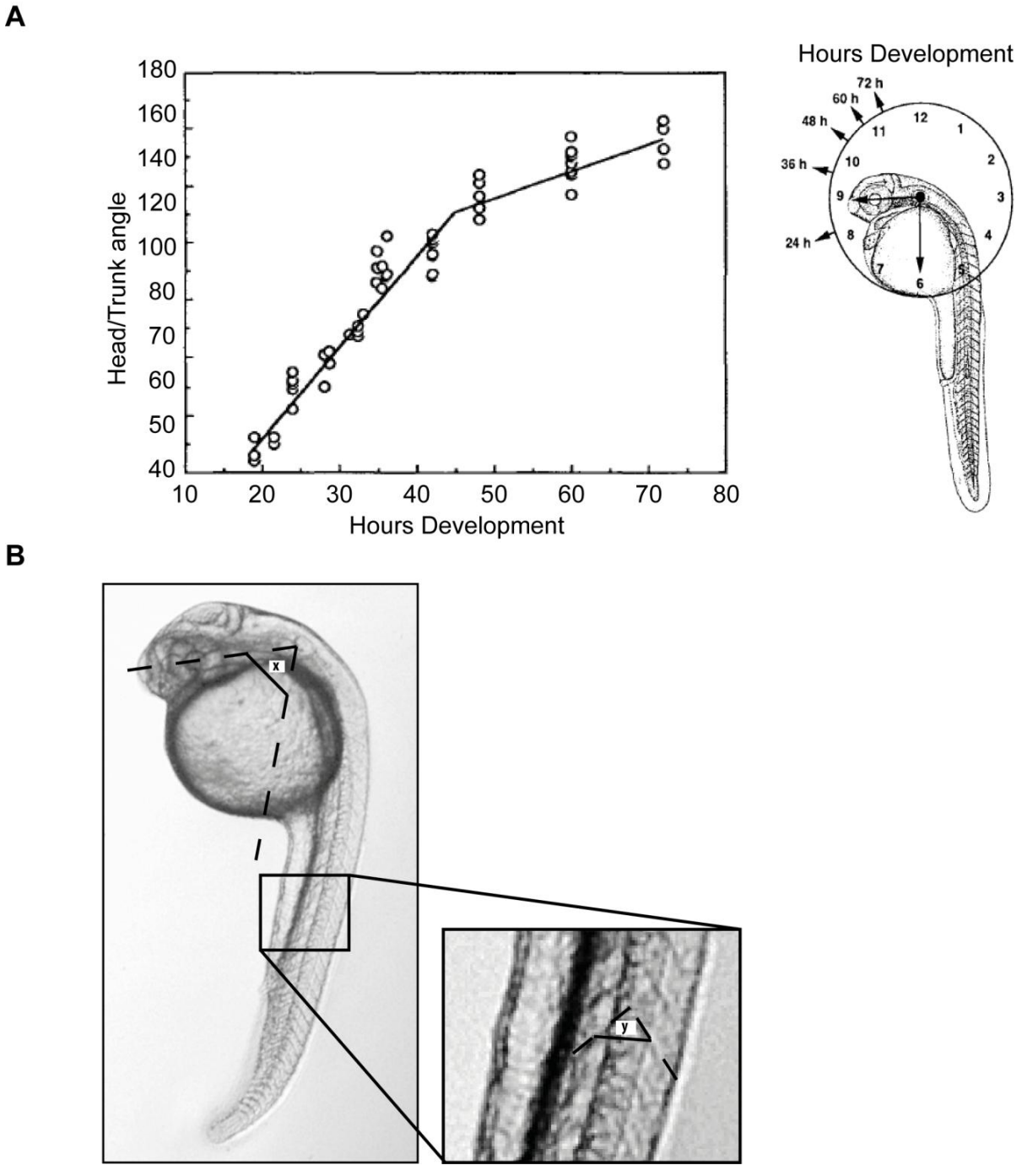


**Figure 3.6 Head/Trunk and somite angle measurements in Zebrafish embryos**
**(A)** Graph demonstrating the change in Zebrafish head trunk angle with development al time (taken from (Kimmel et al. 1995)). **(B)** Schematic demonstrating how head/trunk angle (x) and somite angles (y) are measured using image J software.

## 3.6 Polymerase Chain Reaction (PCR) methods

In this thesis both reverse transcription PCR (RT-PCR) and quantitative real time PCR (qRT-PCR) were used to qualitatively and quantitatively examine gene expression respectively. Studies examine both basal levels of gene expression and changes in response to various stimuli.

### 3.6.1 RNA isolation and reverse transcription

#### 3.6.1.1 RNA isolation

Total RNA was isolated from cells using an RNeasy Kit (Qiagen) according to the manufacturer's instructions. Briefly, cells were lysed in 350µl RLT buffer containing guanidine-thiocyanate which inhibits RNAses. A cell scraper was used to collect the lysate which was subsequently homogenised 7 times with a 20-gauge needle and then applied to a silica based column. The total RNA binds to the column and the remaining lysate passes through the column upon centrifugation (8117g for 30s) and is discarded. Following this the bound RNA is washed once with 700µl RW1 buffer, then twice with 500µl buffer RPE. The column can then be centrifuged in a fresh collection tube to remove any remaining RPE buffer. The column is then transferred to a clean eppendorf tube and the RNA eluted in 30ul of RNAse free water.

RNA was quantified using the Nanodrop ND-1000 spectrophotometer (LabTech, East Sussex, UK) which measures the optical density of the samples at 260nM. The nanodrop can also be used to determine the purity of the RNA sample as pure RNA exhibits an A260/280 absorbance ratio of 2.0. RNA integrity was confirmed by formaldehyde gel electrophoresis (section 3.6.1.2).

#### 3.6.1.2 Formaldehyde gel electrophoresis

RNA integrity was confirmed by denaturing formaldehyde gel electrophoresis. Following isolation, an aliquot containing at least 200ng RNA is removed and mixed with RNA sample loading buffer (Sigma Aldrich) containing 1.14M formaldehyde and 50 µg/ml EtBr. One volume of RNA is mixed with 2 volumes of sample buffer and then heated to 65°C for 10min

and placed on ice. The denatured RNA is loaded onto a 1% agarose gel made using 4-morpholinopropanesulfonic acid (MOPS) buffer (40mM MOPS pH 7.0, 10mM sodium acetate, 1mM EDTA pH 8.0). The gel is run in an electrophoresis tank filled with MOPS buffer for 1hr at 50-60V. The gel is then visualised using a UVP UV transilluminator.

If the RNA is degraded it will appear as a smear and is not suitable for downstream use. If intact then you will see the 18S and 28S bands, the 28S band should be approximately 2X bigger/brighter than the 18S band.

#### 3.6.1.3 cDNA synthesis

RNA was converted to cDNA using the Quantitect reverse transcription kit (Qiagen) according to the manufacturer's instructions. This kit comprises two main steps 1) elimination of genomic DNA and 2) reverse transcription. For the first step 1µg RNA was incubated with gDNA wipe out buffer at 42°C for 2min (see reaction 1 below). This effectively removes all contaminating genomic DNA from the sample.

Reaction 1:

| | |
|---|---|
| gDNA wipe out buffer | 2µl |
| 1µg RNA | variable |
| Nuclease free water | variable |
| **Total volume** | **14µl** |

For reverse transcription, the entire genomic DNA elimination reaction above is incubated for 15min at 42°C according to reaction 2.

Reaction 2:

| | |
|---|---|
| Quantiscript RT Buffer, 5x | 4µl |
| Quantiscript Reverse Transcriptase | 1µl |
| RT Primer Mix | 1µl |
| Entire genomic DNA elimination reaction | 14µl |
| **Total volume** | **20µl** |

This is followed by 3min at 95°C to inactivate the RT enzyme. The resulting cDNA was quantified using the Nanodrop ND-1000 spectrophotometer (LabTech, East Sussex, UK) and subsequently diluted 1:2 in nuclease free water for use in RT-PCR and qRT-PCR. Successful

cDNA synthesis was confirmed by a reduction in the A260/280 absorbance ratio of the sample from 2.0 to 1.8.

### 3.6.2 Reverse Transcription PCR (RT-PCR)

RT-PCR is a non-quantitative method by which to assess the presence of a particular transcript in an experimental sample. It is a variant of PCR that uses RNA reverse transcribed into its cDNA complement as the initial template for the PCR reaction. RT-PCR reactions were performed using *Taq* polymerase (New England Biolabs) according to the following reaction:

RT-PCR Reaction:

| | |
|---|---|
| DNA template | 1µl |
| Primer (10µM) | 0.5 µl |
| dNTPs (10mM) | 0.5 µl |
| *Taq* polymerase | 0.125 µl |
| 10X *Taq* reaction buffer | 1 µl |
| Nuclease free water | 6.875 µl |
| **Total volume** | **10 µl** |

The cycling conditions for RT-PCR reactions were as follows:

| | | |
|---|---|---|
| | 94$^{o}$C 5min | |
| Denaturation | 94$^{o}$C 30s | x25 cycles |
| Annealing | χ $^{o}$C 30s | |
| Extension | 72 $^{o}$C 30s | |
| | 72 $^{o}$C 10min | |
| | 4 $^{o}$C | |

Optimal primer annealing temperatures (χ) were determined for each primer set and are detailed in Table 2.1 and Table 2.2. After amplification, samples were combined with 2µl 6X gel loading dye and subjected to gel electrophoresis (see section 3.6.2).

### 3.6.3 Primer design

For RT and qRT-PCR primers were designed based on the sequences published in GenBank using Primer-3 software and synthesised in Sigma Genosys. Primers were targeted to specific regions of target genes and were designed to amplify regions from 100-250bp in length. To avoid genomic DNA amplification, primers were either located in different exons

or across exon-exon boundaries. Amplicon size and reaction specificity were confirmed by agarose gel electrophoresis (see section 3.6.2). Sequence information and annealing temperatures for primers used in this thesis are available in Table 3.3 and Table 3.4.

**Table 3.3 Bovine primers for PCR**

| Accession no. | Gene | Sequence | Size (bp) | Annealing temperature |
|---|---|---|---|---|
| HQ437693.1 | Sonic Hedgehog | F- GAACCAAGCTGGTGAAGGAC<br>R- TCTCGATGGCGTAGAAGACC | 138 | 60°C |
| XM_001788869.1 | Desert Hedgehog | F- TCTCGATGGCGTAGAAGACC<br>R- AGTCTCCGCGATGCAGTT | 202 | 60°C |
| NM_001076870 | Indian Hedgehog | F- GCTTCGACTGGGTGTATTACG<br>R- GTCTCGATGACCTGGAAAGC | 244 | 60°C |
| NM_001205879 | Patched 1 | F- ATGTCTCGCACATCAACTGG<br>R- TCGTGGTAAAGGAAAGCACC | 131 | 60°C |
| NM_001192220 | Smoothened | F- CCGGGACTATGTGTTATGCC<br>R-TTCTTGATCCGTTTGGGTTC | 243 | 60°C |
| NM_001099000.1 | Gli1 | F-ACCCCACCACCAGTCAGTAG<br>R-TGTCCGACAGAGGTGAGATG | 255 | 60°C |
| NM_001192250.2 | Gli2 | F-CACCGTTCCACGCCCCCTTC<br>R-CGTGCACAGCCCGCAGGTAA | 236 | 60°C |
| XM_002686896.1 | Gli3 | F-CGCTTTGCAAGCCCGGAGCA<br>R-GTACTGGGCTGCGTGCCGTT | 164 | 60°C |
| NM_173981 | Aggrecan | F- GAGTTTGTCAACAACAATGCC<br>R- TGGTAATTACATGGGACATCG | 212 | 60°C |
| NM_001001135.2 | Collagen Type II | F- ACGTCCAGATGACCTTCCTG<br>R- GGATGAGCAGAGCCTTCTTG | 150 | 60°C |
| NM_001166515 | ADAMTS-5 | F-GCCCTGCCCAGCTAACGGTA<br>R- CCCCCGGACACACACGGAA | 248 | 60°C |
| NM_001034034 | GAPDH | F- GACAAAATGGTGAAGGTCGG<br>R- TCCACGACATACTCAGCACC | 290 | 60°C |

**Table 3.4 Murine primers for PCR**

| Accession no. | Gene | Sequence | Size (bp) | Annealing temperature |
|---|---|---|---|---|
| NM_010544.2 | Indian Hedgehog | F-GCTTCGACTGGGTGTATTACG<br>R-GTCTCGATGACCTGGAAAGC | 244 | 60°C |
| NM_008957.2 | Patched 1 | F-GCAGAGGACTTACGTGGAGG<br>R-CTGACAGTGCAACCAACAGG | 245 | 60°C |
| NM_010296.2 | Gli1 | F-CCAAGCCAACTTTATGTCAGGG<br>R-AGCCCGCTTCTTTGTTAATTTGA | 130 | 60°C |
| NM_007424.2 | Aggrecan | F-CACGCTACACCCTGGACTTTG<br>R-CCATCTCCTCAGCGAAGCAGT | 270 | 60°C |
| NM_011782.2 | ADAMTS-5 | F-GGATGTGACGGCATTATTGG<br>R-GGGCTAAGTAGGCAGTGAAT | 211 | 60°C |
| NM_008084.2 | GAPDH | F- GACAAAATGGTGAAGGTCGG<br>R- TCCACGACATACTCAGCACC | 290 | 60°C |

### 3.6.3.1 Gel electrophoresis

Following PCR amplification, reactions were mixed with 6x DNA loading dye (New England Biolabs) containing bromophenol blue and subjected to agarose gel electrophoresis. Samples were loaded onto a 2% agarose gel which was made up in Tris-acetate-EDTA (TAE) buffer (40mM Tris pH8, 20mM glacial acetic acid, 1mM EDTA) containing 0.5µg/ml ethidium bromide. Samples were electrophoresed for 45min at 90V in TAE buffer and then visualised in the gel using a UVP UV transilluminator.

Amplicon size was confirmed by running a low molecular weight marker (New England Biolabs) containing reference bands from 50-766bp in size.

### 3.6.3.2 Gel Extraction

Following electrophoresis, cDNA bands were excised from the gel and dissolved in three volumes of NaI solution (6M NaI, 120mM $Na_2SO_3$) at 55°C for approximately 5 min with frequent vortexing. A 10µl aliquot of glass milk (silica suspension in NaI solution) was then added to the dissolved gel and incubated at room temperature for 5 min to allow DNA binding. The silica was pelleted by centrifugation (1 min, 11337xg) and the supernatant discarded. The pellet was then washed twice in wash buffer (100mM NaCl, 1mM EDTA, 10mMTris-HCl, pH7.5, 50% EtOH) and allowed to air dry for 10 min. The pellet was

resuspended in 20µl nuclease free water and incubated at room temperature for 5 min then centrifuged. The supernatant containing the eluted DNA was removed and transferred to a fresh eppendorf tube and the purified DNA quantified using the Nanodrop ND-1000 spectrophotometer.

### 3.6.4 Quantitative real time PCR (qRT-PCR)

Real time PCR was used to measure changes in gene expression and was conducted using syber-green PCR. Syber-green is a fluorescent DNA binding dye that preferentially binds to dsDNA. It has an excitation and emission maxima of 494nm and 521nm, respectively. In qRT-PCR, syber-green is used to monitor the accumulation of PCR product during the annealing and extension phases of the PCR reaction by measuring increases in fluorescence at 521nm. The cycle number at which this increase in fluorescence becomes exponential is measured and termed the Ct value (threshold cycle). The Ct value is the number of cycles required for the fluorescent signal to cross an arbitrary threshold line and to exceed the background fluorescence. While syber-green PCR has the advantage of being more cost effective than other probe based assays, its main drawback is that this dye will fluoresce in the presence of dsDNA regardless of the specificity of the amplified product. It therefore requires primers to be accurately designed to only amplify the specific region of interest.

Real time PCR was conducted on an MxPro3000P thermal cycler (Stratagene) and analysed using MxPro QPCR software. Changes in gene expression were quantified according to the relative standard curve method. This approach to qRT-PCR is simple and reliable and avoids the practical and theoretical problems associated with efficiency based techniques (Larionov et al. 2005). It uses a standard curve derived from a serial dilution of target cDNA for each gene of interest (GOI) (see section 3.6.4.1). Logarithms (base 10) of standard concentrations are plotted against Ct values and the standard curve interpreted as an ordinary linear function. The concentration of the GOI in each experimental sample is calculated using the Ct value from the amplification reaction in conjunction with the standard curve in the customary way. This value is then normalised to the expression of a reference gene such as glyceraldehyde-3-phosphate (GAPDH), β2-microglobulin (B2M), β-Actin or 18S RNA and expressed as a fold change relative to the experimental control. In this thesis I have

normalised to GAPDH, previous studies have established the expression of this gene in chondrocytes remains stable during mechanical loading (Lee et al. 2011) and I did not observe significant variation in the expression of this gene under the experimental conditions used in this thesis.

#### 3.6.4.1 Standard curve preparation

The standard curve for each target gene was prepared from a dilution series of the amplified PCR product. Firstly a 40µl PCR reaction was prepared and run at the appropriate annealing temperature. The entire reaction was then subjected to agarose gel electrophoresis and purified by gel extraction (section 3.6.2 and 3.6.3.2). The purified product was quantified (typically in the range of 5-30ng/µl and usually ~$10^{16}$copies) using the Nanodrop ND-1000 spectrophotometer.

A dilution series ranging from $10^{-3}$-$10^{-10}$ was prepared in nuclease-free water and syber-green PCR conducted on the MX3500P thermal cycler. When identified as standard wells, the Stratagene software will prepare a standard curve from the resulting Ct values of each reaction and calculate reaction efficiency and $r^2$. Standard curves were deemed suitable for use if reactions were 90-110% efficient and had an $r^2$ value greater than 0.97.

#### 3.6.4.2 qRT-PCR

The KAPA SYBR® FAST Universal qPCR master mix (Kapa Biosystems) containing SYBR® Green I dye and KAPA SYBR® DNA Polymerase was used for qRT-PCR. The passive reference dye ROX (Kapa Biosystems) was used to normalise for non-PCR-related fluctuations in fluorescence signal. PCR reactions were performed as described below:

qRT-PCR Reaction:

| | |
|---|---|
| cDNA | 1µl |
| Primer (5µM) | 1 µl |
| 50X ROX | 0.2 µl |
| KAPA master mix | 5 µl |
| Nuclease free water | 2.8µl |
| **Total volume** | **10 µl** |

Reactions were performed on cDNA generated from 1µg RNA and were diluted 1:10 so that

each reaction contained at least 100ng cDNA (or 5ng of the original RNA). A sample containing nuclease-free water instead of template cDNA, the 'no template control' (NTC) is also run for each GOI to distinguish between actual gene expression and background contamination. All samples are run in triplicate to minimise pipetting error and a mean Ct value is obtained for each experimental replicate. The amount of target DNA in each sample is determined from the standard curve then normalised to GAPDH expression.

PCR reactions were performed according to the following program and contained a final dissociation/melt-curve step to confirm reaction specificity:

Real time PCR program:

| | | |
|---|---|---|
| | 95 °C 3min | |
| Amplification: | 95 °C 30s | |
| | x °C 30s | X40 cycles |
| | 72 °C 30s | |
| | Collect end point fluorescence values | |
| Dissociation: | 95 °C 1min | |
| | 55 °C 30s | |
| | Collect all fluorescence values from 55-95 ºC | |
| | 95 °C 30s | |

Ct and quantification data were extracted into a Microsoft Excel file for statistical analyses. Statistical analyses were performed on normalised expression ratios. For normally distributed data, statistical significance was determined using the students T-test and the threshold for statistical significance was set at $p<0.05$.

## 3.7 Mechanical loading model

The Flexcell system (Tension Plus, FX-4000T™, Flexcell International, USA), was used to apply cyclic tensile strain (CTS) to chondrocytes in 2D-culture (Figure 3.7A). In this system cells are cultured on collagen type I coated flexible elastic membranes in a 6-well plate format and subjected to uniform equibiaxial strain (Dunnlab, Germany). This is achieved by a computer controlled vacuum which pulls the membrane down over a circular loading post positioned below each well subjecting it to uniform radial and circumferential tensile strain (Figure 3.7B)(Vande Geest et al. 2004).

Freshly isolated bovine chondrocytes were cultured on collagen type I coated Bioflex® plates. Membranes were pre-coated at 4°C overnight with 10µg/cm$^2$ collagen Type I (Sigma Aldrich) then allowed to dry at room temperature and UV sterilised for 16hrs. The membranes were then washed twice in PBS and coated for an additional 3hrs with FCS at 37°C. Chondrocytes were seeded at a density of 80,000 cells/cm$^2$ immediately following isolation and cultured until 80-90% confluent for up to 6 days. Only the region directly above the loading post experiences uniform strain (Vande Geest et al. 2004) therefore the cells in the area outside of this loading post were removed 3 days prior to loading by aspiration (Figure 3.7C). The size of the area which experiences uniform loading, and thus the size of the area that needs to be removed, can be calculated according to the following equation:

$$\text{Diameter of uniformly loaded area} = \frac{\text{Diameter of Loading Station}}{1 + (\text{Max \% Elongation}/100)}$$

Chondrocytes were stimulated with 5, 10 or 20% equibiaxial cyclic tensile strain (CTS) at a frequency of 0.33Hz (sinusoidal) from 0-24 hrs. A silicone-based lubricant was used to minimize friction between the membranes and posts. For unstrained controls, Bioflex plates seeded with chondrocytes were maintained in an identical manner but in the absence of strain. Chondrocytes were maintained in serum free DMEM throughout the duration of the experiment, media was changed 30min prior to the application of strain. All cultures were maintained at 37°C in a humidified atmosphere with 5% $CO_2$ throughout the experiment.

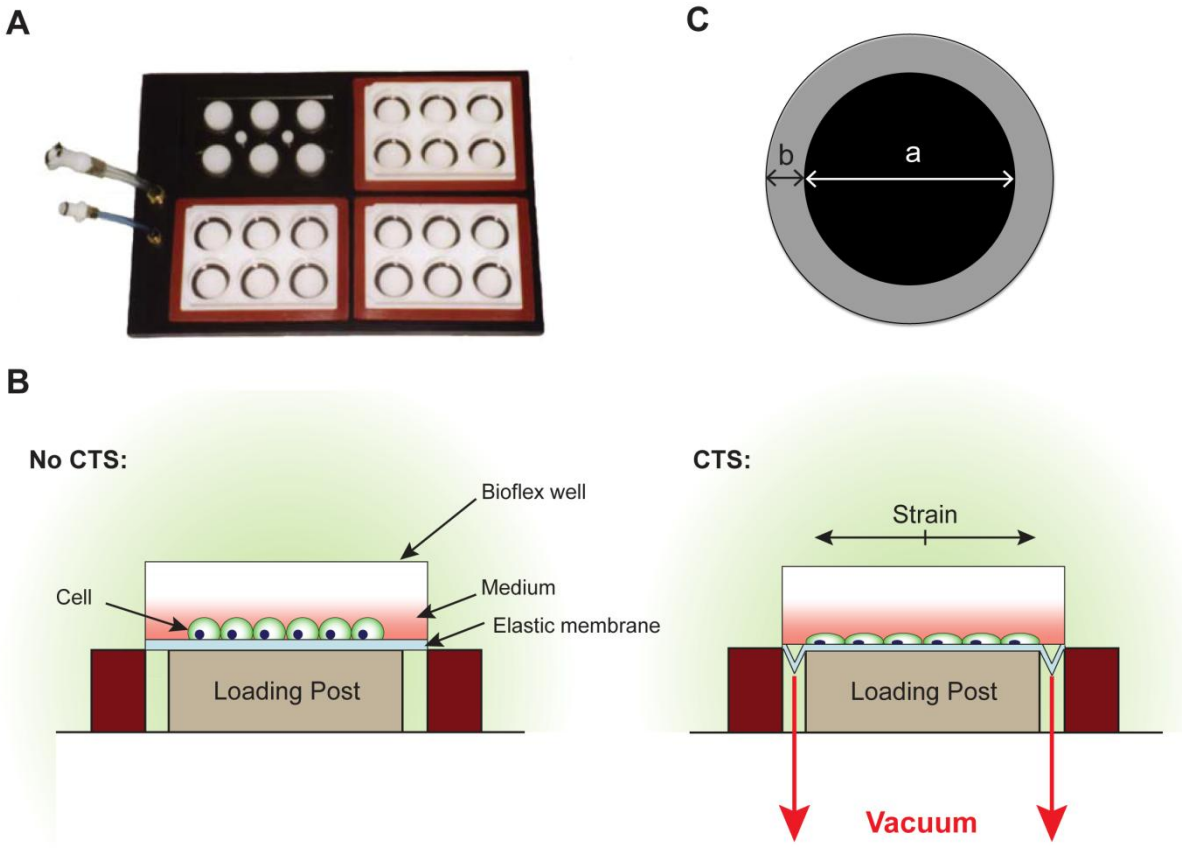


**Figure 3.7 Flexcell 4000T system**
**(A)** Flexcell 400T system. **(B)** Schematic illustrating the Flexcell system demonstrating how the elastic membrane is pulled down over the loading post when the vacuum is applied (No CTS= no load applied, CTS= load applied). **(C)** Schematic representing a single well in the Bioflex plate. Region a (black) experience uniform equibiaxial strain when the vacuum is applied. The cells in region b (grey) do not experience uniform strain and are removed prior to loading.

## 3.7.1 Cell attachment and Viability

### 3.7.1.1 Cell attachment and normalised cell density

Cell attachment was assessed following the application of strain by examining changes in cell density. Nuclei were labelled with DAPI as described in section 3.4.1. Cells were imaged with a Leica DM4000B epifluorescence microscope (Leica, UK) with a x63/1.4-NA oil immersion lens and cell density was determined in 10 representative fields of view for the strained and unstrained groups. Each field was approximately 200µm x 150µm in size. Cell

density was divided by the mean of the unstrained control and expressed as the normalised cell density.

The DNA content of the strained and unstrained media was also examined immediately post loading as described in section 3.3.2. Significant increases in the DNA content of the media would suggest significant cell detachment was occurring.

#### 3.7.1.2 Cell viability

Chondrocyte viability was assessed at the end of the mechanical loading period by measuring the uptake of ethidium homodimer-1 (EthD-1) (Molecular Probes), a high-affinity, red-fluorescent nucleic acid stain that is only able to pass through the compromised membranes of dead cells where it enters the nucleus and intercalates with the DNA. At the end of the mechanical loading period and corresponding control period, cultures were incubated with 1 µM EthD-1, prepared in DMEM+10%FCS, for 15 minutes at 37°C, before being washed thoroughly with phosphate buffered saline (PBS) and fixed with 4% (w/v) PFA. Samples were counterstained with DAPI and mounted as described previously (see section 3.4.1). Cells were imaged with a Leica DM4000B epifluorescent microscope (Leica, UK) with a x63 oil immersion lens and the percentage cell death was determined in 10 representative fields of view from two culture wells (20 fields in total) for each loading regime.

## 3.8 Heat shock methods

### 3.8.1 *In vitro* heat shock of isolated cells in 2D-culture

For the application of heat shock cells were subjected to elevated temperatures for up to 30min at 42°C. Cells were cultured in 35 mm cell culture dishes containing a 10 mm coverslip. To apply heat shock 37°C media was rapidly exchanged for 42°C media and cell culture dishes were sealed with parafilm and immediately transferred to a 42°C water-bath. For experiments involving a recovery period, after heat shock the parafilm was removed and the cell culture dishes returned to a 37°C incubator for a specified amount of time.

### 3.8.2 Thermotolerance

To generate thermotolerant NIH3T3 cells, cells were subjected to a 30 min heat shock at a 42°C 4 hrs prior to passage. Thermotolerant NIH3T3 cells were then seeded into 35mm cell culture dishes containing a 10mm glass coverslip and cultured for a further 24hrs. They were then serum starved for 20 hrs and subjected to heat shock as described in section 3.8.1. To confirm activation of the heat shock response, the expression level of the chaperone protein Hsp70 was assessed by western blotting. Hsp70 expression is induced upon activation of the heat shock response, the expression of this protein was absent from control cells whereas induction of this protein was observed in thermotolerant cells (Figure 3.8).

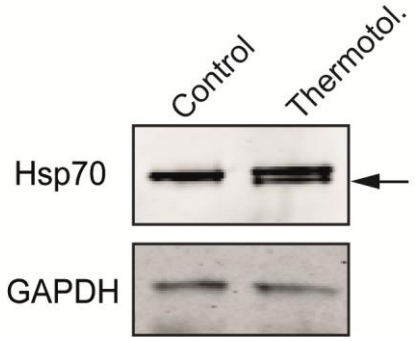


**Figure 3.8 Hsp70 protein expression in thermotolerant cells**
Western blot showing expression of Hsp70 in control and thermotolerant cells (thermotol.). Thermotolerant cells express the inducible chaperone Hsp70 (arrow), while in control cells only a single band representing Hsc70 is present. GAPDH protein expression was examined as a loading control.

### 3.8.3 *In vivo* heat shock of Zebrafish (*Danio Rerio)* embryos

To assess the effects of heat shock on primary cilia length and prevalence *in vivo* Zebrafish embryos were grown until 24hpf in 35mm cell culture dishes. For heat shock, Zebrafish were dechorionated and 28.5$^{o}$C embryo medium was replaced with 42$^{o}$C medium. Cell culture dishes were sealed with parafilm and placed in a water bath set to 42$^{o}$C for 5 min. Zebrafish were immediately fixed and processed for immunofluorescent detection of primary cilia (Section 3.4.2).

To assess the effects of heat shock on Zebrafish gross morphology and development both 12hpf and 24hpf embryos were used. Following heat shock embryos were returned to 28.5$^{o}$C for a set recovery period and changes in head trunk/angles and somite development monitored (Section 3.5.6).

## 3.9 Statistics

For all data sets data is represented as mean ± SEM unless otherwise stated. Normality was assessed using the D'Agostino-Pearson omnibus test. For normally distributed data statistical significance was determined using unpaired students T-test, otherwise the non parametric Mann U Whitney test was used. For all statistics, a two-tailed approach was used with statistically significant differences indicated as *= $p \leq 0.05$, **=$p \leq 0.01$ and ***= $p \leq 0.001$. Statistical analyses were conducted using Graphpad prism v6.

# CHAPTER 4

# Chondrocyte hedgehog signalling requires the primary cilium and is regulated by mechanical strain

## 4.1 Introduction

The role of primary cilia in skeletal development is well established (for review see (Haycraft and Serra 2008)). This is largely due to the influence this organelle has over hedgehog signalling as this pathway regulates key steps in bone formation. However, primary cilia are rapidly coming into focus as essential mediators of chondrocyte function in adult cartilage. In 2012 studies from the Knight lab demonstrated a role for the cilium in the mechanotransduction pathway which acts downstream of mechanosensitive ATP release to regulate $Ca^{2+}$ signalling and gene expression (Wann et al. 2012). Moreover, subsequent studies have shown cilia to be key modulators of inflammatory signalling in chondrocytes (Wann and Knight 2012). These *in vitro* studies complement prior *in vivo* work which suggests the cilium is important for both the formation and maintenance of the articular cartilage and highlight the potential role abnormalities in cilia structure and function may have on the pathogenesis of OA (McGlashan et al. 2007; Chang et al. 2012).

Although hedgehog signalling has been implicated in the initiation and progression of osteoarthritis, its role in healthy adult tissues has not been well characterised. During development, hedgehog signalling is regulated by mechanical stimuli. In osteoarthritic cartilage the mechanical environment of the chondrocyte is altered, suggesting deregulation of this response in articular chondrocytes. Indeed, increased Ihh expression is associated with very early focal cartilage degeneration at the articular surface suggesting the upregulation of Ihh may be one of the earliest markers of OA (Tchetina et al. 2005). However despite this, the effects of mechanical stimuli on Ihh expression and hedgehog pathway activation have not previously been studied in articular chondrocytes.

## 4.2 Aims and Objectives

The aim of this chapter was to investigate the effects of mechanical strain on hedgehog signalling in articular chondrocytes isolated from healthy joints. We hypothesised that Ihh expression is mechanosensitive in adult cells and that hedgehog signalling is activated by mechanical stimuli.

The first objective of this study was to determine if primary articular chondrocytes from healthy adult tissues possess the necessary machinery for hedgehog signalling, can respond to ligand stimulation and to verify the role of the primary cilium in this response.

The second objective was to characterise chondrocyte primary cilia expression in short-term 2D cell culture and to determine the optimal conditions for cilia expression in subsequent experiments. The effects of serum starvation, cell density and short-term culture on chondrocyte ciliation were studied.

The third objective was to develop a 2D mechanical loading model and to investigate the effects of mechanical strain on Ihh expression.

## 4.3 Results

### 4.3.1 Characterising chondrocyte hedgehog signalling in 2D culture

To confirm the expression of Ihh in bovine articular chondrocytes, total RNA was extracted from freshly isolated cells from two different animals and subjected to RT-PCR. Relative to GAPDH, Ihh expression was low but detectable in both animals (Figure 4.1). Shh and Dhh expression were not detected.

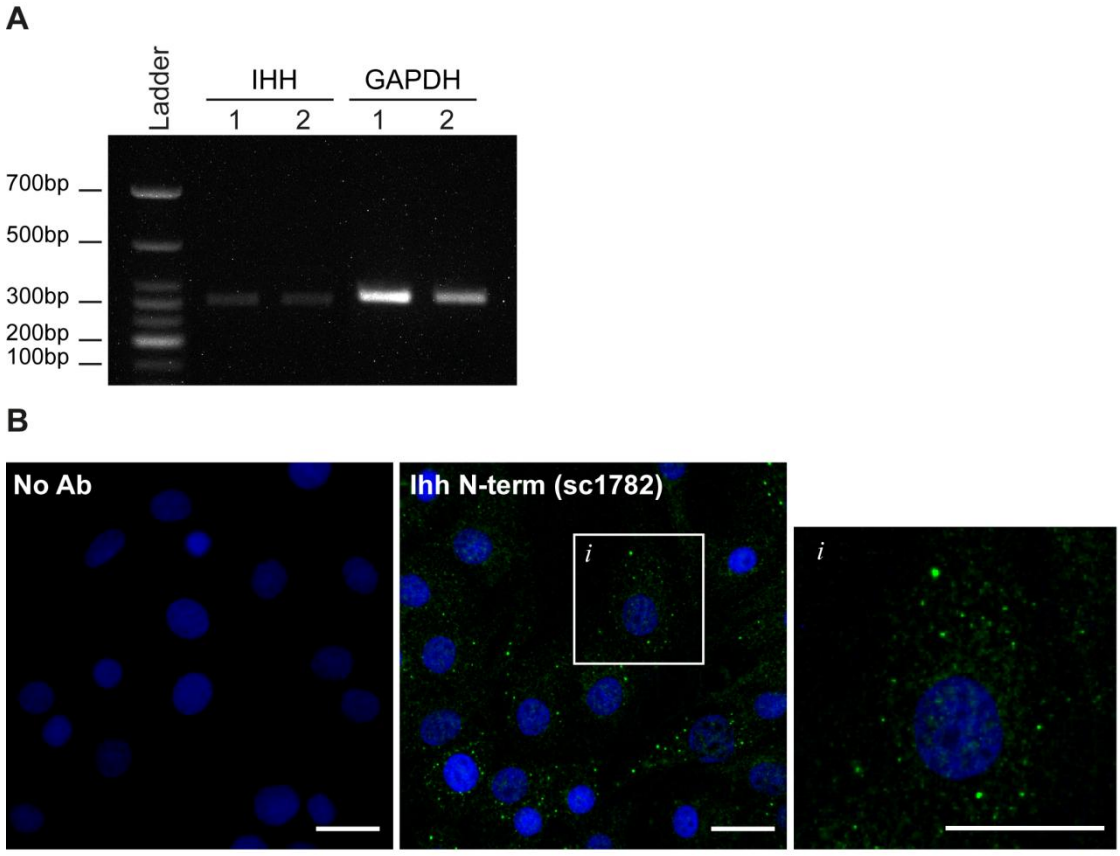


**Figure 4.1 Articular chondrocytes express Ihh**
**(A)** The expression of Ihh was assessed in freshly isolated bovine articular chondrocytes by RT-PCR. GAPDH expression was also examined as a positive control. **(B)** Freshly isolated bovine articular chondrocytes were cultured for six days then fixed and immunofluorescently labelled for Ihh using an N-terminally directed antibody (sc1782, green). Nuclei were counterstained with DAPI and cells were imaged on a Leica SP2 confocal microscope. Inset (i) highlights a single cell to more clearly demonstrate the distribution of Ihh staining. Scale bar represents 20µm.

Ihh protein expression was examined further using a polyclonal antibody directed to the N-terminal portion of the Ihh protein (Santa Cruz, Sc1782). The active hedgehog signal is contained within this region and this antibody should recognise both full length, unprocessed Ihh (~42kDa) and the lipid modified signalling protein (15-20kDa). Ihh protein expression was analysed by both western blotting and cytology. Ihh protein expression was not detectable by western blotting most likely due to its low abundance. However, immunocytochemistry revealed punctate cytoplasmic staining throughout the cell reminiscent of secretory vesicles (Figure 4.1). This staining was similar to that observed with other N-terminally directed antibodies in human cell lines (personal communication, Dr K.F.Cogger). While western blotting was attempted with other C-terminally directed antibodies multiple high intensity non-specific bands were detected in bovine samples and it was not possible to identify a band specific to Ihh.

To confirm the expression of the major hedgehog pathway components in articular chondrocytes, total RNA was extracted from these cells and subjected to RT-PCR. Low but detectable expression of the hedgehog receptor Ptch1 was observed, and the expression of Smo, Gli2 and Gli3 were readily detectable (Figure 4.2).

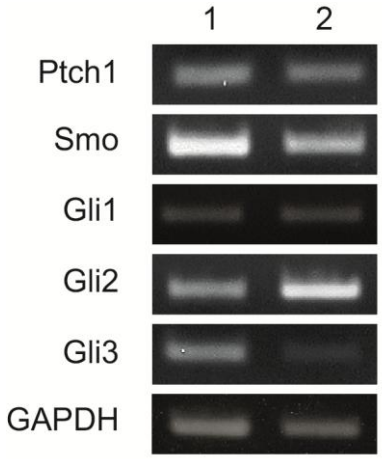


**Figure 4.2 Articular chondrocytes express the major components of the hedgehog signalling pathway**
The expression of the major hedgehog pathway components was examined by RT-PCR in chondrocytes isolated from two different steers (lanes 1 and 2).

#### 4.3.1.1 Chondrocyte hedgehog signalling is activated in response to agonist

To determine if articular chondrocytes were capable of responding to agonist stimulation, chondrocytes were treated with recombinant Indian hedgehog (r-Ihh) ligand (Figure 4.3). Real time PCR was used to examine the expression of Ptch1 and Gli1 as a measure of pathway activation. Freshly isolated chondrocytes were cultured for 5 days then treated for a further 24hrs with 1µg/ml r-Ihh. Ptch1 gene expression was increased by 5.13-fold following r-Ihh treatment (p=0.005) while Gli1 gene expression was increased by 5.4-fold (p=0.004) relative to the untreated control (Figure 4.3). Both differences were statistically significant indicating the hedgehog pathway was activated.

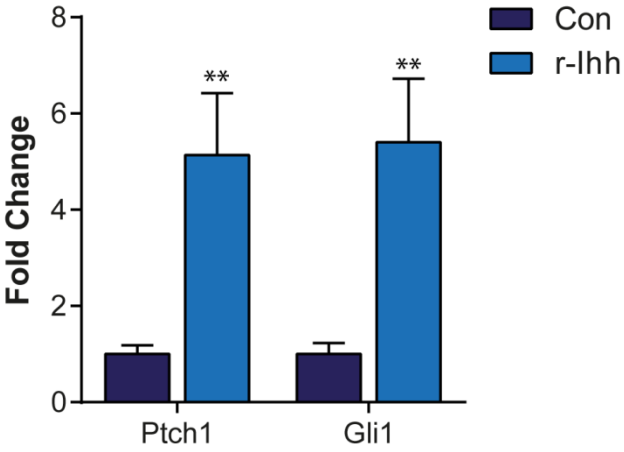


**Figure 4.3 Recombinant Ihh protein activates hedgehog signalling in articular chondrocytes**
Freshly isolated chondrocytes were cultured for 5 days then treated for a further 24hrs with 1µg/ml r-Ihh. Pathway activation was monitored using qRT-PCR for Gli1 and Ptch1 gene expression. Data represents mean ±S.E.M (n=12 experimental replicates from 2 independent experiments). Statistical significance was determined using a Student's T test.

#### 4.3.1.2 Chondrocyte hedgehog signalling requires the primary cilium

An immortalised mutant chondrocyte cell line generated from the $Tg737^{ORPK}$ mouse was used to verify the role of the primary cilium in chondrocyte hedgehog signalling. These cells, kindly donated by CJ Haycraft (University of Alabama), possess a hypomorphic mutation in the gene encoding IFT88 (McGlashan et al. 2007; Wann and Knight 2012). As a consequence of this mutation, primary cilia are either absent or severely truncated in mutant (ORPK) cells (Figure 4.4A). In wild-type (WT) cells approximately 80%±19 of cells exhibit a primary cilium

compared with just 13±13% of ORPK cells (Figure 4.4B). Mean cilia length in WT cells is 2.98µm±0.94, compared to 1.99µm±0.78 in ORPK cells (Figure 4.4C).

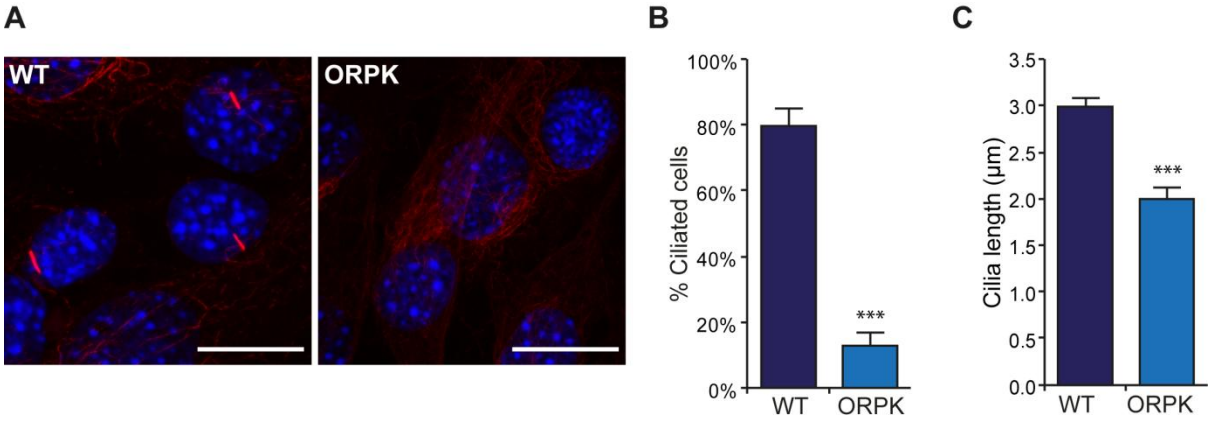


**Figure 4.4 Primary cilia are absent or severely truncated in ORPK chondrocytes**
WT and ORPK chondrocytes were cultured for 4days in the absence of IFN-ɣ. **(A)** Cells were fixed and immunofluorescently labelled for acetylated α-tubulin to detect primary cilia (red) and nuclei were counterstained with DAPI (blue). Scale bar represents 20µm. **(B)** Primary cilia prevalence was quantified in 10 representative fields of view and expressed as mean ±S.E.M. Statistical significance was assessed using Student's T-test. **(C)** Primary cilia length was quantified from 3D confocal images. Data is presented as mean ±S.E.M , n=~100 cilia for each condition. Statistical significance was assessed using Mann Whitney U test.

WT and ORPK chondrocytes were cultured for 4 days in the absence of IFN-ɣ then treated for a further 24hrs with 1µg/ml r-Ihh. In WT chondrocytes, Ptch1 and Gli1 gene expression were significantly increased in r-Ihh treated cultures by 1.59 and 3.57-fold respectively relative to the untreated control, these differences being statistically significant (Ptch1: p=0.03, Gli1: p=0.0057, Figure 4.5). However, no significant changes in the expression of Ptch1 and Gli1 were observed in ORPK chondrocytes relative to the untreated control indicating theses cells are not able to respond to ligand stimulation.

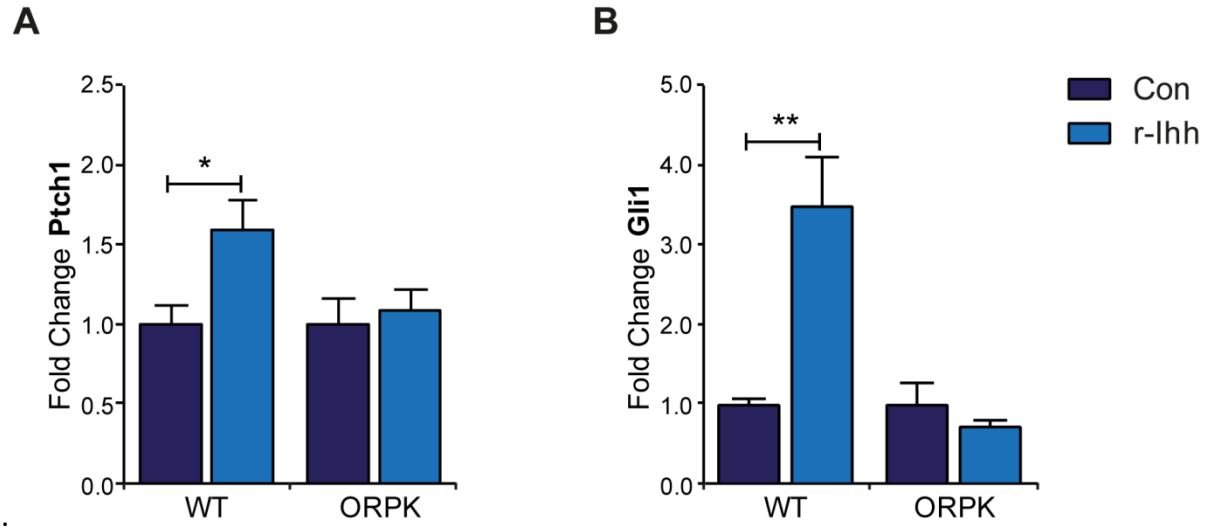


.

**Figure 4.5 ORPK chondrocytes do not respond to r-Ihh stimulation**
WT and ORPK chondrocytes were cultured for 4days in the absence of IFN-ɣ then treated for a further 24hrs with 1µg/ml r-Ihh. Total RNA was isolated and changes in the gene expression of **(A)** Ptch1 and **(B)** Gli1 were assessed by qRT-PCR. Data represents mean ±S.E.M (n=6 replicates). Statistical significance was determined using a Student's T test.

In untreated cells the expression ratios for Ptch1 and Gli1 were often found to be higher in ORPK chondrocytes relative to WT however this did not reach statistical significance (Figure 4.6AB). As the primary cilium is required for both the formation of Gli activators and repressors, cilia disruption often results in aberrant pathway activation (Haycraft et al. 2005; Caspary et al. 2007; Tran et al. 2008; Chang et al. 2012). The increase in Ptch1 and Gli1 expression in ORPK chondrocytes suggests this is likely the case in these cells. To investigate this further, western blotting was performed to examine the proteolytic processing of Gli3. In the absence of hedgehog signals, full length Gli3 (Gli3FL, 170-190kDa) is processed to Gli3R (~80kDa) and gene transcription is inhibited (Wang et al. 2000). In the presence of hedgehog ligand this processing is inhibited and the full length protein accumulates altering the Gli3R:Gli3FL ratio. Low-level Gli3 expression was observed in both WT and ORPK chondrocytes and 190 and 80kDa bands were visible (Figure 4.6C). Densitometry was used to quantify band intensity and the Gli3R:Gli3FL ratio determined, this ratio was significantly lower in ORPK compared to WT chondrocytes indicating Gli3 processing is disrupted (Figure 4.6C).

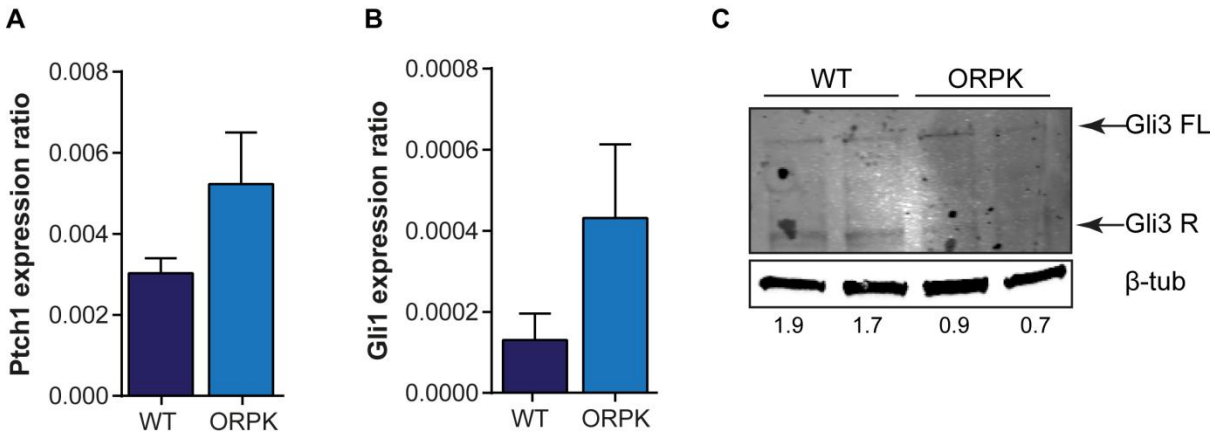


**Figure 4.6 ORPK chondrocytes exhibit elevated hedgehog signalling in the absence of ligand**

WT and ORPK chondrocytes were cultured in the absence of IFNɣ for five days then lysed and processed for RNA and protein extraction. The expression of **(A)** Ptch1 and **(B)** Gli1 were analysed my real time PCR. Data represents mean ±S.E.M (n= 18 replicates). Statistical significance was assessed using a student's T-test. **(C)** Gli3 processing was analysed by western blotting, the Gli3R:FL ratio is shown beneath each column, β-tubulin expression was used as a loading control.

### 4.3.2 Optimising primary cilia expression in 2D cell culture

Double immunofluorescence was performed on bovine articular cartilage explants (Figure 4.7) and isolated chondrocytes in 2D culture (Figure 4.8) to verify the expression of primary cilia in articular chondrocytes, and to validate the use of antibodies commonly used for the detection of ciliary axonemes. Primary cilia were labelled for acetylated α-tubulin and Arl13b. Consistent with the literature, primary cilia were present on chondrocytes *in vivo* (Figure 4.7). Cilia were also present on chondrocytes *in vitro* and were more easily identified due to the spread morphology of the cell (Figure 4.8). The level of tubulin acetylation is higher within the cilium compared to the rest of the cell, thus ciliary staining is more intense and easily distinguished from the cell body in 2D culture. However, it is more difficult to reliably identify a cilium in tissue as the cytoplasmic acetylated tubulin appears more intense, probably due to the rounded morphology of the cell, and this often obscures the cilium.

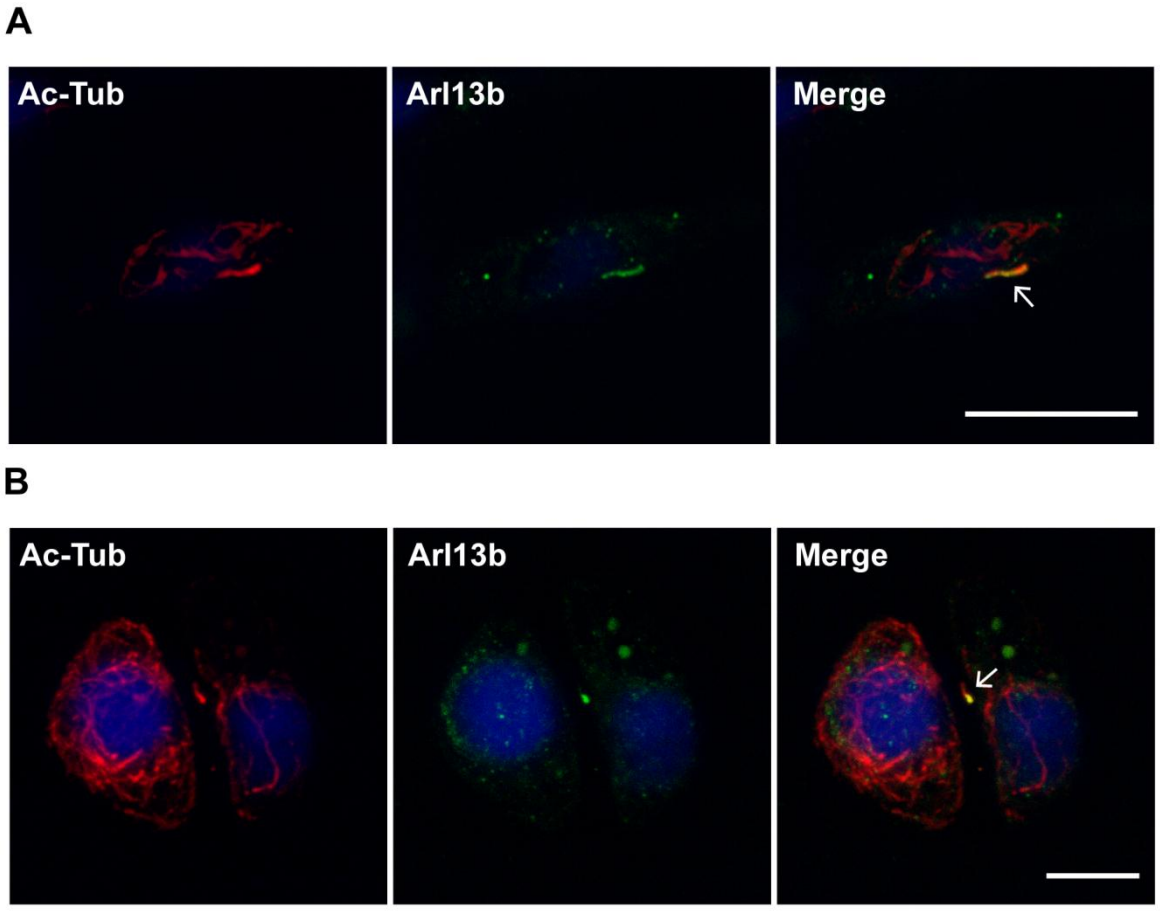


**Figure 4.7 Articular chondrocytes exhibit primary cilia in vivo**
Freshly isolated articular cartilage was removed from the proximal surface of the joint, fixed and snap frozen for embedding and sectioning. Chondrocyte primary cilia (white arrows) were labelled in 20µm thick sections using antibodies directed against both acetylated α-tubulin (red) and Arl13b (green). Nuclei were counter-stained with DAPI. (A) A primary cilium in a discoidal shaped superficial zone chondrocyte. (B) A primary cilium between two cells within a single chondron in the middle/deep zone. Scale bar represents 5µm.

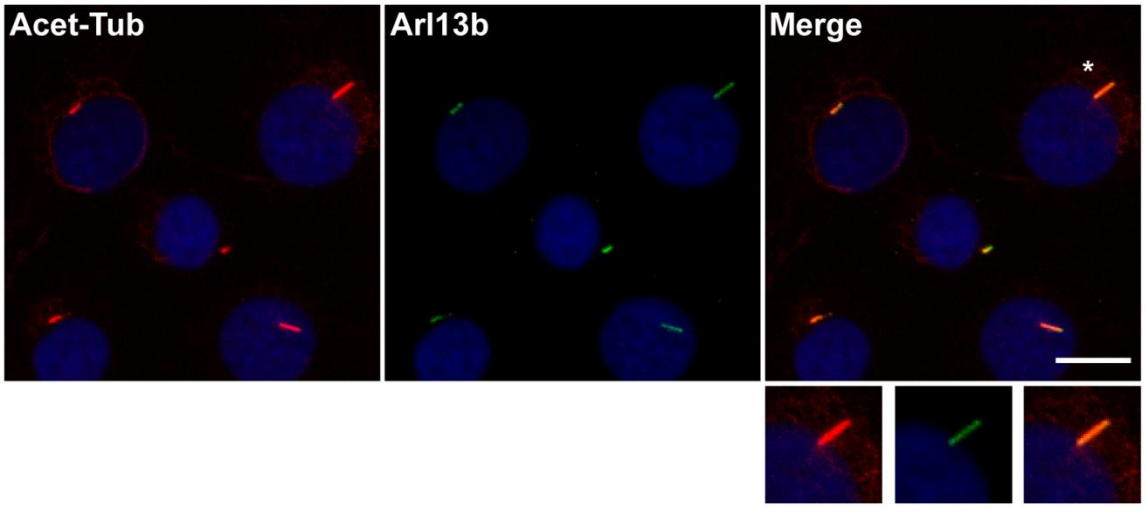


**Figure 4.8 Articular chondrocytes exhibit primary cilia in 2D cell culture**
Freshly isolated bovine articular chondrocytes were cultured for six days then fixed and immunofluorescently labelled for primary cilia. Two ciliary markers were used; acetylated α-tubulin (red) and Arl13b (green). Asterix indicates the cilium chosen for enlargement under the merged image. Nuclei were counterstained with DAPI. Scale bar represents 10µm.

Arl13b is a membrane associated GTPase found within the cilium in numerous cell types. It is important for ciliogenesis and cilia maintenance and has been implicated in hedgehog signalling (Caspary et al. 2007; Larkins et al. 2011). Arl13b labelled cilia both *in vivo* and *in vitro* (Figure 4.7 and Figure 4.8). In 2D culture, Arl13b and acetylated tubulin staining fully co-localised in the majority of cilia (insert, Figure 4.8), however staining was often weaker and less uniform *in vivo* although it represents a useful additional marker to confirm the identity of cilia (Figure 4.7).

The basal body markers, ɣ-tubulin and pericentrin, were also tested however a compatible staining protocol could not be identified for both basal body and axoneme markers. Basal bodies were only labelled successfully in bovine articular chondrocytes using methanol fixation, which disrupted cytoplasmic microtubules and actin and gave cilia a distorted appearance (not shown). Basal body markers are often used to help with the identification of primary cilia. However given the specificity of the axoneme markers in 2D culture (Figure 4.8) basal body staining was not considered to be necessary to identify cilia and therefore was not used in subsequent studies.

While primary cilia are present on nearly every cell type in the mammalian body, they are not typically found on proliferating cells (Wheatley et al. 1996). Therefore a common approach to studying these organelles *in vitro* is to serum-starve cultures to inhibit cell cycle entry and promote ciliation. I examined the effects of serum starvation on chondrocyte ciliation in 2D culture to determine if cilia length and prevalence could be similarly increased. Freshly isolated bovine chondrocytes were cultured for 5 days then subjected to serum starvation for a further 24 hrs prior to fixation. The cilium was immunofluorescently labelled with antibodies directed against acetylated α-tubulin. In the presence of serum, 75%±13 of cells exhibited a primary cilium with a mean length of 1.88μm±0.7. There was no significant difference in either the length or prevalence of cilia in cultures with or without serum starvation (Figure 4.9). These data indicate that serum starvation is not essential for the study of primary cilia in chondrocytes.

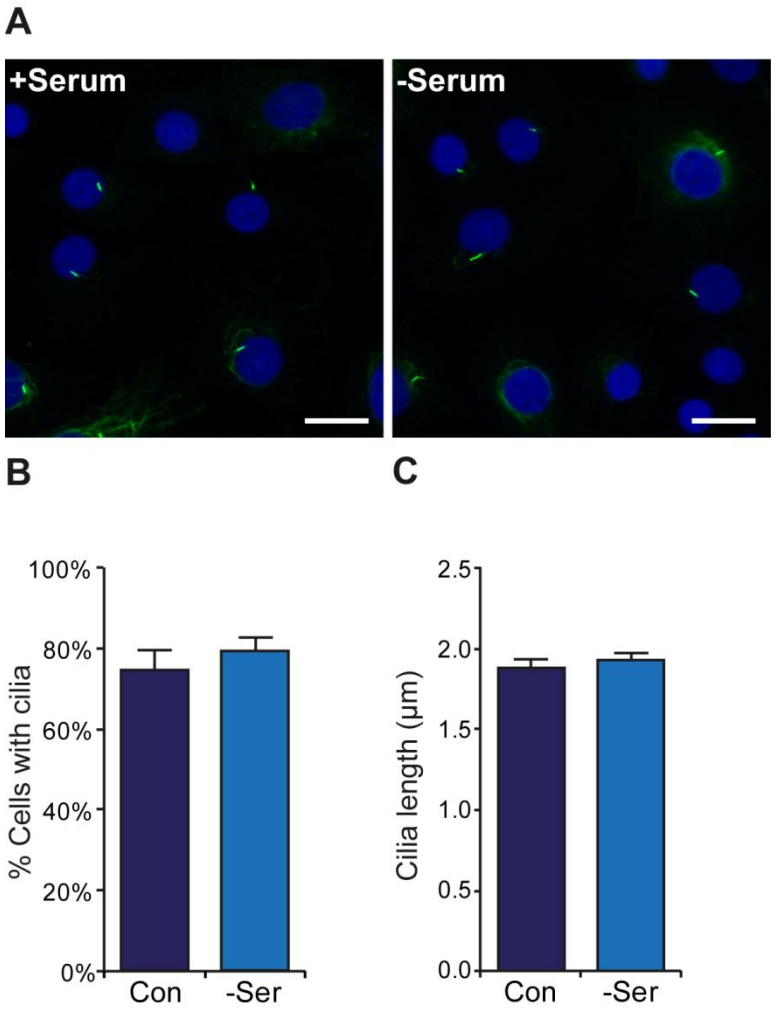


**Figure 4.9 Serum starvation does not influence chondrocyte primary cilia in 2D cell culture** Freshly isolated chondrocytes were cultured for 5 days in the presence of serum. On the fifth day, the media was removed and replaced with serum-free media and cells were cultured for a further 24hrs. Control cells were cultured in an identical manner but in the presence of serum. **(A)** Cells were fixed and primary cilia were immunofluorescently labelled for acetylated α-tubulin. **(B)** Primary cilia prevalence was quantified in 10 representative fields of view and expressed as mean ±S.E.M. Statistical significance was assessed using Student's T-test. **(C)** Primary cilia length was quantified from 3D confocal images. Data is presented as mean ±S.E.M , n=~100 cilia for each condition. Statistical significance was assessed using Mann Whitney U test.

The confluence of cell cultures has been used similarly to induce cell cycle arrest through contact inhibition and thus promote ciliation. Correlation between cell density and the proportion of ciliated cells in a population has been observed previously (Tucker et al. 1979; Wheatley et al. 1994; Pitaval et al. 2010). To examine the effects of cell density on primary cilia expression in articular chondrocytes, cells were seeded at a range of densities from low

($25x10^3$cells/$cm^2$) to high ($150x10^3$cells/$sm^2$) and cultured for 4 days. This time point was chosen to limit the influence of cell cycle status on ciliation. While chondrocyte proliferation increases in 2D culture associated with dedifferentiation, significant increases in cell number are not observed until after day 4 (not shown) therefore most cells remain in interphase and approximate cell seeding density is maintained.

Cells seeded at $25x10^3$ cells/$cm^2$ were significantly less ciliated than cells seeded at $50x10^3$ cells/$cm^2$. However, there was no significant difference in the proportion of ciliated cells between the $50x10^3$ and $80x10^3$ cells/$cm^2$ densities. At seeding densities above $50x10^3$ cells/$cm^2$ ciliation remained stable with 70-75% of cells expressing cilia. These data indicate that chondrocyte ciliation is affected only at very low cell seeding densities; such conditions were avoided in subsequent experiments.

Chondrocyte primary cilia length and prevalence increase with cartilage depth (McGlashan et al. 2008; Farnum and Wilsman 2011). In bovine patellae cartilage, primary cilia length is highest in the deep zone where cilia are present on 65% of cells with a mean length of 1.6μm (McGlashan et al. 2008). Although the chondrocytes examined in this study comprise a heterogeneous population of cells from all cartilage zones, this value is lower than the mean value of 1.88μm observed in 2D culture which suggests cilia length and prevalence are increasing during short-term culture. To investigate this further, freshly isolated chondrocytes were seeded at $80x10^3$ cells/$cm^2$ and cultured for up to 12 days without passage. Changes in primary cilia length and prevalence were examined during this time.

Primary cilia were exhibited by 55±9% of cells 24 hrs after isolation (day 1). The level of ciliation progressively increased during short term culture peaking at 78%±5 on day 3 (Figure 4.11). The proportion of ciliated cells remained constant between days 3 and 12. Similarly, cilia length was significantly increased between day 1 and day 3 with mean values of 1.14±0.3μm and 1.4±0.5μm respectively. Cilia length continued to increase peaking at 1.92μm±0.6 following 6 days in culture. There was no significant difference in cilia length between day 6 and day 12.

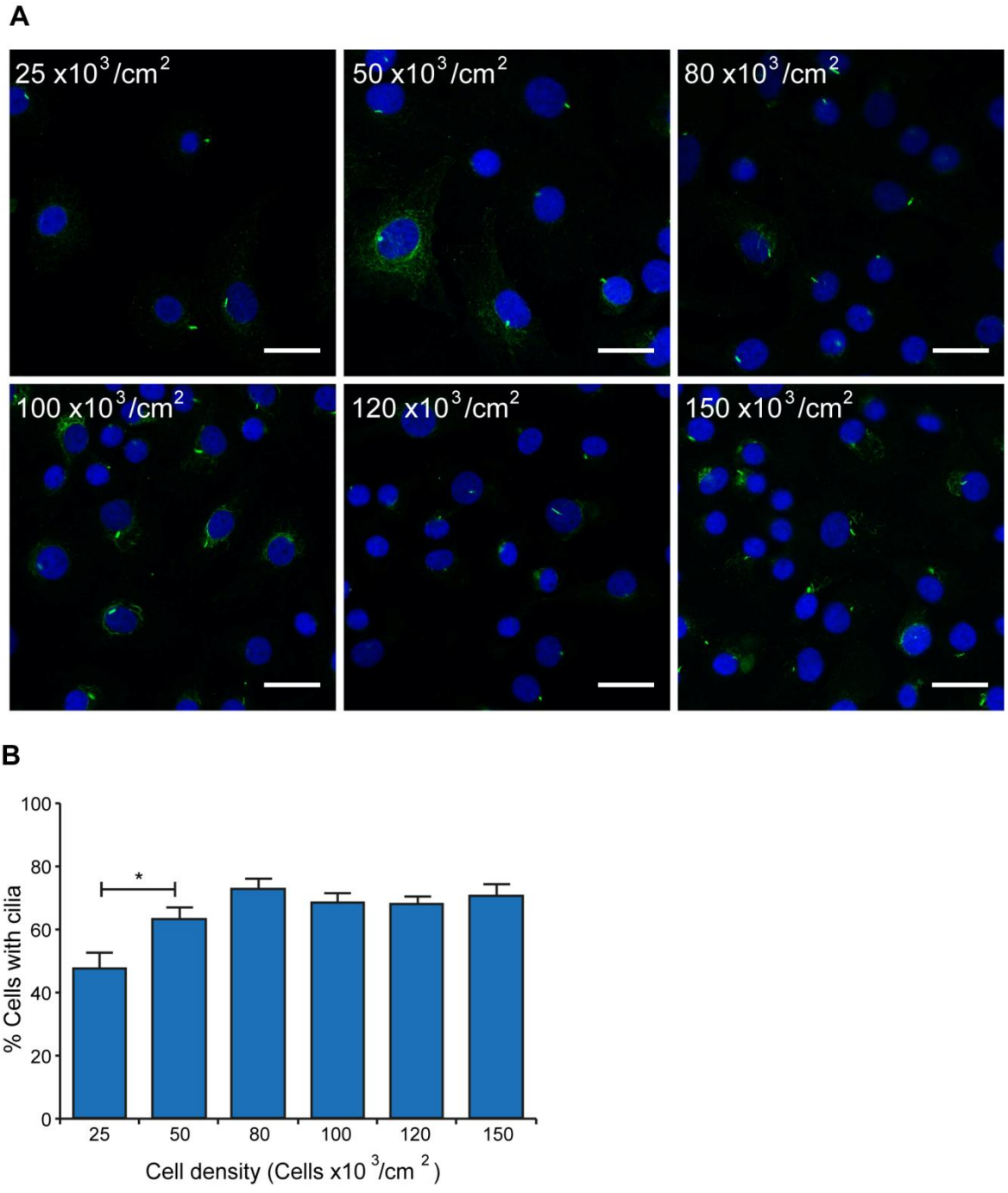


**Figure 4.10 Low cell density influences chondrocyte cilia prevalence**
Freshly isolated chondrocytes were seeded at varying cell densities and cultured for 4 days in the presence of serum. **(A)** Primary cilia were immunofluorescently labelled for acetylated α-tubulin and nuclei were stained with DAPI (blue). Scale bar represents 20μm. **(B)** Primary cilia length was quantified from 3D confocal images and expressed as mean ±S.E.M (n≥100 cilia). Statistical significance was assessed using Student's T-test.

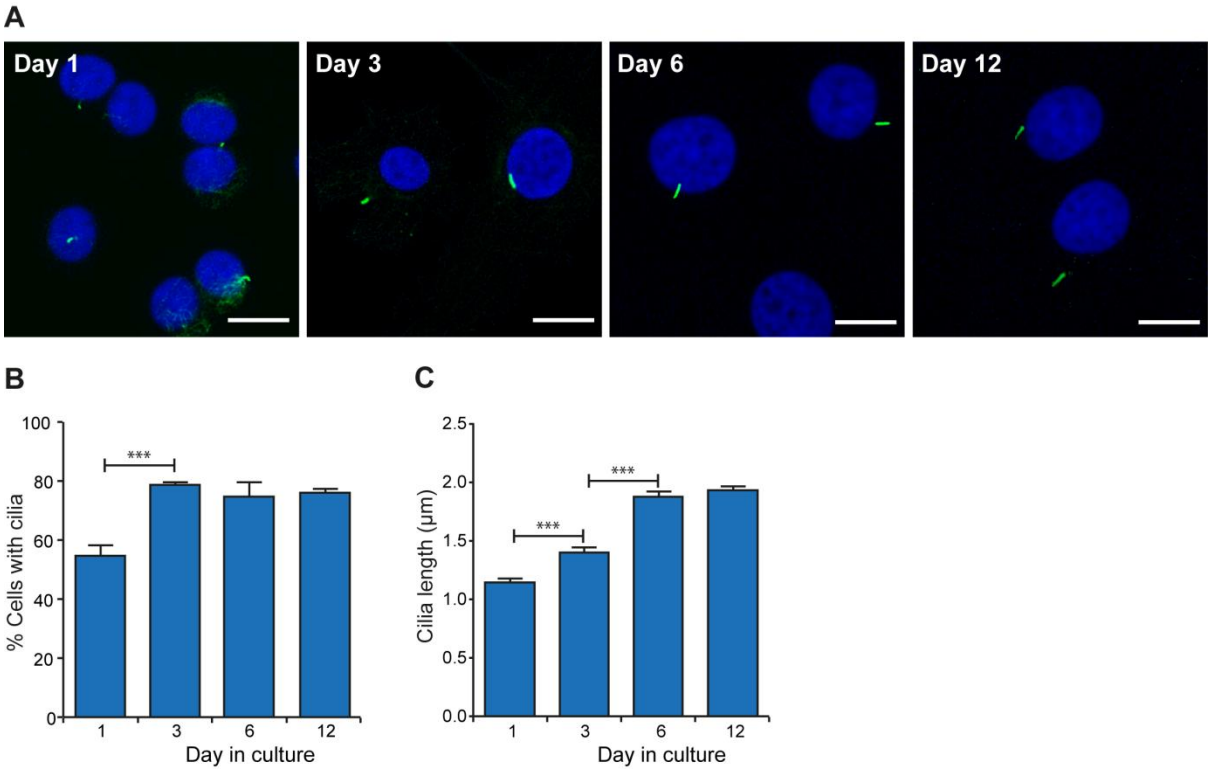


**Figure 4.11 Primary cilia length and prevalence increase with short-term culture**
Freshly isolated chondrocytes were cultured for up to 12 days in the presence of serum. **(A)** Cells were fixed at day 1, 3, 6, 9 and 12 and primary cilia were immunofluorescently labelled for acetylated α-tubulin. **(B)** Primary cilia prevalence was quantified in 10 representative fields of view and expressed as mean ±S.E.M. Statistical significance was assessed using Student's T-test. **(C)** Primary cilia length was quantified from 3D confocal images. Data is presented as mean ±S.E.M (n≥100 cilia). Statistical significance was assessed using Mann Whitney U test.

### 4.3.3 Characterisation of a 2D mechanical loading model

To investigate the influence of mechanical strain on Ihh expression in articular chondrocytes the Flexcell™ system was used. Freshly isolated articular chondrocytes were seeded at $80x10^3$ cells/$cm^2$ and cultured for 6 days on collagen coated Bioflex plates. These conditions were selected as they encourage optimal levels of ciliation and provide chondrocytes enough time to spread and attach to elastic membranes (see section 4.3.2), but not so long that cultures become overly confluent.

Chondrocytes were subjected to 10% mechanical strain for 1hr at 0.33Hz. Unfortunately, in the initial runs of these experiments large numbers of cells detached from the membrane

during loading. To improve attachment, the Bioflex plates were further coated with 10µg/ml collagen type I prior to cell seeding which solved this issue. On re-coated membranes, cells continued to exhibit a polygonal morphology and did not appear fibroblastic (Figure 4.12A) moreover neither the number of ciliated cells nor mean cilia length was altered (not shown). Significant cell detachment was not observed and gross cell morphology was not altered by loading (Figure 4.12A). Cell attachment was quantified by two means, firstly by comparing normalised cell density between the strained and unstrained samples and secondly by examining DNA content. There was no significant difference in the number of cells/cm$^2$ in the strained samples relative to the unstrained control (Figure 4.12B). Moreover, DNA content, measured 24hrs from the start of loading, was not significantly different from unstrained samples further (Figure 4.12C). Together these data indicate that cell attachment is maintained during the loading procedure.

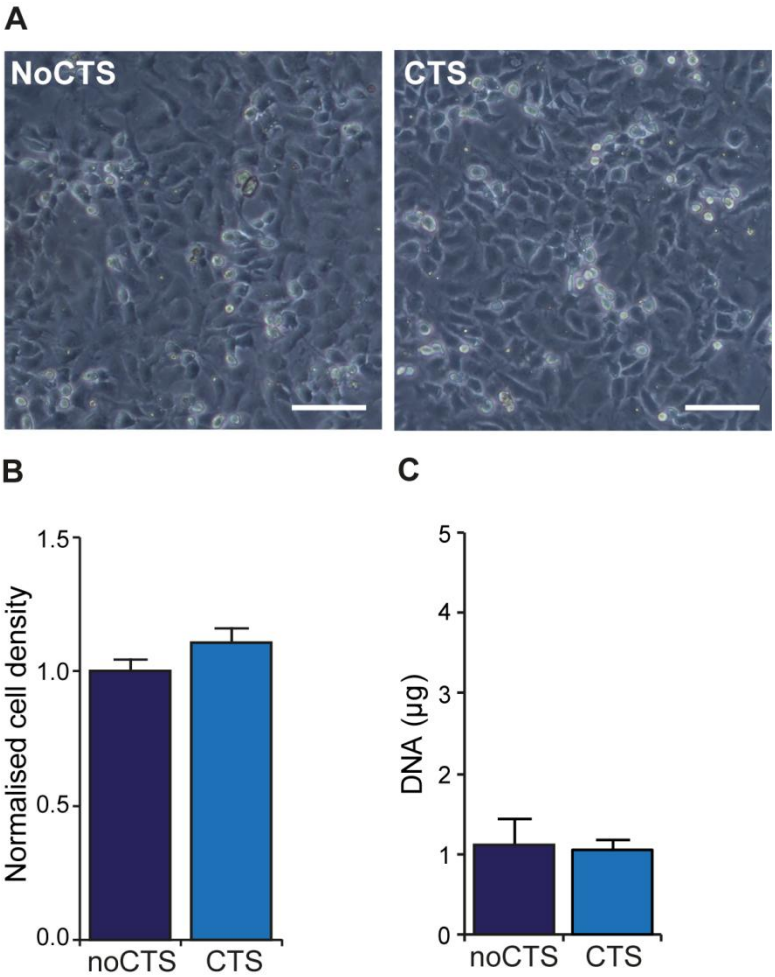


**Figure 4.12 Mechanical strain does not trigger cell detachment**
Freshly isolated bovine articular chondrocytes were subjected to mechanical strain for 1hr. **(A)** Bright field images of strained and unstrained chondrocytes 24hrs post loading. **(B)** Following mechanical strain, cells were fixed and nuclei labelled with DAPI. The number of nuclei were quantified in 10 representative fields of view and expressed as fold change relative to the mean of the unloaded control. Scale bar represents 100µm. **(C)** DNA content was quantified 24hrs after the start of loading n=10 replicates from 2 independent experiments. Data represents mean ±S.E.M and statistical significance was assessed using a student's T-test.

Changes in actin cytoskeletal organisation were monitored post loading to determine if mechanical strain resulted in the formation of stress fibres. The actin cytoskeleton was visualised using AlexaFluor555 conjugated phalloidin (Figure 4.13). There was no obvious difference in actin organisation between strained and unstrained samples. Actin staining was heterogeneous within a cell population both in intensity and structural organisation. Between 15 and 20% of cells exhibited a rounded morphology with more intensely stained cortical actin while the majority showed a spread or flattened morphology. These cells typically exhibited diffuse cytoplasmic staining however stress fibre formation was apparent in some cells. In an attempt to quantify changes in actin organisation following strain, cells were grouped into four categories, namely: cortical organisation, diffuse cytoplasmic organisation, mild fibre formation (some low intensity, stress fibre formation throughout the cell) and intense fibre formation (intensely stained actin cables) (Figure 4.13B). There were no statistically significant differences in the percentage of cells in each group between strained and unstrained cultures (p=0.8092).

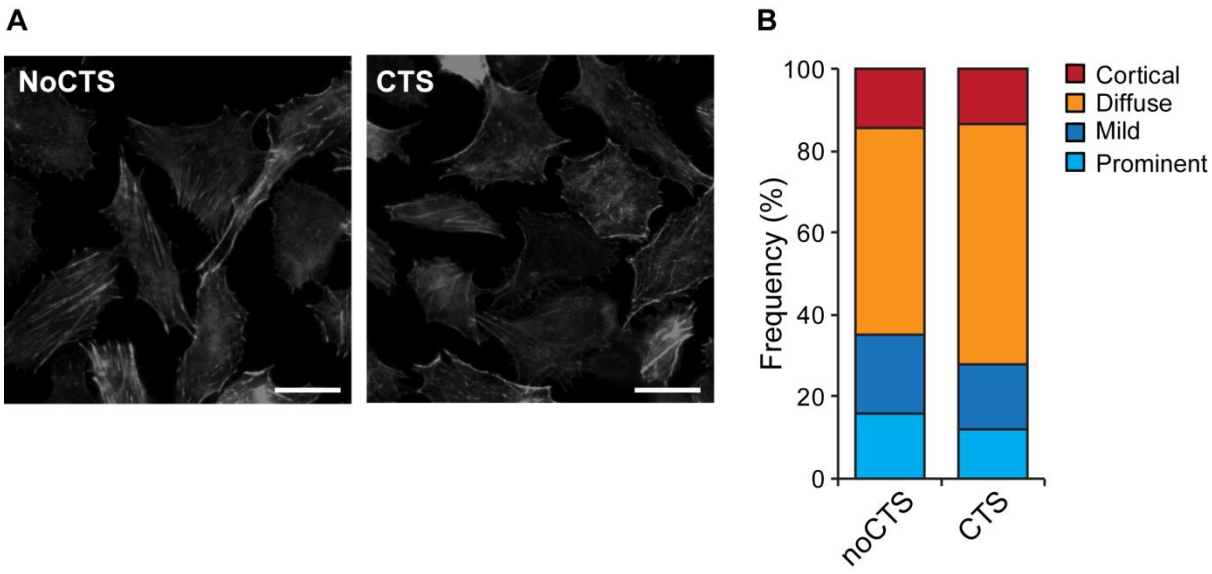


**Figure 4.13 Actin organisation is not dramatically altered by mechanical strain**
Freshly isolated chondrocytes were subjected to 10% mechanical strain for 1hr then immediately fixed and processed for immunofluorescent staining of actin. **(A)** The actin cytoskeleton was labelled with Alexa555 conjugated phalloidin. Scale bar represents 20µm. **(B)** Cytoskeletal organisation was examined in strained and unstrained samples and grouped into cortical, diffuse, mild stress fibre formation and prominent stress fibre formation (n=60 cells). Statistical signifcance was assessed using a Chi-square Test.

Chondrocyte viability was assessed following mechanical loading using Ethidium homo-dimer (EthD-1) as a marker for cell death. Viability was assessed in strained and unstrained groups immediately after loading. There was no significant difference in the proportion of EthD1 positive cells in the strained samples relative to the unstrained control indicating mechanical strain does not induce cell death (Figure 4.14).

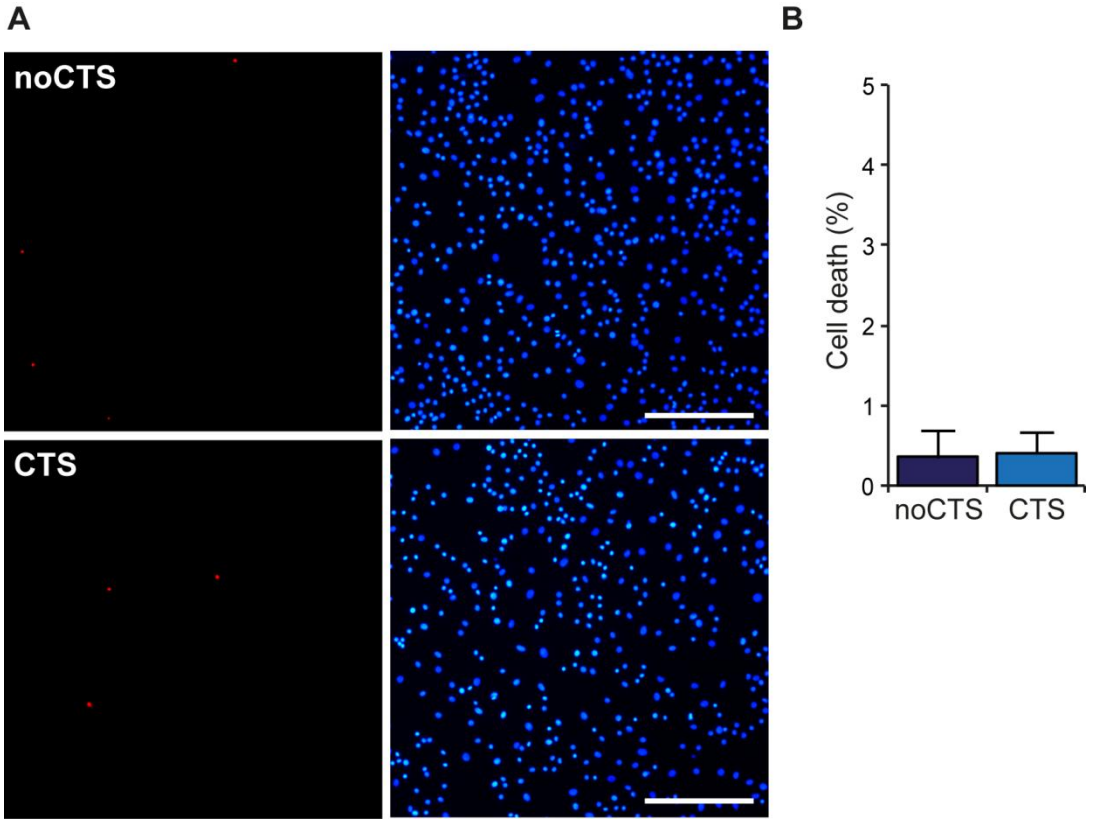


**Figure 4.14 Mechanical strain does not alter chondrocyte viability**
Freshly isolated bovine articular chondrocytes were cultured for six days then subjected to mechanical strain for 1hr. **(A)** Following mechanical strain, cell viability was assessed using ethidium homodimer-1 (red) and nuclei were counter stained with DAPI (blue). Scale bar represents 200µm. **(B)** The number of nuclei and the number of EtHD-1 positive cells was quantified in 10 representative fields of view. Data represents mean ±S.E.M and statistical significance was assessed using a student's T-test.

To determine if the loading regime was sufficient to activate mechanotransduction, changes in the expression of the matrix genes collagen type II and aggrecan were assessed using real time PCR. These genes have been shown to be upregulated as an early component of the mechanotransduction response in numerous *in vitro* and *in situ* chondrocyte loading models (Millward-Sadler et al. 2000; Tanaka et al. 2005; Huang et al. 2007). Following the application of 10% mechanical strain for 1hr the expression of collagen II and aggrecan were increased by 1.90 and 1.82-fold respectively relative to the unstrained control (Figure 4.15AB). These differences were statistically significant ($p \leq 0.0001$). The increase in aggrecan gene expression was not associated with a change in sGAG content measured in the media after a further 24hrs in culture in the absence of strain (Figure 4.15C). This suggests that changes in the expression of aggrecan are reversible following the removal of load.

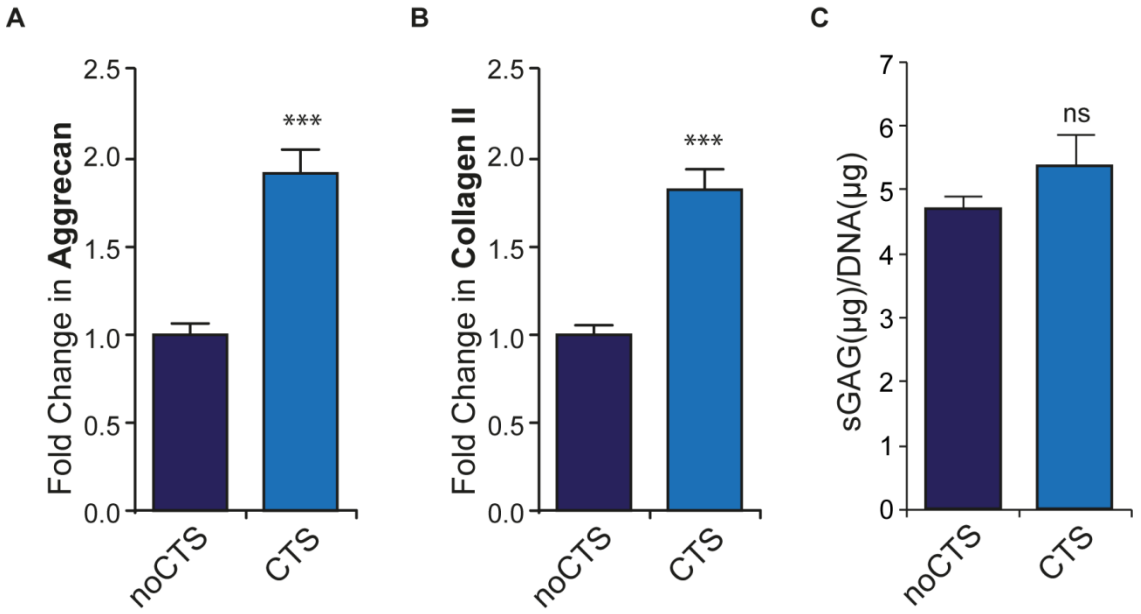


**Figure 4.15 Mechanical strain upregulates the expression of matrix genes**
Freshly isolated bovine articular chondrocytes were cultured for six days then subjected to mechanical strain for 1hr. Total RNA was isolated from cells immediately after loading and sunbjected to real time PCR for **(A)** Aggrecan and **(B)** Collagen type II. **(C)** Following mechanical strain chondrocytes were cultured for a further 24hrs in the absence of strain and the total sGAG production quantified and normalised to DNA. Data represents mean ±S.E.M and statistical significance was assessed using a student's T-test.

### 4.3.4 Mechanical strain upregulates Ihh expression and activates hedgehog signalling

Previous studies have shown mechanical loading regulates the expression of Ihh in chondrocytes isolated from developing tissues (Wu et al. 2001; Shao et al. 2011). Significant increases in Ihh expression were observed in rat growth plate chondrocytes as early as 30min from the start of loading and Ihh expression was found to correlate with an increase in the duration of load (Shao et al. 2011). Real time PCR was use to assess the effects of mechanical strain on hedgehog signalling in articular chondrocytes. Ihh gene expression was increased by 1.9 fold following 10% CTS for 1hr (Figure 4.16A). This was accompanied by significant increases in the expression of Ptch1 and Gli1 ($p \leq 0.05$) indicating the hedgehog signalling pathway was activated (Figure 4.16B).

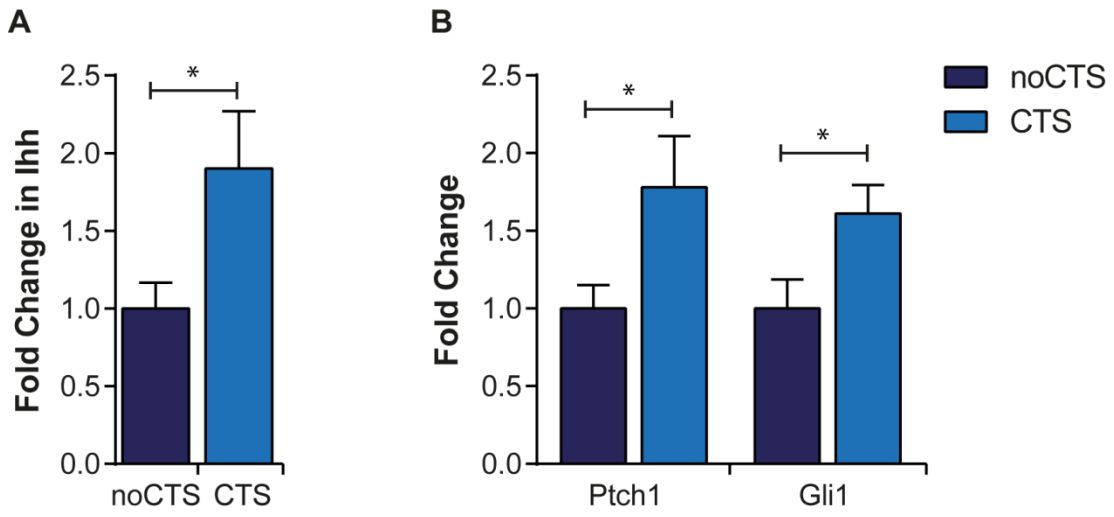


**Figure 4.16 Mechanical strain upregulates Ihh expression and activates hedgehog signalling**
Freshly isolated bovine articular chondrocytes were cultured for six days then subjected to mechanical strain for 1hr. Total RNA was isolated from cells immediately after loading and subjected to real time PCR for **(A)** Ihh and **(B)** Ptch1 and Gli1. Data represents mean ±S.E.M and statistical significance was assessed using a student's T-test.

## 4.4 Discussion

In this chapter I have determined the optimal conditions for the study of chondrocyte primary cilia in 2D culture investigating factors including culture duration, seeding density and serum starvation. I have successfully developed an *in vitro* mechanical loading model with which to subject cultured cells to mechanical strain and have shown that Ihh expression is increased by mechanical stimuli in articular chondrocytes.

### 4.4.1 Characterisation of chondrocyte primary cilia in a 2D cell culture model

In 2D cell culture the majority of chondrocytes were ciliated, although primary cilia length was highly variable ranging from 0.5-5µm with a mean length of 1.88µm. Reports of chondrocyte cilia length and prevalence in the literature vary greatly with the tissue source and preparation (Table 4.1). However, the values reported in this thesis are comparable with other studies using bovine chondrocytes (McGlashan et al. 2008; McGlashan et al. 2010; Wann and Knight 2012). This chapter has highlighted the importance of standardising culture conditions which have significant influence over cilia expression.

**Table 4.1 Chondrocyte cilia length/prevalence reported in the literature**

| Site | Preparation | Species | Age | Prevalence (%) | Length (µm)* | Reference |
|---|---|---|---|---|---|---|
| Humeral head | Explant | Canine | Immature | 100 | 1.76 | (Wilsman 1978) |
| Sterna | Explant | Chick | Embryonic | 100 | 1-4 | Poole et al 2001 |
| Patellae | Explant | Bovine | Adult | 65 | 1.1-1.5 | (McGlashan et al. 2008) |
| Growth plate | Explant | Human | Immature | 70-90 | 0.5-4.5 | (de Andrea et al. 2010) |
| Metacarpal phalangeal joint | 3D agarose culture | Bovine | Adult | 15-45 | 1.3-2.2 | (McGlashan et al. 2010) |
| Growth plate | Explant | Murine | Embryonic | - | 1.1-5.1 | (Ascenzi et al. 2011) |
| Femoral condyle | Ex vivo | Murine | Adult | 87 | 0.75-0.95 | (Rich and Clark 2012) |
| Metacarpal phalangeal joint | 2D culture | Bovine | Adult | >75% | 0.5-5 | (Wann and Knight 2012) |

**mean value or range*

In contrast to other cell types, the removal of serum from cultures did not significantly affect chondrocyte cilia length or prevalence. While interesting, this is not a feature unique to chondrocytes as we have found that IMCD3 cells also exhibit a high level of ciliation in the presence of serum, however this requires high density culture and is more reliant on contact inhibition. Unusually ciliation in chondrocytes was not overly affected by cell seeding density relative to other cell types, as more than 50% of cells exhibited cilia even at low seeding density. The expression and length of cilia is linked to both cell shape and cell cycle status (Pitaval et al. 2010). *In vivo,* articular chondrocytes are quiescent; upon isolation chondrocyte proliferation gradually increases but still remains low with less than 10% of cells exhibiting positive staining for the cell cycle marker Ki-67 (not shown). This low proliferation rate may therefore be responsible for the high level of ciliation in chondrocytes *in vitro* (Figure 4.11).

Consistent with reports in 3D culture (McGlashan et al. 2010), primary cilia length and prevalence increase during the initial stages of 2D culture (Figure 4.11). Chondrocytes undergo changes in cell shape and size as they adopt a 'spread' morphology. In rounded chondrocytes, filamentous actin forms a dense cortical network at the periphery of the cell both *in situ* (Langelier et al. 2000) and in 3D culture (Knight et al. 2006). When chondrocytes attach to substrates and spread this cortical network is disrupted such that the actin is no longer densely packed but spread throughout the cell (Benya and Shaffer 1982; Brown and Benya 1988; Schulze-Tanzil et al. 2002; Schmal et al. 2006). Focal adhesions form containing proteins such FAK and paxillin, and are accompanied by stress fibre formation [for review see (Naumanen et al. 2008)]. Alterations to the actin cytoskeleton have been shown to modulate primary cilia incidence and length (Dawe et al. 2009; Bershteyn et al. 2010; Kim et al. 2010; Pitaval et al. 2010; Sharma et al. 2011; Hernandez-Hernandez et al. 2013). Chemical disruption of the actin cytoskeleton with cytochalsin D, an actin depolymerising agent, is associated with an increase in the availability of free, soluble tubulin and results in cilia elongation (Kim et al. 2010; Sharma et al. 2011). However, the relationship between actin dynamics and cilium size is complex as elongation is also observed in response to Jasplakinolide which has similar effects on soluble tubulin levels yet promotes actin stabilisation (Sharma et al. 2011).

Highly spread cells display more prominent actin stress fibres which are associated with an increase in intracellular tension (McBeath et al. 2004; Polte et al. 2004; Pitaval et al. 2010). Cellular confinement reduces this tension and promotes both cilia formation and elongation (Pitaval et al. 2010). At higher seeding densities, cells are subject to increased confinement and reduced spreading due to cell-cell contacts. Similarly culturing cells on softer substrates also reduces intracellular tension and encourages cilia formation (Sharma et al. 2011). On elastic membranes, chondrocytes do not show significant stress fibre formation regardless of density (Figure 4.13), therefore the high level of ciliation observed in these cells is probably linked to changes in actin organisation. Indeed, I have observed that the proportion of chondrocytes exhibiting cilia was significantly lower on glass relative to elastic membranes when cultured under the same conditions (not shown). Moreover, at 15-45% the incidence of primary cilia reported in 3D agarose culture is significantly lower than in 2D culture (McGlashan et al. 2010). However, mean primary cilia length in this study is comparable between the two culture methods, therefore the cilia elongation observed in short-term culture (Figure 4.11) may be occurring independent of changes in cell morphology and actin organisation.

Primary cilia length did not increase beyond day 6, suggesting cilium length had reached a 'set control length' where the rate of antereograde and retrograde IFT are in equilibrium (Marshall et al. 2005). Previous studies in kidney epithelium have shown that the rate of antereograde IFT can be regulated by mechanical stimuli in a cAMP/PKA dependent manner (Besschetnova et al. 2010). Although this response has not been demonstrated in chondrocytes, chondrocyte cilia length is influenced by agents that modulate cAMP levels (Wann and Knight 2012) while cyclic compression has been shown to trigger cilium disassembly in 3D agarose culture (McGlashan et al. 2010). During *in vitro* culture chondrocytes are subject to stress deprivation which will have significant effects on gene expression and cytoskeletal organisation. The removal of the *in vivo* mechanical stimulus may therefore be the influence that drives cilium growth in culture. Indeed, cilia elongation in response to stress deprivation has been observed in cells isolated from other connective tissues such as tendon (Gardner et al. 2011). Tenocytes exhibit primary cilia *in vivo* which orientate parallel to the arrangement of the collagen fibres in this tissue, and thus parallel

with tissue deformation (Lavagnino et al. 2011). Upon isolation and culture, tenocyte primary cilia dramatically increase in length. This elongation is proposed to function as an adaptive response to increase cell sensitivity to mechanical stimuli and is reversed following the application of mechanical strain (Gardner et al. 2011). Therefore subsequent chapters will examine changes in chondrocyte primary cilia length in response to mechanical strain.

### 4.4.2 Evaluation of the mechanical loading model

In this study the Flexcell™ system was used to apply uniform equibiaxial strain to isolated chondrocytes in 2D culture. The loading regime chosen did not cause significant cell detachment or cell death (Figure 4.12 and Figure 4.14). Previous studies have shown that, in chondrocytes, the actin cytoskeleton rearranges in response to both static and dynamic compression (Knight et al. 2006), increased hydrostatic pressure (Parkkinen et al. 1995; Knight et al. 2006) and changes in osmolarity (Erickson et al. 2003; Chao et al. 2006). Surprisingly, cell morphology was unchanged by 10% CTS for 1hr and there were no significant changes in actin organisation (Figure 4.13) yet strain resulted in the activation of mechanotransductive signalling pathways, as evidenced by increases in the expression of aggrecan and collagen II (Figure 4.15). These changes were comparable to what has been reported in previous studies using 2D loading models (Millward-Sadler et al. 2000; Huang et al. 2007). Actin rearrangements have been associated with chondrocyte mechanotransduction (see chapter 2), specifically loading appears to promote the disassembly of more defined structures in the cell (Parkkinen et al. 1995). On flexcell membranes the majority of cells exhibit only faint micro-fibrillar architecture throughout the cytoplasm therefore it is likely that any change in this structure is simply below the limit of detection.

The loading regime (10% strain, 0.33Hz, 1hr) was chosen based on previous work by Donald Salters group at Edinburgh University which showed that loading at a frequency of 0.33Hz activates a membrane hyperpolarisation response dependent upon apamin sensitive stretch activated (SA) cation channels and α5β1 integrins (Wright et al. 1996; Wright et al. 1997; Millward-Sadler et al. 2000). Membrane hyperpolarisation increases the expression of aggrecan. This response is frequency dependent and as such is not observed in response to

loading at 0.1Hz or 1Hz (Wright et al. 1997; Millward-Sadler et al. 2000). The mechanical regulation of Ihh gene expression in embryonic chick sterna chondrocytes is abolished by the SA channel blocker gadolinium ($Gd^{3+}$) indicating a requirement for these channels in this response (Wu et al. 2001). Therefore the aim was to use a similar frequency to activate these channels in this thesis; however the strain magnitude applied by these studies is very small, measured maximally at 0.3% strain (Millward-Sadler et al. 2000). Within the tissue, the strain a chondrocyte experiences varies with its zone of origin but is much higher than this. Chondrocytes in the superficial zone experience compressive strains of up to 25%, while cells in the middle and deep zones typically experience from 0-15% strain (see chapter 1). The flexcell system can deliver strains between 1% and 20% elongation, a strain magnitude of 10% was therefore chosen to provide a more physiologically relevant stimulus and give scope to vary the amount up/down in later studies. Moreover it had previously been demonstrated that 10% mechanical strain resulted in upregulation of matrix genes (Huang et al. 2007). Chondrocytes were subjected to strain for just 1hr and gene expression examined immediately after loading as hedgehog signalling is rapidly activated following ligand stimulation, with Gli accumulation observed in cilia within minutes of treatment (Wen et al. 2010).

#### 4.4.2.1 Limitations

One of the major advantages to working with chondrocytes in 2D cell culture is that it facilitates the accurate identification and measurement of primary cilia length which will be necessary for later studies. However there are several limitations to this system. In addition to strain cells will also experience an unknown level of fluid flow as the displacement of the membrane will cause some movement of the media over the cells. Furthermore, although 2D culture is advantageous for cilia studies, as it facilitates the identification and measurement of changes in cilia length, it does pose a significant issue for the chondrocyte phenotype.

Isolated chondrocytes maintained in 2D cell culture undergo changes in their morphology and alter their phenotype to a less differentiated state (Benya and Shaffer 1982; Brown and Benya 1988; Newman and Watt 1988; Malleingerin et al. 1991; Brodkin et al. 2004). Serial

culture results in the complete loss of the chondrocyte phenotype and cells become fibroblastic. This phenotypic switch occurs rapidly on an individual cell basis, the metabolic activity of the cell is increased and the normally quiescent chondrocyte begins to proliferate. Expression of collagen type II is down regulated concomitant with an increase in collagen type I expression (Archer et al. 1982; Benya and Shaffer 1982; Glowacki et al. 1983). In addition to a reduction in proteoglycan synthesis, the nature of the proteoglycan produced is also altered. Switching from large to small proteoglycan synthesis has been demonstrated in chick chondrocytes during dedifferentiation in 2D culture (Okayama et al. 1976).

Maintaining the rounded morphology of the chondrocyte during *in vitro* culture, by plating at high density or in 3D culture, reduces the level of dedifferentiation and the chondrocyte phenotype can be maintained for longer (Knight et al. 2001; Trickey et al. 2004; Blain et al. 2006). Moreover, the transfer of anchorage dependent chondrocytes into suspension or into hydrogels such as agarose or alginate recovers the differentiated phenotype (Benya and Shaffer 1982). However, this recovery occurs more slowly the longer the chondrocyte is cultured in monolayer and after 5-8 passages chondrocytes cannot be re-differentiated (Schulze-Tanzil et al. 2002). Thus for many years dedifferentiation was believed to result from the change in cell shape associated with the transition from a rounded to a spread morphology. However, actin depolymerising agents such as cytochalasin D can induce dedifferentiated chondrocytes to re-express collagen type II without a return to the spherical shape suggesting that it is actually changes in cytoskeletal organisation rather than cell shape which are responsible for modulating the chondrocyte phenotype *in vitro* (Malleingerin et al. 1991). Indeed, the synthesis of chondroitin sulphate proteoglycans and collagen type II is coincident with the presence of faint microfibrillar actin architecture whereas cells with more defined actin cables express collagen type I (Malleingerin et al. 1991).

The culture of chondrocytes in 2D is necessary for cell based OA therapies which require *in vitro* expansion such as autologous chondrocyte implantation (ACI). Dedifferentiation reduces the efficiency of cell-based repair methods, as it decreases the capacity for implanted chondrocytes to regenerate a functional cartilage tissue therefore the study of chondrocyte behaviour in monolayer is still necessary. Recent studies have shown that

culturing chondrocytes on a continuously expanding elastomeric substrate without passage produces a large number of chondrocytes that form a cartilage with improved phenotypic properties on subsequent pellet culture (Rosenzweig et al. 2012).

To limit dedifferentiation in this study freshly isolated chondrocytes were used for each experiment to avoid passage. Cells were plated at high density and allowed to attach to substrates for 6 days. Cultured in this way, chondrocytes still express collagen type II and aggrecan, markers of the differentiated phenotype (Figure 4.15) and display a polygonal morphology rather than the elongated phenotype of fibroblastic cells (Figure 4.12A). Although some stress fibre formation was observed, this was minimal when compared to chondrocytes plated on glass that predominantly exhibit intense stress fibre formation (Figure 4.17).This difference most likely arises due to the reduced stiffness of the elastic membranes.

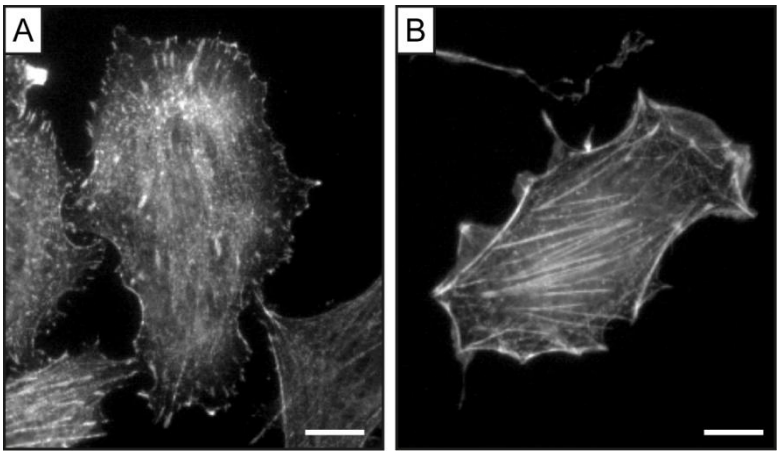


**Figure 4.17 Chondrocyte actin organisation on membrane and glass**
**(A)** Representative image of a chondrocyte cultured for 6 days on collagen coated plastic membranes. **(B)** Representative image of a chondrocyte cultured on serum coated glass coverslip, the majority of chondrocytes exhibit prominent stress fibre formation. Scale bar represents 10µm.

### 4.4.3 Hedgehog signalling in articular chondrocytes

Consistent with published reports (Wei et al. 2012), Ihh expression in articular chondrocytes is low but detectable by both PCR and immunofluorescent staining (Figure 4.1). In fact Ihh expression *in vivo* is likely to be much higher as an 80% reduction in expression was

observed between day 0 and day 6. The majority of cells labelled positive for Ihh which was surprising given that we are dealing with a heterogeneous population of cells from all cartilage zones. Ihh expression has been hypothesised to occur only in cells of the deep zone and regulate a PTHrP-Ihh axis reminiscent of signalling in the growth plate (Macica et al. 2011). Yet others have reported more intense expression of Ihh in the superficial zone which is increased in osteoarthritic cartilage and results in the release of Ihh protein into the synovial fluid (Wei et al. 2012). Furthermore it has recently been shown that Ihh promotes the expression of lubricin in cultures of superficial zone cells (Iwakura et al. 2012).

Articular chondrocytes express the major components of the hedgehog signalling pathway (Ihh, Ptch1, Smo and Gli1-3) and the majority of cells are ciliated in 2D cell culture. Due to a lack of commercially available antibodies with suitable species compatibility, I was unable to demonstrate that these components were expressed at the protein level or examine their ciliary localisation by immunofluorescence. However, this signalling pathway is functional as the addition of r-Ihh to cultures activated hedgehog signalling, as determined by increases in the expression of Ptch1 and Gli1 (Figure 4.3). The level to which the expression of these genes was induced is similar to what has been reported previously for human articular chondrocytes (Lin et al. 2009).

In ORPK cells lacking cilia, Ptch1 and Gli1 gene expression were not altered by r-Ihh treatment relative to untreated control cells confirming the requirement for this organelle in this response (Figure 4.5). However, the primary cilium is essential not only for the ligand dependent activation of Gli transcription factors, but also for the correct processing of the Gli3 repressor (Gli3R) in the absence of signals (Haycraft et al. 2005). Chang et al recently showed that Gli3 is an important regulator of articular cartilage maintenance in mice and that the conditional deletion of *Ift88* in chondrocytes increases hedgehog pathway activity *in vivo.* The elevated hedgehog signalling meant the cartilage that formed in these mice had altered mechanical properties and an increased susceptibility to osteoarthritis (Chang et al. 2012). It was found that hedgehog signalling was aberrantly activated in these mice due to a reduction in the formation of Gli3R and the de-repression of hedgehog target genes. Interestingly, this activation is not observed in chondrocytes of the growth plate where ligand dependent hedgehog signalling and Gli2 activation is of greater functional importance

(Song et al. 2007; Chang et al. 2012). In light of this study, I analysed the baseline level of hedgehog signalling in ORPK chondrocytes relative to WT chondrocytes (Figure 4.6). The expression of Ptch1 and Gli1 expression were higher in ORPK chondrocytes relative to WT cells, however this was not significant (Figure 4.6AB). This prompted the assessment of Gli3 processing, the ratio of Gli3R:Gli3A was found to be reduced in ORPK cells (Figure 4.6C), indicating that hedgehog signalling may be similarly disrupted in these cells. This disruption is much less severe than that reported by Chang et al, most likely due to the fact that this study used a knock out model while the cells used in this thesis originated from a hypomorphic mutant which may still have some functionality and is known to exhibit a less severe phenotype (Zhang et al. 2003).

While these data demonstrate the importance of the primary cilium for ligand mediated hedgehog signalling in articular chondrocytes, they also indicate that a mechanically induced reduction in primary cilia prevalence could also result in pathway activation due to reduced Gli3R. Studies by Caspary et al suggest that Gli3 processing is unaffected by the size of the ciliary signalling compartment (Caspary and Anderson 2006) therefore it will be interesting to study the effects of co-ordinated cilium disassembly on this processing.

Hedgehog proteins are lipid modified and can associate with the plasma membrane and function in an autocrine manner. They can also be released from cells and thus function in a paracrine manner (for review see (Gallet 2011)). In response to mechanical strain, the expression of Ihh was increased by almost 2-fold (Figure 7.4). This level of induction is comparable to that observed in rat growth plate chondrocytes following 1hr hydrostatic loading (Shao et al. 2011). Previous studies have shown that Ihh is released from embryonic chondrocytes in response to loading (Wu et al. 2001). The existence of mechanosensitive microRNAs has been reported in growth plate chondrocytes and shown to modulate Ihh expression (Guan et al. 2011). The lack of suitable antibodies for Ihh detection by western blotting means that we cannot be certain that the levels of Ihh protein are actually increased in response to strain. However, this is likely as significant pathway activation was observed.

### 4.4.4 Summary

To summarise, in this chapter I have shown that healthy articular chondrocytes are capable of responding to hedgehog ligands and that the cilium is essential for this response. Furthermore, I have established that mechanical strain upregulates Ihh expression and activates hedgehog signalling in these cells. Thus I have identified a suitable model with which to study the relationship between mechanics, the cilium and mechanically induced hedgehog signalling.

# CHAPTER 5

# Modulation of primary cilia structure and function by cyclic tensile strain

## 5.1 Introduction

Mechanical stimuli trigger primary cilia disassembly in numerous cell types (Iomini et al. 2004; Besschetnova et al. 2010; McGlashan et al. 2010; Gardner et al. 2011; Rich and Clark 2012). This phenomenon is proposed to regulate cilia-mediated signalling pathways, reigning in cellular responses to immoderate stimuli and preventing over stimulation. For example, in kidney epithelial cells fluid flow through the renal tubules causes deflection of the primary cilium and results in a $Ca^{2+}$ signalling event (Praetorius and Spring 2001, 2003), the magnitude of which is proportional to cilia length (Resnick and Hopfer 2007). Fluid shear stress triggers cilium disassembly, providing a feedback mechanism by which the cell can adapt intracellular signalling to external cues (Besschetnova et al. 2010).

Chondrocyte primary cilia length and prevalence increase with cartilage depth such that the shortest cilia are observed in the cells of the superficial zone closest to the articular surface (McGlashan et al. 2008). In this zone chondrocytes experience higher levels of fluid flow, tensile strain and compression relative to the cells in the middle and deep zones (O'Connor et al. 1988; Guilak et al. 1995; Wong et al. 1997). This highlights the possibility that a relationship exists between cilium length and strain magnitude. In line with this, McGlashan et al reported that the chondrocyte primary cilium disassembles in response to extended periods of cyclic mechanical compression (McGlashan et al. 2010).

While genetic models exist to study the effects of cilia loss on chondrocyte function, the consequences of length modulation on cilia mediated signalling pathways have not been well analysed and the mechanisms of ciliary disassembly are not well understood.

## 5.2 Aims and objectives

The aim of this chapter was to investigate the effects of cyclic tensile strain on primary cilia length and prevalence in articular chondrocytes and to determine the consequences of cilium disassembly for mechanically induced hedgehog signalling. It was hypothesised that increasing levels of mechanical strain would result in strain dependent cilium disassembly, and that this disassembly might inhibit ligand mediated hedgehog signalling.

The first objective of this study was to determine the role of the primary cilium in mechanically induced Ihh expression and hedgehog pathway activation using the $Tg737^{ORPK}$ mutant cell line in which cilia are either absent or severely truncated.

The second objective was to determine whether cyclic tensile strain triggers cilium disassembly in primary cells, similar to what is observed with cyclic compression (McGlashan et al. 2010). Primary cilia length and prevalence were examined by confocal microscopy and the effect of strain duration and strain magnitude examined.

Aurora A kinase (AurA) and the tubulin deacetylase HDAC6 have been implicated in cilium disassembly in response to serum growth factors (see chapter 1). More recently, over activation of HDAC6 has been implicated in cilia loss in cholangiocarcinoma (Gradilone et al. 2013). The third objective of this study was therefore to assess the role of HDAC6 and AurA in mechanically induced cilium disassembly.

The final objective was to examine hedgehog pathway activation in response to strain and to assess the consequences of cilium disassembly on pathway activity and the downstream targets of hedgehog signalling.

## 5.3 Results

### 5.3.1 The primary cilium is required for mechanosensitive hedgehog signalling

Hedgehog signalling is mechanosensitive in primary articular chondrocytes (see chapter 4). To explore the role of the cilium in this response, hedgehog signalling was examined in WT and ORPK chondrocytes following 1 hr 10% CTS. WT and ORPK chondrocytes were plated at 50,000 cells/$cm^2$ onto collagen coated elastic membranes and cultured in the absence of IFNɣ at 37$^oC$ for four days. On the fourth day the cells were subjected to 10% CTS for 1 hr and gene expression analysed by real time PCR immediately after loading. The expression of Ihh was increased approximately 1.5 fold above the unstrained control cells in both WT and ORPK chondrocytes (Figure 5.1A). These differences were statistically significant (WT: p=0.0258, ORPK: p=0.0447) indicating the cilium is not required for the mechanosensitive upregulation of Ihh. Although no significant changes in the expression of Ptch1 were observed (Figure 5.1C), Gli1 expression was significantly increased in WT chondrocytes following strain (p=0.0301, Figure 5.1B) suggesting hedgehog signalling was activated. No significant changes in gene expression were observed in ORPK chondrocytes showing a functioning primary cilium is required for this response.

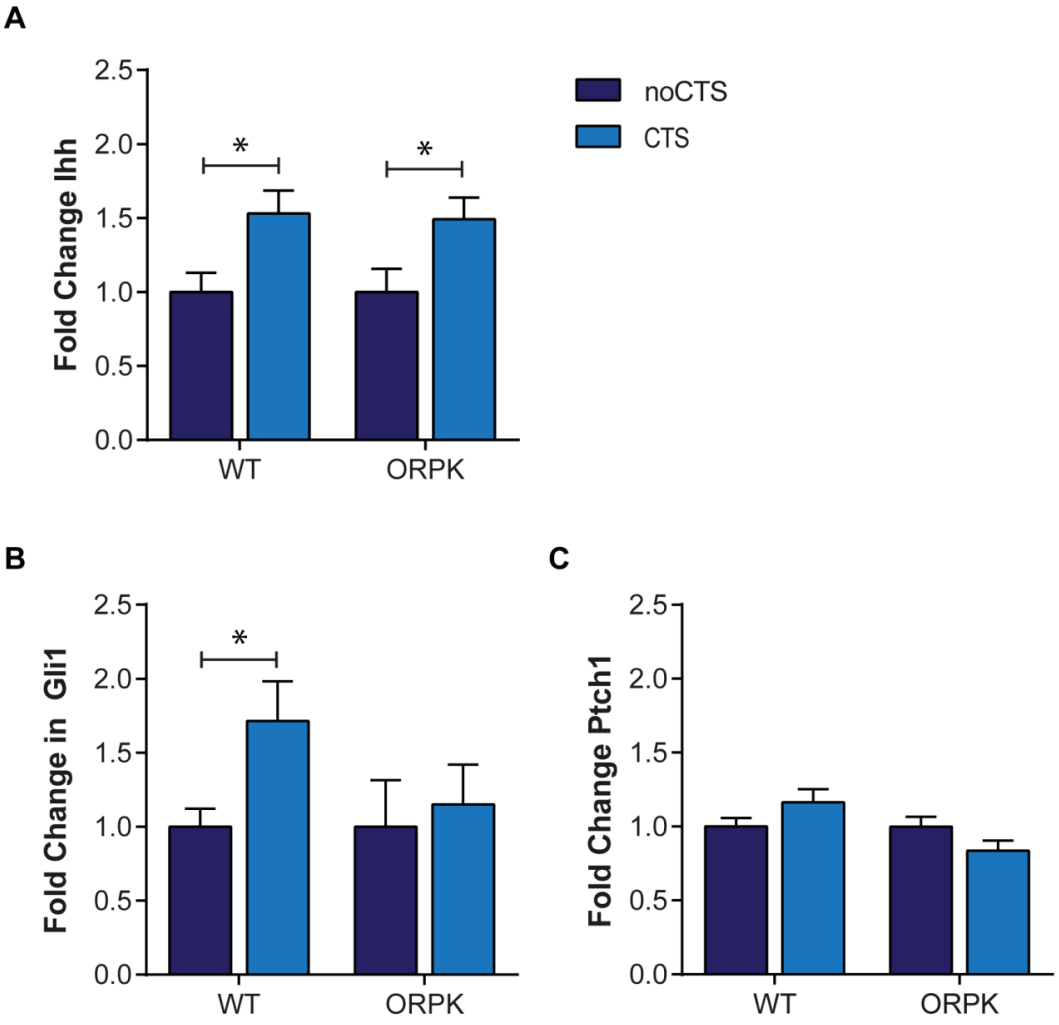


**Figure 5.1 Primary cilia are required for mechanical induced hedgehog signalling**
WT and ORPK chondrocytes were subjected to 10% CTS for 1 hr and the effects on **(A)** Ihh **(B)** Gli1 and **(C)** Ptch1 gene expression assessed by qRT-PCR immediately after strain. Data represents mean ± S.E.M (n= 8 per experimental group). All data are normalised to the expression of GAPDH and expressed as a fold change relative to the mean of the unstrained control group. Statistical significance was assessed using a Student's T test.

### 5.3.2 Mechanical strain triggers primary cilia resorption in adult articular chondrocytes

Having established the importance of a functioning cilium in the mechanical regulation of chondrocyte hedgehog signalling, the effects of mechanical strain on cilia length and prevalence were examined in primary articular chondrocytes. Chondrocytes were subjected to 10% CTS for 1 hr and cilia examined by confocal microscopy with acetylated α-tubulin used as a ciliary marker. There was no difference in the proportion of ciliated cells following strain which was approximately 75% in all cases. However mean primary cilia length was reduced from 2.39µm±0.03 (mean±S.E.M) in unstrained cells to 2.24µm±0.03 in strained cells (Figure 5.2A), this difference was statistically significant (p=0.002).

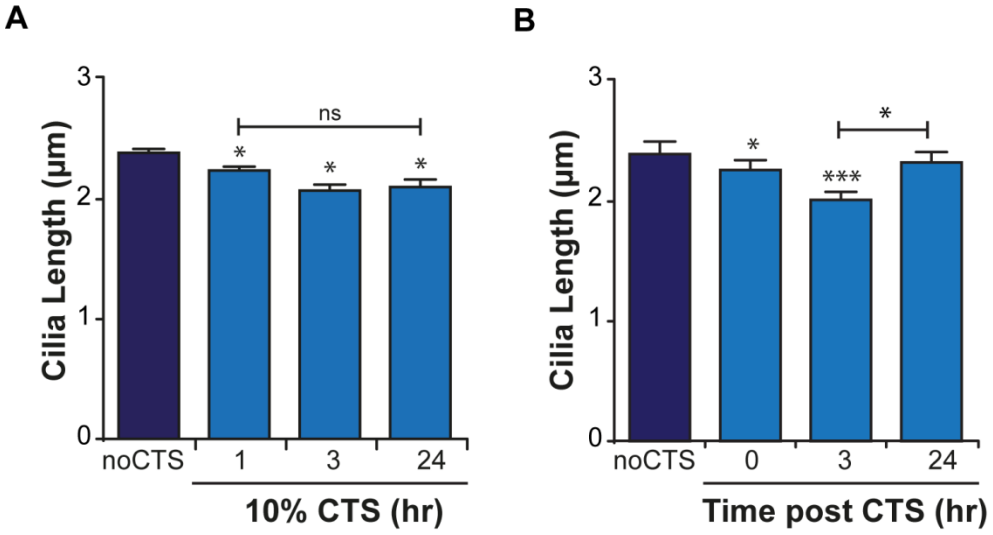


**Figure 5.2 Primary cilia length is reduced following 10% CTS**
Freshly isolated bovine articular chondrocytes were cultured for 6 days on elastic membranes then subjected to 10% CTS. **(A)** CTS was applied for 1, 3 and 24 hrs and cells were fixed immediately. **(B)** CTS was applied for 1hr and cells were allowed to recover in the absences of strain for 3 and 24hrs . Primary cilia length was by confocal microscopy. Data represents mean±S.E.M (n≥150 cilia per experimental group). Statistical significance was assessed using a Mann Whitney U test.

Previous studies used prolonged exposure to supra-physiological levels of compressive strain for 24-48 hrs to induce changes in cilia length and prevalence (McGlashan et al. 2010). Therefore the duration of the loading regime was increased to 3 and 24 hrs. Following 3 hrs

CTS, mean cilia length was significantly reduced relative to the unstrained control ($p=0.038$), increasing the loading duration to 24 hrs did not result in further axoneme disassembly. There were no significant differences in cilia length between groups following 1, 3 and 24 hrs loading (Figure 5.2A).

The resorption observed in response to 10% CTS was reversible (Figure 5.2B). Articular chondrocytes were subjected to 10% CTS for 1 hr then cultured for a further 3 and 24 hrs in the absence of strain. Primary cilia exhibited a further reduction in mean length following a 3hr recovery period such that they were significantly shorter than in unstrained controls ($p=0.001$). However 24 hrs after loading cilia length was not significantly different from the unstrained control cells ($p=0.246$, Figure 5.2B).

To explore the effects of strain magnitude on primary cilia, freshly isolated articular chondrocytes were subjected to CTS at 5, 10 and 20% strain for 1 hr at 0.33Hz. In unstrained populations, 77±7% of cells possessed a primary cilium with a mean length of 2.46±0.04μm. Cilia prevalence was not affected by strain at any magnitude; however cilia length was significantly reduced by CTS at all three strain magnitudes (Figure 5.3). Maximum disassembly was observed following 20% strain where mean cilia length was reduced by approximately 13% (Figure 5.3). Although subtle, this response was highly reproducible as shown by five separate repeat experiments (Table 5.1). Cilia were significantly shorter following 20% strain relative to cells subjected to 5% or 10% strain indicating more disassembly was occurring at this strain magnitude.

To confirm that the observed shortening of primary cilia was due to cilia resorption and not a reduction in the levels of acetylated tubulin staining in the ciliary axoneme, cells were also labelled for Arl13b. Articular chondrocytes were subjected to CTS at 20% strain for 1 hr and then processed for dual-immunofluorescence. In articular chondrocytes Arl13b localised almost exclusively to the cilium co-localising with acetylated tubulin in the axoneme both in strained and unstrained preparations (Figure 5.4A). Consistent with the acetylated tubulin staining, a significant reduction in cilia length was observed using Arl13b as a ciliary marker (Figure 5.4B).

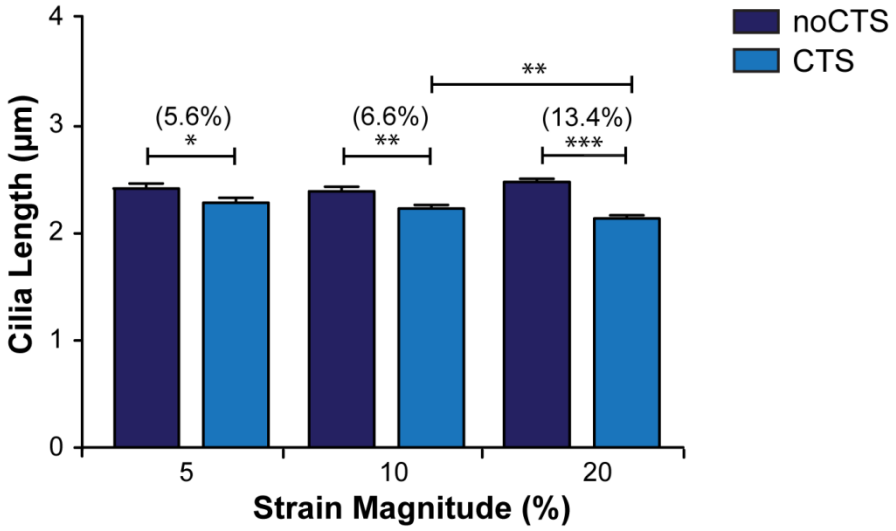


**Figure 5.3 Primary cilia length is reduced in a strain dependent manner**
Freshly isolated bovine articular chondrocytes were cultured for 6 days on Bioflex membranes then subjected to 1hr CTS at 5%, 10% and 20% strain. Primary cilia length was quantified by confocal microscopy. Data represents mean ±S.E.M (n ≥400 cilia per experimental group). Statistical significance was assessed using a Mann Whitney U test.

**Table 5.1 Primary cilia length is consistently reduced following 20% CTS**

| | noCTS | | | 20% CTS | | | | |
|---|---|---|---|---|---|---|---|---|
| Exp | Cilia Length (µm) | ±S.E.M | n | Cilia Length (µm) | ±S.E.M | n | Difference | p-value |
| 1 | 2.669 | 0.066 | 222 | 2.125 | 0.048 | 231 | 17.38% | < 0.0001 |
| 2 | 2.711 | 0.071 | 274 | 2.41 | 0.071 | 216 | 9.92% | 0.0027 |
| 3 | 2.418 | 0.058 | 292 | 2.15 | 0.055 | 325 | 13.70% | < 0.0001 |
| 4 | 2.232 | 0.043 | 308 | 2.052 | 0.048 | 284 | 11.14% | 0.0013 |
| 5 | 2.469 | 0.062 | 204 | 2.29 | 0.065 | 199 | 10.34% | 0.0204 |

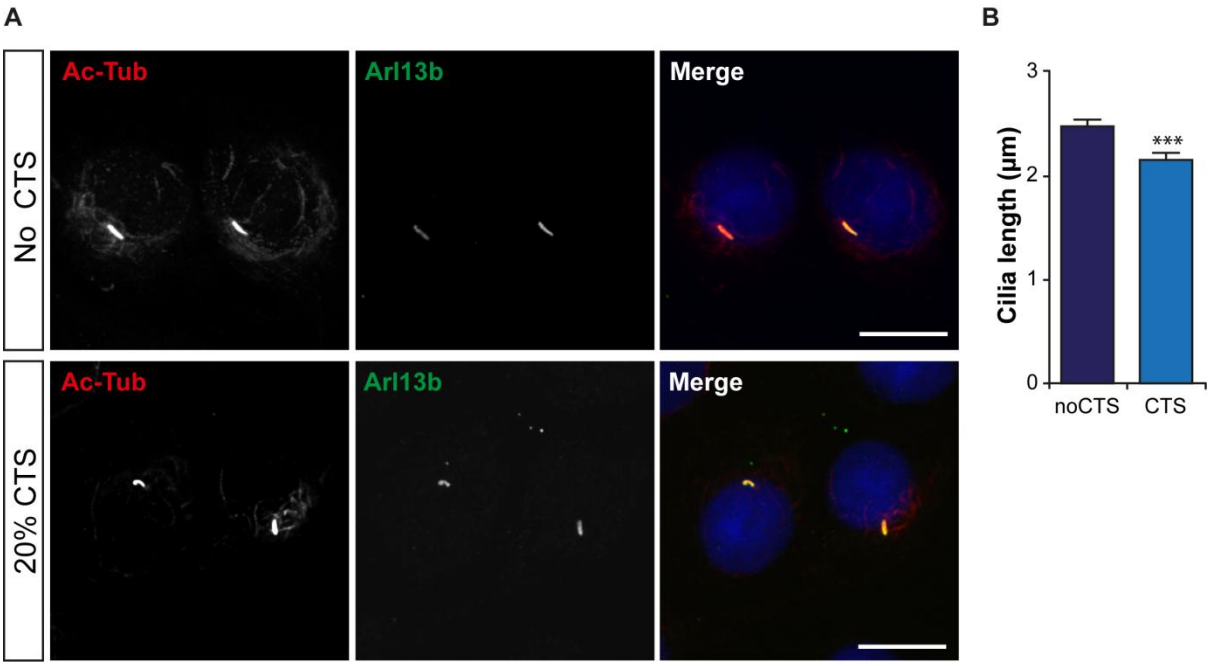


**Figure 5.4 Changes in cilia length are also observed using Arl13b as an axoneme marker**
Freshly isolated chondrocytes were subjected to 20% CTS for 1 hr then immediately fixed and processed for the immunofluorescent detection of primary cilia. **(A)** Primary cilia were labelled using antibodies directed against acetylated α-tubulin (red) and Arl13b (green). Nuclei were counterstained with DAPI, scale bar represents 20 µm. **(B)** Cilia length was quantified in the Arl13b channel by confocal microscopy. Data represent mean ±S.E.M (n≥150 cilia per experimental group). Statistical significance was assessed using a Mann U Whitney test.

Primary cilia are expressed on cells during interphase and are typically resorbed prior to cell division due to the requirement for the basal body in mitotic spindle formation (Seeley and Nachury 2010). To determine if the reduction in cilia length occurred as a consequence of cell cycle re-entry, immunofluorescent staining for the nuclear marker Ki-67 was performed (Figure 5.5). Ki-67 is expressed by cells during all active phases of the cell cycle (G1, S, G2, and mitosis), but is absent from resting cells (G0). Articular chondrocytes were subjected to 5%, 10% and 20% CTS and allowed to recover in the absence of strain for a further 24 hrs. The proportion of chondrocytes exhibiting nuclear Ki-67 staining varied slightly from 5-10% between different chondrocyte isolations. However for all loading regimes (5, 10 and 20% CTS) there was no statistically significant difference between strained and unstrained cells (Figure 5.5B). These data show that the changes in cilia length are not caused by cell cycle re-entry.

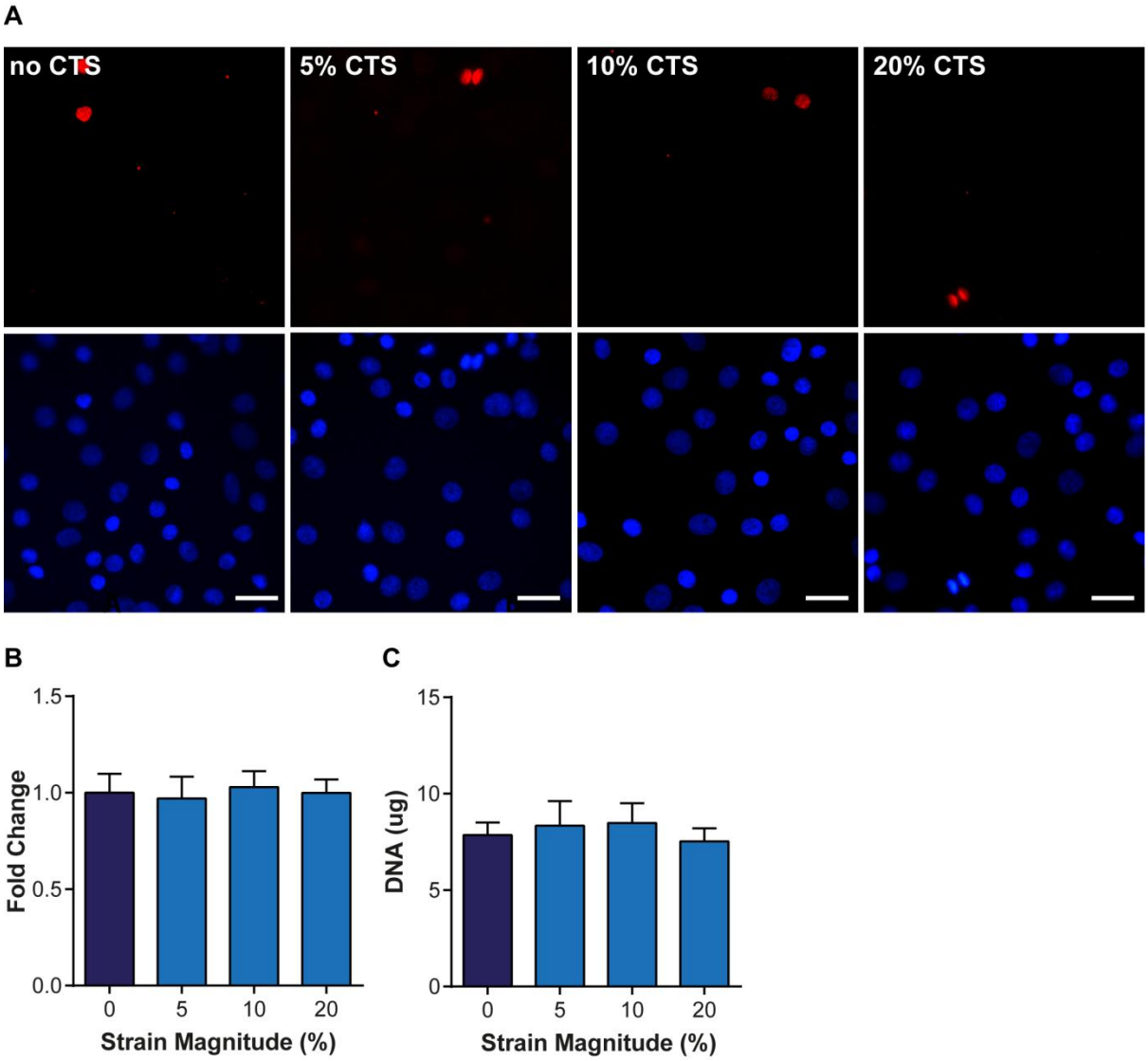


**Figure 5.5 CTS does not induce chondrocyte proliferation**

Primary articular chondrocytes were cultured for six days then subjected to CTS for 1hr or an equivalent unlstrained period. (**A)** Chondrocytes were labelled with Ki-67 (red) and counterstained with DAPI (blue) 24 hrs after the start of loading. Scale bar represents 20µm **(B)** The number of nuclei and the number of Ki-67 positive cells was quantified in 10 representative fields of view and expressed as a fold change relative to the mean of the unloaded control ( n=40 fields for each experimental group). **(C)** Cells were lysed and DNA content analysed by Hoescht 33342 assay (n=8 per experimental group). Data represents mean ±S.E.M and statistical significance was assessed using a student's T-test.

### 5.3.3 Mechanical strain increases Ihh expression and activates hedgehog signalling in a strain dependent manner

To explore the effects of strain magnitude on hedgehog signalling primary chondrocytes were subjected to 1 hr CTS at 5%, 10% and 20% strain and pathway activation assessed by real time PCR. Ihh expression was significantly increased following 10% and 20% CTS ($p=0.0405$ and $p=0.0269$) however there was no significant induction in response to 5% CTS (Figure 5.6A).

Hedgehog pathway activation was determined by monitoring the expression of Ptch1 and Gli1. Ptch1 and Gli1 expression were increased following 5% and 10% strain (Figure 5.6), these differences were statistically significant from unstrained controls (Ptch1: 5%:$p=0.0041$, 10%:$p=0.0206$, Gli1: 5%:$p=0.0186$, 10%:$p=0.0211$). Thus at 5% strain there is significant activation of the hedgehog pathway despite no significant mechanosensitive upregulation of Ihh. This may be due to inability to detect small changes in Ihh expression. Alternatively CTS may trigger the release of endogenous Ihh protein sufficient to activate the hedgehog pathway. However without a suitable antibody that recognises bovine Ihh protein this cannot be confirmed. No significant activation of the hedgehog pathway was observed following 20% CTS (Ptch1: $p=0.6376$ Gli1: $p=0.4926$) despite the induction of Ihh expression at this strain magnitude. Given the importance of the cilium in this pathway it is possible that the reduction in cilia length at this strain magnitude (Figure 5.3) is preventing mechanosensitive pathway activation (Figure 5.6).

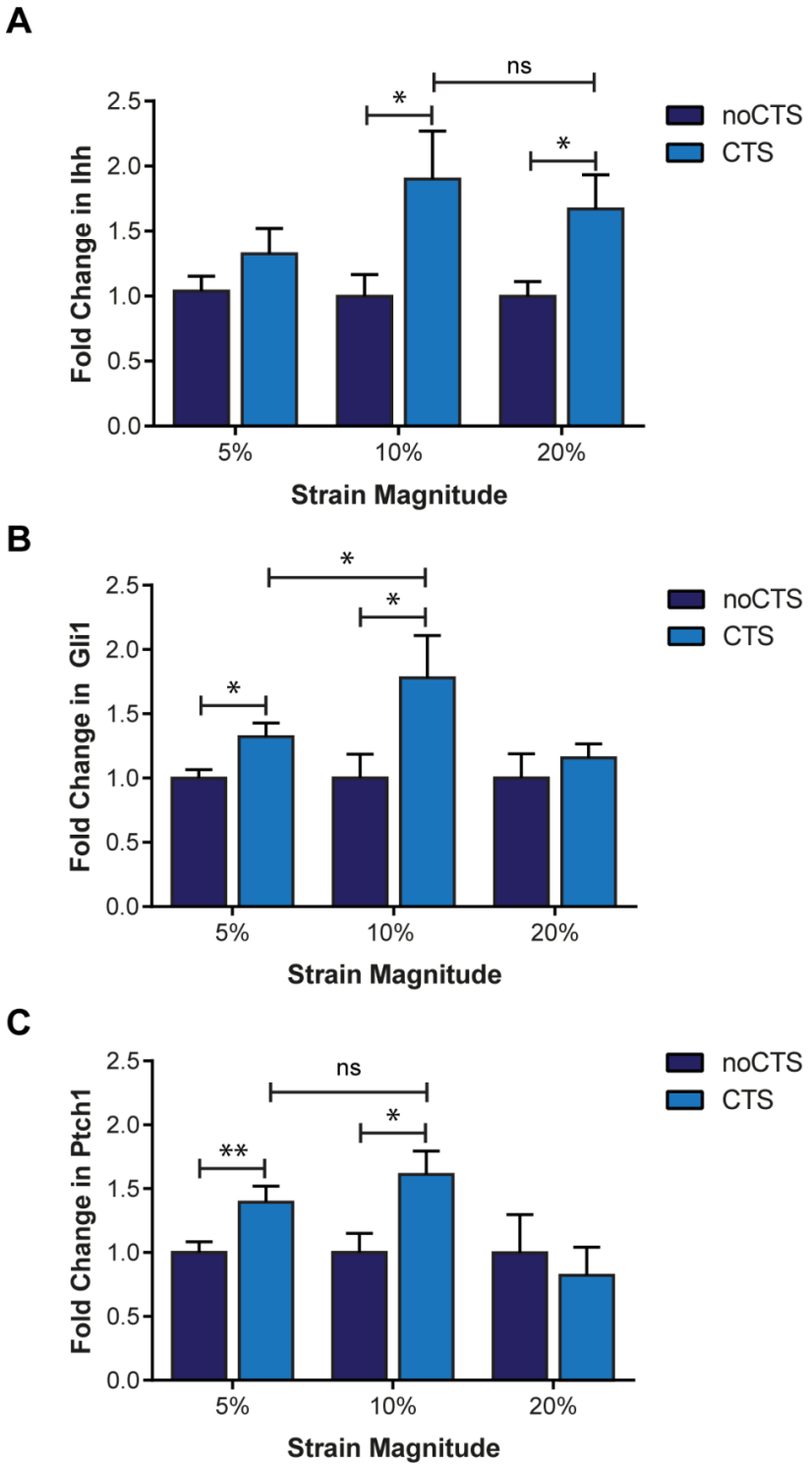


**Figure 5.6 Hedgehog signalling is attenuated at higher strains**
Primary articular chondrocytes subjected to CTS at 5%, 10% or 20% strain for 1 hr and the effects on gene expression assessed by real time PCR immediately after strain. Changes in **(A)** Ihh **(B)** Gli1 and **(C)** Ptch1 expression were analysed. All data are normalised to the expression of GAPDH and expressed as a fold change relative to the mean of the unstrained control group. Statistical significance was assessed using a Student's T test. Data represents mean ± S.E.M (n≥10 per experimental group).

### 5.3.4 Strain-induced cilium resorption is dependent upon HDAC6 and AurA function

The HDAC dependent deacetylation of ciliary microtubules has been implicated in cilia resorption (see chapter 1). Specifically the tubulin deacetylase HDAC6 has been linked to cilium disassembly and shown to localise to the ciliary axoneme. HDAC6 protein distribution was examined in articular chondrocytes using immunocytochemistry. HDAC6 staining was present throughout the cytoplasm and partially co-localised with acetylated tubulin in the ciliary axoneme (Figure 5.7). To examine the role of HDAC6 in mechanically-induced ciliary resorption, HDAC6 function was inhibited using trichostatin A (TSA) and tubacin. TSA is a broad specificity inhibitor that targets class I and class II HDAC function, while tubacin specifically targets HDAC6. Chondrocytes were pre-incubated with 7nM TSA, 500nM Tubacin or the carrier DMSO for 3hrs prior to the application of 20% CTS for 1 hr. In control cells, statistically significant reductions in primary cilia length were observed following 20% strain (Figure 5.8A). By contrast, no significant differences were observed between the strained and unstrained groups following treatment with HDAC inhibitors (Figure 5.8A). TSA and tubacin affected cilia length in an identical manner indicating HDAC6 is required for strain induced cilium disassembly.

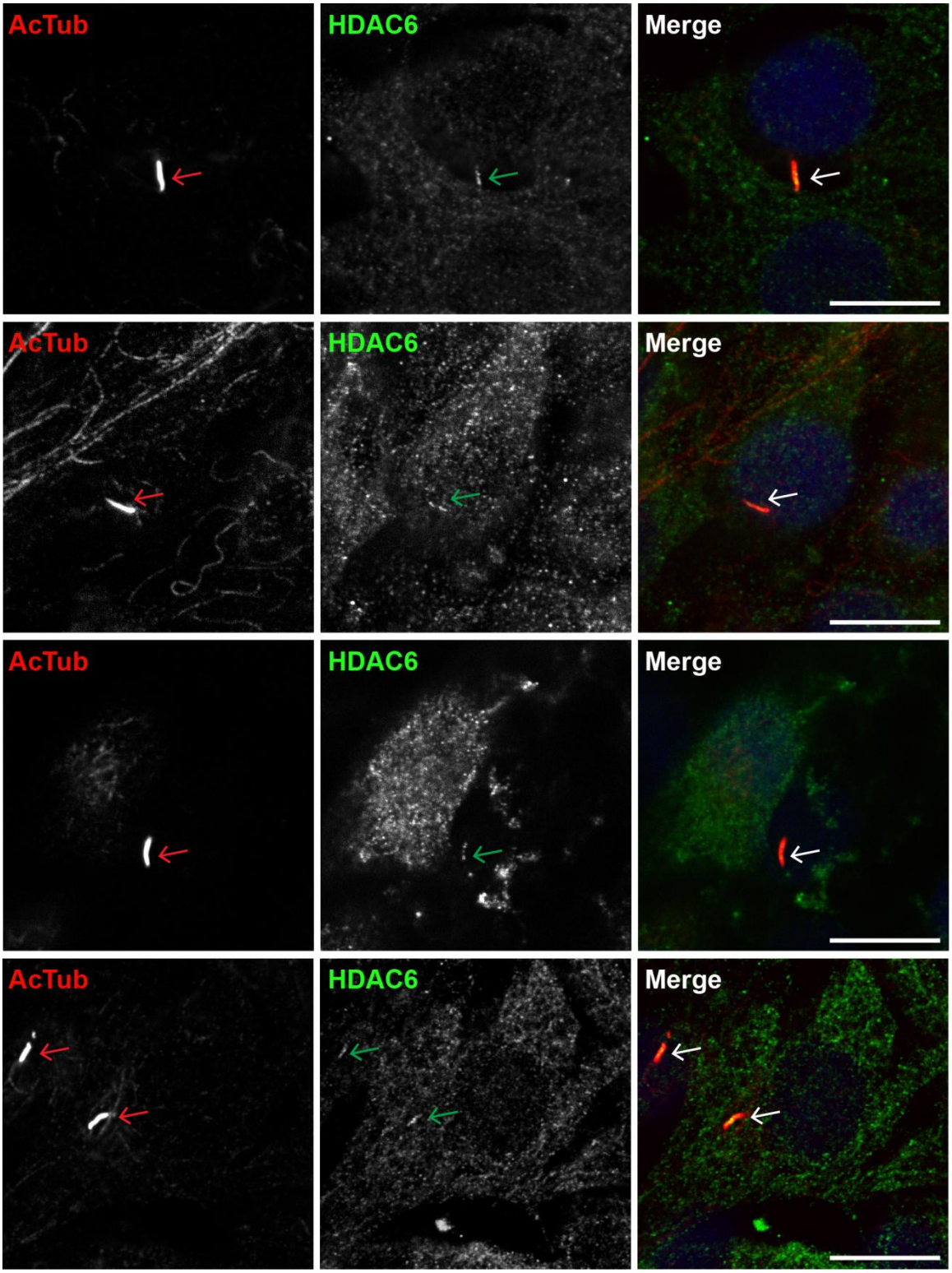


**Figure 5.7 HDAC6 localises to the ciliary axoneme in articular chondrocytes**
Freshly isolated bovine articular chondrocytes were cultured for six days then fixed and immunofluorescently labelled for HDAC6 (ab12173, green) and acetylated α-tubulin (red). Nuclei were counterstained with DAPI. Arrows indicate primary cilia and scale bar represents 10µm.

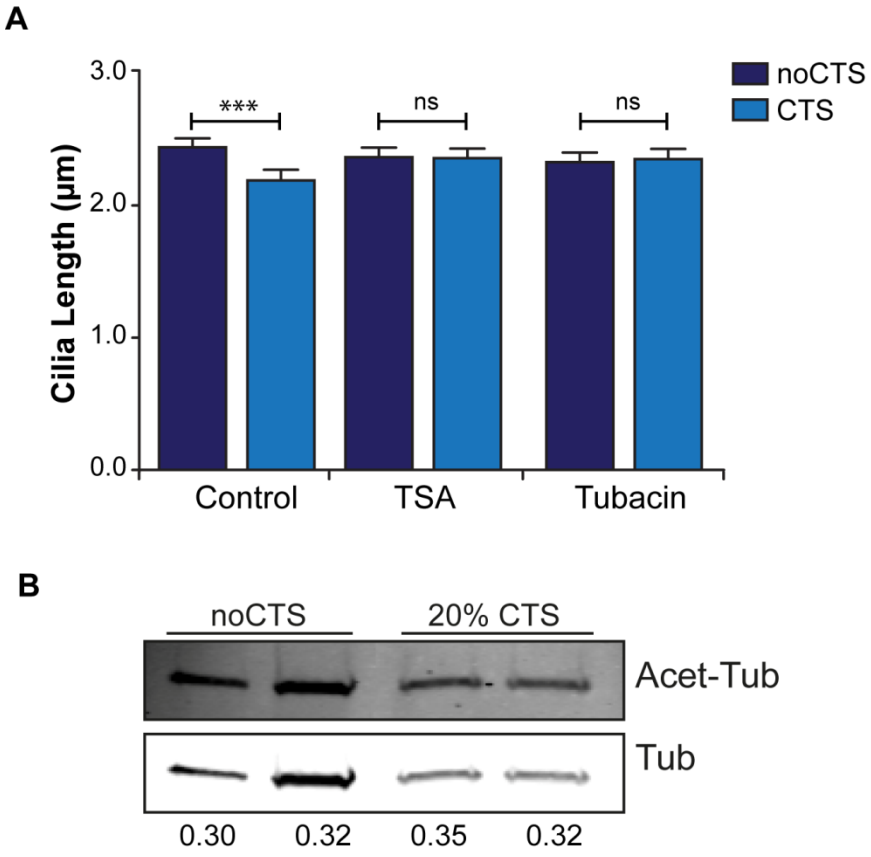


**Figure 5.8 HDAC function is required for strain-induced axoneme disassembly**
Freshly isolated bovine articular chondrocytes were cultured for 6 days on Bioflex membranes then subjected to 20% CTS ± DMSO (control) TSA or Tubacin for 1hr. **(A)** Primary cilia length was quantified in 5 representative fields of view. Data represents mean ±S.E.M (n≥400 cilia per experimental group). Statistical significance was assessed using a Mann Whitney U test. **(B)** Cell lysates were subjected to SDS-PAGE and western blotting for α-tubulin(Tub) and acetylated α-tubulin (Acet-Tub). Band intensity was quantified using the Licor Odyssey and the Acet-Tub:Tub ratio determined for each column.

Studies in lung epithelial cells have shown that the distribution of tubulin acetylation is altered in response to mechanical strain (Geiger et al. 2009). This prompted examination of whole cell acetylated tubulin levels by western blotting. There was no significant difference in the levels of acetylated α-tubulin relative to total tubulin between strained and unstrained samples and the ratio of acetylated:deacetylated tubulin remained unchanged (Figure 5.8B). The distribution of acetylated microtubules is not homogenous within a cell population. Some cells exhibit higher levels of acetylation than others often displaying a peri-nuclear distribution that radiates out from the microtubule organising centre at the base of the cilium. While no overt changes in this distribution were observed, the

proportion of cells exhibiting more prominent acetylated microtubules at the base of the cilium was increased from 29%±1 to 38%±4 in response to 20% CTS (Figure 5.9). This difference was statistically significant (p=0.0176) suggestive of a subtle reorganisation of tubulin PTMs.

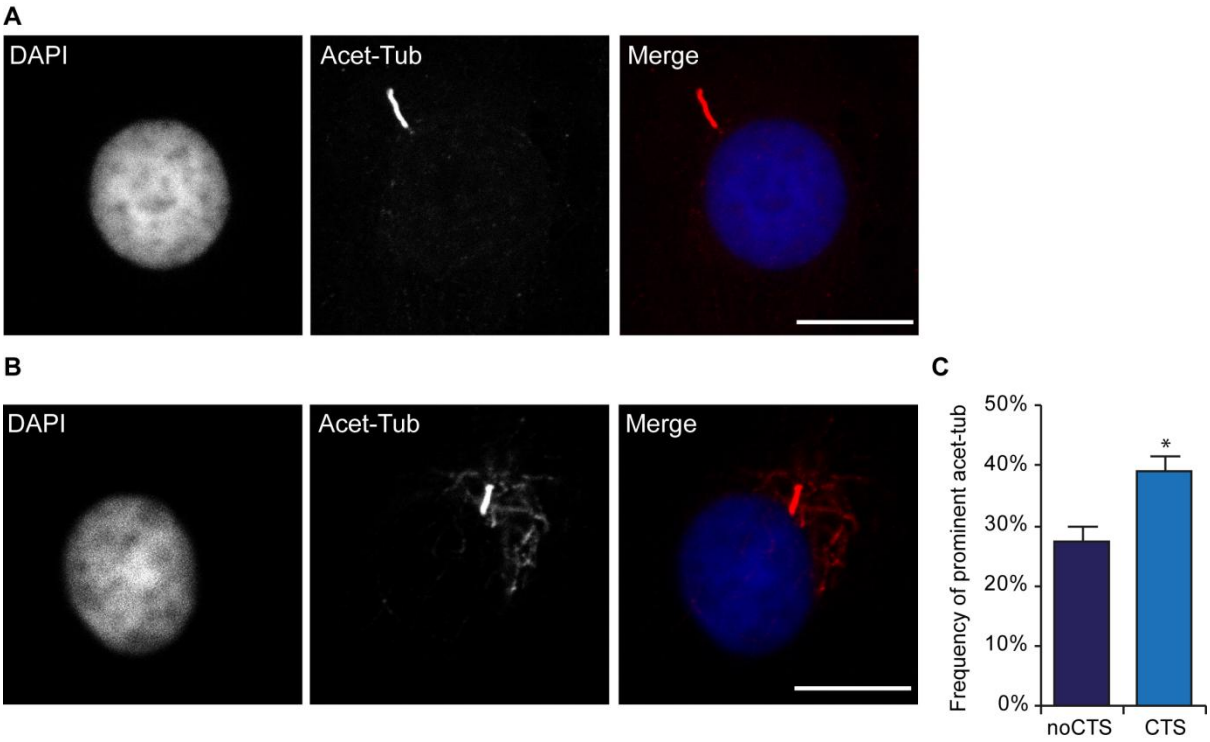


**Figure 5.9 Prominent tubulin staining increases at the ciliary base**
Primary articular chondrocytes were cultured for six days on Bioflex membranes, subjected to 20% CTS for 1 hr then fixed and immunofluorescently labelled for acetylated α-tubulin (red). Nuclei were counterstained with DAPI. Scale bar represents 10µm. Representative image of a cell with **(A)** low level and **(B)** prominent acetylated tubulin staining at the ciliary base- cells exhibiting this staining were present in both strained and unstrained populations. **(C)** The proportion of cells exhibiting prominent staining was quantified in 5 representative fields of view. Data represents mean ±S.E.M (n=10 fields per experimental group). Statistical significance was assessed using a student's T-test.

Given that HDAC6 inhibition rescues the cilia disassembly observed at 20% strain, if the absence of hedgehog pathway activation at this strain magnitude occurs as the result of

axoneme destabilisation then inhibiting tubulin deacetylation should also rescue the mechanosensitive hedgehog signalling. In unstrained cells, Gli1 expression was significantly increased (p=0.0003) in response to TSA treatment (Figure 5.10A) however no significant changes in Ptch1 expression (p=0.2187) were observed (Figure 5.10A). Previous studies have reported that class I HDACs are required for Gli3 repressor activity (Dai et al. 2002) therefore the increase in Gli1 expression may occur due to the loss of Gli3R function. Consistent with this hypothesis, no significant changes were observed in unstrained cells following tubacin treatment which specifically targets HDAC6 (Figure 5.10A). Chondrocytes were therefore subjected to 20% CTS in the presence of tubacin only and the effects on hedgehog pathway activity examined by real time PCR.

Consistent with previous results, there was no significant difference in Ptch1 and Gli1 expression in untreated control cells following 20% CTS (Figure 5.10AB). In tubacin treated cells, there was no significant difference in Gli1 expression following 20% CTS (p=0.073; Figure 5.10B). However, the expression of Ptch1 was upregulated by approximately 1.5 fold (Figure 5.10C). This difference was statistically significant (p= 0.003). These results suggest that perhaps a partial rescue has been achieved and that HDAC6 exerts a negative influence over mechanosensitive hedgehog signalling at higher strains potentially through changes in ciliary structure. However the hedgehog response could not be fully restored by HDAC6 inhibition suggesting other mechanisms are likely to be involved.

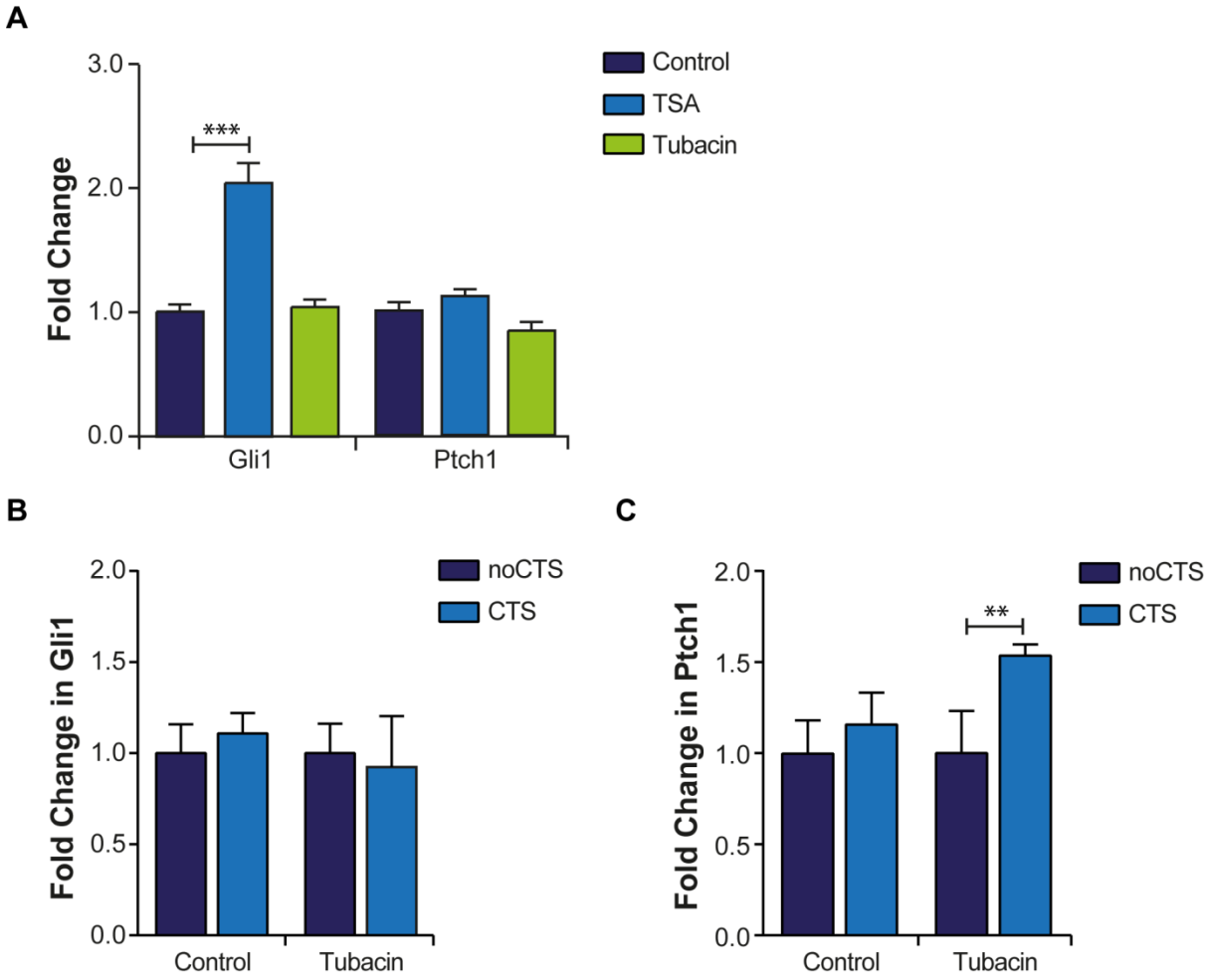


**Figure 5.10 HDAC6 inhibition modulates hedgehog signalling in response to 20% CTS**
Primary articular chondrocytes were treated with TSA (7nM), Tubacin (500nM) or the carrier DMSO (control) and the effects on hedgehog pathway activation assessed by real time PCR immediately after strain. Changes in (A) Gli1 and Ptch1 expression were analysed. All data are normalised to the expression of GAPDH and expressed as a fold change relative to the mean of the untreated control group. Primary articular chondrocytes were subjected to 20% CTS for 1 hr in the presence of Tubacin (500nM) or the carrier DMSO (control) and changes in (B) Gli1 and (C) Ptch1 expression were analysed by real time PCR. All data are normalised to the expression of GAPDH and expressed as a fold change relative to the mean of the unstrained control for each subgroup. Statistical significance was assessed using a Student's T test. Data represents mean ± S.E.M (n=6 per experimental group).

Interactions between the pro-metastatic scaffolding protein HEF-1 and AurA kinase at the basal body result in the phosphorylation and activation of HDAC6 promoting cilia disassembly in response to growth factors (see chapter 1). To assess the role of AurA in mechanically induced cilium resorption, articular chondrocytes were treated for 3 hrs with the AurA inhibitor PHA-680632 (500nM) prior to the application of 20% CTS for 1hr. In the unstrained cells, AurA inhibition had no effect on primary cilia length (Figure 5.11A). Furthermore, mechanosensitive cilium disassembly was not observed in cells treated with the AurA inhibitor such that there was no statistically significant difference in cilia length between unstrained control cells and those subjected to CTS (Figure 5.11A). This suggests that AurA is functioning upstream of HDAC6 in this response.

In contrast to HDAC inhibition, PHA-680632 did not rescue hedgehog signalling in response to 20% CTS (Figure 5.11B and C). Surprisingly the expression of Gli1 was significantly down regulated by AurA inhibition in both strained and unstrained groups ($p=0.0019$ and $p=0.0002$ respectively). In contrast Ptch1 expression was significantly increased in unstrained cells, however this induction was abrogated by 1hr 20% CTS (Figure 5.11C).

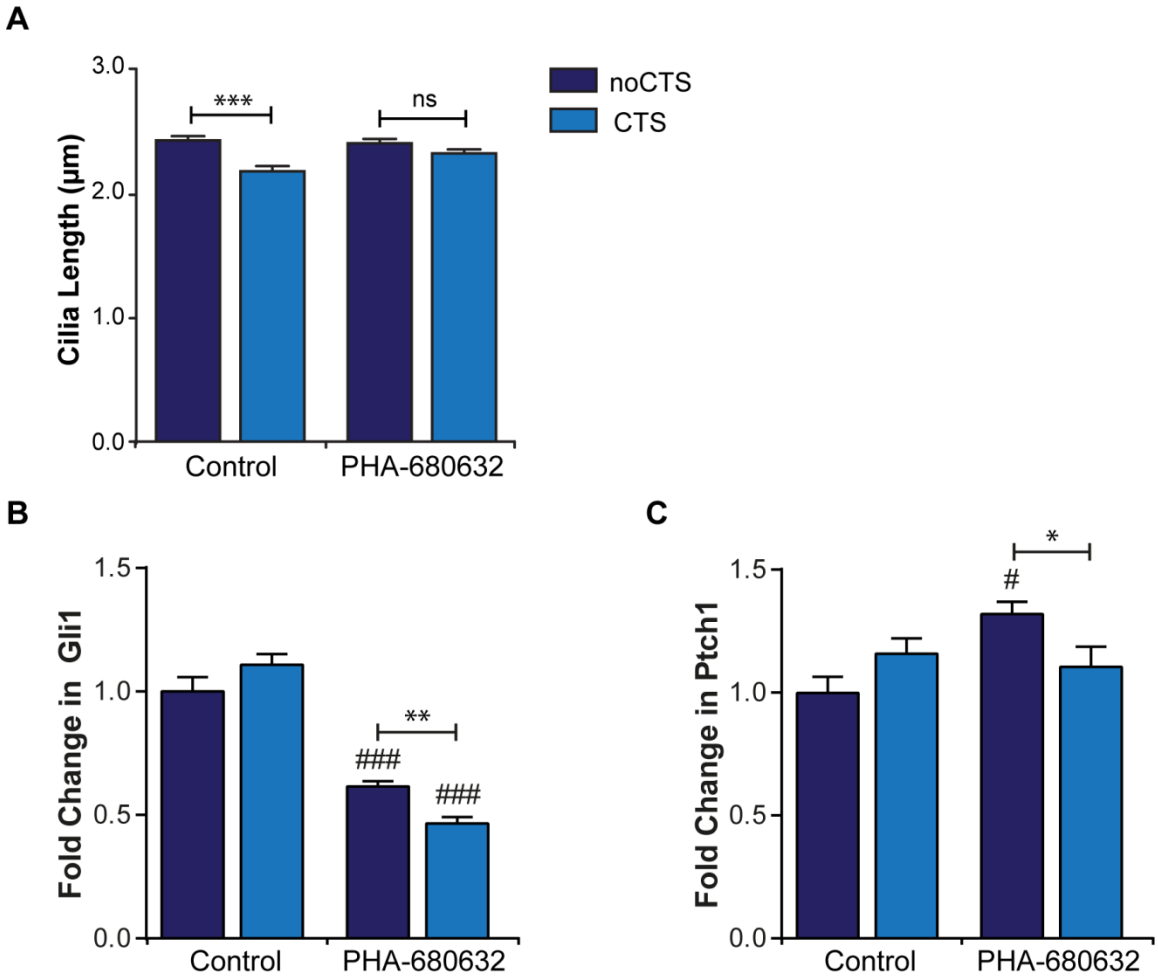


**Figure 5.11 PHA-680632 inhibits strain induced cilia resorption and modulates hedgehog signalling in response to CTS**

Primary articular chondrocytes were subjected to 20% CTS ±PHA-680632 for 1hr. **(A)** Primary cilia length was quantified in 5 representative fields of view. Data represents mean ±S.E.M (n≥400 cilia per experimental group). Statistical significance was assessed using a Mann Whitney U test. **(B)** The effects on **(B)** Gli1 and **(C)** Ptch1 gene expression were assessed by real time PCR immediately after strain. All data are normalised to the expression of GAPDH and expressed as a fold change relative to the mean of the unstrained (noCTS) control group. Data represents mean ± S.E.M (n=6 per experimental group). Statistical signifcance was assessed using a Student's T-test relative to the unstrained control group (without AurA inhibitor, shown as '#') or to the unstrained control for each sub group (with AurA inhibitor, shown as '*').

### 5.3.5 Examination of downstream targets of mechanically induced hedgehog signalling

In chondrocytes isolated from embryonic tissues, *in vitro* mechanical loading triggers Ihh release which promotes chondrocyte proliferation (Wu et al. 2001). However mechanical strain did not induce chondrocyte proliferation (Figure 5.5). Chondrocyte proliferation was subsequently examined in response to 24 hrs r-Ihh treatment (Figure 5.12). While the proportion of Ki-67 positive cells was increased from 3.22% to 4.51% following r-Ihh treatment (Figure 5.12A) there were no significant changes in DNA content between treated and untreated samples (Figure 5.12B).

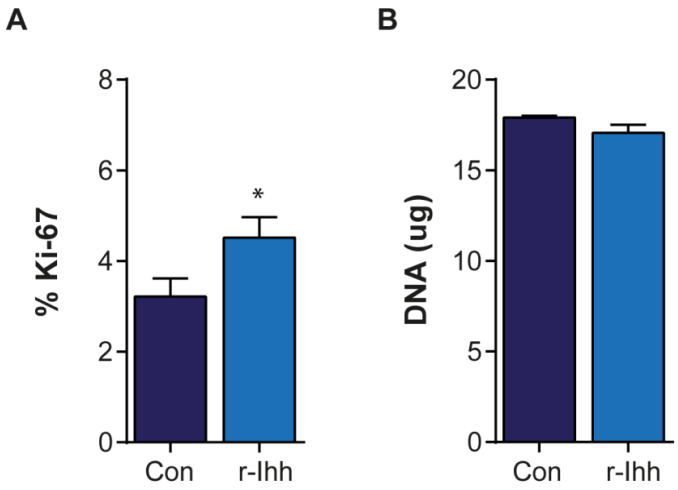


**Figure 5.12 The effects of r-Ihh treatment on chondrocyte proliferation**
Freshly islated articular chondrocytes were cultured for 5 days then treated for a further 24hrs with r-Ihh (1µg/ml). **(A)** Cells were labelled for Ki-67 to monitor changes in cell cycle status. The number of nuclei and the number of Ki-67 positive cells was quantified in 10 representative fields of view and expressed as a fold change relative to the mean of the unstrained control (n=40 fields per experimental group). **(B)** Cells were lysed and DNA content analysed by Hoescht 33342 assay. Data represents mean ±S.E.M (n=6 per experimental group) and statistical significance was assessed using a student's T-test.

Previous studies have reported that hedgehog signalling promotes the expression of catabolic genes such as ADAMTS-5 and MMP-13 in osteoarthritic cartilage (Lin et al. 2009; Wei et al. 2012). In light of these studies, the expression of ADAMTS-5 was examined following mechanical strain. At 5% and 10% strain ADAMTS-5 expression was significantly

increased however no significant changes were observed in cells subjected to 20% strain (Figure 5.13A). These findings correlate with hedgehog pathway activation (Figure 5.6BC).

To confirm that ADAMTS-5 can be regulated by hedgehog signalling, cells were subjected to r-Ihh treatment for 24 hrs. Surprisingly, there was no difference in the expression of ADAMTS-5 in response to ligand stimulation in apparent contrast to previous studies (Figure 5.13B). Moreover, when isolated cartilage explants were subjected to r-Ihh treatment over a period of 6 days significant cartilage degradation, as measured by sGAG release, was not observed (Figure 5.13C). Therefore it seems unlikely that the mechanically induced hedgehog signalling is directly responsible for the changes in ADAMTS-5 expression in response to strain.

In ORPK chondrocytes ADAMTS-5 expression is elevated above that of WT cells (unpublished data and (Chang et al. 2012)) this suggests that ADAMTS-5 may still be dependent upon ciliary function. Moreover, mechanosensitive ADAMTS-5 expression has been linked to HDAC function (Saito et al. 2013). Chondrocytes were therefore subjected to 20% CTS in the presence of tubacin and PHA-680632 and the effects on ADAMTS-5 expression examined. No statistically significant differences in ADAMTS-5 expression were observed in unstrained control cells; however in both PHA-680632 and tubacin treated preparations ADAMTS-5 was significantly upregulated in response to strain (Figure 5.14).

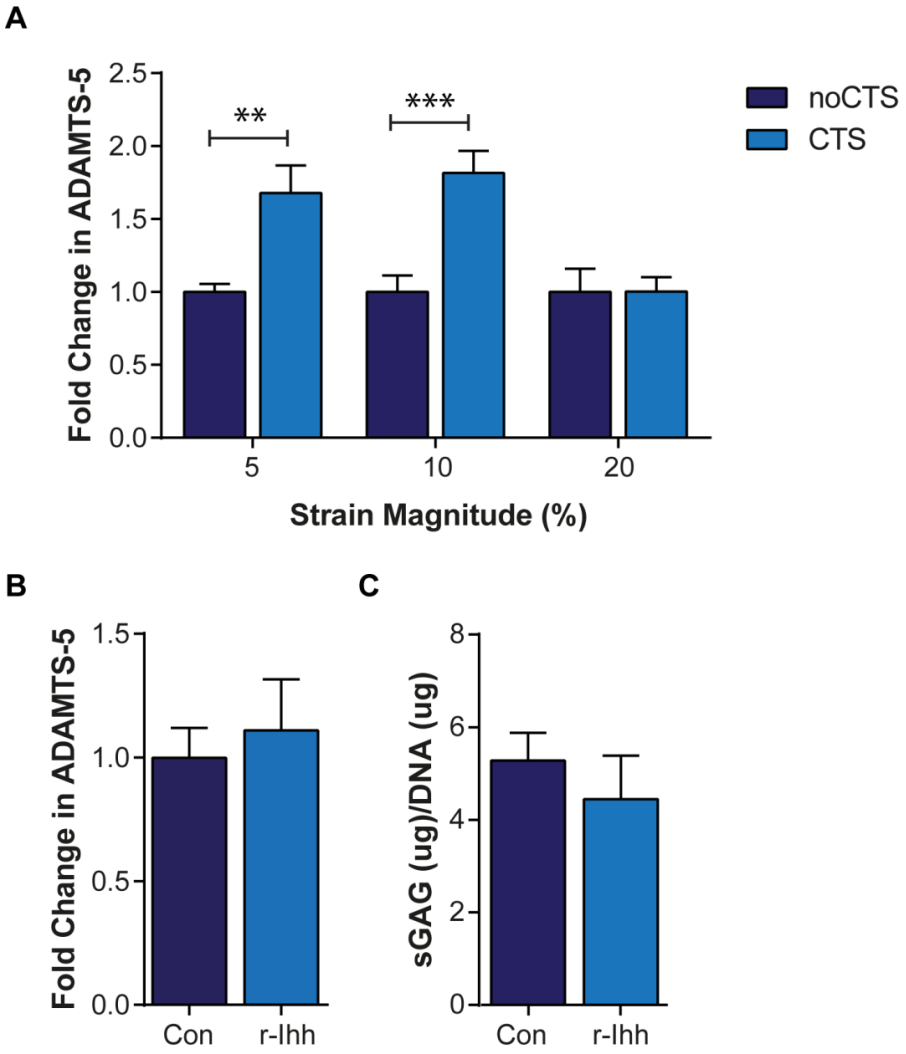


**Figure 5.13 Mechanically induced ADAMTS-5 is reduced at high strain but is independent of hedgehog signalling**

**(A)** Primary articular chondrocytes were subjected to mechanical strain for 1 hr and the effects on ADAMTS-5 gene expression assessed by qRT-PCR immediately after strain. Data represents mean ± S.E.M (n= 10 per experimental group). **(B)** The effects on ADAMTS-5 gene expression were also analysed following treatment with r-Ihh (1µg/ml) (n=10 per experimental group). All data are normalised to the expression of GAPDH and expressed as a fold change relative to the mean of the untreated or unstrained control group. Statistical significance was assessed using a Student's T test.

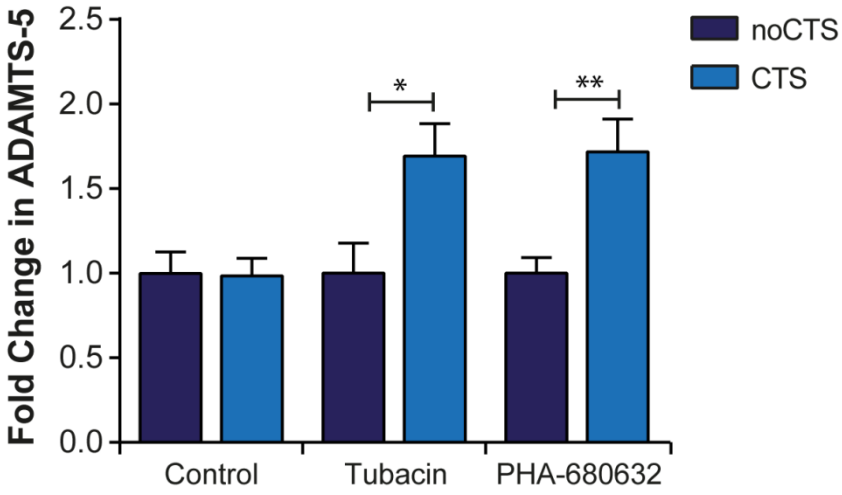


**Figure 5.14 HDAC6/AurA inhibition rescues ADAMTS-5 expression following 20% CTS**
Primary articular chondrocytes were subjected to 20% CTS ± Tubacin or PHA-680632 for 1hr. The effects on ADAMTS-5 gene expression were assessed by real time PCR immediately after strain. Data represents mean ± S.E.M (n=6 per experimental group). All data are normalised to the expression of GAPDH and expressed as a fold change relative to the mean of the unstrained (noCTS) control group. Statistical signifcance was assessed using a Student's T-test relative to the unstrained control for each group.

## 5.4 Discussion

In this chapter, I have determined that a functioning primary cilium is essential for mechanosensitive hedgehog signalling in articular chondrocytes. In primary chondrocytes the cilium disassembles in response to high levels of mechanical strain in a HDAC6 dependent manner coincident with the loss of mechanosensitive hedgehog signalling and ADAMTS-5 expression suggesting ciliary resorption modulates these responses.

### 5.4.1 Mechanical strain regulates Ihh signalling in a strain dependent manner

The expression of Ihh was increased in response to 10% and 20% CTS however hedgehog pathway activation was observed following 5% and 10% CTS (Figure 5.6). Low level Ihh gene expression is observed in unstrained chondrocytes (Figure 4.1). Therefore pathway activation at 5% suggests that either the upregulation of Ihh is below the limit of detection or that in addition to *de novo* synthesis mechanosensitive hedgehog signalling occurs due to the release of endogenous Ihh protein. Ihh release has been observed in embryonic chick sternal chondrocytes cultured in 3D scaffolds following cyclic stretch (Wu et al. 2001). Unfortunately, an antibody that convincingly recognises bovine Indian hedgehog protein could not be found, hence mechanosensitive Ihh release could not be examined in our system. Future studies should perhaps try to examine the strain dependent Ihh production in a different species.

### 5.4.2 Mechanosensitive hedgehog signalling requires the primary cilium

In response to CTS, the expression of Gli1 is significantly increased in WT cells suggesting hedgehog signalling is activated (Figure 5.1B). Gene expression was not significantly altered by CTS in ORPK cells (Figure 5.1) indicating a functioning cilium is required for mechanosensitive hedgehog signalling. This agrees with the findings in chapter 4 showing that the primary cilium is necessary for ligand induced hedgehog signalling (Figure 4.5). In WT chondrocytes, the expression of Ptch1 was not significantly upregulated by mechanical strain despite the induction of Gli1 (Figure 5.1). In chapter 4 I demonstrated a 50% increase

in Ptch1 expression following r-Ihh treatment for 24 hrs (Figure 4.5B). At 1µg/ml this dose is likely much higher than what the cells experience during mechanical loading therefore it is unsurprising that the pathway is regulated to a lesser extent.

*Ift88* disruption and cilia loss appears to increase the basal level of hedgehog signalling (see chapter 3). Therefore one concern with this study is the validity of ORPK chondrocytes as a model for studying the role of the cilium in hedgehog signalling. It is possible that the failure of these cells to activate hedgehog signalling in response to CTS and ligand stimulation is not due to disrupted signal reception, but rather because signalling is already maximally elevated and cannot be increased further. However studies in rat growth plate chondrocytes suggest this is not the case as mechanosensitive hedgehog signalling was also abrogated in these cells following chemical deciliation with chloral hydrate (Shao et al. 2011). Interestingly, Shao et al also reported that Ihh gene expression was reduced by chloral hydrate treatment (Shao et al. 2011). In contrast, the data presented in this thesis indicates that mechanosensitive Ihh expression in articular chondrocytes is not dependent upon ciliary function (Figure 5.1A) suggesting there may be key differences in the role of the cilium between mature and immature cells.

### 5.4.3 Mechanical strain triggers chondrocyte primary cilia disassembly

While the number of ciliated cells was not altered by CTS, primary cilia became progressively shorter with increasing strain magnitude, such that the mean length of cilia was reduced by approximately 13% following 20% CTS (Figure 5.3). Studies conducted at 10% strain suggest that this alteration in cilium length will perhaps be maintained for several hours after the removal of the mechanical stimulus (Figure 5.2B). Additional studies will be required to determine if extending the duration of the loading regime at 20% strain results in further cilium disassembly.

Previous studies have also reported that the chondrocyte primary cilium disassembles in response to physical stimuli like those experienced during joint loading. For example chondrocytes cultured in 3D agarose constructs undergo dramatic cilia loss in response to prolonged periods of cyclic compression such that the proportion of ciliated cells is reduced

from 35% to 25% following 24 hrs of loading (McGlashan et al. 2010). However, it is not until 48 hrs that a significant reduction in cilium length is observed at which time the cilia of loaded cells were 30% shorter (McGlashan et al. 2010). The mechanically induced cilia resorption observed in this thesis occurs earlier and is more subtle, the magnitude of disassembly being reminiscent of the differences observed between cartilage zones *in vivo* where cilia are 20% shorter in the superficial zone relative to the deep zone (McGlashan et al. 2008). This likely reflects differences in the loading models as Rich et al have recently demonstrated that changes in osmolarity also trigger ciliary resorption (Rich and Clark 2012). In this study, live imaging of chondrocytes in isolated mouse femora was used to explore the effects of osmolarity on primary cilia (Rich and Clark 2012). While cilia prevalence was not altered by changes in osmolarity, axoneme length was reduced by approximately 10%.

The reigning hypothesis regarding ciliary length control is that a set axoneme length is maintained as the velocity of retrograde and antereograde IFT are in equilibrium (Marshall and Rosenbaum 2001). Disruption of this equilibrium will result in a change in axoneme length however the mechanisms regulating IFT velocity are not well understood. Studies in kidney epithelia have shown that cilia disassembly in response to fluid flow is regulated by the intracellular levels of $Ca^{2+}$ and cAMP which influence IFT velocity (Besschetnova et al. 2010). Agents that reduce $Ca^{2+}$ levels, increase cAMP or result in cAMP-dependent PKA activation, increase antereograde IFT and result in cilia elongation. Conversely, agents that reduce cAMP levels or trigger intracellular $Ca^{2+}$ release result in cilia disassembly (Besschetnova et al. 2010). While neither cAMP nor $Ca^{2+}$ levels were examined in this thesis, numerous studies have shown that mechanical loading modulates $Ca^{2+}$/cAMP signalling (Wright et al. 1996; Yellowley et al. 1997; Edlich et al. 2001; Roberts et al. 2001; Erickson et al. 2003; Browning et al. 2004; Fitzgerald et al. 2004; Mizuno 2005; Pingguan-Murphy et al. 2005; Tanaka et al. 2005; Chao et al. 2006; Pingguan-Murphy et al. 2006; Degala et al. 2012; Wann and Knight 2012). Therefore it is possible that mechanosensitive disassembly in chondrocytes is also $Ca^{2+}$/cAMP mediated. This hypothesis is further supported by previous studies showing chondrocyte cilia length can be regulated by cAMP resulting from treatment with 8-Bromo-adenosine (Wann and Knight 2012). Ideally, one

would test this by measuring the rate of IFT in chondrocyte primary cilia under strain. Unfortunately, this cannot be done using current techniques as chondrocyte primary cilia are relatively short compared to those in kidney epithelia, which can reach 10 µm in length. However, the reduction in cilia length observed in response to CTS suggests IFT equilibrium might be disrupted.

### 5.4.4 Cilia disassembly requires HDAC6 and the AurA kinase

Primary cilia disassembly in response to growth factor stimulation occurs via an HDAC6/AurA dependent mechanism in retinal pigment epithelial (RPE) cells (Pugacheva et al. 2007). The HEF-1 dependent activation of AurA results in phosphorylation and activation of HDAC6 and the deacetylation and destabilisation of ciliary microtubules which likely occurs upstream of changes in IFT (Pugacheva et al. 2007).

The HDAC family is divisible into four classes (class I, IIa, IIb and IV), HDAC6 belongs to class IIb. HDAC6 is structurally different to other HDACs as it has two catalytic deacetylase domains (Figure 5.15). While possessing some activity towards histones, it mainly functions as a tubulin deacetylase (Hubbert et al. 2002). It predominantly localises to the cytoplasm where, in addition to tubulin it deacetylates substrates such as the actin regulatory protein cortactin and Hsp90 (Kovacs et al. 2005; Murphy et al. 2005; Zhang et al. 2007). Consequently HDAC6 plays essential roles in cytoskeletal dynamics and the mis-folded protein response [for review see (Boyault et al. 2007)].

Inhibition of HDAC6 abrogated chondrocyte cilia disassembly in response to 20% CTS, indicating a role for this enzyme in strain induced cilia resorption (Figure 5.8). Consistent with this finding, HDAC6 localised to the ciliary axoneme in articular chondrocytes (Figure 5.7). Tubulin acetylation is proposed to reduce the dynamic instability of microtubules thus stabilising the structures they form (Mitchison and Kirschner 1984; Rochlin et al. 1996). Deacetylation may therefore facilitate changes in axoneme length by creating a more labile structure. Indeed, current studies in the Knight lab have shown that microtubule deacetylation is also required for ciliary elongation in response to IL-1 (paper submitted).

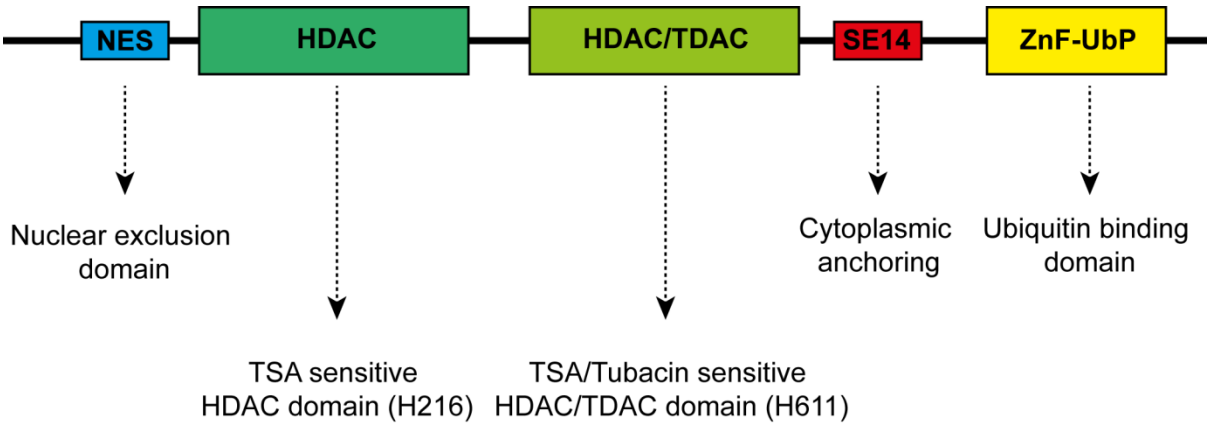


**Figure 5.15 HDAC6 domain organisation**
Schematic representation of the functional domain organisation of HDAC6. HDAC6 is the only member of the histone deacetylase family containing tandem catalytic domains, H216 and H611. While both deacetylase domains possess histone deacetyase (HDAC) activity only H611 posesses tubulin deacetylase (TDAC) activity (Haggarty et al. 2003). In human HDAC6, two different domains ensure the stable maintenance of the protein in the cytoplasm. In the human protein a conserved, N-terminal nuclear export signal (NES) mediates the active export of HDAC6 from the nucleus while a C-terminal domain called SE14 stably anchors the protein in the cytoplasm. The ZnF-UBP domain constitutes a highly conserved, high affinity ubiquitin-binding motif at the C-terminus. Adapted from (Boyault et al. 2007) and (Haggarty et al. 2003).

The mechanical regulation of the chondrocyte cytoskeleton has been extensively studied (see chapter 2) and while the microtubule network appears to be essential for cartilage maintenance (Jortikka et al. 2000; Capin-Gutierrez et al. 2004; Guo et al. 2011) little is known about the effects of mechanical loading on tubulin post translational modifications (PTMs) such as acetylation, glutamylation and de-tyrosination. Berbari et al reported that tubulin PTMs are disrupted in *Ift88* and *Kif3a* mutants lacking cilia (Berbari et al. 2013). This study demonstrated that in the absence of a cilium the acetylation of cytosolic microtubules is disrupted due to the altered expression and activity of, αTAT1/MEC7-17 and HDAC6. The authors suggest that the primary cilium has an important function in regulating the balance between HDAC6 and αTAT1/MEC7-17 and thus regulating tubulin acetylation throughout the cell. Tubulin acetylation status has been shown to influence the binding and processivity of kinesin-1 and consequently can influence cellular processes that are dependent upon microtubule transport (Reed et al. 2006). This raises the intriguing possibility that the mechanical regulation of primary cilia structure could provide a novel

mechanism by which microtubule transport, and hence the metabolic activity of the chondrocyte, might be regulated by mechanical stimuli. Consistent with this hypothesis, chemical disruption of the microtubule network in chondrocytes with taxol or nocadozole has been shown to inhibit the mechanosensitive upregulation of proteoglycan synthesis in response to cyclic hydrostatic pressure (Jortikka et al. 2000).

AurA is a centrosome-localised kinase that regulates cell cycle entry and passage through mitosis (Pugacheva and Golemis 2006). Surprisingly in the present study the activation of AurA was found to be necessary for strain induced ciliary resorption despite the fact that mechanical strain did not trigger chondrocyte proliferation and cell cycle re-entry (Figure 5.11). Transient calmodulin-dependent activation of AurA has been reported in response to $Ca^{2+}$ release from intracellular endoplasmic reticulum stores which triggers cilia disassembly in kidney epithelia via HDAC6 (Plotnikova et al. 2010; Plotnikova et al. 2012). This study suggests that loading induced changes in $Ca^{2+}$ signalling might be responsible for AurA activation. However, although mechanosensitive $Ca^{2+}$ signalling in chondrocytes has been reported (see chapter 2) further studies would be required to investigate this.

## 5.4.5 Mechanically induced changes in cilia length modulate ciliary function

### 5.4.5.1 Hedgehog signalling

In adult primary chondrocytes, hedgehog pathway activation was not observed in response to 20% CTS, despite the fact that loading at this strain magnitude upregulates Ihh expression (Figure 5.6). Primary cilia disassemble in response to mechanical stimuli in numerous cell types and this disassembly is proposed to limit cilia mediated signalling as part of a negative feed-back response. Indeed, in kidney epithelial cells fluid flow triggers cilium disassembly and reduces the levels of intracellular cAMP. When cilium disassembly is inhibited, either genetically or pharmacologically, cAMP levels cannot be regulated by flow (Besschetnova et al. 2010).

The greatest reductions in cilia length were observed in response to 20% CTS suggesting cilium disassembly might function to attenuate hedgehog signalling at higher strains. That some cilium disassembly is observed in response to 5% and 10% CTS suggests a threshold

exists above which this disruption will have functional consequences. However, although a role for tubulin deacetylation was demonstrated in strain-dependent ciliary resorption (Figure 5.8), as cilia disassembly was abrogated by HDAC6 inhibition, this inhibition was not sufficient to fully restore mechanosensitive hedgehog signalling (Figure 5.10). These data indicate that a change in the size of ciliary signalling compartment per se is not responsible for the loss of pathway activity at 20% strain. However, a partial rescue was observed as Ptch1 expression was increased by strain following tubacin treatment (Figure 5.10). Therefore it is still likely that the HDAC6-dependent destabilisation of the ciliary axoneme contributes to the loss of hedgehog signalling at higher strains which perhaps is mediated by other processes such as IFT alternatively the translocation of activated Gli proteins to the nucleus might be affected by changes in microtubule transport in the cell body.

While AurA has been shown to act upstream of HDAC6 in cilia disassembly, inhibiting this kinase did not rescue the hedgehog response at 20% strain. In fact Ptch1 and Gli1 exhibited a statistically significant down regulation following strain (Figure 5.10). Plotnikova et al reported that AurA directly interacts with the $Ca^{2+}$ channel PC-2 and phosphorylates its intracellular C-terminal domain to reduce channel activity as part of a negative feedback response (Plotnikova et al. 2011). Indeed, the authors demonstrated that AurA dependent PC-2 phosphorylation reduces the amplitude of the $Ca^{2+}$ response in kidney epithelia following the application of fluid flow (Plotnikova et al. 2011) . PC-2 localises to the cilium in chondrocytes and has been linked to ciliary function in these cells (Wann et al. 2012), therefore, PHA-680632 treatment might be expected to increase $Ca^{2+}$ signalling in these cells which will undoubtedly affect a multitude of signalling pathways and could mask any role AurA plays in hedgehog signalling. Further studies would be required to confirm if AurA activation is necessary for the HDAC6 dependent deacetylation of ciliary microtubules and cilium disassembly in response to strain.

#### 5.4.5.2 ADAMTS-5 expression

ADAMTS-5 gene expression was increased in response to 5% and 10% CTS but not by 20% CTS correlating with hedgehog pathway activity (Figure 5.13A). Although previous studies have shown that ligand dependent hedgehog signalling upregulates ADAMTS-5 expression

in human chondrocytes (Lin et al. 2009) I was not able to reproduce this response (Figure 5.13B). Therefore I find it unlikely that the mechanosensitive ADAMTS-5 expression observed in this thesis is hedgehog mediated.

Saito et al have reported mechanosensitive ADAMTS-5 expression to be dependent on HDAC-mediated MAPK-dependent activation of RUNX-2 (Saito et al. 2013). In this study, TSA or MS-275 inhibited ADAMTS-5 upregulation in response to 10% CTS. While TSA has broad specificity, MS-275 is specific to class I HDACs implicating HDAC 1, 2, 3, and 8 in this response. In the current study, Tubacin treatment restored mechanosensitive ADAMTS-5 expression at 20% CTS suggesting that strain-dependent HDAC6 activation might function to counteract the class I HDAC-dependent ADAMTS-5 expression at higher strains. Indeed, a physical interaction between HDAC6 and RUNX-2 has been reported and shown to promote the repressor function of RUNX-2 (Westendorf et al. 2002). Moreover, strain dependent regulation of HDAC6 has been reported in lung epithelia (Geiger et al. 2009). Remarkably, AurA inhibition also resulted in the upregulation of ADAMTS-5 following strain (Figure 5.14) consistent with a role for this kinase upstream of HDAC6. The pathways regulating cilia disassembly therefore appear linked to strain dependent changes in ADAMTS-5 expression. Future studies could perhaps investigate the activation of RUNX-2 and determine the influence HDAC6 exerts over this transcription factor in the context of tensile strain.

### 5.4.6 Summary

In summary, the data presented in this thesis shows that mechanical strain regulates primary cilia structure in a strain dependent manner via the activation of AurA and HDAC6, however further studies are required to establish the nature of the interaction between these enzymes. Mechanosensitive hedgehog signalling and ADAMTS-5 expression are activated in response to low but not high strain suggesting that the effects of strain on primary cilia exert a negative influence over signalling. Further questions remain as to the function of this mechanosensitive hedgehog signalling and the regulation of ADAMTS-5 in response to strain.

# Chapter 6

# Modulation of primary cilia structure and function by thermal stress

The work conducted in this chapter was performed in collaboration with N. Prodromou at the William Harvey Institute.

## 6.1 Introduction

In the previous chapter I have shown that primary cilia disassemble in response to mechanical strain. This appears to modulate mechanosensitive hedgehog signalling and ADAMTS-5 expression. To further investigate the influence extracellular stress exerts over the cilia structure-function relationship, the following chapter will examine the behaviour of cilia in response to thermal stress, or heat shock. The majority of this work will be conducted in NIH3T3 cells, a common model used to study primary cilia function. The use of this cell type will not only facilitate experiments by resolving the species compatibility issues experienced in previous chapters, but the use of a more generic cell type will hopefully target this study to a wider audience.

Joint inflammation is a common component of arthritis and leads to an increase in intra-articular temperature. This increase in temperature has been suggested to promote cartilage damage by increasing enzyme activity and matrix degradation (Harris and McCroskery 1974; Woolley and Evanson 1977). Elevated temperature activates the cellular stress response and affects multiple cellular compartments however the consequences for primary cilia have not been well analysed. Several publications have identified that elevated temperature during development can have significant consequences for processes regulated by hedgehog signalling such as endochondral ossification and neurogenesis. Serrat et al reported that chondrocyte proliferation and extracellular matrix volume strongly correlate with tissue temperature in metatarsals cultured *in vitro* without vasculature (Serrat et al. 2008). While a study by Khan et al demonstrated that in pregnant rats exposure to 42°C for 45 min on day 17 of gestation increased apoptosis in the cerebral cortex of the foetus (Khan and Brown 2002). Interestingly, this may also have relevance for human disease as hyperthermia *in utero*, due to maternal influenza, is widely accepted as an environmental risk factor for schizophrenia (Edwards 2007). Moreover, the protein disrupted-in-schizophrenia (DISC) has been shown to localise to the cilium where it regulates the formation and/or maintenance of primary cilia containing dopamine receptors (Marley and von Zastrow 2010; Domire et al. 2011).

### 6.1.1 The cellular stress response

The cellular stress response is induced by the exposure of cells to acute or chronic environmental stress such as elevated temperature and functions to promote cell survival. It is regulated mostly at the level of transcription and is characterised by enhanced synthesis of heat shock proteins (Hsps) and a reduction in the normal level of translation (Kultz 2005). Hsps are molecular chaperones and play a role in the cellular repair process by restraining protein aggregation and facilitating the refolding or degradation of mis-folded proteins to encourage cell survival. Accumulated Hsps also play a role in thermotolerance, a protective mechanism whereby cellular resistance to a subsequent stress is increased (Lowenstein et al. 1991; Mailhos et al. 1993). A family of transcription factors called heat shock factors (HSFs) regulate the stress-inducible expression of hsps (Cotto and Morimoto 1999; Anckar and Sistonen 2007). Vertebrates possess four HSF isoforms (HSF1-4), HSF-1 is the key responder to heat stress in mammals (Pirkkala et al. 2001).

In response to cellular stress, inactive HSF monomers present in the nucleus and cytoplasm trimerise and acquire DNA binding activity for the heat shock element (HSE). Binding of active HSF trimers to the HSE promotes the transcription of heat shock genes such as Hsp70 and Hsp90, which are crucial for protection against stress induced damage (Cotto and Morimoto 1999; Anckar and Sistonen 2007) (Figure 6.1).

### 6.1.2 HSF-1 and Hsp90 in ciliary function

A role for components of the cellular stress response in ciliary function was demonstrated by Takaki et al who observed that HSF-1 defective mice exhibit defects in the motile, beating cilia of the respiratory epithelium (Takaki et al. 2007). Consequently these mice develop chronic sinusitis due to impaired mucociliary clearance (Takaki et al. 2007). The cause of this defective beating was shown to be a reduction in the stability of the tubulin protein. Consequently these mice exhibited cilia that have reduced tubulin content and abnormal ultra structure such that microtubule doublets were either missing or transposed. Hsp90 expression was reduced in these mutant mice and is the most likely cause for the reduction in tubulin stability in the cilium (Takaki et al. 2007). Hsp90 is a constitutively expressed chaperone and localises to the cytoplasm and ciliary axoneme in epithelial cells (Takaki et al.

2007). The expression of Hsp90 was specifically lost from the cilia of the nasal respiratory epithelium in HSF-1 null mice. *In vitro* studies show that Hsp90 specifically interacts with ciliary tubulin and promotes its polymerisation indicating a crucial role for this chaperone in the maintenance of motile cilia (Takaki et al. 2007; Weis et al. 2010).

HDAC6 is an Hsp90 deacetylase and can modulate the activity of this chaperone (Bali et al. 2005; Kovacs et al. 2005; Murphy et al. 2005). Boyault et al demonstrated the existence of an inhibitory complex of HDAC6, Hsp90 and HSF-1 which exists in the cytoplasm of unstressed cells (Boyault et al. 2007). In response to the accumulation of ubiquitinated protein, HDAC6 is activated and triggers dissociation of this complex resulting in HSF-1 activation and the subsequent expression of stress inducible molecular chaperones such as Hsp70 (Boyault et al. 2007).

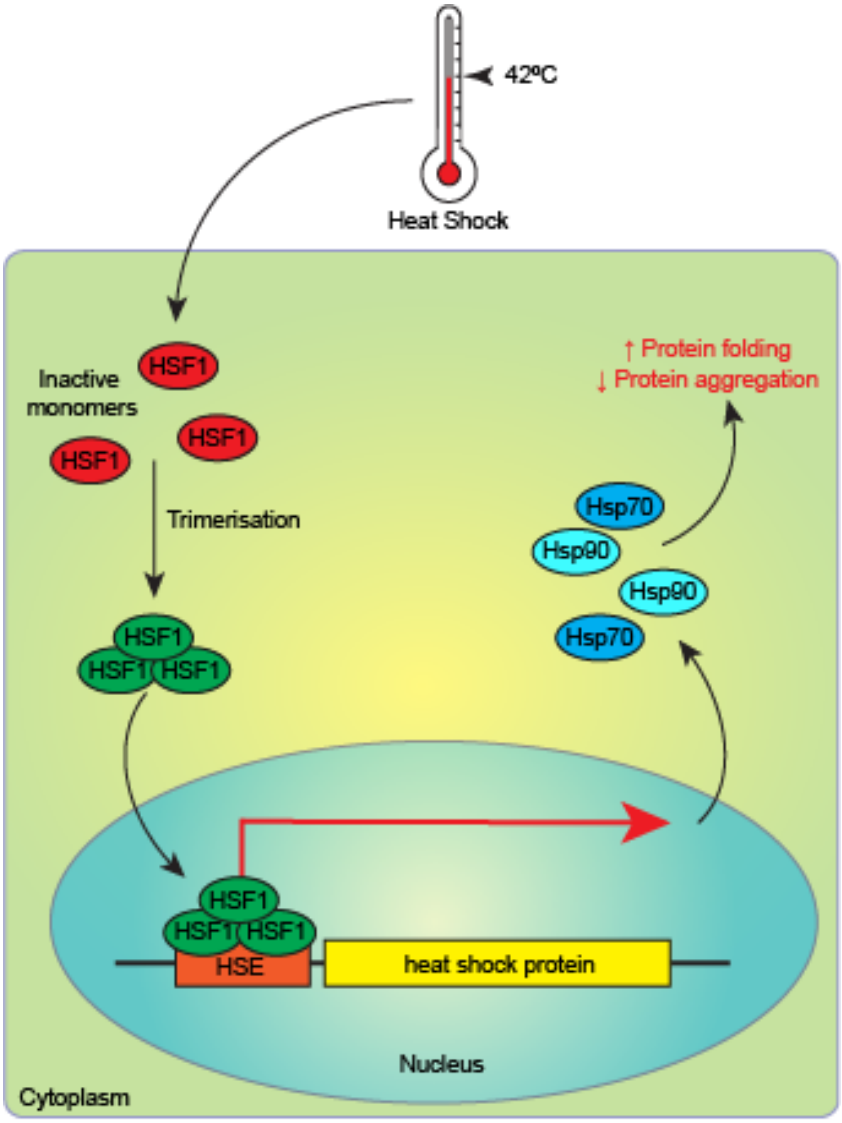


**Figure 6.1 The heat shock response**
Inactive Hsf-1 monomers in the cytoplasm are induced to trimerise in response to elevated temperature, or heat shock. Hsf-1 trimers translocate to the nucleus where they bind to heat shock response elements (HSE) *upstream of stress induced genes such* as Hsp70 and Hsp90. The expression of these proteins is increased and they facilitate protein folding and reduce the accumulation of protein aggregates in stressed cells.

### 6.1.3 Aims and Objectives

The aim of this chapter was to develop a second, more dramatic model of cilium disassembly with which to explore the cilia structure-function relationship identified in chapter 4. Previous studies in *Chlamydomonas* have identified numerous extracellular stressors that trigger flagella resorption or excision such as pH and temperature (Lefebvre and Rosenbaum 1986; Quarmby and Hartzell 1994; Pan and Snell 2005). Preliminary data collected by the Chapple group identified thermal stress, or heat shock, as an effective inducer of primary cilia resorption in mammalian cells.

The first objective of this chapter was to verify that heat shock induces cilia resorption in articular chondrocytes. The second objective was to characterise this response using the NIH3T3 murine fibroblast cell line, a model system commonly used for the study of primary cilia function, and to assess the effect this resorption has on ligand mediated hedgehog signalling. As part of this objective this response was also examined *in vivo* using a zebrafish model and the effects on development and gross morphology briefly examined.

The third objective of this study was to examine the mechanism of ciliary resorption. In chapter 5, it was shown that the AurA/HDAC6 response is activated in response to CTS therefore the role of this pathway in temperature-induced ciliary resorption was examined. As studies suggested that resorption was not occurring by this mechanism, a role for the molecular chaperone Hsp90 was examined in this response.

## 6.2 Results

### 6.2.1 Heat shock triggers primary cilia loss by resorption

Freshly isolated bovine articular chondrocytes were cultured for 6 days then subjected to heat shock for 30 min to determine the effects of thermal stress on cilia prevalence. Following heat shock cells were fixed and processed for the immunofluorescent detection of primary cilia. Primary cilia were detected on 66%±5% of the cells maintained at 37°C. Exposure to a sub-lethal 42°C heat shock for 30 min resulted in a significant reduction in the number of cells exhibiting a cilium ($p<0.001$) such that just 39%±3% of cells had detectable primary cilia (Figure 6.2).

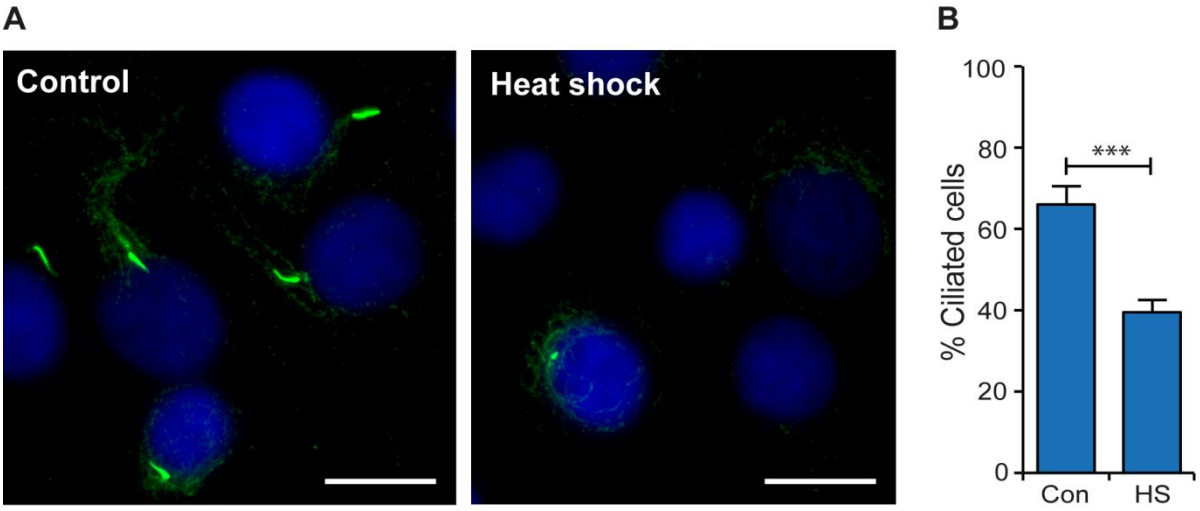


**Figure 6.2 Primary cilia loss occurs in articular chondrocytes following heat shock**
Freshly isolated articular chondrocytes were cultured for 6 days then subjected to a 42° heat shock for 30 min. **(A)** Primary cilia were labelled for acetylated α-tubulin (green) and nuclei were counter-stained with DAPI (blue). Scale bar represents 20µm. **(B)** Primary cilia prevalence was quantified in 10 representative fields of view and expressed as mean ±S.E.M. Statistical significance was assessed using Student's T-test.

To study this phenomenon more closely the NIH3T3 mouse fibroblast cell line was used, these cells provide a more widely used in vitro model in which to study cilia function. The cells were cultured for 24 hours after seeding, until 70-80% confluency was reached. They were then transferred to serum free conditions for a further 20hrs to promote ciliation then either maintained at 37°C or exposed to a 42°C heat shock for 5, 15 or 30 min (Figure 6.3). Heat shock resulted in the progressive loss of primary cilia with increasing duration (Figure

6.3B) such that following 30 min cilia prevalence was reduced to 35±3% compared to 65±2% in the control group ($p<0.001$). Like the ciliary axoneme, the cytoplasmic bridges connecting daughter cells in cytokinesis are known to be highly enriched in acetylated tubulin. As the cells used in these experiments were serum starved these structures were rare appearing at a frequency of less than 2% under control conditions (Figure 6.3C). The frequency of these structures was not significantly altered in cell populations subjected to a 42°C heat shock indicating that this response is specific to the cilium (Figure 6.3C).

The bi-flagellated green alga *Chlamydomonas reinhardtii* regulates the length of its two flagella by resorption in response to numerous stimuli. Moreover it possesses additional mechanisms for flagella elimination in response to environmental stresses such as low pH, altered tonicity and temperature (Lefebvre and Rosenbaum 1986; Quarmby and Hartzell 1994; Pan and Snell 2005). Previous studies demonstrate that primary cilia can also be lost from mammalian cells by deciliation in response to chemical agents like chloral hydrate (Taipale et al. 2000). To determine whether cilia were lost from mammalian cells by resorption or due to microtubule severing and excision at the transition zone (deciliation), primary cilia length was quantified in NIH3T3 cells maintained at 37 °C and cells subjected to heat shock for 5, 15 and 30 min using confocal microscopy (Figure 6.4). On average, cilia became progressively shorter with increased exposure to elevated temperature (Figure 6.4B). This was suggestive of primary cilia resorption, rather than excision which would be expected to cause a more immediate and dramatic reduction in length not the progressive shortening seen in Figure 6.4.

An increase in disorganised acetylated α-tubulin was observed throughout the cell after heat shock which is particularly evident at 30 min (Figure 6.4A). The reason for this is unknown, interestingly similar disorganisation has been reported in mutant cells lacking cilia due to disruption of the IFT machinery (McGlashan et al. 2007; Wann et al. 2012; Berbari et al. 2013). However the total cellular levels of acetylated tubulin were not altered by heat shock as determined by western blot (Figure 6.4C).

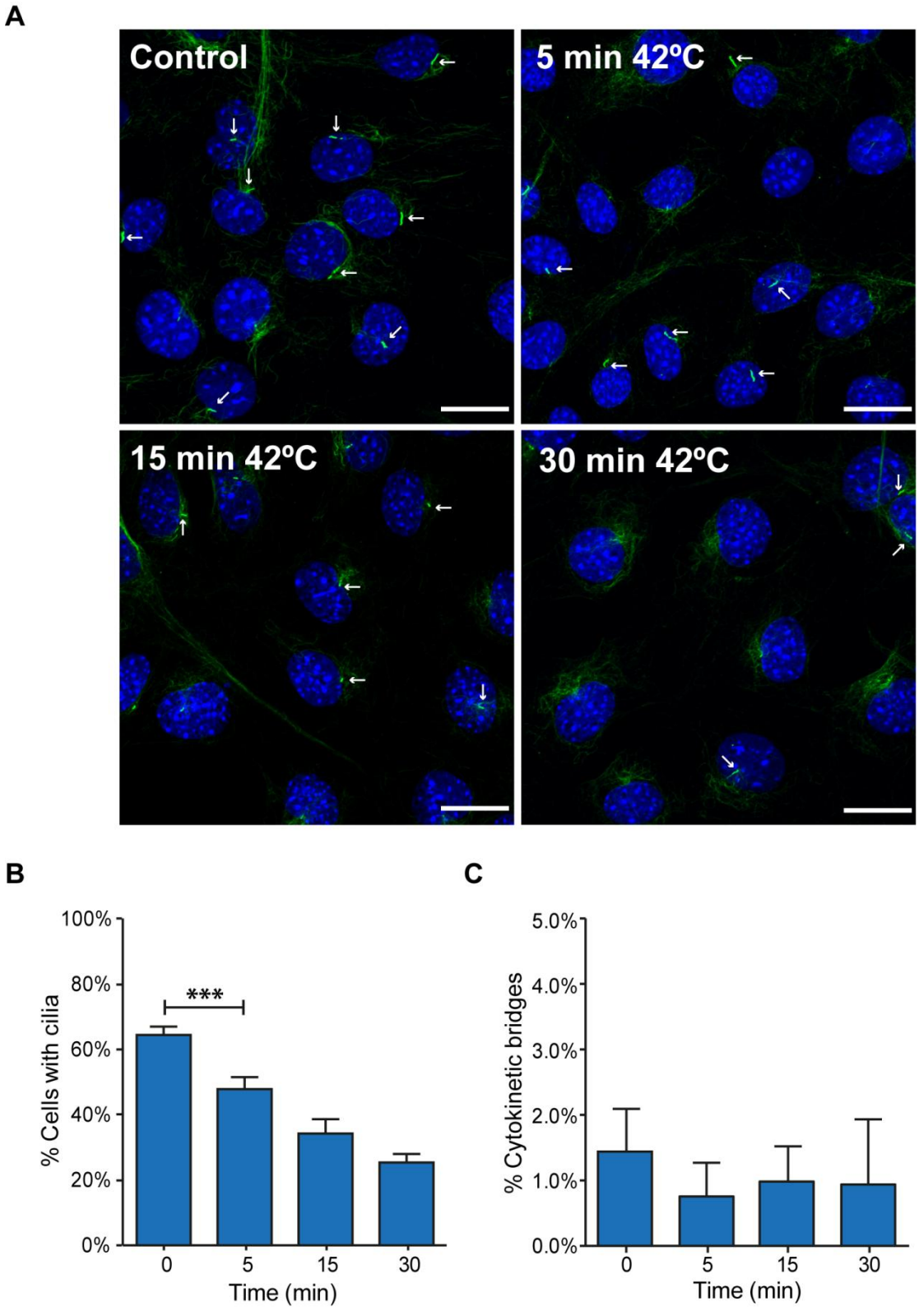


**Figure 6.3 Primary cilia loss occurs in NIH3T3 cells following heat shock**
NIH3T3 cells were exposed to heat shock at 42°C for 5, 15 and 30min. **(A)** Primary cilia were labelled for acetylated α-tubulin (green) and nuclei were counter-stained with DAPI (blue). Scale bar represents 20µm. The prevalence of **(B) p**rimary cilia prevalence and **(C)** cytokinetic bridges was quantified in 10 representative fields of view and expressed as mean ±S.E.M. Statistical significance was assessed using Student's T-test.

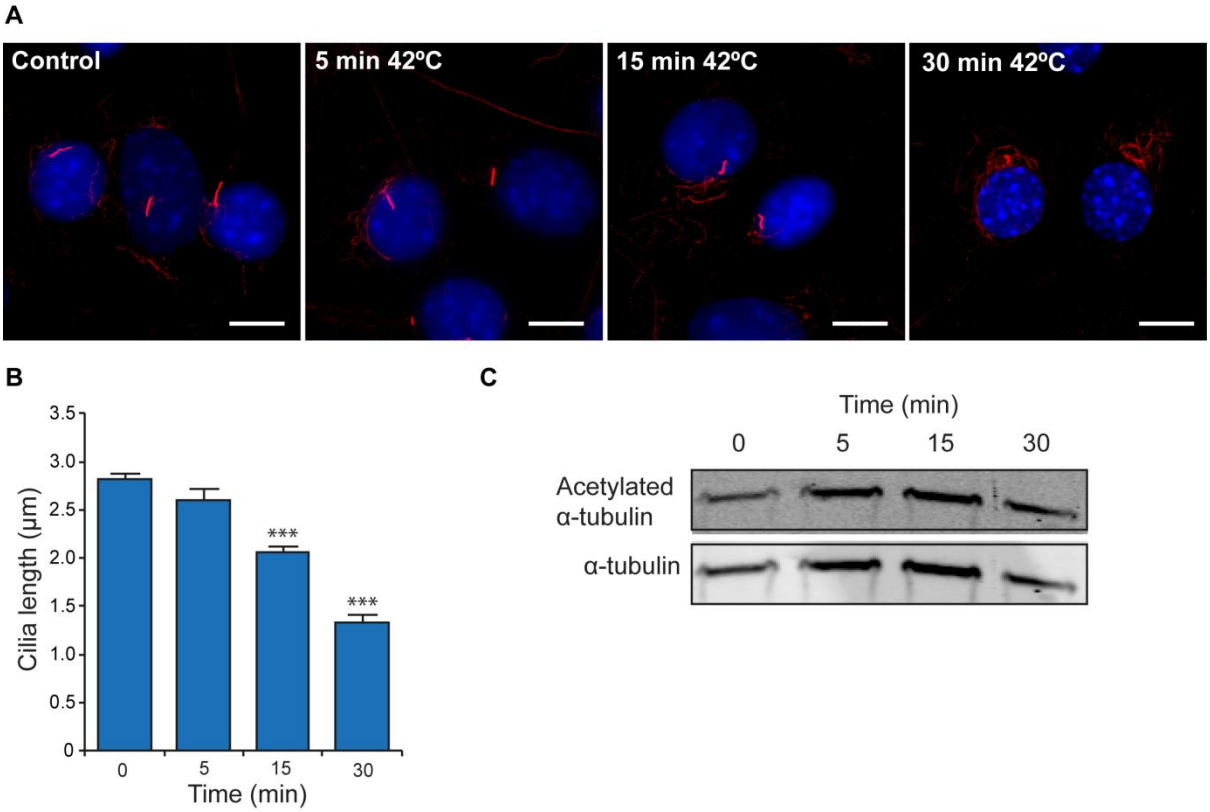


**Figure 6.4 Primary cilia disassemble in response to heat shock**

NIH3T3 cells were subjected to heat shock at 42°C for 5, 15 and 30min. **(A)** The ciliary axoneme was labelled for acetylated α-tubulin (red) and nuclei were counterstained with DAPI (blue). Scale bar represents 10µm. **(B)** Mean cilia length was measured for at least 30 cilia over 5 representative fields of view. Error bars represent ±S.E.M (90 cilia total) and statistical significance was determined using a student's T-test. **(C)** Cells were cultured for 3hrs at 37°C and were then lysed in laemelli buffer and subjected to SDS-PAGE and western blotting with antibodies directed against acetylated α-tubulin and α-tubulin were used.

To confirm that the disassembly observed was due to a true shortening of the axoneme and not the loss of acetylated tubulin within the cilium, primary cilia were co-labelled for Arl13b (Figure 6.5). Arl13b localised to the axoneme in NIH3T3 cells overlapping with acetylated tubulin in both control cells and those subjected to heat shock (Figure 6.5).

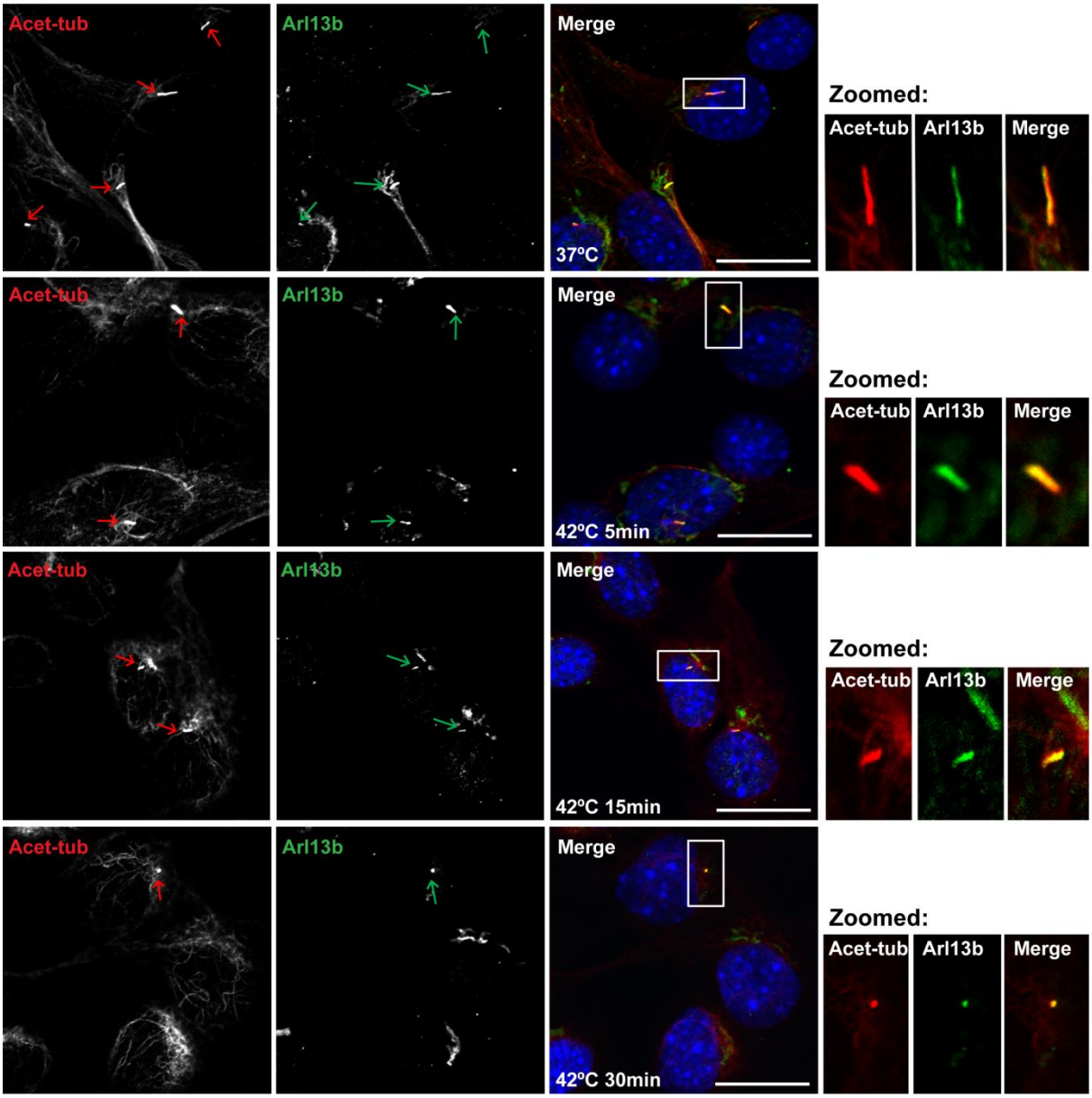


**Figure 6.5 Arl13b and acetylated tubulin co-localise within the primary cilium of NIH3T3 cells**

NIH3T3 cells were subjected to heat shock at 42°C for 5, 15 and 30min. Immediately after heat shock, NIH3T3 cells were fixed and processed for the immunofluorescent detection of primary cilia. The ciliary axoneme was labelled for acetylated α-tubulin (red) and arl13b (green). Nuclei were counterstained with DAPI (blue). Scale bar represents 20µm.

### 6.2.2 Primary cilia reassembly occurs after heat shock

To determine the rate of ciliary reassembly following heat shock, NIH3T3 cells were subjected to heat shock at 42$^{o}$C for 30 min then allowed to recover at 37$^{o}$C for up to 24hrs. A low level of cilia recovery is observable from 6hrs, at which time a small but significant ($p<0.001$) increase in cilia prevalence is observed (Figure 6.6A). However, at 58±3% the percentage of ciliated cells remains significantly lower following heat shock relative to control cells after a recovery period of 16hrs. Following 24 hrs at 37°C cilia prevalence returned to the level observed in control cells. By contrast, mean cilia length did not fully recover within 24 hrs (Figure 6.6B). While significant cilia reassembly was observed as early as 6hrs post heat shock, primary cilia remained significantly shorter in cells subjected to heat shock compared to control cells after 24hrs ($p<0.001$). Interestingly, one way ANOVA confirmed that the rate of cilia assembly was not constant over the 24 hr period ($p<0.01$) (Figure 6.6B). In fact the mean rate of cilia assembly following heat shock (growth rate) decreased significantly over time. Trend analysis was performed on the mean growth rate from 4 to 24 hrs, where cilia assembly was observed. These analyses revealed a strong, negative correlation between growth rate and time post heat shock with a Pearson's r-value of -0.976 (Figure 6.6C). This is consistent with previously published reports that suggest the rate of flagella assembly negatively correlates with flagella length (Engel et al. 2009). Indeed a negative correlation was observed between growth rate and cilia length (Pearson's r-value = -0.733, Figure 6.6D).

These data show that stress induced changes in cilia length can persist for some time after the initial application of stress therefore heat shock would be expected to have a lasting effect on cilia mediated signalling.

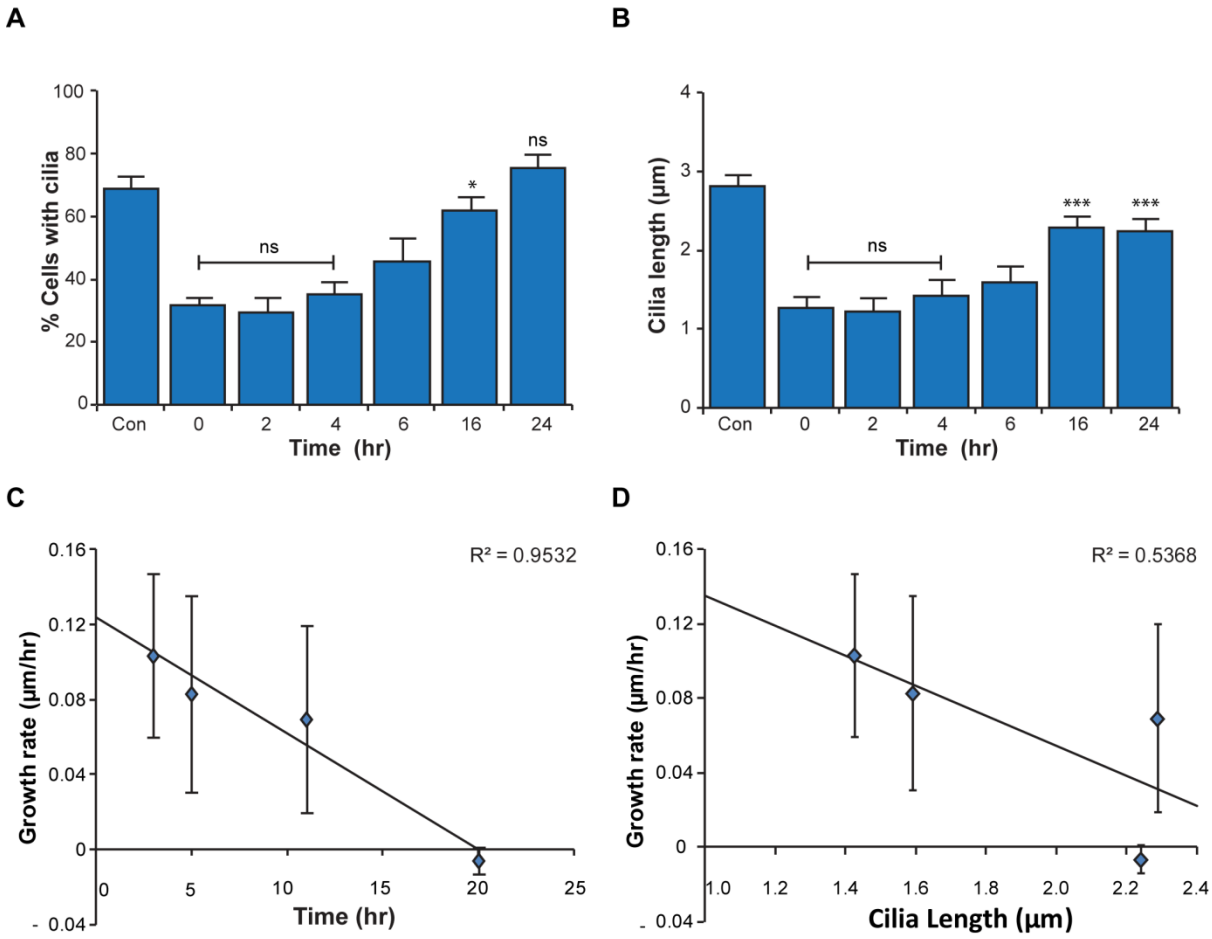


**Figure 6.6 Primary cilia reassemble following heat shock**

NIH3T3 cells were subjected to heat shock at 42°C for 30min. Cells were then allowed to recover in serum-free media at 37°C for up to 24hrs. They were then fixed and processed for the immunofluorescent detection of primary cilia. **(A)** Primary cilia prevalence was quantified in 10 representative fields of view and expressed as mean ±S.E.M. Statistical significance was assessed using Student's T-test. **(B)** Mean cilia length was assessed using confocal microscopy. Data represents mean ±S.E.M (n=90 cilia) and statistical significance was determined using a Mann Whitney U -test. The growth rate (µm/hr) was calculated from the start of recovery and plotted **(C)** against time (between adjacent time points) and **(D)** mean cilia length. Linear regression analysis demonstrated a negative correlation between growth rate and time.

### 6.2.3 Heat shock induced ciliary resorption attenuates ligand mediated hedgehog signalling

NIH3T3 cells contain all of the components required for ligand-dependent hedgehog signalling (Taipale et al. 2000; Rohatgi et al. 2007). Therefore the functional consequences of heat shock-induced ciliary resorption on cilia mediated signal transduction were tested by analysing hedgehog pathway activation using a Gli-dependent luciferase assay. This assay provides a highly sensitive measure of hedgehog pathway activity.

NIH3T3 cells were transfected with a Gli-dependent luciferase reporter which becomes activated in response to ligand stimulation providing a measure of the transcriptional activity of Gli1. Following a 20hr recovery period the transfected cells were subjected to heat shock at 42°C for 15 and 30 min. The cells were then allowed to recover at 37°C for 4hrs then treated with 2μM Purmorphamine, a hedgehog agonist, for a further 12hrs. At the end of the treatment period the cells were lysed and luciferase activity measured. In control cells maintained at 37°C, purmorphamine treatment triggered a highly significant increase in luciferase activity indicative of hedgehog pathway activation ($p<0.001$) (Figure 6.7). Significant pathway activity was also observed in cells subjected to heat shock ($p<0.001$) (Figure 6.7). This finding is unsurprising given that significant cilia recovery occurs during the treatment period (Figure 6.6). However, the level of hedgehog pathway activation observed following a 30 min heat shock was significantly attenuated compared to the response in control cells (Figure 6.7). This is consistent with the finding that cilia remain significantly shorter and less prevalent throughout the treatment period in cell populations subjected to heat shock (Figure 6.6) suggesting cilia resorption attenuates hedgehog signalling.

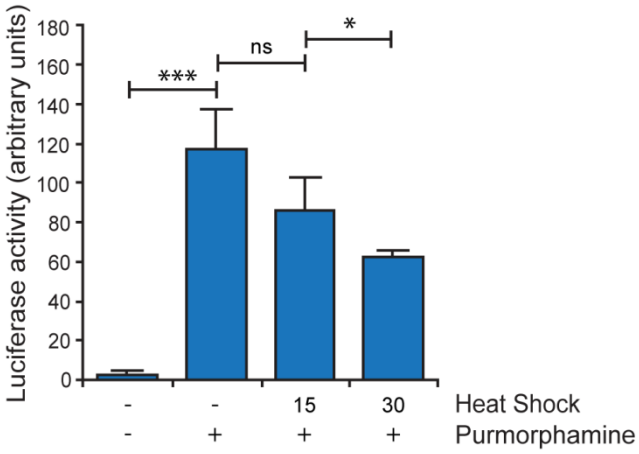


**Figure 6.7 Primary cilia disassembly attenuates ligand mediated hedgehog signalling**
NIH3T3 cells were transfected with a Gli luciferase reporter than subjected to heat shock at 42°C for 15 and 30min. Cells were allowed to recover at 37°C for 4hrs then treated for a further 12hrs with 2µm Purmorphamine. Hedgehog pathway activity was assessed by luciferase assay. Data represents mean ±S.E.M. Statistical significance was assessed using Student's T-test.

### 6.2.4 Primary cilia are sensitive to heat shock *in vivo*

Zebrafish (*Danio rerio*) were used to investigate the effect of elevated temperature on cilia *in vivo*. Exposure to a 42°C heat shock for 30 min proved to be lethal for Zebrafish embryos therefore a 5 min heat shock was used. Zebrafish embryos were used at the 24 hours post fertilisation (hpf) stage to facilitate ciliary staining. Confocal analysis of primary cilia in the caudal region of embryos was performed for control embryos maintained at 28.5°C and embryos subjected to heat shock. The tip of the tail was used as a reference for orientation and primary cilia were detected in control embryos by labelling acetylated α-tubulin (Figure 6.8A). Cilia prevalence was 78±11% in control embryos with a mean axoneme length of 1.35±0.4µm. Following heat shock primary cilia prevalence was significantly reduced to 42%±6% and at 1.08±0.4µm the remaining primary cilia were significantly shorter ($p<0.001$) (Figure 6.8)

Although primary cilia loss was observed, the heat shock conditions used were sub-lethal and all embryos survived until the end of the experimental period. No obvious deformities such as body axis curvature, reduced body length or increased somite angles were apparent in Zebrafish subjected to heat shock (Figure 6.9A-C). To track the progress of development

head-trunk (H/T) angles were measured, this angle increases from 20hpf as a consequence of embryo straightening (Kimmel et al. 1995). The H/T angle increased significantly from 24hpf to 32hpf in control embryos and embryos subjected to heat shock demonstrating a strong positive correlation with experimental time (Pearson's r-value= 0.96 and 0.99 respectively). While the H/T angle was consistently greater in embryos subjected to heat shock (Figure 6.9D) this did not reach statistical significance. Analysis of covariance (ANCOVA) was performed but did not find this trend to be statistically significant either indicating there were no obvious defects in the rate of embryo development.

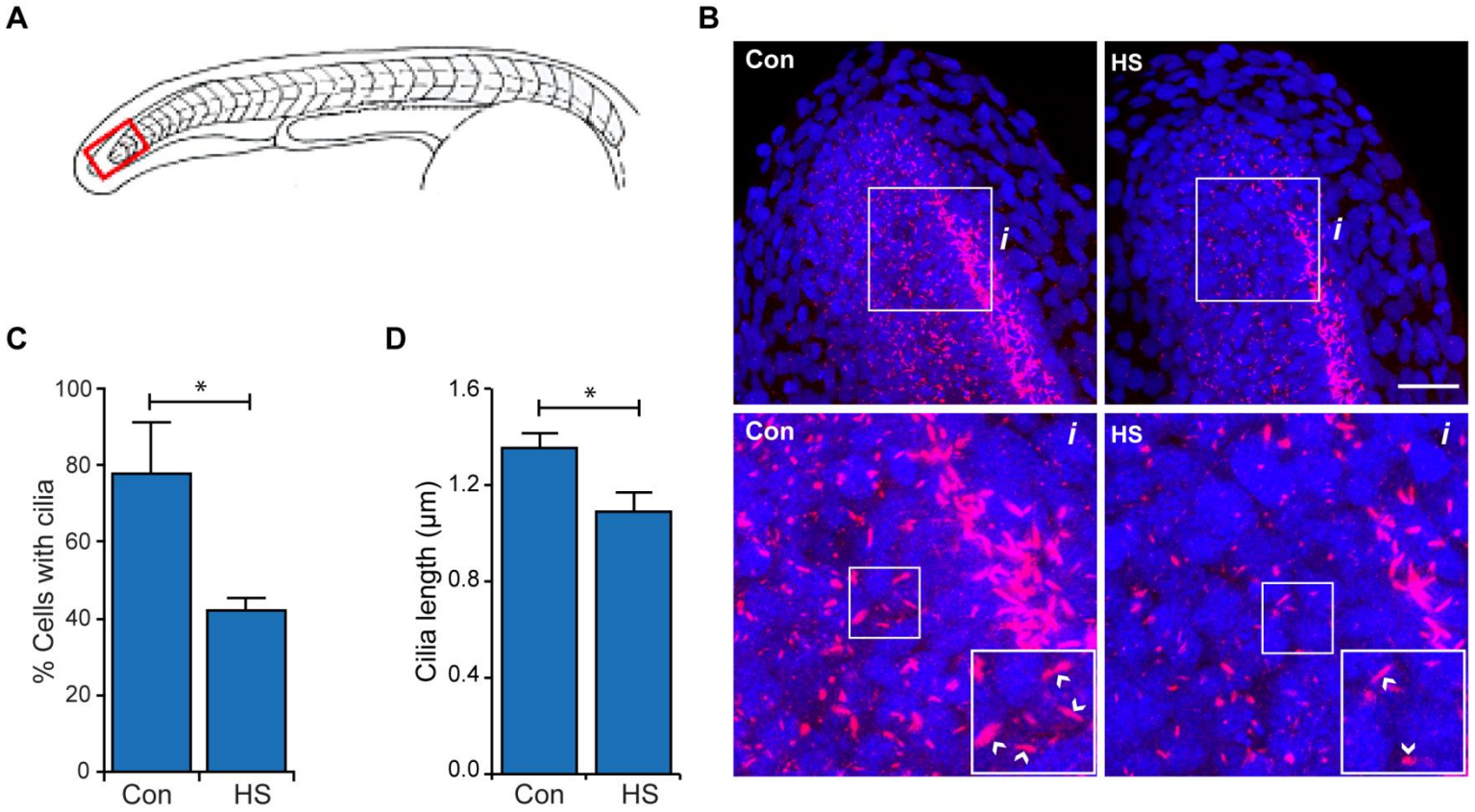


**Figure 6.8 Stress induced primary cilia resorption occurs in vivo**

Zebrafish embryos were subjected to a 5 min heat shock at 42°C at the 24hpf stage. **(A)** Cilia length and prevalence were analysed in the tail region. **(B)** Following heat shock embryos were fixed and primary cilia labelled with acetylated α-tubulin (red). Nuclei were counter stained with DAPI (blue). Scale bar represents 100µm. Primary cilia **(C)** prevalence and **(D)** length were quantified from maximum intensity projections of confocal z-stacks. Data represents mean ± S.E.M (n= 5 embryos per group).

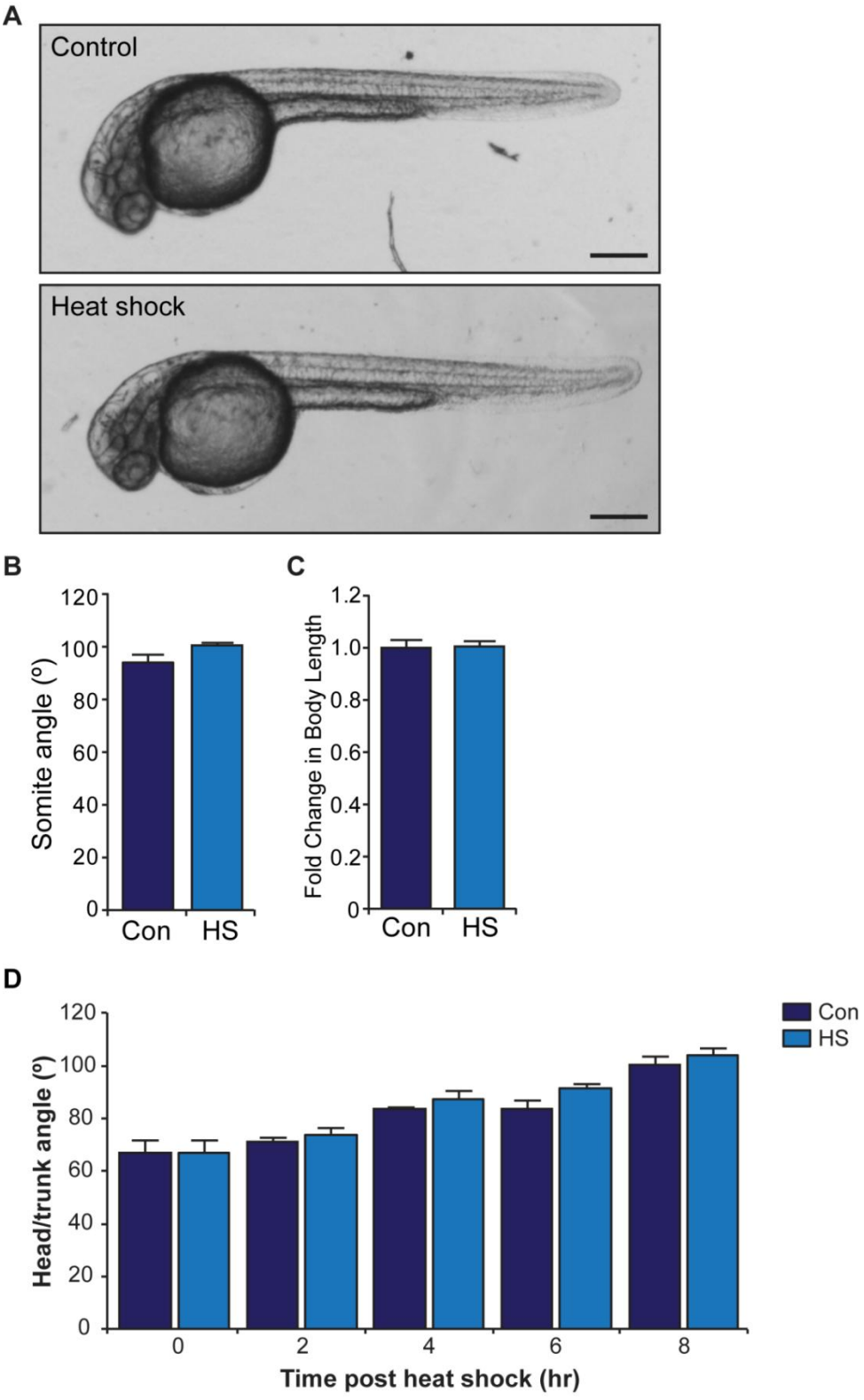


**Figure 6.9 Heat shock does not overtly effect development in 24hpf Zebrafish embryos**
Zebrafish embryos were subjected to a 5min heat shock at 42$^{o}$C at the 24hpf stage. **(A)** Heat shock did not alter zebrafish morphology. There were no significant differences in **(B)** somite angle **(C)** body length or **(D)** H/T angles between control embryos and those subjected to heat shock. Data represents mean ± S.E.M (n= 10 embryos per group).

### 6.2.5 Heat shock induced cilia loss is dependent on a HDAC6 mediated pathway but does require AurA

In mammalian cells the resorption of primary cilia in response to serum has previously been shown to depend on an AurA/HDAC6 pathway (Pugacheva et al. 2007), in chapter 5 I demonstrated that the activity of these proteins is required for chondrocyte cilia disassembly in response to strain. In the following section I test the role of these two proteins in heat-shock induced cilia resorption.

In RPE cells serum induced cilia disassembly occurs in 2 waves; an early wave at 2 hrs post serum addition, and a later wave between 18-24 hrs. In this early wave cells remain in the $G_1$ phase of the cell cycle, whereas in the second wave most cells are entering mitosis. PHA-680632 inhibits cilia disassembly at both these points (Pugacheva et al. 2007). To confirm the efficacy of the AurA inhibitor NIH3T3 cells were serum starved for 20hrs to induce ciliation, then pre-treated with 500nM PHA-680632 for 3hrs and subsequently returned to serum containing medium for 2 or 24 hrs to induce cilia disassembly. Mean cilia prevalence in control cells was 62±7%, this was significantly reduced to 45±2% following serum addition for just 2hrs ($p<0.001$). A greater reduction was observed following 24 hrs of serum addition where mean cilia prevalence was reduced to 22±3% (Figure 6.10A). Cilia disassembly was significantly inhibited by 500nM PHA-680632 at 2 hrs. In contrast the reduction in prevalence was not inhibited at 24hrs (Figure 6.10A). These data suggest that while in NIH3T3 cells the first wave of disassembly is regulated by AurA, these cells may have additional AurA-independent mechanisms for regulating the second wave of ciliary disassembly prior to mitosis.

To assess the potential role for AurA in heat shock induced ciliary resorption, ciliated NIH3T3 cells were pre-treated with 500nM PHA-680632 for 3 hrs then subjected to a 30 min heat shock at 42$^{o}$C (Figure 6.10B and C). PHA-680632 treatment did not inhibit stress induced ciliary disassembly and mean primary cilia length and prevalence were not significantly different between treated and untreated cells subjected to heat shock suggesting AurA is not involved in this response (Figure 6.10B and C).

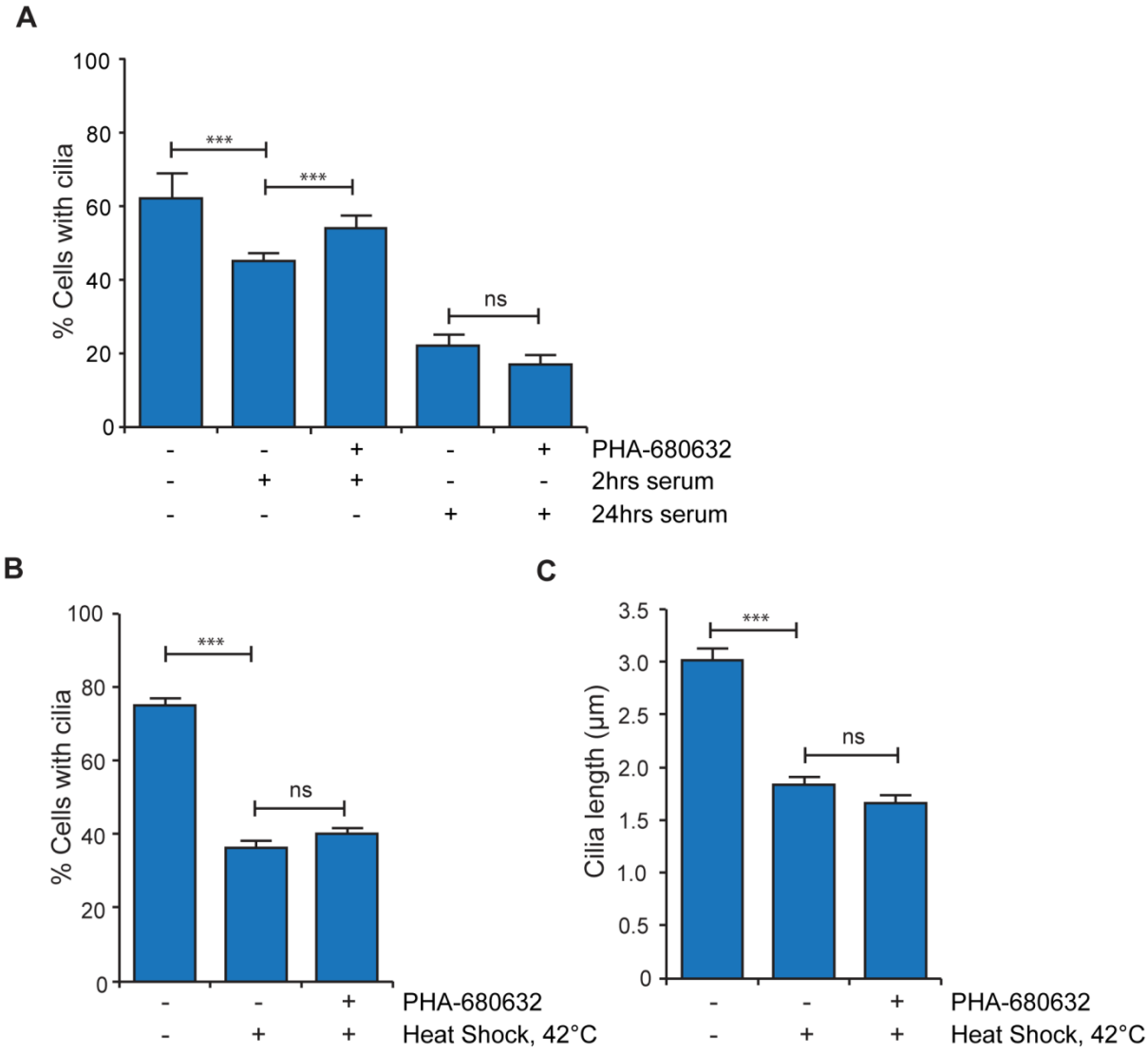


**Figure 6.10 AurA is required for serum induced cilia disassembly at 2hrs**

NIH3T3 cells were cultured for 24 hrs then serum starved for a further 20 hrs to induce ciliation (con). The effect of serum addition in the presence of PHA-680632 was assessed at 2 and 24 hrs. **(A)** Primary cilia prevalence was quantified in 10 representative fields of view and expressed as mean ±S.E.M. Statistical significance was assessed using Student's T-test. NIH3T3 cells were subjected to heat shock for 30 min in the presence of PHA-680632. **(B)** Primary cilia prevalence was quantified in 10 representative fields of view and expressed as mean ±S.E.M. Statistical significance was assessed using Student's T-test. **(C)** Mean cilia length was measured by confocal microscopy. Data represents mean ±S.E.M (n=90 cilia) and statistical significance was determined using a Mann Whitney U -test.

Immunofluorescent labelling of HDAC6 confirmed that, as in chondrocytes, HDAC6 was present both in the cytoplasm and the ciliary axoneme (Figure 6.11). In NIH3T3 cells HDAC6 localised along the length of the cilium although stronger labelling was often observed at the more distal end of the axoneme. In longer cilia this staining was more punctate suggesting HDAC6 localises to IFT particles; it was not always possible to distinguish individual particles in shorter cilia. The intensity of HDAC6 ciliary staining was variable within different cells and was often masked by more intense cytoplasmic staining. Staining was readily observable in approximately 30% of cells; however the true value for this is likely to be higher.

Following heat shock, HDAC6 remained localised to the primary cilium (Figure 6.12A) and there was no significant difference in the number of HDAC6 positive cilia between control cells and those subjected to heat shock for 30min ($p=0.667$), suggesting that localisation in this population of HDAC6-positive cells at least is not affected by thermal stress. To assess the role of HDAC6 in heat shock induced cilia resorption NIH3T3 cells were pre-treated with either 7nM TSA or 500nM tubacin for 3 hrs then subjected to a 30 min heat shock. The loss of primary cilia following heat shock was significantly attenuated by both TSA and tubacin ($p<0.0001$) (Figure 6.12B). The remaining primary cilia in treated cells subjected to heat shock were also longer than in untreated cells (Figure 6.12C). These data indicate that the deacetylation of microtubules is at least partially required for cilia disassembly in response to heat shock.

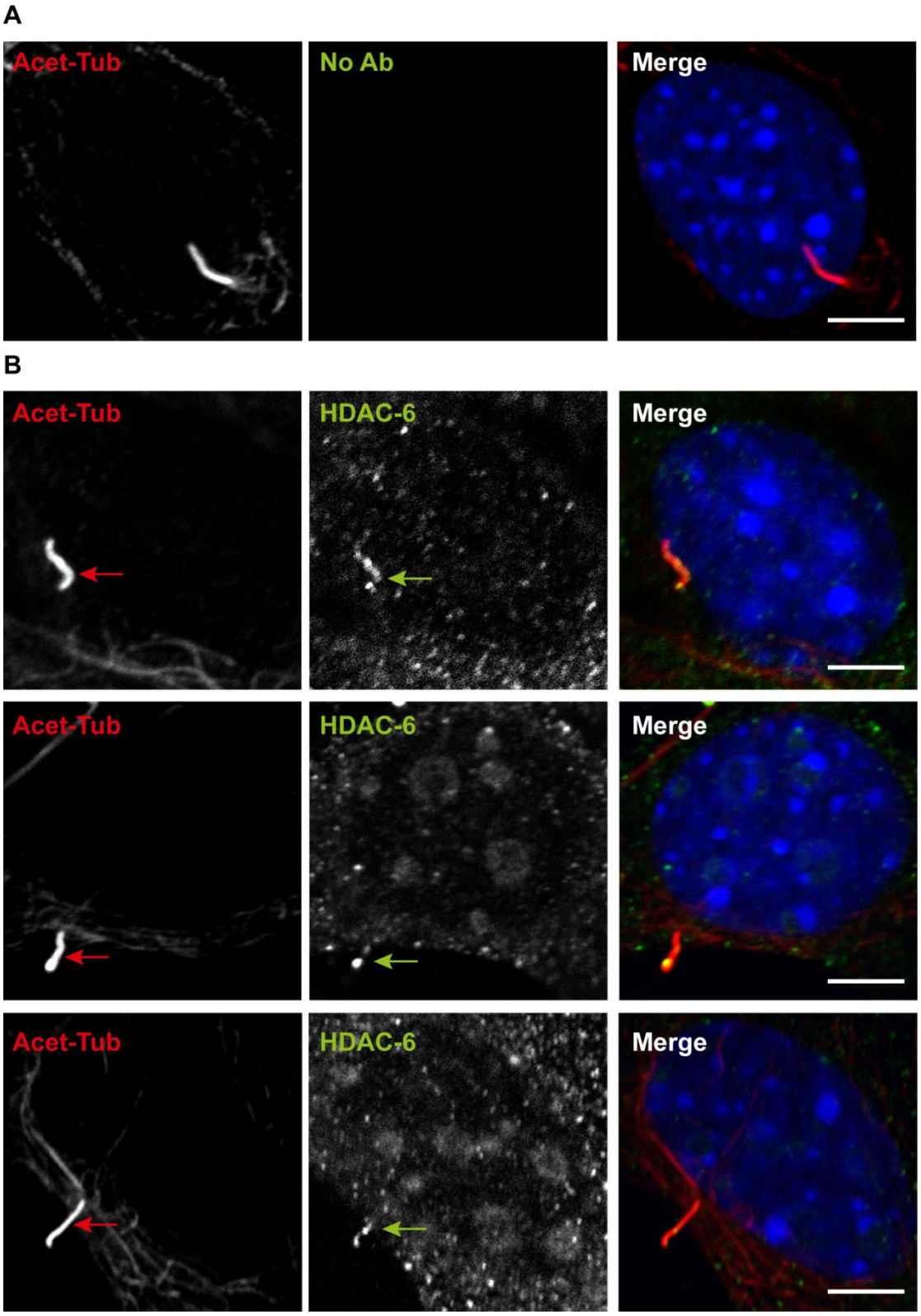


**Figure 6.11 HDAC6 localises to the ciliary axoneme in NIH3T3 cells**
NIH3T3 cells were serum starved for 20 hrs to induce ciliation then fixed and immunofluorescently labelled for HDAC6 (ab12173, green) and acetylated α-tubulin (red). Nuclei were counterstained with DAPI. **(A)** no HDAC6 antibody control **(B)** with HDAC6 antibody. Scale bar represents 5µm.

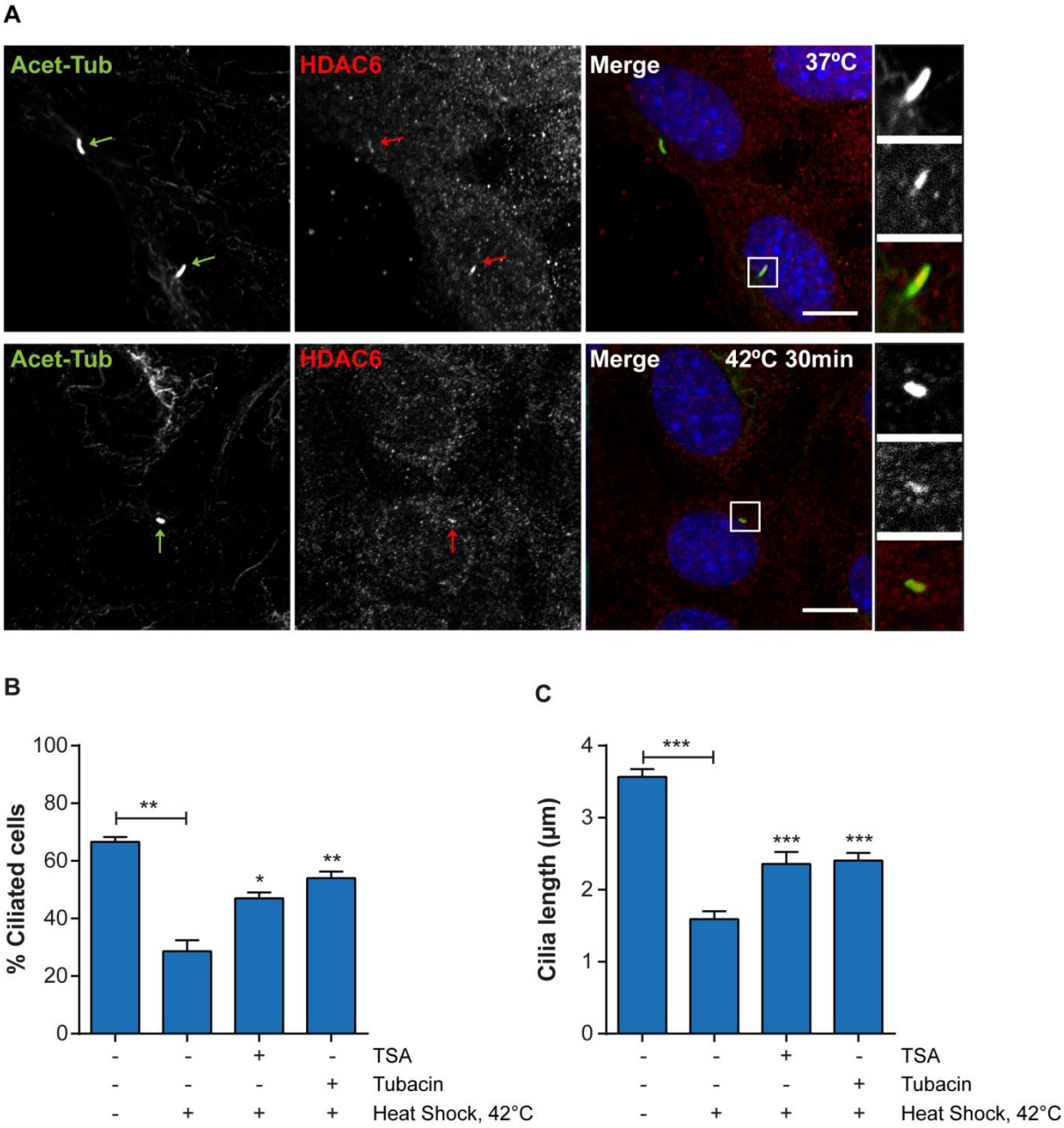


**Figure 6.12 Heat shock induced ciliary resorption requires HDAC6**
NIH3T3 cells were subjected to a 30 min heat shock. **(A)** Following heat shock cells were fixed and immunofluorescently labelled for HDAC6 (red) and acetylated α-tubulin (green). Nuclei were counterstained with DAPI. Scale bar represents 10µm. NIH3T3 cells were subjected to a 30 min heat shock in the presence of TSA or Tubacin. **(B)** Primary cilia prevalence and **(C)** length were quantified in 10 representative fields of view and expressed as mean ±S.E.M (n=90 cilia). Statistical significance for cilia prevalence was assessed using Student's T-test and a Mann Whitney U test was used for cilia length.

### 6.2.6 Heat shock induced primary cilia resorption is reduced in thermotolerant cells

Thus far, a partial requirement for HDAC6 in heat shock induced ciliary disassembly has been demonstrated. However, in contrast to mechanically induced disassembly, AurA is not required for this response. Given the multitude of disassembly pathways reported in the literature, and the rapidity of the heat shock induced response, it is unsurprising that heat shock induced resorption occurs by a different mechanism. Hsp90 is constitutively expressed by cells and has been reported to associate with ciliary microtubules in protozoa (Williams and Nelsen 1997). HDAC6 is an Hsp90 deacetylase (Fuino et al. 2003; Nimmanapalli et al. 2003; Bali et al. 2005) moreover Hsp90 has also been implicated in motile cilia function in mice (Takaki et al. 2007). Therefore the potential role of this chaperone was examined in heat shock-induced ciliary resorption.

In addition to the synthesis of heat shock proteins, the cellular response to sub-lethal heat shock involves the development of thermotolerance. If a role in cilia maintenance exists for Hsp90 or heat shock proteins in general, primary cilia would be expected to be less sensitive to thermal stress in thermotolerant cells where the levels of these proteins are elevated. NIH3T3 cells were exposed to a 30 min priming heat shock 4 hours prior to passage to make them thermotolerant. After seeding these cells were cultured for 24 hours and then transferred to serum free media for 20 hours to promote cilia formation. Primary cilia resorption in response to heat shock was significantly reduced in thermotolerant cells ($p<0.01$) (Figure 6.13A). Furthermore the remaining cilia were longer than in control cells ($p<0.01$) (Figure 6.13B). These data suggest a possible role for Hsps in cilia maintenance.

To specifically target the function of Hsp90 cells were treated with geldanamycin benzoquinone ansamycin (GA), a broad specificity Hsp90 inhibitor. GA treatment resulted in a reduction in the prevalence and mean length of primary cilia in a population of NIH3T3 cells maintained at 37°C (Figure 6.13C). In cells exposed to a 30 min heat shock, GA treatment further reduced cilia prevalence and length relative to heat shock alone (Figure 6.13D). Together these data indicate a possible protective role for Hsp90 in the maintenance of primary cilia.

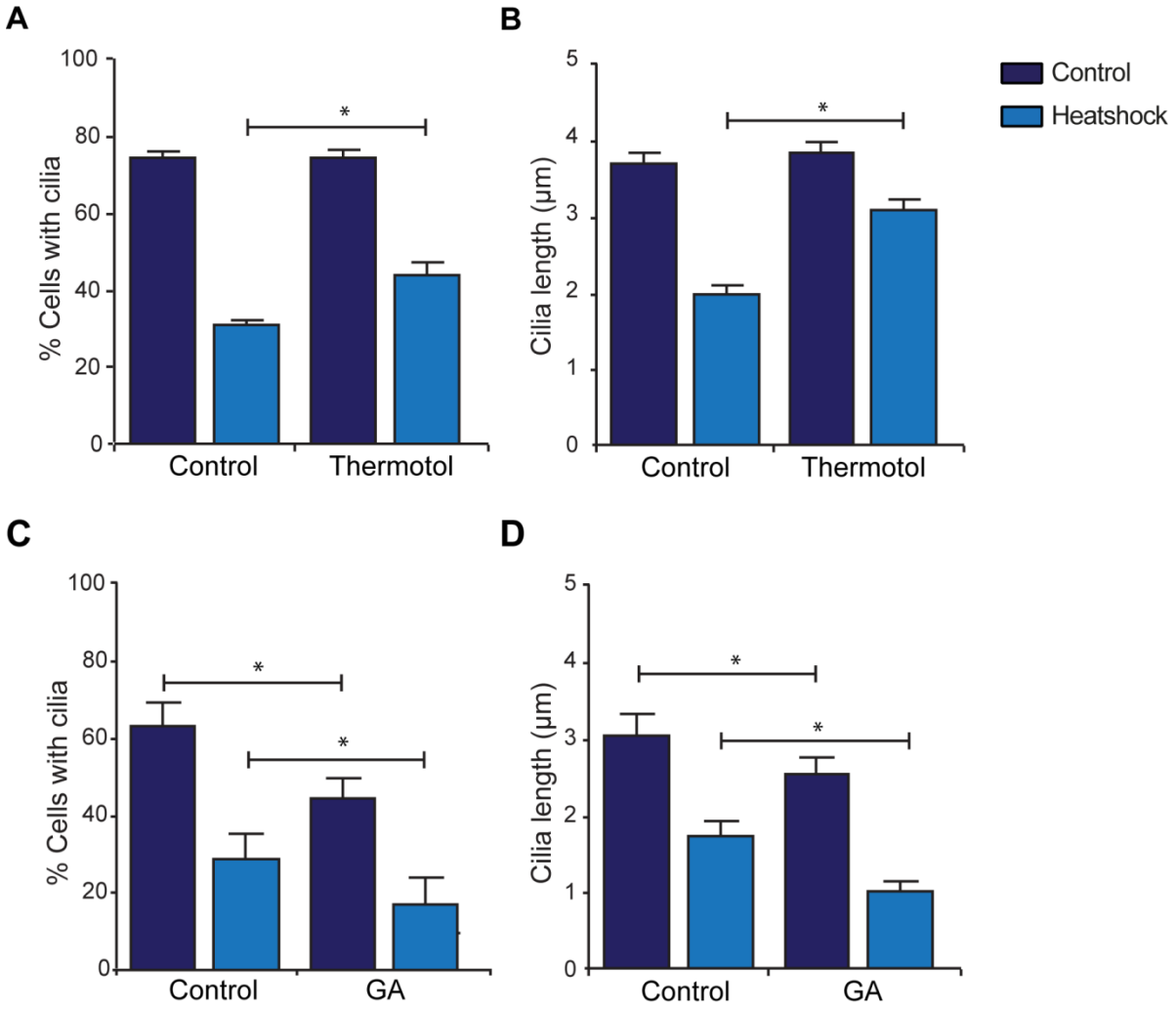


**Figure 6.13 Hsp90 is required for primary cilia maintenance**

NIH3T3 cells were subjected to a priming heat shock for 30 min then recovered for 24 hr at 37°C. These cells were then passaged and cultured for a further 24 hrs and then serum starved for 20 hrs to induce ciliation before the application of a 30 min heat shock. Primary cilia **(A)** prevalence and **(B)** length were assessed immediately after heat shock. NIH3T3 cells were treated for 3 hrs with 2µm geldanamycin benzoquinone ansamycin (GA) then subjected to a 30 min heat shock Primary cilia **(C)** prevalence and **(D)** length were assessed immediately after heat shock. Cilia prevalence was quantified in 10 representative fields of view and expressed as mean ±S.E.M (n=90 cilia). Statistical significance for cilia prevalence was assessed using Student's T-test and a Mann Whitney U test was used for cilia length.

### *6.2.7* Hsp90 localises to the ciliary axoneme in NIH3T3 cells

It has previously been reported that Hsp90 is present in the nucleus and cytoplasm with some enrichment at centrosomes and within the axonemes of motile cilia (Lange et al. 2000; Takaki et al. 2007). Immunofluorescent labelling of Hsp90 revealed this protein localises to the ciliary axoneme in NIH3T3 cells in addition to the cell cytoplasm (Figure 6.14). Hsp90 staining was detected in 71±3% of axonemes in control cells (Figure 6.15A and B). For cells that retained primary cilia after heat shock, the incidence of Hsp90 positive axonemes was significantly reduced to 42±7% (Figure 6.15B). Moreover, Hsp90 ciliary staining in these remaining axonemes was significantly less intense ($p<0.01$) (Figure 6.15C). Hsp90 intensity was quantified by measuring the Hsp90 immunofluorescent signal that co-localised with acetylated tubulin in individual primary cilia. Together these data suggest that Hsp90 levels are decreased in cilia upon heat shock. They could also indicate that cilia that are positive for Hsp90 are more readily lost upon heat shock, however given that GA treatment also reduces cilia frequency this is unlikely (Figure 6.13C).

HDAC6 and Hsp90 have previously been reported to interact, forming a complex in the cytoplasm of unstressed cells which dissociates in response to the accumulation of ubiquitinated protein and results in Hsp90 activation (Boyault et al. 2007). To examine the existence of this complex in the primary cilium, co-localisation of these proteins was assessed by triple immunofluorescent labelling for HDAC6, Hsp90 and acetylated α-tubulin (Figure 6.16). A partial co-localisation was observed in ciliary axonemes in control cells. Co-localisation was observed in both short (<2µm) and long (>2µm) cilia (Figure 6.16A-C). This was particularly evident in puncta along longer cilia suggesting HDAC6 and Hsp90 co-localise within IFT particles which have been reported to become smaller and more punctate with increases in cilia length (Pan and Snell 2005). In cells exposed to 42°C for 30 min it was more difficult to identify Hsp90 staining in the remaining shortened ciliary axonemes due the reduction in Hsp90 intensity (Figure 6.16D-F). However, this co-localisation was still present in some cilia, albeit less so. Coupled with the previous observation that HDAC6 ciliary localisation remains constant following heat shock, these data provide support for the existence of an HDAC6/Hsp90 complex within the cilium that dissociates upon heat shock.

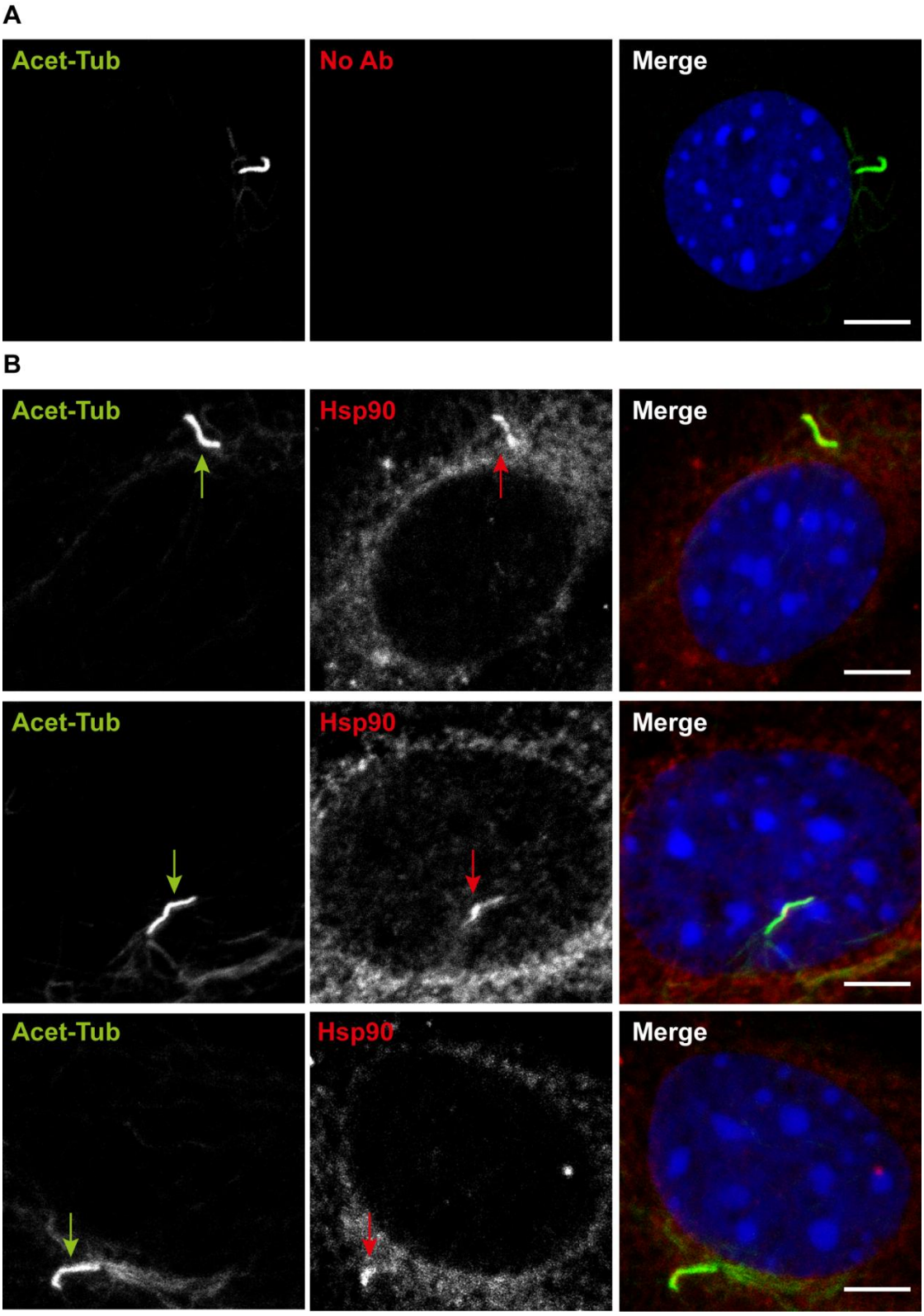


**Figure 6.14 Hsp90 localises to the ciliary axoneme in NIH3T3 cells**
NIH3T3 cells were serum starved for 20hrs to induce ciliation then fixed and immunofluorescently labelled for Hsp90 (ab13495, green) and acetylated α-tubulin (red). Nuclei were counterstained with DAPI. **(A)** without Hsp90 primary antibody **(B)** with Hsp90 primary antibody. Scale bar represents 5µm.

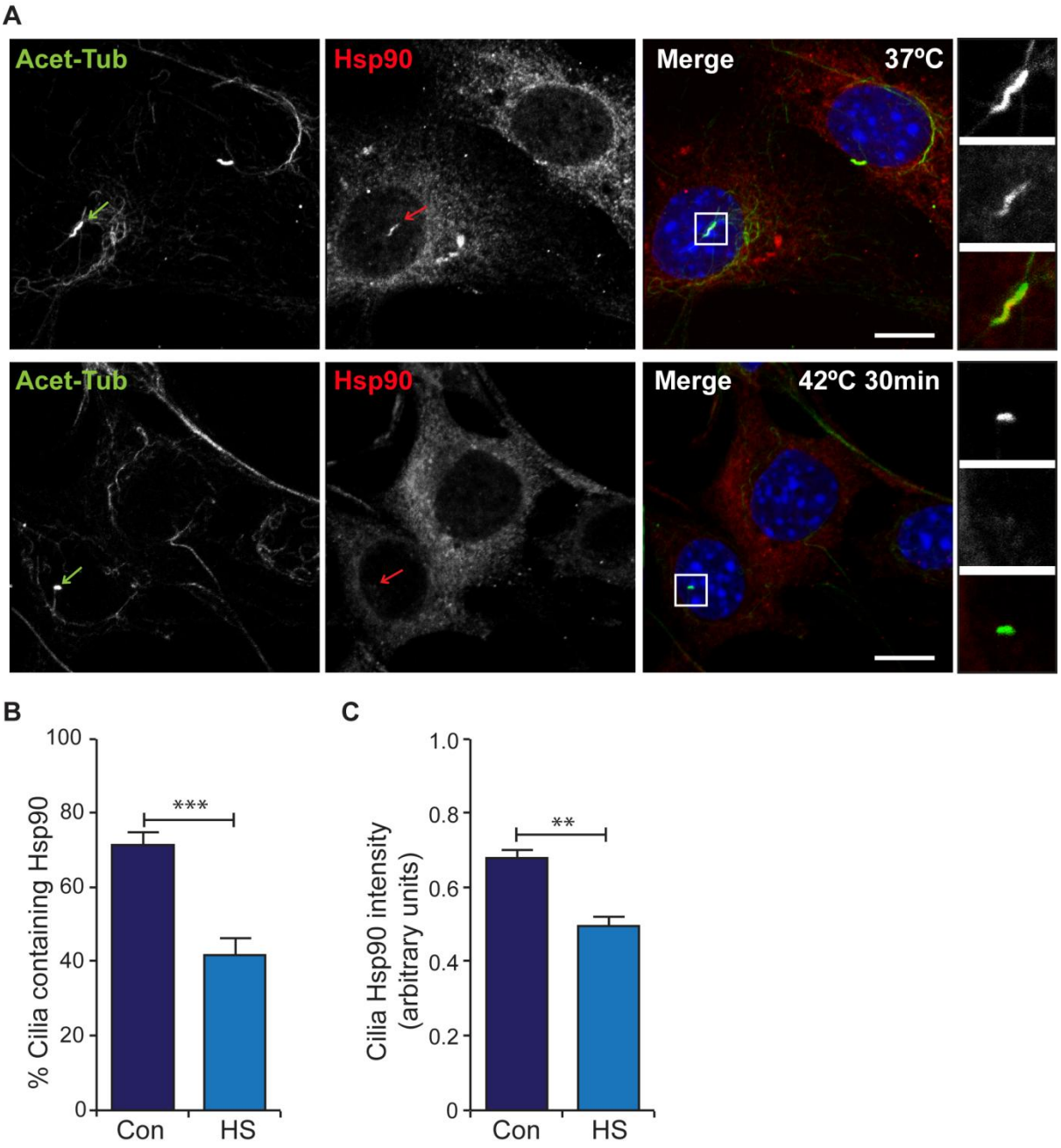


**Figure 6.15 Heat shock reduces Hsp90 localisation to the axoneme**
NIH3T3 cells were serum starved for a 20 hrs to induce ciliation then subjected to a 30 min heat shock. **(A)** Immediately after heat shock, cells were immunofluorescently labelled for Hsp90 (red) and acetylated α-tubulin (green). Nuclei were counterstained with DAPI. Scale bar represents 10µm. **(B)** The proportion of Hsp90 positive cilia was quantified in 10 representative fields of view. **(C)** Hsp90 fluorescence intensity was quantified in 50 randomly selected axonemes. Data represents mean ±S.E.M. Statistical significance was assessed using Student's T-test.

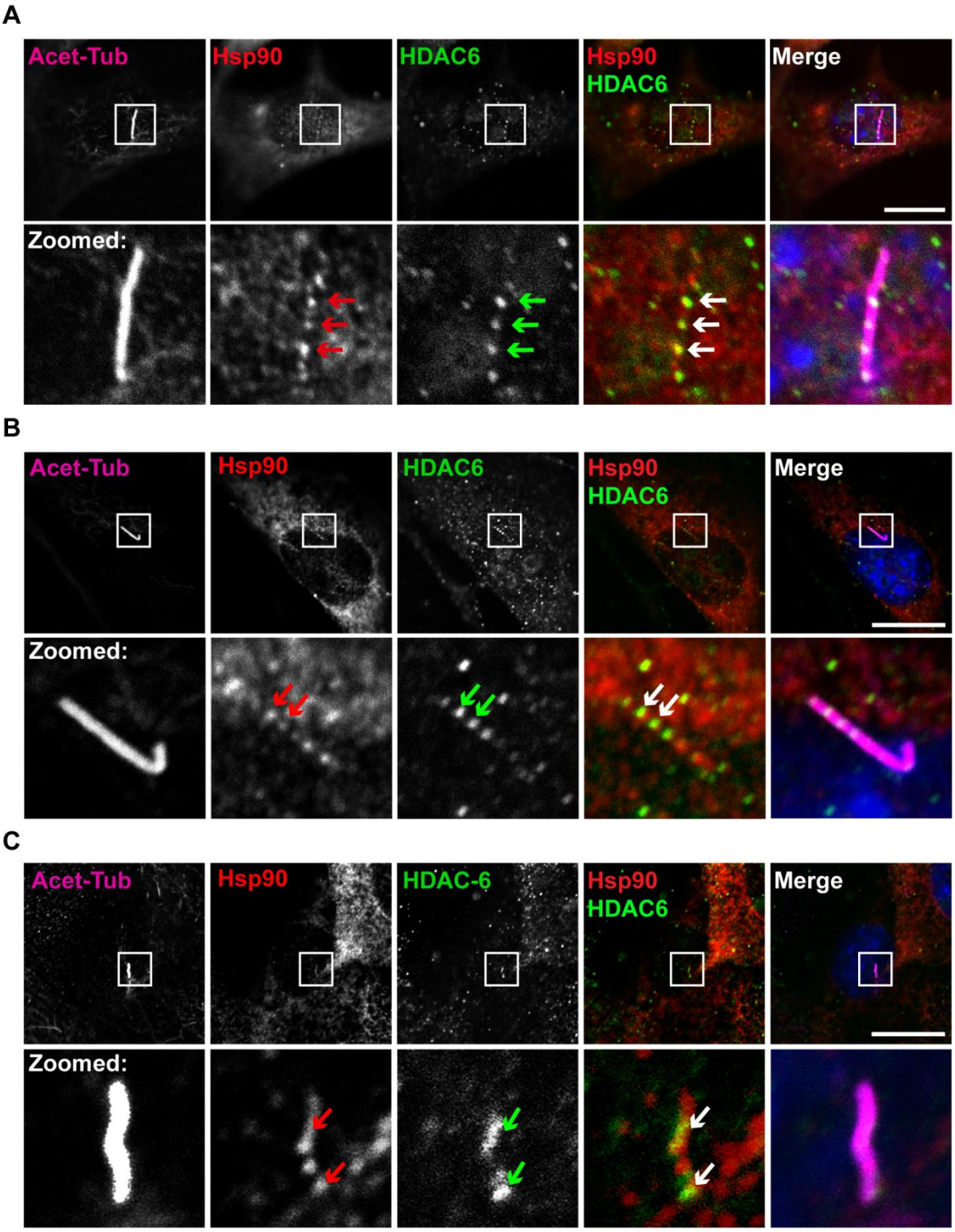
A
Acet-Tub
Hsp90
HDAC6
Hsp90
HDAC6
Merge
Zoomed:
B
Acet-Tub
Hsp90
HDAC6
Hsp90
HDAC6
Merge
Zoomed:
C
Acet-Tub
Hsp90
HDAC-6
Hsp90
HDAC6
Merge
Zoomed:

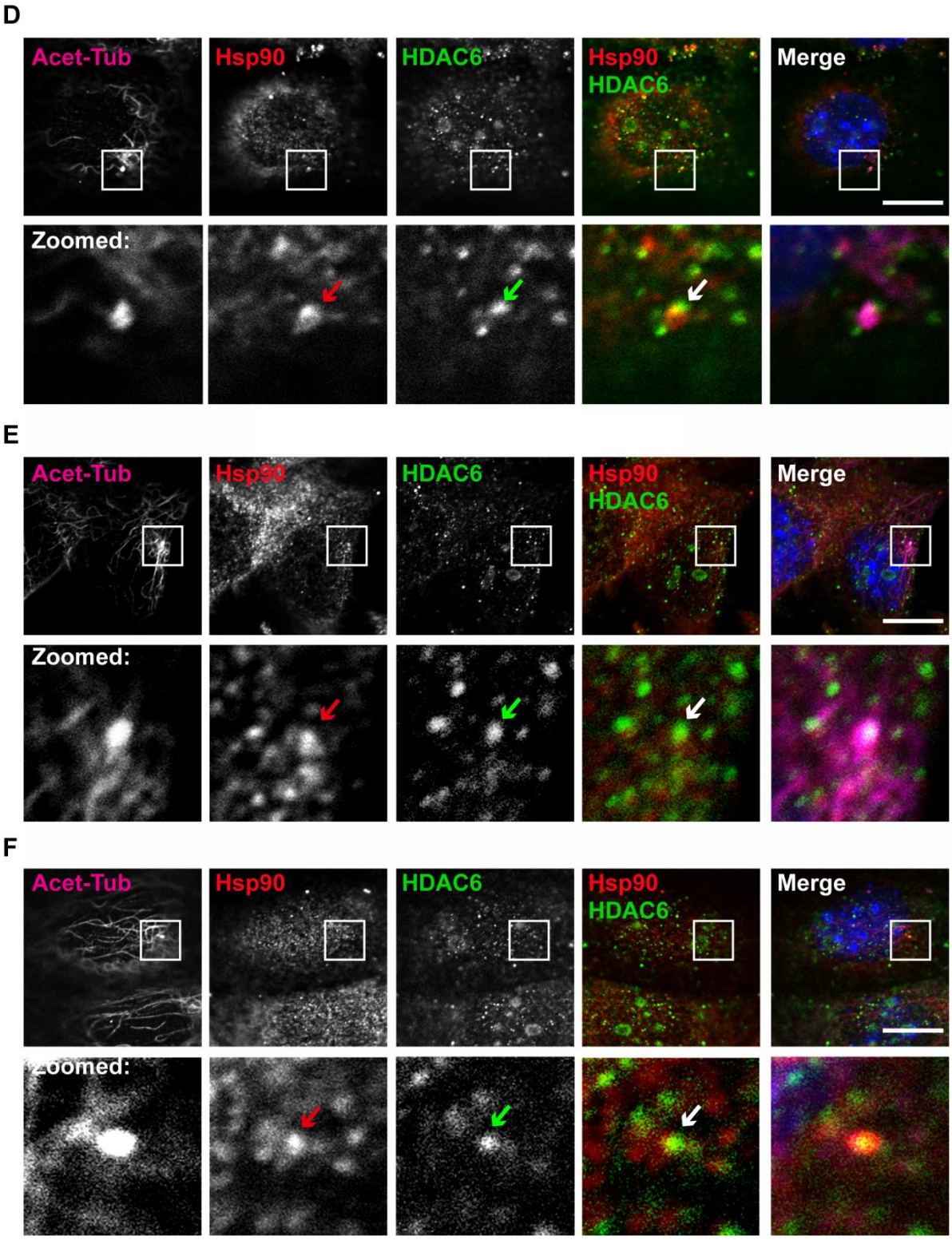


**Figure 6.16 HDAC6 and Hsp90 co-localise within the ciliary axoneme and dissociate upon heat shock**

**(A-C)** NIH3T3 cells cultured under control conditions and **(D-F)** subjected to heat shock at 42°C for 30min. Cells were labelled for anti-acetylated tubulin (magenta) to detect the ciliary axoneme and co-stained for HDAC (green), Hsp90 (red). Nuclei were counterstained with DAPI. Boxed regions in the top panel are shown enlarged in the lower panel (zoom). Arrows indicate areas where HDAC6 and Hsp90 co-localise. Scale bar represents 10µm.

In addition to HDAC6 and Hsp90, Boyault et al. reported that the transcription factor Hsf-1 also formed part of this inhibitory complex. Hsf-1 localisation was therefore examined in cells cultured at 37°C. Consistent with its role as a transcription factor, Hsf-1 strongly localised to the nucleus (Figure 6.17). While some cytoplasmic staining was also evident, Hsf-1 was not observed within the ciliary axoneme (Figure 6.17).

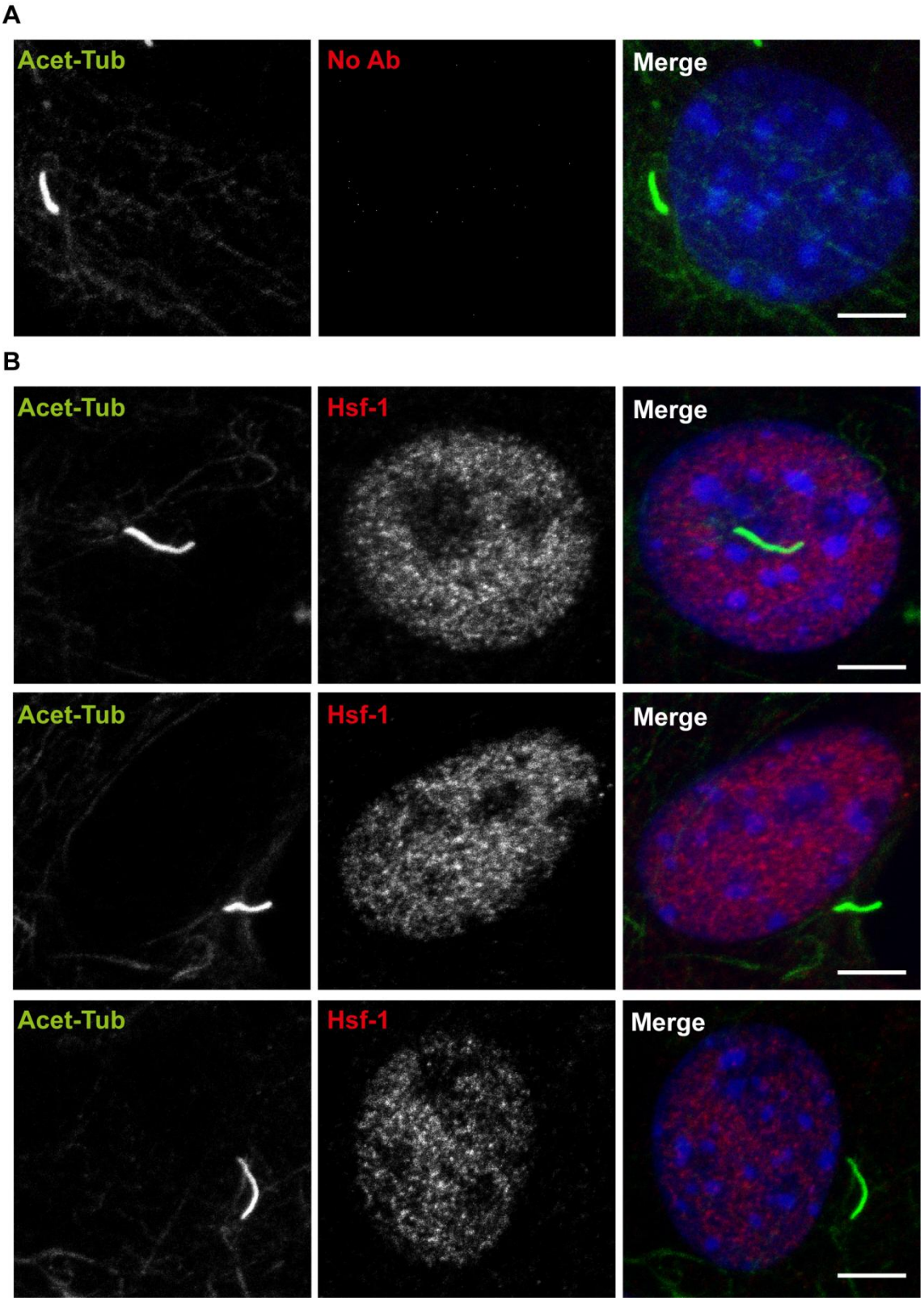


**Figure 6.17 Hsf-1 does not localise to primary cilia**
NIH3T3 cells were serum starved for 20 hrs to induce ciliation then fixed and immunofluorescently labelled for HSF-1 (ADI-SPA-901, red) and acetylated α-tubulin (green). Nuclei were counterstained with DAPI. **(A)** without HSF-1 primary antibody **(B)** with Hsf-1 primary antibody. Scale bar represents 5µm.

## 6.3 Discussion

In this chapter I have shown that primary cilia are rapidly disassembled in response to heat shock both in mammalian cells *in vitro* and in Zebrafish *in vivo.* Ciliary resorption occurs through a HDAC6/Hsp90 dependent mechanism and results in a reduction in cilia mediated signalling. This disassembly may represent an important component of the cellular stress response which results in the down regulation of non-essential proteins during times of stress to promote cell survival.

### 6.3.1 Heat shock triggers cilia resorption *in vitro* and reduces cilia signalling

Joint inflammation is a common component of arthritis and leads to an increase in intra-articular temperature this has been suggested to promote cartilage damage by increasing enzyme activity and matrix degradation (Harris and McCroskery 1974; Woolley and Evanson 1977). Inflammatory stimuli have been shown to regulate ciliary structure and promote cilia elongation in chondrocytes (Wann and Knight 2012). Moreover the presence of a cilium is necessary for inflammatory signalling such that in its absence IL-1 treatment does not trigger NO and $PGE_2$ release in articular chondrocytes (Wann and Knight 2012). In this chapter I show that heat shock triggers the rapid resorption of primary cilia in isolated articular chondrocytes (Figure 6.2) this could therefore function as part of a protective mechanism to reduce inflammatory signalling in OA.

To explore the mechanism of cilia resorption, this response was further characterised in NIH3T3 cells which provide a more established *in vitro* cell culture model for the study of primary cilia. In response to heat shock primary cilia are rapidly disassembled (Figure 6.3). Primary cilia length and prevalence remain significantly reduced for a considerable time following the initial thermal assault (Figure 6.6). These changes would therefore be expected to have long-term consequences for cilia-mediated signalling pathways. Indeed, ligand dependent hedgehog signalling was found to be attenuated following heat shock, even after the cells were allowed to recover for 16 hr at 37$^{o}$C (Figure 6.7).

### *6.3.2* Heat shock triggers cilia resorption *in vivo*

Studies conducted in Zebrafish indicate that primary cilia are also sensitive to a non-lethal exposure to elevated temperature *in vivo* and that this is not simply an *in vitro* phenomenon (Figure 6.8). However, heat shock did not appear to significantly affect Zebrafish development and gross morphology (Figure 6.9). While cilia dependent morphogens such as hedgehog and wnt are responsible for patterning embryo development, much of this patterning occurs before the 24hpf stage when the stressor was applied. For example mono-ciliated cells in Kupffers vesicle, an organ of asymmetry analogous to the mammalian embryonic node, initiate the left-right development of the brain, heart and gut (Essner et al. 2005). These ciliated cells arise in the tail bud at the end of gastrulation, around 10hpf, and establish a directional fluid flow that determines left/right asymmetry (Essner et al. 2002). This developmental stage would perhaps be a more suitable point at which to investigate the consequences of stress induced ciliary resorption in future studies.

That elevated temperatures reduce cilia length and prevalence in both mammalian cell culture and in Zebrafish suggests that this response is likely to be an evolutionarily conserved phenomenon amongst vertebrates.

### 6.3.3 Cilia disassembly requires HDAC6

It has been reported that cilia can be induced to disassemble by inhibiting antereograde IFT, however axoneme shortening occurs slowly at a constant, cell type-specific rate independent of axoneme length (Pan and Snell 2005). The rapidity of stress induced resorption suggests it is an active process, indeed HDAC6 inhibition attenuated this response however it did not completely prevent cilia loss. Tubulin deacetylation is therefore not absolutely necessary for resorption to occur but more likely enhances the rate of disassembly by increasing the inherent instability of the ciliary microtubules and facilitating deconstruction of the axoneme. Pugacheva et al reported that HDAC6 inhibition was sufficient to almost fully inhibit cilia loss in response to serum addition (Pugacheva et al. 2007). This response was also found to require AurA function; similarly a role for both HDAC6 and AurA function was identified in strain dependent cilia resorption in chondrocytes (chapter 5). These data indicate that multiple mechanisms exist to regulate

cilia shortening in response to different stimuli which is unsurprising given the crucial role of this organelle in so many different signalling pathways. That these mechanisms have differing dependencies on tubulin deacetylation is intriguing and may be linked to the presence or absence of other tubulin post translational modifications in the cilium which have been reported to vary with the maturation status of the cilium (Gaertig and Wloga 2008).

Cilia resorption is likely to be a multi-faceted response dependent on both tubulin deacetylation and changes in IFT. In *Chlamydomonas*, flagella shortening can occur through both an increase in the rate of retrograde and in antereograde IFT as cargo loading can be uncoupled at the ciliary base such that 'empty' transport modules are transported to the ciliary tip (Pan and Snell 2005). While further studies would be required to determine the effects of heat shock on IFT, one can speculate that IFT might be altered. While alterations in temperature would be expected to affect motor processivity, tubulin acetylation status has also been shown to modulate Kinesin-1 motor recruitment and can affect the velocity at which it moves along microtubules (Dompierre et al. 2007). Alternatively, the increased protein aggregation observed at elevated temperature could potentially affect cargo loading at the ciliary base and/or block the entry of IFT particles into the cilium.

HDAC6 binds to the poly ubiquitinated protein aggregates which accumulate in response to cellular stress. Dynein motors transport these aggregates via the microtubule network to a cellular organelle called the aggresome where they are processed and degraded. Intriguingly, HDAC6 co-localises extensively with the $p150^{glued}$ subunit of the dyenin motor complex (Hubbert et al. 2002). Neither the dynein motor, nor its associated dynactin complex, possess binding capacity for ubiquitin unlike HDAC6 which has been shown to function as an adaptor between this motor and its cargo (Kawaguchi et al. 2003). The ubiquitination of axonemal proteins, including α-tubulin, increases during ciliary resorption and it has been suggested that these ubiquitinated proteins are disassembly products that have been tagged for retrograde IFT to the cell body (Huang et al. 2009). HDAC6 ciliary labelling is consistent with a localisation to IFT particles and was found in both the larger IFT trains of smaller cilia and within the smaller more punctate particles observed in longer cilia (Engel et al. 2009). An adaptor function for HDAC6 in IFT is an interesting and novel concept which has not previously been explored.

### 6.3.4 Hsp90 is required for cilia maintenance and protects against stress induced resorption

Hsp90 functions as a chaperone for tubulin and promotes protein stability and polymerisation (Takaki et al. 2007). Consequently a role for hsp90 has been identified in the maintenance of the motile cilia of the airway epithelium (Takaki et al. 2007). In control cells hsp90 inhibition results in the loss of cilia indicating that hsp90 is also required for the maintenance of primary cilia (Figure 6.13). While the data presented in this thesis supports resorption as part of a regulated response, it is also likely that heat shock reduces the size/stability of the cytoplasmic pool of soluble tubulin available for IFT and thus reduces its subsequent incorporation into ciliary microtubules influencing ciliary length (Sharma et al. 2011). Indeed, it has recently been demonstrated *in vitro* that soluble tubulin is prone to aggregation even at physiological temperatures and furthermore that hsp90 protects tubulin against this thermal denaturation (Weis et al. 2010). This is consistent with the observation that hsp90 inhibition exacerbated cilia loss in response to heat shock. Moreover in thermotolerant cells, where the relative levels of Hsp90 and Hsp70 proteins are elevated, primary cilia were more resistant to stress-induced ciliary resorption.

Stress induced ciliary resorption did not occur in all cells; many cells maintained their cilia even after a 30 min heat shock. However the length of these cilia was significantly reduced relative to control cells indicating resorption was occurring. It is possible that the Hsp90 content within these cilia was greater than average and afforded more protection against resorption, this would fit with the observation that Hsp90 staining varied between cells. However, not all remaining cilia were found to contain Hsp90 after heat shock suggesting additional protective mechanisms may exist in these cells independent of Hsp90.

### 6.3.5 An Hsp90-HDAC6 complex functions within the cilium

The HDAC dependent deacetylation of Hsp90 modulates the chaperone function of this protein (Fuino et al. 2003; Nimmanapalli et al. 2003). HDAC6 inhibition leads to Hsp90 acetylation which inhibits its ability to bind ATP and function as a chaperone consequently promoting the proteasomal degradation of Hsp90 client proteins (Fuino et al. 2003; Nimmanapalli et al. 2003; Bali et al. 2005). Consistent with reports that HDAC6 and Hsp90

are binding partners (Bali et al. 2005; Boyault et al. 2007); co-localisation of these proteins was observed in the ciliary axonemes of NIH3T3 cells (Figure 6.16). This co-localisation was reduced following heat shock suggesting that the dissociation of an Hsp90-HDAC6 complex had occurred (Figure 6.16). Despite reports that within the cytoplasm of unstressed cells this complex also contains HSF-1 (Boyault et al. 2007); localisation of this protein to the ciliary axoneme was not observed (Figure 6.17).

HDAC6 is activated in response to the accumulation of cytotoxic ubiquitinated protein aggregates (Kawaguchi et al. 2003; Boyault et al. 2007). As evidence exists for an increase in the ubiquitination of axonemal proteins, including α-tubulin, during ciliary resorption (Huang et al. 2009), it is possible to propose a model whereby the heat shock dependent activation of HDAC6 promotes cilia disassembly by two means. Firstly by deacetylating ciliary microtubules and destabilising the axoneme. Secondly by deacetylating Hsp90 and activating this protein such that the HDAC6/Hsp90 complex dissociates and Hsp90 exits the cilium to conduct its chaperone function elsewhere in the cell. As Hsp90 function is required for the folding and maintenance of tubulin, the loss of function of this chaperone within the axoneme means the susceptibility of ciliary tubulin to stress-induced damage is increased and the disassembly of ciliary microtubules promoted.

## 6.4 Summary

Rapid cilia resorption occurs in response to elevated temperature in mammalian cells and in Zebrafish embryos *in vivo*. Primary cilia loss significantly attenuates ligand mediated hedgehog signalling in cultured mammalian cells and may function as part of the cellular stress response to down regulate unnecessary signalling pathways in times of stress. The molecular chaperone Hsp90 is required for primary cilia maintenance under control conditions and co-localises with the tubulin deacetylase HDAC6 within the ciliary axoneme. Stress induced ciliary resorption is partially dependent upon HDAC function which may serve to destabilise the ciliary microtubules and facilitate cilia disassembly. Hsp90 staining within the ciliary axoneme is reduced following heat shock, whereas HDAC6 staining remains constant. These data suggest that an inhibitory complex of these two proteins exists within the cilium, is activated by thermal stress whereupon it dissociates resulting in primary cilia resorption.

# CHAPTER 7

# General discussion and future work

This thesis demonstrates that the structure and function of the primary cilium is regulated by extracellular stress. Co-ordinated cilium disassembly occurs in response to mechanical and thermal stress which in turn exerts a negative influence over hedgehog signalling and mechanosensitive ADAMTS-5 expression in chondrocytes. While cilia disassembly in response to these biophysical stressors occurs through distinct mechanisms, the mechanisms examined in this thesis exhibit a shared requirement for the tubulin deacetylase HDAC6.

## 7.1 Experimental considerations

In addition to tensile strain, chondrocytes experience a variety of mechanical stimuli during physiological joint loading such as compressive strain, fluid flow and osmolarity (for review see (Urban 1994)). While tensile strain may be only a small component of this physiological load, subjecting chondrocytes to mechanical stimuli in 2D culture is advantageous as it provides a more sensitive and highly reproducible assay with which to reliably measure small changes in cilia length. Culturing cells in 3D makes identification of primary cilia quite difficult due to the higher intensity of the cytoplasmic tubulin stain. Moreover it reduces the sensitivity of cilia length measurements as the cilium can project from the cell at any angle. Indeed, despite observing significant cilia loss in chondrocytes subjected to 24 hrs cyclic compression in 3D culture, McGlashan et al were unable to observe significant changes in length before 48 hrs of loading (McGlashan et al. 2010).

Furthermore, several studies have shown that chondrocytes exhibit a mechanotransduction response to tensile strain that is comparable to other studies in which cells have been subjected to cyclic compression, hydrostatic pressure and changes in osmolarity. It has been suggested that 2D systems over estimate the influence of integrins in the mechanotransduction response, however one could argue that culturing cells in an inert matrix would underestimate this influence. No *in vitro* system is perfect, however they do provide useful tools with which to study the potential mechanisms involved in chondrocyte mechanotransduction.

In this thesis, cilia length was measured from maximum intensity projections created by imaging confocal z-stacks throughout the entirety of the cellular profile. In cells where cilia are located on the apical surface such as in epithelial cells, there is potential for significant variation when measuring cilium length in this way. The projected length of the cilium can be influenced by the cosine of the angle at which it protrudes from the cell and consequently cilia length is likely to be underestimated (Figure 7.1).

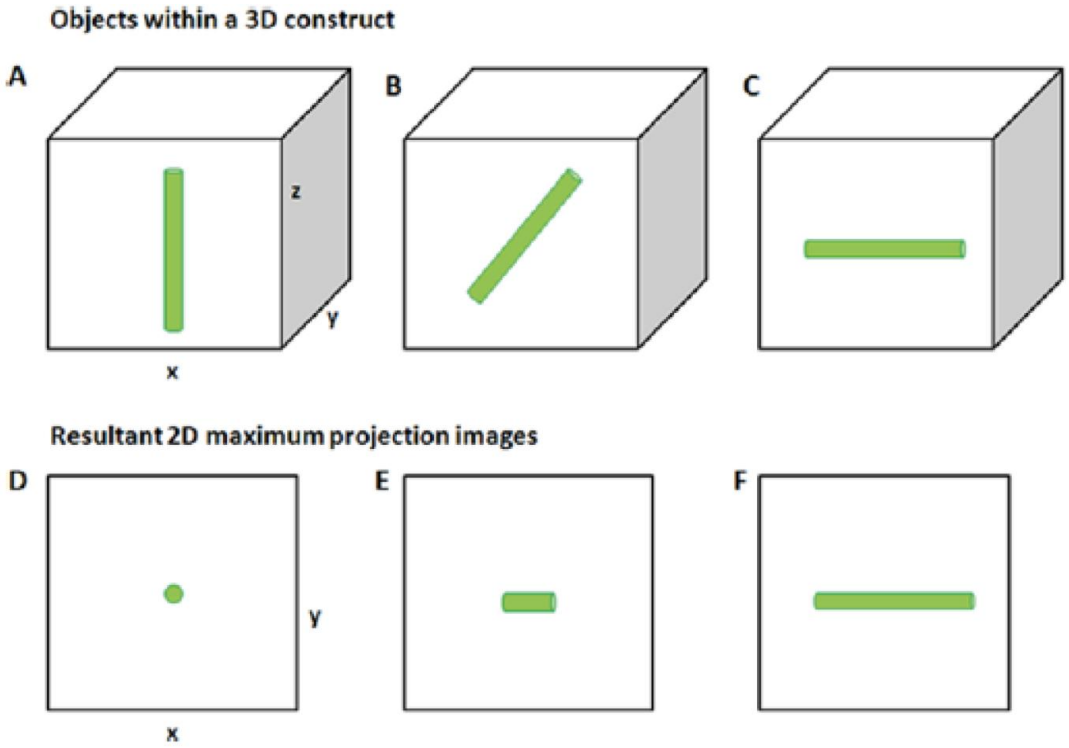


**Figure 7.1 Measurement error in 2D culture**
Schematic highlighting the potential for error when measuring cilia from 2D projected images (taken from (Saggese et al. 2012)). A vertical cilium will appear as a single point (A, D) while the measured length of an extended cilium will vary with the cosine of the angle from which the cilium protrudes from the focal plane (B, C, E, F).

Fortunately in chondrocytes and fibroblasts cilia are typically found on the basal surface of the cell between the cell membrane and the substrate and thus the size of this angle is constrained. Nonetheless, Z-stacks must be carefully monitored as a change in cellular morphology, such as rounding up, could affect cilia positioning and orientation. The mean angle of projection was determined from confocal z-stacks and found to be ≤25° for

chondrocyte cilia and there was no significant difference in the size of this angle between strained and unstrained groups. Therefore the length changes presented in this thesis are unlikely to have been caused by an imaging artefact.

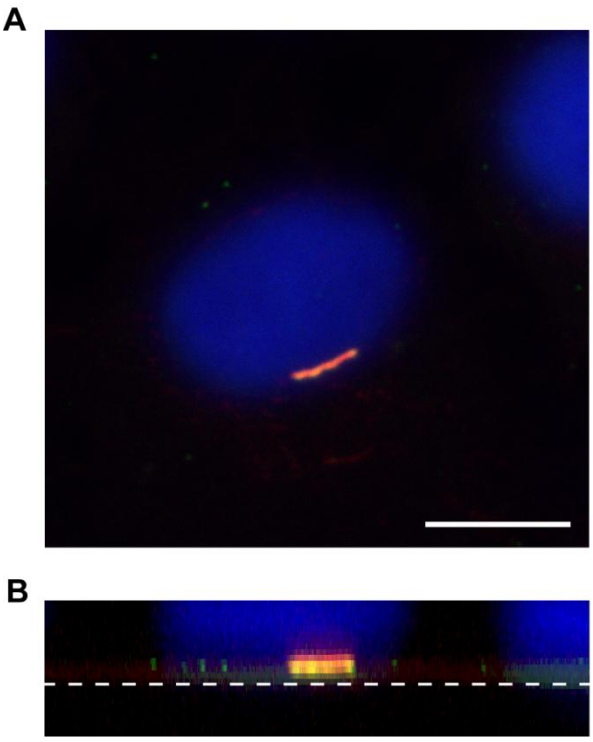


**Figure 7.2 Cilia are positioned on the base of the cell in chondrocytes**
**(A)** Maximum intensity projection of a chondrocyte in 2D culture. The cilium is double labelled for acetylated α-tubulin (red) and Arl13b (green) such that co-localisation within the ciliary axoneme appears yellow. Nuclei are counterstained with DAPI, scale bar represents 10µm. **(B)** Side projection of image A, the bottom of the cover slip is highlighted by a white dotted line in this image, the cilium is clearly shown extended and on the base of the cell between the cell membrane and the glass.

A further advantage to 2D culture is that more than 75% of chondrocytes exhibit a cilium (Figure 4.9B). This is a much greater proportion than reported *in situ* where ciliation through the cartilage depth is approximately 45% (McGlashan et al. 2008), and is also significantly greater than reported for 3D agarose models where less than 50% of cells elaborate this structure (McGlashan et al. 2010).

## 7.2 Cilia structure-function relationship

In line with the findings of this thesis, an increasing number of studies have demonstrated that cilia length, and associated antereograde and retrograde IFT, correlates with functionality (Caspary et al. 2007; Tran et al. 2008; Besschetnova et al. 2010). This might have important implications in diseases where altered cilia length has been reported, such as in osteoarthritis (McGlashan et al. 2008), contact dermatitis (Elofsson et al. 1984) and in response to acute renal injury (Verghese et al. 2009). The relationship between

mechanically induced cilia disassembly and function is most clearly demonstrated in the polarised epithelial cells of the renal tubules. In kidney epithelia, flow induced ciliary deflection activates a $Ca^{2+}$ dependent signalling cascade that regulates the mechanotransduction response (Praetorius and Spring 2001). The magnitude of the $Ca^{2+}$ response is proportional to cilia length (Resnick and Hopfer 2007). As well as activating this cilia mechanotransduction pathway, the shear forces generated by fluid flow also influence cilia structure by triggering disassembly (Iomini et al. 2004; Masyuk et al. 2006; Besschetnova et al. 2010). This creates a negative feedback loop as axoneme shortening reduces the length of the lever arm. Consequently, the amount of ciliary deflection that occurs in response to a given flow is reduced thereby reducing the sensitivity of the cell to fluid shear stress (Schwartz et al. 1997). Thus coordinated cilia disassembly provides a mechanism by which the cell can adapt intracellular signalling to external cues. Indeed, Besschetnova et al demonstrated that when flow-mediated cilia disassembly is inhibited the mechanical regulation of $Ca^{2+}$/cAMP signalling is disrupted (Besschetnova et al. 2010).

For the first time, we show that in chondrocytes and fibroblasts primary cilia disassemble in a dose dependent manner in response to biophysical stress and that this disassembly inhibits cilia mediated signalling. Surprisingly, the length changes observed in chondrocytes were not large despite producing almost total inhibition of hedgehog pathway activation and mechanosensitive ADAMTS-5 expression at 20% strain (Figure 5.6 and Figure 5.13). Even more striking was the fact that the 13% reduction in length at 20% strain inhibited mechanosensitive hedgehog while the 6% reduction in length at 10% strain had no effect. These findings highlight the importance of the integrity of the ciliary structure and suggest that this organelle is highly sensitised to the cellular microenvironment. That some disassembly was also observed in response to 10% strain suggests a threshold exists above which cilia resorption has functional consequences. Consistent with this assumption, disassembly in response to a 15 min heat shock did not significantly attenuate hedgehog signalling following ligand stimulation despite triggering significant cilia disassembly, while 30 min produced greater disassembly and attenuated hedgehog signalling (Figure 6.4 and Figure 6.7).

### 7.2.1 Cilia length in articular cartilage

The observation that primary cilia prevalence and length increase with *in vitro* cell culture (Figure 4.11) is reminiscent of studies conducted in tendon showing that stress deprivation results in significant cilia elongation (Gardner et al. 2011). This elongation was reversed upon the application of mechanical strain suggesting that the 'set length' of a cilium is modulated by its mechanical environment. The primary cilium is required for mechanosensitive matrix production in chondrocytes (Wann et al. 2012). In the absence of a cilium, chondrocytes fail to upregulate aggrecan gene expression and do not synthesise proteoglycan. Therefore ciliary elongation in the absence of strain might represent a mechanism by which the cell can increase its sensitivity to mechanical stimuli and maintain the articular cartilage under conditions where loading is insufficient. However, given the correlation between mechanosensitive ADAMTS-5 expression and cilia length presented in this thesis, if elongation occurs *in vivo* as the result of stress deprivation one might also expect it to promote mechanosensitive cartilage degeneration. Indeed, in the 1980's Palmoski et al conducted seminal studies in canines examining the effects of stress deprivation on articular cartilage form and function. This study reported that in the absence of strain the articular cartilage deteriorated (Palmoski and Brandt 1982). Spontaneous cartilage degradation occurs in cartilage explants *in situ*, which may in part be due to stress deprivation. Future studies could therefore examine changes in cilia length *in situ* in response to stress deprivation and test whether cilia length modulators such as tubacin inhibit this degradation.

*In vivo* the length of the chondrocyte primary cilium varies with cartilage depth such that cilia in the superficial zone are significantly shorter than those of the deep zone chondrocytes (McGlashan et al. 2008). The data presented in chapter 5 suggests that this may be the result of zonal variations in a chondrocytes mechanical environment as several studies have reported that the cells of the superficial zone are subject to the greatest levels of both compressive and tensile strain (Guilak et al. 1995; Gratz et al. 2009). The extent of cilium disassembly observed in the current study is significantly less dramatic than that observed following dynamic compression (McGlashan et al. 2010). While this may indicate that different types of stimuli activate the disassembly response to varying degrees, it is

most likely the result of differences in the intensity and duration of the loading regime. Indeed, a low level of cilia disassembly similar to that reported in this thesis was observed for chondrocytes *in situ* during short-term osmotic loading (Rich and Clark 2012).

## 7.3 Mechanistic insights

### 7.3.1 Actin

It is well established that mechanical loading influences chondrocyte actin dynamics and cytoskeletal organisation (see chapter 2). Such changes are suggested to be involved in chondrocyte mechanotransduction through the stabilisation of membrane ion channels, control of cell deformation and distortion of intracellular structures including the nucleus. Recent studies have identified a role for changes in actin dynamics in the regulation of primary cilia length (Bershteyn et al. 2010; Kim et al. 2010; Sharma et al. 2011; Hernandez-Hernandez et al. 2013). In a genomic screen Kim et al identified a number of proteins involved in actin dynamics as modulators of cilia length (Kim et al. 2010). More recently, Sharma et al showed that cytochalsin D and Jasplakinolide, agents which destabilise or stabilise actin respectively, result in significant cilia elongation (Sharma et al. 2011). This length control is achieved through the modulation of the amount of free soluble tubulin within the cytoplasm and thus its availability for IFT. However the mechanism controlling this is unknown (Sharma et al. 2011).

The actin regulatory protein cortactin (CTTN) is a substrate of HDAC6. HDAC6 deacetylates CTTN increasing its ability to bind F-actin and regulate microtubule-dependent cell movement (Zhang et al. 2007). CTTN regulates ciliogenesis through an antagonistic relationship with the protein missing-in-metastasis (MIM) (Bershteyn et al. 2010). MIM and CTTN co-localise at the basal body where MIM inhibits p60 Src kinase activity and antagonises CTTN function to promote ciliogenesis. In the absence of MIM, CTTN phosphorylation is increased and it inhibits ciliogenesis and promotes cilia disassembly (Bershteyn et al. 2010).

Changes in actin organisation at 20% strain were not investigated in this thesis; however these studies suggest that the ciliary length changes and subsequent defects in signalling

might be occurring as the result of strain-induced changes in actin organisation. Therefore future work should focus on the effects of mechanical strain on actin organisation and the influence this exerts over the availability of soluble tubulin, such studies might provide further insight as to the mechanism of strain-induced cilia resorption.

### 7.3.2 Tubulin acetylation

The primary cilium has recently been shown to influence the post translational modification (PTM) of cytoplasmic microtubules (Berbari et al. 2013). The stability of cytoplasmic microtubules is increased in cilia mutants lacking the IFT88 protein due to the hyper-acetylation of tubulin which occurs as a result of increased tubulin acetyl-transferase activity (Berbari et al. 2013). Interestingly, this is accompanied by a compensatory increase in HDAC6 expression suggesting the cilium/IFT88 regulates the balance between acetylation and deacetylation throughout the cell modulating both cellular integrity and microtubule transport. The protein expression of HDAC6 was not analysed in this thesis, however it would be interesting to examine the mechanosensitivity of this protein in future studies.

Gradilone et al have recently reported that increased HDAC6 expression in cholangiocarcinoma disrupts hedgehog signalling and promotes tumour growth through the modulation of cilia structure (Gradilone et al. 2013). Aberrant hedgehog pathway activation is observed in these cells due to complete cilia loss. Consequently hedgehog signalling is activated as the processing of the Gli3 repressor is disrupted resulting in the loss of pathway repression (see chapter 1). This results in an increase in cell proliferation and tumour growth which is reversible through the restoration of HDAC6 expression. This study highlights the complexity of the relationship between HDAC6/tubulin acetylation and the cilium. Gradilone et al showed that restoring the correct level of HDAC6 expression in cholangiocarcinoma cells allows the cell to build a cilium and thus reduces ligand independent hedgehog signalling. The data presented in this thesis reveals a new level to this signalling showing that a lower level of HDAC6 activation, which does not cause cilia loss, triggers cilia disassembly which can modulate the responsiveness of the cell to hedgehog ligands (a schematic representation of this can be found in Figure 7.3). This altered responsiveness most likely arises due to an effect of tubulin deacetylation on IFT however further studies

examining the trafficking and levels of activated Gli proteins in the cilium, or of the transmembrane protein smoothened, would be required to investigate this.

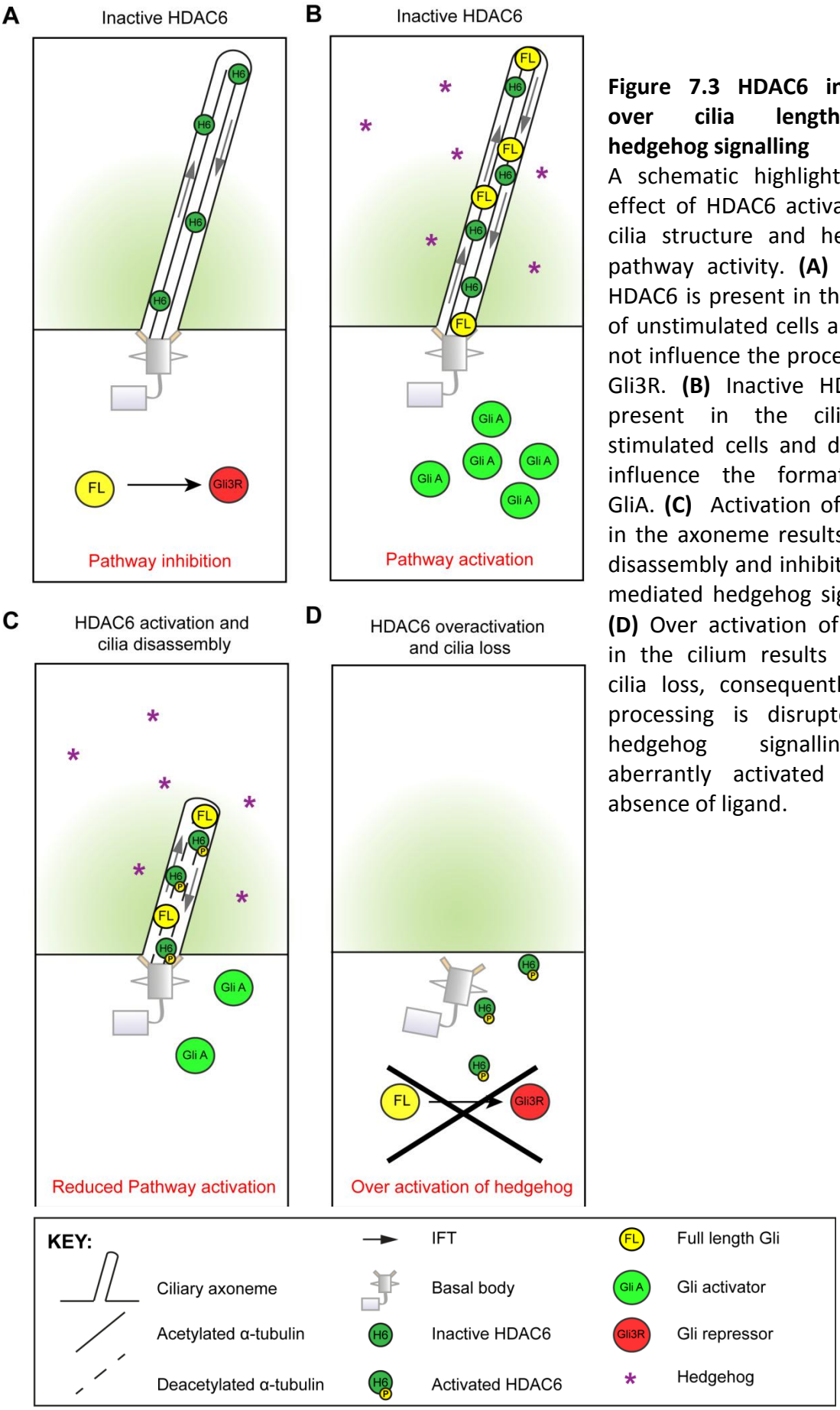


**Figure 7.3 HDAC6 influence over cilia length and hedgehog signalling**
A schematic highlighting the effect of HDAC6 activation on cilia structure and hedgehog pathway activity. **(A)** Inactive HDAC6 is present in the cilium of unstimulated cells and does not influence the processing of Gli3R. **(B)** Inactive HDAC6 is present in the cilium of stimulated cells and does not influence the formation of GliA. **(C)** Activation of HDAC6 in the axoneme results in cilia disassembly and inhibits ligand mediated hedgehog signalling. **(D)** Over activation of HDAC6 in the cilium results in total cilia loss, consequently Gli3R processing is disrupted and hedgehog signalling is aberrantly activated in the absence of ligand.

### 7.3.3 Hsp90 client proteins

The hsp90 chaperone machinery regulates the activity of hundreds of client proteins in the eukaryotic cytosol and has been implicated in the development of cancer (Bagatell and Whitesell 2004) and neurodegenerative disease (Luo et al. 2010; Salminen et al. 2011). Therefore the recent finding that ciliary changes occur in mouse models of Alzheimer's disease is particularly interesting given the function of Hsp90 in primary cilia maintenance (Chakravarthy et al. 2012). Alzheimer's disease is characterised by the formation of amyloid plaques and neurofibrillary tangles, the latter of which involves the deposition of the microtubule associated protein Tau. The hyper-phosphorylation of tau within these tangles is hypothesised to play a role in fibril formation, potentially through its disruption of microtubule binding (Salminen et al. 2011). Hsp90 influences the clearance of tau aggregates as it promotes the folding/re-folding pathway through collaboration with CHIP, a co-chaperone with E3 ligase activity (Dickey et al. 2007). Characteristically hsp90 complexes have a higher affinity for their aberrant clients (Luo et al. 2007). One might therefore hypothesise that tau accumulation could divert hsp90 function from the cilium and account for the reduction in cilia length reported much like what is hypothesised to occur in response to heat shock (see chapter 6).

Intriguingly, Chakravarthy et al also reported age dependent reductions in neuronal primary cilia length (Chakravarthy et al. 2012). Given that neuritic plaques have also been observed in patients with senile dementia (Goedert 2009), changes in cilia length might therefore be linked to a decline in brain function with old age. Age dependent changes in cilia structure and function have not been well studied and may prove to be an interesting avenue for future research.

## 7.4 Hedgehog signalling in articular cartilage

Previous studies have shown that mechanical loading regulates the expression of Ihh in chondrocytes isolated from developing tissues (Wu et al. 2001; hjTang et al. 2004; Shao et al. 2011). Significant increases in Ihh expression were observed in rat growth plate chondrocytes as early as 30 min following the application of hydrostatic loading and the

increase in Ihh expression was found to correlate with loading duration such that expression was upregulated by almost 20 fold following 24 hrs (Shao et al. 2011). In contrast extending the loading regime from 1 to 24 hrs in articular chondrocytes did not up regulate Ihh expression (Figure 7.4). There are several possible explanations for this observation, the first being that Ihh expression is not as responsive in mature cells relative to immature cells. Secondly, the increase in Ihh expression following extended periods of loading in growth plate chondrocytes is associated with chondrocyte differentiation and hypertrophy. Ihh is expressed by the pre-hypertrophic cells of the growth plate, therefore the increased Ihh expression in growth plate cells over time may in fact be due to increased chondrocyte differentiation rather than a direct effect on the mechanosensitive expression of this gene. Finally, in this study a heterogeneous pool of chondrocytes from all cartilage zones is under investigation. Chondrocytes from different zones do not always behave in an identical manner (Lee et al. 1998; Heywood et al. 2010; Motaung et al. 2011); therefore it is possible that not all cells up regulate Ihh in response to load reducing the overall population response. Indeed, a chondrocyte progenitor population has been identified in the superficial zone of articular cartilage constituting less than 10% of the cell population (Dowthwaite et al. 2004; Williams et al. 2010). A similar population of progenitor cells has been identified in the adrenal gland, which have been shown to produce Shh and regulate adrenal development (King et al. 2009). To elucidate the contribution of progenitor cells to the response observed in articular chondrocytes, these cells could be isolated by their differential adhesion to fibronectin coated surfaces (Dowthwaite et al. 2004) and subsequently cultured and subjected to CTS. A greater induction of Ihh expression in these cells might suggest that the 1.5 fold induction observed in the mixed population is largely due to mechanosensitive Ihh expression in this subpopulation.

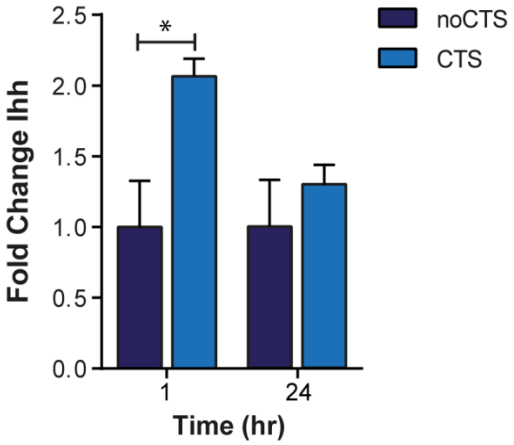


**Figure 7.4 Regulation of Ihh expression by CTS**
Freshly isolated bovine articular chondrocytes were cultured for six days then subjected to mechanical strain for 1 and 24 hrs. All data are normalised to the expression of GAPDH and expressed as a fold change relative to the mean of the unstrained (noCTS) control group. Data represents mean ± S.E.M (n=6 per experimental group).

Despite previous reports that Ihh regulates chondrocyte proliferation in response to mechanical stimuli (Wu et al. 2001; hjTang et al. 2004; Shao et al. 2011); mechanical strain did not induce proliferation in articular chondrocytes (Figure 5.5). Consistent with this finding, r-Ihh treatment did not induce chondrocyte proliferation in the absence of strain (Figure 5.12). These data suggest that the function of Ihh in adult cartilage differs to its role during development. Indeed a recent publication by Ikawura et al showed that hedgehog ligands increased the expression of superficial zone protein (SZP), or lubricin, in isolated articular chondrocytes and cartilage explants (Iwakura et al. 2012). Moreover, hedgehog signalling did not induce chondrocyte proliferation in this model system either. Of particular interest, this study demonstrated reciprocal regulation of SZP accumulation by both hedgehog and wnt signalling (Iwakura et al. 2012). While, Shh treatment increased the level of SZP in the culture medium of isolated superficial zone chondrocytes, Wnt3a dose dependently reduced SZP accumulation. Conversely, when wnt signalling was inhibited a statistically significant increase in SZP accumulation occurred. In the post natal growth plate Ift88 mutation disrupts ligand mediated hedgehog signalling and the hedgehog dependent expression of Sfrp5, a negative regulator of wnt signalling (Chang and Serra 2013). Consequently, increased wnt signalling is observed in the columnar cells of the growth plate. The effects of CTS on Wnt signalling were not investigated in this study; however Thomas et al recently reported a partial nuclear localisation of β-catenin in response to CTS that synergised with Wnt3a treatment to promote the expression of catabolic mediators such as MMP3 and ADAMTS-4 (Thomas et al. 2011). Given the interplay between wnt and

hedgehog, and the role of the cilium in these signalling pathways future studies will need to explore the relationship between these pathways in response to CTS.

### 7.4.1 Pathological implications for osteoarthritis

Focal defects in articular cartilage, such as those sustained following an injury to the joint, cause alterations in the mechanical environment of the chondrocyte (Brown et al. 1991; Braman et al. 2005; Gratz et al. 2008). If left untreated these defects frequently progress to symptomatic OA. That Ihh expression was induced by 10% and 20% CTS yet not in response to 5% CTS suggests a relationship with strain magnitude. Therefore, such changes in the mechanical environment might be responsible for the increased expression of Ihh reported in osteoarthritic cartilage (Wei et al. 2012). Consistent with this, studies in the murine temporo-mandibular joint (TMJ) observed a similar correlation between increasing mechanical stress and Ihh expression and subsequent regulation of chondroprogenitor proliferation (Rabie and Al-Kalaly 2008). Future studies could therefore investigate this relationship more closely perhaps using models of injurious mechanical loading.

While our understanding of the role of the primary cilium in articular cartilage remains limited numerous studies agree that this organelle plays a key role in the maintenance of articular cartilage and that its dysfunction might lead to the development of OA (McGlashan et al. 2007; Kaushik et al. 2009; Chang et al. 2012; Wann et al. 2012). The data presented in this thesis suggests the regulated disassembly of the cilium in response to mechanical strain modulates the mechanosensitive expression of ADAMTS-5 (chapter 5). ADAMTS-5 is a major target in OA as studies have shown that it is the predominant enzyme responsible for aggrecan cleavage and cartilage degeneration in this disease (Majumdar et al. 2007). Over time the cartilage surface is subject to micro-damage due to normal ‘wear and tear' such that the tissue becomes rougher and more fibrillated with age while fatigue resistance is decreased (Weightman 1976; Sah et al. 1992; Urban 1994). Such damage does not always lead to the development of OA suggesting protective mechanisms exist to prevent this. One such mechanism could be cilium disassembly which would be expected to reduce ADAMTS-5 expression in response to high levels of strain preventing enzymatic degradation of the tissue and further damage. Future studies should therefore aim to determine the effects of

cilia elongation on cartilage homeostasis *in vivo* and determine the efficacy of chemical interventions on cilia structure and function in the context of tissue degradation.

Studies conducted in human and mouse quite clearly demonstrate a role for the hedgehog pathway in the development and progression of OA (Lin et al. 2009). However, the findings of the current study do not support the previous suggestion of a direct link between hedgehog signalling and ADAMTS-5 expression. I was unable to induce ADAMTS-5 expression in murine (not shown) or bovine chondrocytes with r-Ihh treatment (Figure 5.13B). A potential explanation for this lies in the differences in the cell populations used in these studies. Lin et al used chondrocytes isolated from 'healthy' regions of human osteoarthritic tissue, while in the current study bovine chondrocytes were isolated from healthy joints with no signs of trauma or degeneration. Chondrocytes isolated from osteoarthritic tissue will be exposed to soluble factors in the synovial fluid, such as pro-inflammatory signals like IL-1 that could alter their response. IL-1 has been shown to trigger cilia elongation which could potentially increase the sensitivity of the cells to hedgehog ligands. Indeed other factors known to promote ciliary elongation, such as the monovalent cation lithium, have been associated with the development of arthritis (Black and Waziri 1984; Skerritt 1987).

Given that a relationship between inflammatory and hedgehog signalling has been demonstrated in other tissues (Amankulor et al. 2009; Schumacher et al. 2012; Zhou et al. 2012), future studies investigating the interactions between these pathways in the context of cartilage degeneration could be insightful. Indeed, preliminary data suggests that a potential interaction may exist as cartilage degradation, as determined by sGAG release, was increased in explants following co-treatment with IL-1 and r-Ihh (Figure 7.5A). However, it is unlikely that IL-1 is inducing degradation through direct hedgehog pathway activation as 10 µM cyclopamine, a hedgehog inhibitor, was not able to reduce sGAG release in response to IL-1 treatment alone (Figure 7.5B) nor was hedgehog pathway activation observed when isolated cells were treated with IL-1 (Figure 7.5C).

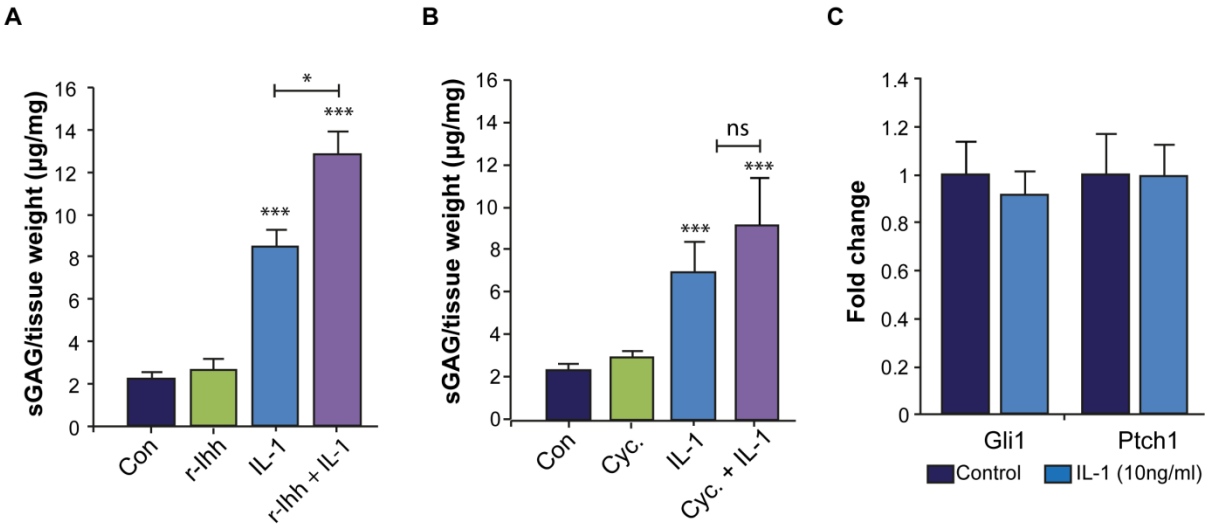


**Figure 7.5 Potential for cross-talk between hedgehog signalling and IL-1**
**(A)** Bovine cartilage explants were isolated and cultured in serum free media for three days in the presence or absence of IL-1 (10ng/ml) and **(A)** r-Ihh (1µg/ml or **(B)** cyclopamine (10µM). After three days the culture media was collected and assayed for sGAG content. Data is normalised to explant weight determined prior to experimental treatment. Data represents mean ±S.E.M (n=6 per experimental group). **(C)** Isolated primary chondrocytes were treated with IL-1 (10ng/ml) for 24hrs and the effects on hedgehog pathway activation determined by real time PCR. All data are normalised to the expression of GAPDH and expressed as a fold change relative to the mean of the unteated control group. Statistical significance was assessed using a Student's T test. Data represents mean ± S.E.M (n=10 per experimental group).Statistical significance was assessed using a Student's T-test relative to the untreated control group.

In summary, I have shown that mechanically induced cilia disassembly occurs in an HDAC6 dependent manner and attenuates hedgehog signalling and ADAMTS-5 expression at higher strains. We propose that this might function as a protective mechanism in healthy cartilage to prevent hedgehog-mediated matrix degradation in response to damaging stimuli. That cilia length and prevalence are increased in osteoarthritic cartilage suggests that this response is disrupted in OA chondrocytes highlighting the potential of the cilium as a therapeutic target in this disease.

# References


Abdul-Majeed, S., Moloney, B. C. and Nauli, S. M. (2011). Mechanisms regulating cilia growth and cilia function in endothelial cells. Cell Mol Life Sci 69: 165-173.

Amankulor, N. M., Hambardzumyan, D., Pyonteck, S. M., Becher, O. J., Joyce, J. A. and Holland, E. C. (2009). Sonic hedgehog pathway activation is induced by acute brain injury and regulated by injury-related inflammation. J Neurosci 29(33): 10299-10308.

Anckar, J. and Sistonen, L. (2007). Heat shock factor 1 as a coordinator of stress and developmental pathways. Adv Exp Med Biol 594: 78-88.

Anderson, C. T. and Stearns, T. (2009). Centriole age underlies asynchronous primary cilium growth in mammalian cells. Curr Biol 19(17): 1498-1502.

Archer, C. W., Rooney, P. and Wolpert, L. (1982). CELL-SHAPE AND CARTILAGE DIFFERENTIATION OF EARLY CHICK LIMB BUD CELLS IN CULTURE. Cell Differentiation 11(4): 245-251.

Ascenzi, M. G., Blanco, C., Drayer, I., Kim, H., Wilson, R., Retting, K. N., Lyons, K. M. and Mohler, G. (2011). Effect of localization, length and orientation of chondrocytic primary cilium on murine growth plate organization. J Theor Biol 285(1): 147-155.

Badano, J. L., Mitsuma, N., Beales, P. L. and Katsanis, N. (2006). The ciliopathies: an emerging class of human genetic disorders. Annu Rev Genomics Hum Genet 7: 125-148.

Bagatell, R. and Whitesell, L. (2004). Altered Hsp90 function in cancer: a unique therapeutic opportunity. Mol Cancer Ther 3(8): 1021-1030.

Bai, C. B., Stephen, D. and Joyner, A. L. (2004). All mouse ventral spinal cord patterning by hedgehog is Gli dependent and involves an activator function of Gli3. Dev Cell 6(1): 103-115.

Bali, P., Pranpat, M., Bradner, J., Balasis, M., Fiskus, W., Guo, F., Rocha, K., Kumaraswamy, S., Boyapalle, S., Atadja, P., Seto, E. and Bhalla, K. (2005). Inhibition of histone deacetylase 6 acetylates and disrupts the chaperone function of heat shock protein 90: a novel basis for antileukemia activity of histone deacetylase inhibitors. J Biol Chem 280(29): 26729-26734.

Barnfield, P. C., Zhang, X., Thanabalasingham, V., Yoshida, M. and Hui, C. C. (2005). Negative regulation of Gli1 and Gli2 activator function by Suppressor of fused through multiple mechanisms. Differentiation 73(8): 397-405.

Bavington, C., Wright, M. O., Jobanputra, P., Brennan, F. R., Salter, D. M. and Nuki, G. (1995). Accelerated proteoglycan synthesis in human articular chondrocytes following pressure-induced mechanical strain: Regulation by gadolinium-sensitive stretch-activated ion channels. Bone (New York) 17(6): 592-592.

Behrens, F., Kraft, E. L. and Oegema, T. R., Jr. (1989). Biochemical changes in articular cartilage after joint immobilization by casting or external fixation. J Orthop Res 7(3): 335-343.

Benya, P. D. and Shaffer, J. D. (1982). Dedifferentiated chondrocytes re-express the differentiated collagen phenotype when cultured in agarose gels. Cell 30(1): 215-224.

Berbari, N. F., Lewis, J. S., Bishop, G. A., Askwith, C. C. and Mykytyn, K. (2008). Bardet-Biedl syndrome proteins are required for the localization of G protein-coupled receptors to primary cilia. Proceedings of the National Academy of Sciences of the United States of America 105(11): 4242-4246.

Berbari, N. F., O'Connor, A. K., Haycraft, C. J. and Yoder, B. K. (2009). The primary cilium as a complex signaling center. Curr Biol 19(13): R526-535.

Berbari, N. F., Sharma, N., Malarkey, E. B., Pieczynski, J. N., Boddu, R., Gaertig, J., Guay-Woodford, L. and Yoder, B. K. (2013). Microtubule modifications and stability are altered by cilia perturbation and in cystic kidney disease. Cytoskeleton (Hoboken) 70(1): 24-31.

Bergmann, C. (2012). Educational paper: ciliopathies. Eur J Pediatr 171(9): 1285-1300.

Bershteyn, M., Atwood, S. X., Woo, W. M., Li, M. and Oro, A. E. (2010). MIM and cortactin antagonism regulates ciliogenesis and hedgehog signaling. Dev Cell 19(2): 270-283.

Besschetnova, T. Y., Kolpakova-Hart, E., Guan, Y., Zhou, J., Olsen, B. R. and Shah, J. V. (2010). Identification of signaling pathways regulating primary cilium length and flow-mediated adaptation. Curr Biol 20(2): 182-187.

Bitgood, M. J. and McMahon, A. P. (1995). Hedgehog and bmp genes are co-expressed at many diverse sites of cell-cell interaction in the mouse embryo. Developmental Biology 172(1): 126-138.

Black, D. W. and Waziri, R. (1984). Arthritis associated with lithium toxicity: case report. J Clin Psychiatry 45(3): 135-136.

Blain, E. J. (2009). Involvement of the cytoskeletal elements in articular cartilage homeostasis and pathology. International Journal of Experimental Pathology 90(1): 1-15.

Blain, E. J., Gilbert, S. J., Hayes, A. J. and Duance, V. C. (2006). Disassembly of the vimentin cytoskeleton disrupts articular cartilage chondrocyte homeostasis. Matrix Biology 25(7): 398-408.

Blain, E. J., Gilbert, S. J., Wardale, R. J., Capper, S. J., Mason, D. J. and Duance, V. C. (2001). Up-regulation of matrix metalloproteinase expression and activation following cyclical compressive loading of articular cartilage in vitro. Arch Biochem Biophys 396(1): 49-55.

Blain, E. J., Mason, D. J. and Duance, V. C. (2002). The effect of thymosin beta4 on articular cartilage chondrocyte matrix metalloproteinase expression. Biochem Soc Trans 30(Pt 6): 879-882.

Blain, E. J., Mason, D. J. and Duance, V. C. (2003). The effect of cyclical compressive loading on gene expression in articular cartilage. Biorheology 40(1-3): 111-117.

Blair, H. J., Tompson, S., Liu, Y. N., Campbell, J., MacArthur, K., Ponting, C. P., Ruiz-Perez, V. L. and Goodship, J. A. (2011). Evc2 is a positive modulator of Hedgehog signalling that interacts with Evc at the cilia membrane and is also found in the nucleus. BMC Biol 9: 14.

Bockholt, S. M. and Burridge, K. (1993). Cell spreading on extracellular matrix proteins induces tyrosine phosphorylation of tensin. J Biol Chem 268(20): 14565-14567.

Bootman, M. D., Collins, T. J., Peppiatt, C. M., Prothero, L. S., MacKenzie, L., De Smet, P., Travers, M., Tovey, S. C., Seo, J. T., Berridge, M. J., Ciccolini, F. and Lipp, P. (2001). Calcium signalling--an overview. Semin Cell Dev Biol 12(1): 3-10.

Boyault, C., Sadoul, K., Pabion, M. and Khochbin, S. (2007). HDAC6, at the crossroads between cytoskeleton and cell signaling by acetylation and ubiquitination. Oncogene 26(37): 5468-5476.

Boyault, C., Zhang, Y., Fritah, S., Caron, C., Gilquin, B., Kwon, S. H., Garrido, C., Yao, T.-P., Vourc'h, C., Matthias, P. and Khochbin, S. (2007). HDAC6 controls major cell response pathways to cytotoxic accumulation of protein aggregates. Genes & Development 21(17): 2172-2181.

Braman, J. P., Bruckner, J. D., Clark, J. M., Norman, A. G. and Chansky, H. A. (2005). Articular cartilage adjacent to experimental defects is subject to atypical strains. Clinical Orthopaedics and Related Research(430): 202-207.

Brodkin, K. R., Garcia, A. J. and Levenston, M. E. (2004). Chondrocyte phenotypes on different extracellular matrix monolayers. Biomaterials 25(28): 5929-5938.

Brown, J. M., Marsala, C., Kosoy, R. and Gaertig, J. (1999). Kinesin-II is preferentially targeted to assembling cilia and is required for ciliogenesis and normal cytokinesis in Tetrahymena. Mol Biol Cell 10(10): 3081-3096.

Brown, P. D. and Benya, P. D. (1988). Alterations in chondrocyte cytoskeletal architecture during phenotypic modulation by retinoic acid and dihydrocytochalasin B-induced reexpression. J Cell Biol 106(1): 171-179.

Brown, T. D., Pope, D. F., Hale, J. E., Buckwalter, J. A. and Brand, R. A. (1991). Effects of osteochondral defect size on cartilage contact stress. Journal of Orthopaedic Research 9(4): 559-567.

Browning, J. A., Saunders, K., Urban, J. P. and Wilkins, R. J. (2004). The influence and interactions of hydrostatic and osmotic pressures on the intracellular milieu of chondrocytes. Biorheology 41(3-4): 299-308.

Burke, R., Nellen, D., Bellotto, M., Hafen, E., Senti, K. A., Dickson, B. J. and Basler, K. (1999). Dispatched, a novel sterol-sensing domain protein dedicated to the release of cholesterol-modified hedgehog from signaling cells. Cell 99(7): 803-815.

Burridge, K., Turner, C. E. and Romer, L. H. (1992). Tyrosine phosphorylation of paxillin and pp125FAK accompanies cell adhesion to extracellular matrix: a role in cytoskeletal assembly. J Cell Biol 119(4): 893-903.

Buschmann, M. D., Gluzband, Y. A., Grodzinsky, A. J. and Hunziker, E. B. (1995). Mechanical compression modulates matrix biosynthesis in chondrocyte/agarose culture. J Cell Sci 108 ( Pt 4): 1497-1508.

Buttitta, L., Mo, R., Hui, C. C. and Fan, C. M. (2003). Interplays of Gli2 and Gli3 and their requirement in mediating Shh-dependent sclerotome induction. Development 130(25): 6233-6243.

Calvet, J. P. and Grantham, J. J. (2001). The genetics and physiology of polycystic kidney disease. Semin Nephrol 21(2): 107-123.

Campbell, J. J., Blain, E. J., Chowdhury, T. T. and Knight, M. M. (2007). Loading alters actin dynamics and up-regulates cofilin gene expression in chondrocytes. Biochem Biophys Res Commun 361(2): 329-334.

Caparros-Martin, J. A., Valencia, M., Reytor, E., Pacheco, M., Fernandez, M., Perez-Aytes, A., Gean, E., Lapunzina, P., Peters, H., Goodship, J. A. and Ruiz-Perez, V. L. (2013). The ciliary Evc/Evc2 complex interacts with Smo and controls Hedgehog pathway activity in chondrocytes by regulating Sufu/Gli3 dissociation and Gli3 trafficking in primary cilia. Hum Mol Genet 22(1): 124-139.

Capin-Gutierrez, N., Talamas-Rohana, P., Gonzalez-Robles, A., Lavalle-Montalvo, C. and Kouri, J. B. (2004). Cytoskeleton disruption in chondrocytes from a rat osteoarthrosic (OA) -induced model: its potential role in OA pathogenesis. Histol Histopathol 19(4): 1125-1132.

Caspary, T. and Anderson, K. V. (2006). Hennin: Dual roles for cilia proteins in mammalian development. Developmental Biology 295(1): 413-413.

Caspary, T., Larkins, C. E. and Anderson, K. V. (2007). The graded response to sonic hedgehog depends on cilia architecture. Developmental Cell 12(5): 767-778.

Chailley, B. and Boisvieux-Ulrich, E. (1985). Detection of plasma membrane cholesterol by filipin during microvillogenesis and ciliogenesis in quail oviduct. J Histochem Cytochem 33(1): 1-10.

Chakravarthy, B., Gaudet, C., Menard, M., Brown, L., Atkinson, T., Laferla, F. M., Ito, S., Armato, U., Dal Pra, I. and Whitfield, J. (2012). Reduction of the immunostainable length of the hippocampal dentate granule cells' primary cilia in 3xAD-transgenic mice producing human Abeta(1-42) and tau. Biochem Biophys Res Commun 427(1): 218-222.

Chamoun, Z., Mann, R. K., Nellen, D., von Kessler, D. P., Bellotto, M., Beachy, P. A. and Basler, K. (2001). Skinny hedgehog, an acyltransferase required for palmitoylation and activity of the hedgehog signal. Science 293(5537): 2080-2084.

Chang, C. F., Ramaswamy, G. and Serra, R. (2012). Depletion of primary cilia in articular chondrocytes results in reduced Gli3 repressor to activator ratio, increased Hedgehog signaling, and symptoms of early osteoarthritis. Osteoarthritis Cartilage 20(2): 152-161.

Chang, C. F. and Serra, R. (2013). Ift88 regulates Hedgehog signaling, Sfrp5 expression, and beta-catenin activity in post-natal growth plate. J Orthop Res 31(3): 350-356.

Chang, J. K., Chang, L. H., Hung, S. H., Wu, S. C., Lee, H. Y., Lin, Y. S., Chen, C. H., Fu, Y. C., Wang, G. J. and Ho, M. L. (2009). Parathyroid hormone 1-34 inhibits terminal differentiation of human articular chondrocytes and osteoarthritis progression in rats. Arthritis Rheum 60(10): 3049-3060.

Chao, P.-h. G., West, A. C. and Hung, C. T. (2006). Chondrocyte intracellular calcium, cytoskeletal organization, and gene expression responses to dynamic osmotic loading. American Journal of Physiology-Cell Physiology 291(4): C718-C725.

Chauvet, V., Tian, X., Husson, H., Grimm, D. H., Wang, T., Hiesberger, T., Igarashi, P., Bennett, A. M., Ibraghimov-Beskrovnaya, O., Somlo, S. and Caplan, M. J. (2004). Mechanical stimuli induce cleavage and nuclear translocation of the polycystin-1 C terminus. J Clin Invest 114(10): 1433-1443.

Chen, C. T., Burton-Wurster, N., Borden, C., Hueffer, K., Bloom, S. E. and Lust, G. (2001). Chondrocyte necrosis and apoptosis in impact damaged articular cartilage. J Orthop Res 19(4): 703-711.

Chen, F. H., Rousche, K. T. and Tuan, R. S. (2006). Technology Insight: adult stem cells in cartilage regeneration and tissue engineering. Nat Clin Pract Rheumatol 2(7): 373-382.

Chen, X., Tukachinsky, H., Huang, C. H., Jao, C., Chu, Y. R., Tang, H. Y., Mueller, B., Schulman, S., Rapoport, T. A. and Salic, A. (2011). Processing and turnover of the Hedgehog protein in the endoplasmic reticulum. J Cell Biol 192(5): 825-838.

Chiang, C., Litingtung, Y., Harris, M. P., Simandl, B. K., Li, Y., Beachy, P. A. and Fallon, J. F. (2001). Manifestation of the limb prepattern: limb development in the absence of sonic hedgehog function. Dev Biol 236(2): 421-435.

Chih, B., Liu, P., Chinn, Y., Chalouni, C., Komuves, L. G., Hass, P. E., Sandoval, W. and Peterson, A. S. (2012). A ciliopathy complex at the transition zone protects the cilia as a privileged membrane domain. Nat Cell Biol 14(1): 61-72.

Choi, J. B., Youn, I., Cao, L., Leddy, H. A., Gilchrist, C. L., Setton, L. A. and Guilak, F. (2007). Zonal changes in the three-dimensional morphology of the chondron under compression: the relationship among cellular, pericellular, and extracellular deformation in articular cartilage. J Biomech 40(12): 2596-2603.

Clark, A. L., Votta, B. J., Kumar, S., Liedtke, W. and Guilak, F. (2010). Chondroprotective Role of the Osmotically Sensitive Ion Channel Transient Receptor Potential Vanilloid 4 Age- and Sex-Dependent Progression of Osteoarthritis in Trpv4-Deficient Mice. Arthritis and Rheumatism 62(10): 2973-2983.

Cole, D. G. (1999). Kinesin-II, the heteromeric kinesin. Cell Mol Life Sci 56(3-4): 217-226.

Cole, D. G., Diener, D. R., Himelblau, A. L., Beech, P. L., Fuster, J. C. and Rosenbaum, J. L. (1998). Chlamydomonas kinesin-II-dependent intraflagellar transport (IFT): IFT particles contain proteins required for ciliary assembly in Caenorhabditis elegans sensory neurons. J Cell Biol 141(4): 993-1008.

Corbit, K. C., Aanstad, P., Singla, V., Norman, A. R., Stainier, D. Y. and Reiter, J. F. (2005). Vertebrate Smoothened functions at the primary cilium. Nature 437(7061): 1018-1021.

Corbit, K. C., Shyer, A. E., Dowdle, W. E., Gaulden, J., Singla, V., Chen, M. H., Chuang, P. T. and Reiter, J. F. (2008). Kif3a constrains beta-catenin-dependent Wnt signalling through dual ciliary and non-ciliary mechanisms. Nat Cell Biol 10(1): 70-76.

Cotto, J. J. and Morimoto, R. I. (1999). Stress-induced activation of the heat-shock response: cell and molecular biology of heat-shock factors. Biochem Soc Symp 64: 105-118.

Creanga, A., Glenn, T. D., Mann, R. K., Saunders, A. M., Talbot, W. S. and Beachy, P. A. (2012). Scube/You activity mediates release of dually lipid-modified Hedgehog signal in soluble form. Genes Dev 26(12): 1312-1325.

Cruz, C., Ribes, V., Kutejova, E., Cayuso, J., Lawson, V., Norris, D., Stevens, J., Davey, M., Blight, K., Bangs, F., Mynett, A., Hirst, E., Chung, R., Balaskas, N., Brody, S. L., Marti, E. and Briscoe, J. (2010). Foxj1 regulates floor plate cilia architecture and modifies the response of cells to sonic hedgehog signalling. Development 137(24): 4271-4282.

D'Andrea, P. and Vittur, F. (1996). Ca2+ oscillations and intercellular Ca2+ waves in ATP-stimulated articular chondrocytes. J Bone Miner Res 11(7): 946-954.

Dabdoub, A. and Kelley, M. W. (2005). Planar cell polarity and a potential role for a Wnt morphogen gradient in stereociliary bundle orientation in the mammalian inner ear. J Neurobiol 64(4): 446-457.

Dai, P., Akimaru, H., Tanaka, Y., Maekawa, T., Nakafuku, M. and Ishii, S. (1999). Sonic Hedgehog-induced activation of the Gli1 promoter is mediated by GLI3. J Biol Chem 274(12): 8143-8152.

Dai, P., Shinagawa, T., Nomura, T., Harada, J., Kaul, S. C., Wadhwa, R., Khan, M. M., Akimaru, H., Sasaki, H., Colmenares, C. and Ishii, S. (2002). Ski is involved in transcriptional regulation by the repressor and full-length forms of Gli3. Genes Dev 16(22): 2843-2848.

Dawe, H. R., Adams, M., Wheway, G., Szymanska, K., Logan, C. V., Noegel, A. A., Gull, K. and Johnson, C. A. (2009). Nesprin-2 interacts with meckelin and mediates ciliogenesis via remodelling of the actin cytoskeleton. Journal of Cell Science 122(15): 2716-2726.

de Andrea, C. E., Wiweger, M., Prins, F., Bovee, J. V., Romeo, S. and Hogendoorn, P. C. (2010). Primary cilia organization reflects polarity in the growth plate and implies loss of polarity and mosaicism in osteochondroma. Lab Invest 90(7): 1091-1101.

Deane, J. A., Cole, D. G., Seeley, E. S., Diener, D. R. and Rosenbaum, J. L. (2001). Localization of intraflagellar transport protein IFT52 identifies basal body transitional fibers as the docking site for IFT particles. Curr Biol 11(20): 1586-1590.

Degala, S., Williams, R., Zipfel, W. and Bonassar, L. J. (2012). Calcium signaling in response to fluid flow by chondrocytes in 3D alginate culture. J Orthop Res 30(5): 793-799.

Dickey, C. A., Kamal, A., Lundgren, K., Klosak, N., Bailey, R. M., Dunmore, J., Ash, P., Shoraka, S., Zlatkovic, J., Eckman, C. B., Patterson, C., Dickson, D. W., Nahman, N. S., Jr., Hutton, M., Burrows, F. and Petrucelli, L. (2007). The high-affinity HSP90-CHIP complex recognizes and selectively degrades phosphorylated tau client proteins. J Clin Invest 117(3): 648-658.

Ding, Q., Fukami, S., Meng, X., Nishizaki, Y., Zhang, X., Sasaki, H., Dlugosz, A., Nakafuku, M. and Hui, C. (1999). Mouse suppressor of fused is a negative regulator of sonic hedgehog signaling and alters the subcellular distribution of Gli1. Curr Biol 9(19): 1119-1122.

Ding, Q., Motoyama, J., Gasca, S., Mo, R., Sasaki, H., Rossant, J. and Hui, C. C. (1998). Diminished Sonic hedgehog signaling and lack of floor plate differentiation in Gli2 mutant mice. Development 125(14): 2533-2543.

Dishinger, J. F., Kee, H. L., Jenkins, P. M., Fan, S., Hurd, T. W., Hammond, J. W., Truong, Y. N., Margolis, B., Martens, J. R. and Verhey, K. J. (2010). Ciliary entry of the kinesin-2 motor KIF17 is regulated by importin-beta2 and RanGTP. Nat Cell Biol 12(7): 703-710.

Doi, H., Nishida, K., Yorimitsu, M., Komiyama, T., Kadota, Y., Tetsunaga, T., Yoshida, A., Kubota, S., Takigawa, M. and Ozaki, T. (2008). Interleukin-4 downregulates the cyclic tensile stress-induced matrix metalloproteinases-13 and cathepsin B expression by rat normal chondrocytes. Acta Med Okayama 62(2): 119-126.

Domire, J. S., Green, J. A., Lee, K. G., Johnson, A. D., Askwith, C. C. and Mykytyn, K. (2011). Dopamine receptor 1 localizes to neuronal cilia in a dynamic process that requires the Bardet-Biedl syndrome proteins. Cell Mol Life Sci 68(17): 2951-2960.

Dompierre, J. P., Godin, J. D., Charrin, B. C., Cordelieres, F. P., King, S. J., Humbert, S. and Saudou, F. (2007). Histone deacetylase 6 inhibition compensates for the transport deficit in Huntington's disease by increasing tubulin acetylation. J Neurosci 27(13): 3571-3583.

Dorn, K. V., Hughes, C. E. and Rohatgi, R. (2012). A Smoothened-Evc2 Complex Transduces the Hedgehog Signal at Primary Cilia. Dev Cell.

Dowthwaite, G. P., Bishop, J. C., Redman, S. N., Khan, I. M., Rooney, P., Evans, D. J., Haughton, L., Bayram, Z., Boyer, S., Thomson, B., Wolfe, M. S. and Archer, C. W. (2004). The surface of articular cartilage contains a progenitor cell population. J Cell Sci 117(Pt 6): 889-897.

Dreier, R. (2010). Hypertrophic differentiation of chondrocytes in osteoarthritis: the developmental aspect of degenerative joint disorders. Arthritis Res Ther 12(5): 216.

Dudhia, J. (2005). Aggrecan, aging and assembly in articular cartilage. Cell Mol Life Sci 62(19-20): 2241-2256.

Edlich, M., Yellowley, C. E., Jacobs, C. R. and Donahue, H. J. (2001). Oscillating fluid flow regulates cytosolic calcium concentration in bovine articular chondrocytes. J Biomech 34(1): 59-65.

Edwards, M. J. (2007). Hyperthermia in utero due to maternal influenza is an environmental risk factor for schizophrenia. Congenit Anom (Kyoto) 47(3): 84-89.

Elofsson, R., Andersson, A., Falck, B. and Sjoborg, S. (1984). The ciliated human keratinocyte. J Ultrastruct Res 87(3): 212-220.

Engel, B. D., Ludington, W. B. and Marshall, W. F. (2009). Intraflagellar transport particle size scales inversely with flagellar length: revisiting the balance-point length control model. J Cell Biol 187(1): 81-89.

Erickson, G. R., Northrup, D. L. and Guilak, F. (2003). Hypo-osmotic stress induces calcium-dependent actin reorganization in articular chondrocytes. Osteoarthritis Cartilage 11(3): 187-197.

Essner, J. J., Amack, J. D., Nyholm, M. K., Harris, E. B. and Yost, H. J. (2005). Kupffer's vesicle is a ciliated organ of asymmetry in the zebrafish embryo that initiates left-right development of the brain, heart and gut. Development 132(6): 1247-1260.

Essner, J. J., Vogan, K. J., Wagner, M. K., Tabin, C. J., Yost, H. J. and Brueckner, M. (2002). Conserved function for embryonic nodal cilia. Nature 418(6893): 37-38.

Fan, S., Fogg, V., Wang, Q., Chen, X. W., Liu, C. J. and Margolis, B. (2007). A novel Crumbs3 isoform regulates cell division and ciliogenesis via importin beta interactions. J Cell Biol 178(3): 387-398.

Fan, S., Whiteman, E. L., Hurd, T. W., McIntyre, J. C., Dishinger, J. F., Liu, C. J., Martens, J. R., Verhey, K. J., Sajjan, U. and Margolis, B. (2011). Induction of Ran GTP drives ciliogenesis. Mol Biol Cell 22(23): 4539-4548.

Farndale, R. W., Sayers, C. A. and Barrett, A. J. (1982). A direct spectrophotometric microassay for sulfated glycosaminoglycans in cartilage cultures. Connect Tissue Res 9(4): 247-248.

Farnum, C. E. and Wilsman, N. J. (2011). Orientation of Primary Cilia of Articular Chondrocytes in Three-Dimensional Space. Anat Rec (Hoboken) 294(3): 533-549.

Fitzgerald, J. B., Jin, M., Dean, D., Wood, D. J., Zheng, M. H. and Grodzinsky, A. J. (2004). Mechanical compression of cartilage explants induces multiple time-dependent gene expression patterns and involves intracellular calcium and cyclic AMP. J Biol Chem 279(19): 19502-19511.

Fuino, L., Bali, P., Wittmann, S., Donapaty, S., Guo, F., Yamaguchi, H., Wang, H. G., Atadja, P. and Bhalla, K. (2003). Histone deacetylase inhibitor LAQ824 down-regulates Her-2 and sensitizes human breast cancer cells to trastuzumab, taxotere, gemcitabine, and epothilone B. Mol Cancer Ther 2(10): 971-984.

Fukasawa, K. (2007). Oncogenes and tumour suppressors take on centrosomes. Nat Rev Cancer 7(12): 911-924.

Gaertig, J. and Wloga, D. (2008). Ciliary tubulin and its post-translational modifications. Curr Top Dev Biol 85: 83-113.

Gallet, A. (2011). Hedgehog morphogen: from secretion to reception. Trends Cell Biol 21(4): 238-246.

Gao, B., Guo, J., She, C., Shu, A., Yang, M., Tan, Z., Yang, X., Guo, S., Feng, G. and He, L. (2001). Mutations in IHH, encoding Indian hedgehog, cause brachydactyly type A-1. Nat Genet 28(4): 386-388.

Garcia-Gonzalo, F. R., Corbit, K. C., Sirerol-Piquer, M. S., Ramaswami, G., Otto, E. A., Noriega, T. R., Seol, A. D., Robinson, J. F., Bennett, C. L., Josifova, D. J., Garcia-Verdugo, J. M., Katsanis, N., Hildebrandt, F. and Reiter, J. F. (2011). A transition zone complex regulates mammalian ciliogenesis and ciliary membrane composition. Nat Genet 43(8): 776-784.

Garcia, M. and Knight, M. M. (2010). Cyclic loading opens hemichannels to release ATP as part of a chondrocyte mechanotransduction pathway. J Orthop Res 28(4): 510-515.
Gardner, K., Arnoczky, S. P. and Lavagnino, M. (2011). Effect of in vitro stress-deprivation and cyclic loading on the length of tendon cell cilia in situ. J Orthop Res 29(4): 582-587.
Geiger, R. C., Kaufman, C. D., Lam, A. P., Budinger, G. R. and Dean, D. A. (2009). Tubulin acetylation and histone deacetylase 6 activity in the lung under cyclic load. Am J Respir Cell Mol Biol 40(1): 76-82.
Gerdes, J. M. and Katsanis, N. (2008). Ciliary function and Wnt signal modulation. Curr Top Dev Biol 85: 175-195.
Gilbert, S. F. (2006). Development of the Tetrapod Limb. Developmental Biology. Sunderland, Sinauer Associates**:** 23.
Gilula, N. B. and Satir, P. (1972). The ciliary necklace. A ciliary membrane specialization. J Cell Biol 53(2): 494-509.
Glowacki, J., Trepman, E. and Folkman, J. (1983). Cell-shape and phenotypic-expression in chondrocytes. Proceedings of the Society for Experimental Biology and Medicine 172(1): 93-98.
Goedert, M. (2009). Oskar Fischer and the study of dementia. Brain 132(Pt 4): 1102-1111.
Goetz, S. C. and Anderson, K. V. (2010). The primary cilium: a signalling centre during vertebrate development. Nat Rev Genet 11(5): 331-344.
Goldring, M. B. and Goldring, S. R. (2007). Osteoarthritis. Journal of Cellular Physiology 213(3): 626-634.
Goldring, S. R. and Goldring, M. B. (2010). Bone and cartilage in osteoarthritis: is what's best for one good or bad for the other? Arthritis Res Ther 12(5): 143.
Gonzalez-Perrett, S., Kim, K., Ibarra, C., Damiano, A. E., Zotta, E., Batelli, M., Harris, P. C., Reisin, I. L., Arnaout, M. A. and Cantiello, H. F. (2001). Polycystin-2, the protein mutated in autosomal dominant polycystic kidney disease (ADPKD), is a Ca2+-permeable nonselective cation channel. Proc Natl Acad Sci U S A 98(3): 1182-1187.
Gradilone, S. A., Radtke, B. N., Bogert, P. S., Huang, B. Q., Gajdos, G. B. and Larusso, N. F. (2013). HDAC6 inhibition restores ciliary expression and decreases tumor growth. Cancer Res.
Graff, R. D., Lazarowski, E. R., Banes, A. J. and Lee, G. M. (2000). ATP release by mechanically loaded porcine chondrons in pellet culture. Arthritis Rheum 43(7): 1571-1579.
Gratz, K. R., Wong, B. L., Bae, W. C. and Sah, R. L. (2008). The effects of focal articular defects on intra-tissue strains in the surrounding and opposing cartilage. Biorheology 45(3-4): 193-207.
Gratz, K. R., Wong, B. L., Bae, W. C. and Sah, R. L. (2009). The Effects of Focal Articular Defects on Cartilage Contact Mechanics. Journal of Orthopaedic Research 27(5): 584-592.
Greene, G. W., Banquy, X., Lee, D. W., Lowrey, D. D., Yu, J. and Israelachvili, J. N. (2011). Adaptive mechanically controlled lubrication mechanism found in articular joints. Proc Natl Acad Sci U S A 108(13): 5255-5259.
Guan, Y. J., Yang, X., Wei, L. and Chen, Q. (2011). MiR-365: a mechanosensitive microRNA stimulates chondrocyte differentiation through targeting histone deacetylase 4. FASEB J 25(12): 4457-4466.
Guilak, F., Ratcliffe, A. and Mow, V. C. (1995). Chondrocyte deformation and local tissue strain in articular cartilage: a confocal microscopy study. J Orthop Res 13(3): 410-421.
Guo, H., Duan, W. P., Li, Q., Cao, X. M., Wang, L. and Wei, X. C. (2011). [Disassembly of tubulin cytoskeleton disrupts the homeostasis of articular cartilage chondrocytes]. Zhonghua Yi Xue Za Zhi 91(15): 1036-1040.
Haggarty, S. J., Koeller, K. M., Wong, J. C., Grozinger, C. M. and Schreiber, S. L. (2003). Domain-selective small-molecule inhibitor of histone deacetylase 6 (HDAC6)-mediated tubulin deacetylation. Proc Natl Acad Sci U S A 100(8): 4389-4394.

Hammond, J. W., Huang, C. F., Kaech, S., Jacobson, C., Banker, G. and Verhey, K. J. (2010). Posttranslational modifications of tubulin and the polarized transport of kinesin-1 in neurons. Mol Biol Cell 21(4): 572-583.

Handel, M., Schulz, S., Stanarius, A., Schreff, M., Erdtmann-Vourliotis, M., Schmidt, H., Wolf, G. and Hollt, V. (1999). Selective targeting of somatostatin receptor 3 to neuronal cilia. Neuroscience 89(3): 909-926.

Harris, E. D., Jr. and McCroskery, P. A. (1974). The influence of temperature and fibril stability on degradation of cartilage collagen by rheumatoid synovial collagenase. N Engl J Med 290(1): 1-6.

Haycraft, C. J., Banizs, B., Aydin-Son, Y., Zhang, Q., Michaud, E. J. and Yoder, B. K. (2005). Gli2 and Gli3 localize to cilia and require the intraflagellar transport protein polaris for processing and function. PLoS Genet 1(4): e53.

Haycraft, C. J. and Serra, R. (2008). Cilia involvement in patterning and maintenance of the skeleton. Curr Top Dev Biol 85: 303-332.

Haycraft, C. J., Zhang, Q., Song, B., Jackson, W. S., Detloff, P. J., Serra, R. and Yoder, B. K. (2007). Intraflagellar transport is essential for endochondral bone formation. Development 134(2): 307-316.

Heldin, C. H. and Westermark, B. (1999). Mechanism of action and in vivo role of platelet-derived growth factor. Physiol Rev 79(4): 1283-1316.

Hellemans, J., Coucke, P. J., Giedion, A., De Paepe, A., Kramer, P., Beemer, F. and Mortier, G. R. (2003). Homozygous mutations in IHH cause acrocapitofemoral dysplasia, an autosomal recessive disorder with cone-shaped epiphyses in hands and hips. Am J Hum Genet 72(4): 1040-1046.

Hernandez-Hernandez, V., Pravincumar, P., Diaz-Font, A., May-Simera, H., Jenkins, D., Knight, M. and Beales, P. L. (2013). Bardet-Biedl syndrome proteins control the cilia length through regulation of actin polymerization. Hum Mol Genet.

Heywood, H. K., Knight, M. M. and Lee, D. A. (2010). Both superficial and deep zone articular chondrocyte subpopulations exhibit the Crabtree effect but have different basal oxygen consumption rates. J Cell Physiol 223(3): 630-639.

Hildebrand, J. D., Schaller, M. D. and Parsons, J. T. (1995). Paxillin, a tyrosine phosphorylated focal adhesion-associated protein binds to the carboxyl terminal domain of focal adhesion kinase. Mol Biol Cell 6(6): 637-647.

Hirokawa, N., Tanaka, Y., Okada, Y. and Takeda, S. (2006). Nodal flow and the generation of left-right asymmetry. Cell 125(1): 33-45.

hjTang, G. H., Rabie, A. B. and Hagg, U. (2004). Indian hedgehog: a mechanotransduction mediator in condylar cartilage. J Dent Res 83(5): 434-438.

Holledge, M. M., Millward-Sadler, S. J., Nuki, G. and Salter, D. M. (2008). Mechanical regulation of proteoglycan synthesis in normal and osteoarthritic human articular chondrocytes--roles for alpha5 and alphaVbeta5 integrins. Biorheology 45(3-4): 275-288.

Horoyan, M., Benoliel, A. M., Capo, C. and Bongrand, P. (1990). Localization of calcium and microfilament changes in mechanically stressed cells. Cell Biophys 17(3): 243-256.

Hou, Y., Pazour, G. J. and Witman, G. B. (2004). A dynein light intermediate chain, D1bLIC, is required for retrograde intraflagellar transport. Mol Biol Cell 15(10): 4382-4394.

Hou, Y., Qin, H., Follit, J. A., Pazour, G. J., Rosenbaum, J. L. and Witman, G. B. (2007). Functional analysis of an individual IFT protein: IFT46 is required for transport of outer dynein arms into flagella. J Cell Biol 176(5): 653-665.

Hsu, S. H., Zhang, X., Yu, C., Li, Z. J., Wunder, J. S., Hui, C. C. and Alman, B. A. (2011). Kif7 promotes hedgehog signaling in growth plate chondrocytes by restricting the inhibitory function of Sufu. Development 138(17): 3791-3801.

Hu, Q. and Nelson, W. J. (2011). Ciliary diffusion barrier: the gatekeeper for the primary cilium compartment. Cytoskeleton (Hoboken) 68(6): 313-324.
Huang, J., Ballou, L. R. and Hasty, K. A. (2007). Cyclic equibiaxial tensile strain induces both anabolic and catabolic responses in articular chondrocytes. Gene 404(1-2): 101-109.
Huang, K., Diener, D. R. and Rosenbaum, J. L. (2009). The ubiquitin conjugation system is involved in the disassembly of cilia and flagella. J Cell Biol 186(4): 601-613.
Huangfu, D. and Anderson, K. V. (2005). Cilia and Hedgehog responsiveness in the mouse. Proc Natl Acad Sci U S A 102(32): 11325-11330.
Huangfu, D. and Anderson, K. V. (2005). Cilia and Hedgehog responsiveness in the mouse. Proceedings of the National Academy of Sciences of the United States of America 102(32): 11325-11330.
Huangfu, D., Liu, A., Rakeman, A. S., Murcia, N. S., Niswander, L. and Anderson, K. V. (2003). Hedgehog signalling in the mouse requires intraflagellar transport proteins. Nature 426(6962): 83-87.
Hubbert, C., Guardiola, A., Shao, R., Kawaguchi, Y., Ito, A., Nixon, A., Yoshida, M., Wang, X. F. and Yao, T. P. (2002). HDAC6 is a microtubule-associated deacetylase. Nature 417(6887): 455-458.
Hung, C. T. (2010). Transient receptor potential vanilloid 4 channel as an important modulator of chondrocyte mechanotransduction of osmotic loading. Arthritis Rheum 62(10): 2850-2851.
Hurd, T. W., Fan, S. and Margolis, B. L. (2011). Localization of retinitis pigmentosa 2 to cilia is regulated by Importin beta2. J Cell Sci 124(Pt 5): 718-726.
Hynes, R. O. (1992). Integrins: versatility, modulation, and signaling in cell adhesion. Cell 69(1): 11-25.
Idowu, B. D., Knight, M. M., Bader, D. L. and Lee, D. A. (2000). Confocal analysis of cytoskeletal organisation within isolated chondrocyte sub-populations cultured in agarose. Histochem J 32(3): 165-174.
Infante, R. E., Wang, M. L., Radhakrishnan, A., Kwon, H. J., Brown, M. S. and Goldstein, J. L. (2008). NPC2 facilitates bidirectional transfer of cholesterol between NPC1 and lipid bilayers, a step in cholesterol egress from lysosomes. Proc Natl Acad Sci U S A 105(40): 15287-15292.
Ingham, P. W. and McMahon, A. P. (2001). Hedgehog signaling in animal development: paradigms and principles. Genes & Development 15(23): 3059-3087.
Iomini, C., Babaev-Khaimov, V., Sassaroli, M. and Piperno, G. (2001). Protein particles in Chlamydomonas flagella undergo a transport cycle consisting of four phases. J Cell Biol 153(1): 13-24.
Iomini, C., Li, L., Esparza, J. M. and Dutcher, S. K. (2009). Retrograde intraflagellar transport mutants identify complex A proteins with multiple genetic interactions in Chlamydomonas reinhardtii. Genetics 183(3): 885-896.
Iomini, C., Tejada, K., Mo, W., Vaananen, H. and Piperno, G. (2004). Primary cilia of human endothelial cells disassemble under laminar shear stress. J Cell Biol 164(6): 811-817.
Ishikawa, H. and Marshall, W. F. (2011). Ciliogenesis: building the cell's antenna. Nat Rev Mol Cell Biol 12(4): 222-234.
Iwakura, T., Inui, A. and Reddi, A. H. (2012). Stimulation of superficial zone protein accumulation by hedgehog and wnt signaling in surface zone articular chondrocytes. Arthritis Rheum.
Jat, P. S., Noble, M. D., Ataliotis, P., Tanaka, Y., Yannoutsos, N., Larsen, L. and Kioussis, D. (1991). Direct derivation of conditionally immortal cell lines from an H-2Kb-tsA58 transgenic mouse. Proc Natl Acad Sci U S A 88(12): 5096-5100.
Jensen, C. G., Davison, E. A., Bowser, S. S. and Rieder, C. L. (1987). Primary cilia cycle in PtK1 cells: effects of colcemid and taxol on cilia formation and resorption. Cell Motil Cytoskeleton 7(3): 187-197.

Jensen, C. G., Poole, C. A., McGlashan, S. R., Marko, M., Issa, Z. I., Vujcich, K. V. and Bowser, S. S. (2004). Ultrastructural, tomographic and confocal imaging of the chondrocyte primary cilium in situ. Cell Biol Int 28(2): 101-110.

Johnson, K. A. and Rosenbaum, J. L. (1992). Polarity of flagellar assembly in Chlamydomonas. J Cell Biol 119(6): 1605-1611.

Johnson, P. F. (2005). Molecular stop signs: regulation of cell-cycle arrest by C/EBP transcription factors. J Cell Sci 118(Pt 12): 2545-2555.

Joly, D., Hummel, A., Ruello, A. and Knebelmann, B. (2003). Ciliary function of polycystins: a new model for cystogenesis. Nephrol Dial Transplant 18(9): 1689-1692.

Jortikka, M. O., Parkkinen, J. J., Inkinen, R. I., Karner, J., Jarvelainen, H. T., Nelimarkka, L. O., Tammi, M. I. and Lammi, M. J. (2000). The role of microtubules in the regulation of proteoglycan synthesis in chondrocytes under hydrostatic pressure. Arch Biochem Biophys 374(2): 172-180.

Karaplis, A. C., Luz, A., Glowacki, J., Bronson, R. T., Tybulewicz, V. L., Kronenberg, H. M. and Mulligan, R. C. (1994). Lethal skeletal dysplasia from targeted disruption of the parathyroid hormone-related peptide gene. Genes Dev 8(3): 277-289.

Kaushik, A. P., Martin, J. A., Zhang, Q., Sheffield, V. C. and Morcuende, J. A. (2009). Cartilage abnormalities associated with defects of chondrocytic primary cilia in Bardet-Biedl syndrome mutant mice. J Orthop Res 27(8): 1093-1099.

Kawaguchi, Y., Kovacs, J. J., McLaurin, A., Vance, J. M., Ito, A. and Yao, T. P. (2003). The deacetylase HDAC6 regulates aggresome formation and cell viability in response to misfolded protein stress. Cell 115(6): 727-738.

Kee, H. L., Dishinger, J. F., Blasius, T. L., Liu, C. J., Margolis, B. and Verhey, K. J. (2012). A size-exclusion permeability barrier and nucleoporins characterize a ciliary pore complex that regulates transport into cilia. Nat Cell Biol 14(4): 431-437.

Kempson, G. E., Spivey, C. J., Swanson, S. A. and Freeman, M. A. (1971). Patterns of cartilage stiffness on normal and degenerate human femoral heads. J Biomech 4(6): 597-609.

Khan, V. R. and Brown, I. R. (2002). The effect of hyperthermia on the induction of cell death in brain, testis, and thymus of the adult and developing rat. Cell Stress Chaperones 7(1): 73-90.

Kiani, C., Chen, L., Wu, Y. J., Yee, A. J. and Yang, B. B. (2002). Structure and function of aggrecan. Cell Res 12(1): 19-32.

Kim, C. H., You, L., Yellowley, C. E. and Jacobs, C. R. (2006). Oscillatory fluid flow-induced shear stress decreases osteoclastogenesis through RANKL and OPG signaling. Bone 39(5): 1043-1047.

Kim, E., Guilak, F. and Haider, M. A. (2008). The dynamic mechanical environment of the chondrocyte: a biphasic finite element model of cell-matrix interactions under cyclic compressive loading. J Biomech Eng 130(6): 061009.

Kim, J., Lee, J. E., Heynen-Genel, S., Suyama, E., Ono, K., Lee, K., Ideker, T., Aza-Blanc, P. and Gleeson, J. G. (2010). Functional genomic screen for modulators of ciliogenesis and cilium length. Nature 464(7291): 1048-1051.

Kim, Y. J., Sah, R. L., Doong, J. Y. and Grodzinsky, A. J. (1988). Fluorometric assay of DNA in cartilage explants using Hoechst 33258. Anal Biochem 174(1): 168-176.

Kimmel, C. B., Ballard, W. W., Kimmel, S. R., Ullmann, B. and Schilling, T. F. (1995). Stages of embryonic development of the zebrafish. Dev Dyn 203(3): 253-310.

King, P., Paul, A. and Laufer, E. (2009). Shh signaling regulates adrenocortical development and identifies progenitors of steroidogenic lineages. Proc Natl Acad Sci U S A 106(50): 21185-21190.

Kinzel, D., Boldt, K., Davis, E. E., Burtscher, I., Trumbach, D., Diplas, B., Attie-Bitach, T., Wurst, W., Katsanis, N., Ueffing, M. and Lickert, H. (2010). Pitchfork regulates primary cilia disassembly and left-right asymmetry. Dev Cell 19(1): 66-77.

Kiviranta, I., Tammi, M., Jurvelin, J. and Helminen, H. J. (1987). Topographical variation of glycosaminoglycan content and cartilage thickness in canine knee (stifle) joint cartilage. Application of the microspectrophotometric method. J Anat 150: 265-276.

Knight, M. M., Idowu, B. D., Lee, D. A. and Bader, D. L. (2001). Temporal changes in cytoskeletal organisation within isolated chondrocytes quantified using a novel image analysis technique. Medical & Biological Engineering & Computing 39(3): 397-404.

Knight, M. M., McGlashan, S. R., Garcia, M., Jensen, C. G. and Poole, C. A. (2009). Articular chondrocytes express connexin 43 hemichannels and P2 receptors - a putative mechanoreceptor complex involving the primary cilium? J Anat 214(2): 275-283.

Knight, M. M., Toyoda, T., Lee, D. A. and Bader, D. L. (2006). Mechanical compression and hydrostatic pressure induce reversible changes in actin cytoskeletal organisation in chondrocytes in agarose. J Biomech 39(8): 1547-1551.

Knudson, C. B. and Knudson, W. (2001). Cartilage proteoglycans. Semin Cell Dev Biol 12(2): 69-78.

Kolpakova-Hart, E., McBratney-Owen, B., Hou, B., Fukai, N., Nicolae, C., Zhou, J. and Olsen, B. R. (2008). Growth of cranial synchondroses and sutures requires polycystin-1. Dev Biol 321(2): 407-419.

Kovacs, J. J., Murphy, P. J., Gaillard, S., Zhao, X., Wu, J. T., Nicchitta, C. V., Yoshida, M., Toft, D. O., Pratt, W. B. and Yao, T. P. (2005). HDAC6 regulates Hsp90 acetylation and chaperone-dependent activation of glucocorticoid receptor. Mol Cell 18(5): 601-607.

Kozminski, K. G., Johnson, K. A., Forscher, P. and Rosenbaum, J. L. (1993). A motility in the eukaryotic flagellum unrelated to flagellar beating. Proc Natl Acad Sci U S A 90(12): 5519-5523.

Kronenberg, H. M. (2003). Developmental regulation of the growth plate. Nature 423(6937): 332-336.

Kultz, D. (2005). Molecular and evolutionary basis of the cellular stress response. Annu Rev Physiol 67: 225-257.

Kuwabara, P. E. and Labouesse, M. (2002). The sterol-sensing domain: multiple families, a unique role? Trends Genet 18(4): 193-201.

Lai, L. P. and Mitchell, J. (2005). Indian hedgehog: its roles and regulation in endochondral bone development. J Cell Biochem 96(6): 1163-1173.

Lancaster, M. A., Schroth, J. and Gleeson, J. G. (2011). Subcellular spatial regulation of canonical Wnt signalling at the primary cilium. Nat Cell Biol 13(6): 700-707.

Lange, B. M., Bachi, A., Wilm, M. and Gonzalez, C. (2000). Hsp90 is a core centrosomal component and is required at different stages of the centrosome cycle in Drosophila and vertebrates. EMBO J 19(6): 1252-1262.

Langelier, E., Suetterlin, R., Hoemann, C. D., Aebi, U. and Buschmann, M. D. (2000). The chondrocyte cytoskeleton in mature articular cartilage: structure and distribution of actin, tubulin, and vimentin filaments. J Histochem Cytochem 48(10): 1307-1320.

Larionov, A., Krause, A. and Miller, W. (2005). A standard curve based method for relative real time PCR data processing. BMC Bioinformatics 6: 62.

Larkins, C. E., Aviles, G. D., East, M. P., Kahn, R. A. and Caspary, T. (2011). Arl13b regulates ciliogenesis and the dynamic localization of Shh signaling proteins. Mol Biol Cell 22(23): 4694-4703.

Lavagnino, M., Arnoczky, S. P. and Gardner, K. (2011). In situ deflection of tendon cell-cilia in response to tensile loading: an in vitro study. J Orthop Res 29(6): 925-930.

Lee, D. A. and Bader, D. L. (1997). Compressive strains at physiological frequencies influence the metabolism of chondrocytes seeded in agarose. J Orthop Res 15(2): 181-188.

Lee, D. A., Brand, J., Salter, D., Akanji, O. O. and Chowdhury, T. T. (2011). Quantification of mRNA using real-time PCR and Western blot analysis of MAPK events in chondrocyte/agarose constructs. Methods Mol Biol 695: 77-97.

Lee, D. A., Noguchi, T., Knight, M. M., O'Donnell, L., Bentley, G. and Bader, D. L. (1998). Response of chondrocyte subpopulations cultured within unloaded and loaded agarose. J Orthop Res 16(6): 726-733.

Lee, J. H., Fitzgerald, J. B., Dimicco, M. A. and Grodzinsky, A. J. (2005). Mechanical injury of cartilage explants causes specific time-dependent changes in chondrocyte gene expression. Arthritis Rheum 52(8): 2386-2395.

Lefebvre, P. A. and Rosenbaum, J. L. (1986). Regulation of the synthesis and assembly of ciliary and flagellar proteins during regeneration. Annu Rev Cell Biol 2: 517-546.

Li, A., Saito, M., Chuang, J. Z., Tseng, Y. Y., Dedesma, C., Tomizawa, K., Kaitsuka, T. and Sung, C. H. (2011). Ciliary transition zone activation of phosphorylated Tctex-1 controls ciliary resorption, S-phase entry and fate of neural progenitors. Nat Cell Biol 13(4): 402-411.

Liem, K. F., Jr., He, M., Ocbina, P. J. and Anderson, K. V. (2009). Mouse Kif7/Costal2 is a cilia-associated protein that regulates Sonic hedgehog signaling. Proc Natl Acad Sci U S A 106(32): 13377-13382.

Lin, A. C., Seeto, B. L., Bartoszko, J. M., Khoury, M. A., Whetstone, H., Ho, L., Hsu, C., Ali, S. A. and Alman, B. A. (2009). Modulating hedgehog signaling can attenuate the severity of osteoarthritis. Nat Med 15(12): 1421-1425.

Litingtung, Y., Dahn, R. D., Li, Y., Fallon, J. F. and Chiang, C. (2002). Shh and Gli3 are dispensable for limb skeleton formation but regulate digit number and identity. Nature 418(6901): 979-983.

Liu, A., Wang, B. and Niswander, L. A. (2005). Mouse intraflagellar transport proteins regulate both the activator and repressor functions of Gli transcription factors. Development 132(13): 3103-3111.

Liu, Q., Zhang, Q. and Pierce, E. A. (2010). Photoreceptor sensory cilia and inherited retinal degeneration. Adv Exp Med Biol 664: 223-232.

Loening, A. M., James, I. E., Levenston, M. E., Badger, A. M., Frank, E. H., Kurz, B., Nuttall, M. E., Hung, H. H., Blake, S. M., Grodzinsky, A. J. and Lark, M. W. (2000). Injurious mechanical compression of bovine articular cartilage induces chondrocyte apoptosis. Arch Biochem Biophys 381(2): 205-212.

Logan, C. Y. and Nusse, R. (2004). The Wnt signaling pathway in development and disease. Annu Rev Cell Dev Biol 20: 781-810.

Lopes, S. S., Lourenco, R., Pacheco, L., Moreno, N., Kreiling, J. and Saude, L. (2010). Notch signalling regulates left-right asymmetry through ciliary length control. Development 137(21): 3625-3632.

Low, S. H., Vasanth, S., Larson, C. H., Mukherjee, S., Sharma, N., Kinter, M. T., Kane, M. E., Obara, T. and Weimbs, T. (2006). Polycystin-1, STAT6, and P100 function in a pathway that transduces ciliary mechanosensation and is activated in polycystic kidney disease. Dev Cell 10(1): 57-69.

Lowenstein, D. H., Chan, P. H. and Miles, M. F. (1991). The stress protein response in cultured neurons: characterization and evidence for a protective role in excitotoxicity. Neuron 7(6): 1053-1060.

Luo, W., Dou, F., Rodina, A., Chip, S., Kim, J., Zhao, Q., Moulick, K., Aguirre, J., Wu, N., Greengard, P. and Chiosis, G. (2007). Roles of heat-shock protein 90 in maintaining and facilitating the neurodegenerative phenotype in tauopathies. Proc Natl Acad Sci U S A 104(22): 9511-9516.

Luo, W., Sun, W., Taldone, T., Rodina, A. and Chiosis, G. (2010). Heat shock protein 90 in neurodegenerative diseases. Mol Neurodegener 5: 24.

Ma, Y., Erkner, A., Gong, R., Yao, S., Taipale, J., Basler, K. and Beachy, P. A. (2002). Hedgehog-mediated patterning of the mammalian embryo requires transporter-like function of dispatched. Cell 111(1): 63-75.

Macica, C., Liang, G., Nasiri, A. and Broadus, A. E. (2011). Genetic evidence of the regulatory role of parathyroid hormone-related protein in articular chondrocyte maintenance in an experimental mouse model. Arthritis Rheum 63(11): 3333-3343.

Maeda, Y., Schipani, E., Densmore, M. J. and Lanske, B. (2009). Partial rescue of postnatal growth plate abnormalities in Ihh mutants by expression of a constitutively active PTH/PTHrP receptor. Bone.

Mahjoub, M. R. and Stearns, T. (2012). Supernumerary Centrosomes Nucleate Extra Cilia and Compromise Primary Cilium Signaling. Curr Biol.

Mailhos, C., Howard, M. K. and Latchman, D. S. (1993). Heat shock protects neuronal cells from programmed cell death by apoptosis. Neuroscience 55(3): 621-627.

Majumdar, M. K., Askew, R., Schelling, S., Stedman, N., Blanchet, T., Hopkins, B., Morris, E. A. and Glasson, S. S. (2007). Double-knockout of ADAMTS-4 and ADAMTS-5 in mice results in physiologically normal animals and prevents the progression of osteoarthritis. Arthritis Rheum 56(11): 3670-3674.

Malleingerin, F., Garrone, R. and Vanderrest, M. (1991). Proteoglycan and collagen-synthesis are correlated with actin organization in dedifferentiating chondrocytes. European Journal of Cell Biology 56(2): 364-373.

Malone, A. M., Anderson, C. T., Tummala, P., Kwon, R. Y., Johnston, T. R., Stearns, T. and Jacobs, C. R. (2007). Primary cilia mediate mechanosensing in bone cells by a calcium-independent mechanism. Proc Natl Acad Sci U S A 104(33): 13325-13330.

Marley, A. and von Zastrow, M. (2010). DISC1 regulates primary cilia that display specific dopamine receptors. PLoS One 5(5): e10902.

Marshall, W. F., Qin, H., Rodrigo Brenni, M. and Rosenbaum, J. L. (2005). Flagellar length control system: testing a simple model based on intraflagellar transport and turnover. Mol Biol Cell 16(1): 270-278.

Marshall, W. F. and Rosenbaum, J. L. (2001). Intraflagellar transport balances continuous turnover of outer doublet microtubules: implications for flagellar length control. J Cell Biol 155(3): 405-414.

Massinen, S., Hokkanen, M. E., Matsson, H., Tammimies, K., Tapia-Paez, I., Dahlstrom-Heuser, V., Kuja-Panula, J., Burghoorn, J., Jeppsson, K. E., Swoboda, P., Peyrard-Janvid, M., Toftgard, R., Castren, E. and Kere, J. (2011). Increased expression of the dyslexia candidate gene DCDC2 affects length and signaling of primary cilia in neurons. PLoS One 6(6): e20580.

Masyuk, A. I., Masyuk, T. V., Splinter, P. L., Huang, B. Q., Stroope, A. J. and LaRusso, N. F. (2006). Cholangiocyte cilia detect changes in luminal fluid flow and transmit them into intracellular Ca2+ and cAMP signaling. Gastroenterology 131(3): 911-920.

Matsuura, K., Lefebvre, P. A., Kamiya, R. and Hirono, M. (2002). Kinesin-II is not essential for mitosis and cell growth in Chlamydomonas. Cell Motil Cytoskeleton 52(4): 195-201.

May-Simera, H. L., Kai, M., Hernandez, V., Osborn, D. P., Tada, M. and Beales, P. L. (2010). Bbs8, together with the planar cell polarity protein Vangl2, is required to establish left-right asymmetry in zebrafish. Dev Biol 345(2): 215-225.

McBeath, R., Pirone, D. M., Nelson, C. M., Bhadriraju, K. and Chen, C. S. (2004). Cell shape, cytoskeletal tension, and RhoA regulate stem cell lineage commitment. Developmental Cell 6(4): 483-495.

McGlashan, S. R., Cluett, E. C., Jensen, C. G. and Poole, C. A. (2008). Primary cilia in osteoarthritic chondrocytes: from chondrons to clusters. Dev Dyn 237(8): 2013-2020.

McGlashan, S. R., Haycraft, C. J., Jensen, C. G., Yoder, B. K. and Poole, C. A. (2007). Articular cartilage and growth plate defects are associated with chondrocyte cytoskeletal abnormalities in Tg737orpk mice lacking the primary cilia protein polaris. Matrix Biol 26(4): 234-246.

McGlashan, S. R., Jensen, C. G. and Poole, C. A. (2006). Localization of extracellular matrix receptors on the chondrocyte primary cilium. J Histochem Cytochem 54(9): 1005-1014.

McGlashan, S. R., Knight, M. M., Chowdhury, T. T., Joshi, P., Jensen, C. G., Kennedy, S. and Poole, C. A. (2010). Mechanical loading modulates chondrocyte primary cilia incidence and length. Cell Biology International 34(5): 441-446.

Meier-Vismara, E., Walker, N. and Vogel, A. (1979). Single cilia in the articular cartilage of the cat. Exp Cell Biol 47(3): 161-171.

Milenkovic, L., Scott, M. P. and Rohatgi, R. (2009). Lateral transport of Smoothened from the plasma membrane to the membrane of the cilium. J Cell Biol 187(3): 365-374.

Millward-Sadler, S. J. and Salter, D. M. (2004). Integrin-dependent signal cascades in chondrocyte mechanotransduction. Ann Biomed Eng 32(3): 435-446.

Millward-Sadler, S. J., Wright, M. O., Davies, L. W., Nuki, G. and Salter, D. M. (2000). Mechanotransduction via integrins and interleukin-4 results in altered aggrecan and matrix metalloproteinase 3 gene expression in normal, but not osteoarthritic, human articular chondrocytes. Arthritis Rheum 43(9): 2091-2099.

Millward-Sadler, S. J., Wright, M. O., Flatman, P. W. and Salter, D. M. (2004). ATP in the mechanotransduction pathway of normal human chondrocytes. Biorheology 41(3-4): 567-575.

Millward-Sadler, S. J., Wright, M. O., Lee, H., Caldwell, H., Nuki, G. and Salter, D. M. (2000). Altered electrophysiological responses to mechanical stimulation and abnormal signalling through alpha5beta1 integrin in chondrocytes from osteoarthritic cartilage. Osteoarthritis Cartilage 8(4): 272-278.

Mitchison, T. and Kirschner, M. (1984). Dynamic instability of microtubule growth. Nature 312(5991): 237-242.

Miyoshi, K., Kasahara, K., Miyazaki, I. and Asanuma, M. (2011). Factors that influence primary cilium length. Acta Med Okayama 65(5): 279-285.

Mizuno, S. (2005). A novel method for assessing effects of hydrostatic fluid pressure on intracellular calcium: a study with bovine articular chondrocytes. Am J Physiol Cell Physiol 288(2): C329-337.

Molla-Herman, A., Ghossoub, R., Blisnick, T., Meunier, A., Serres, C., Silbermann, F., Emmerson, C., Romeo, K., Bourdoncle, P., Schmitt, A., Saunier, S., Spassky, N., Bastin, P. and Benmerah, A. (2010). The ciliary pocket: an endocytic membrane domain at the base of primary and motile cilia. J Cell Sci 123(Pt 10): 1785-1795.

Morris, R. L. and Scholey, J. M. (1997). Heterotrimeric kinesin-II is required for the assembly of motile 9+2 ciliary axonemes on sea urchin embryos. J Cell Biol 138(5): 1009-1022.

Moser, J. J., Fritzler, M. J., Ou, Y. and Rattner, J. B. (2010). The PCM-basal body/primary cilium coalition. Semin Cell Dev Biol 21(2): 148-155.

Motaung, S. C., Di Cesare, P. E. and Reddi, A. H. (2011). Differential response of cartilage oligomeric matrix protein (COMP) to morphogens of bone morphogenetic protein/transforming growth factor-beta family in the surface, middle and deep zones of articular cartilage. J Tissue Eng Regen Med 5(6): e87-96.

Mow, V. C., Wang, C. C. and Hung, C. T. (1999). The extracellular matrix, interstitial fluid and ions as a mechanical signal transducer in articular cartilage. Osteoarthritis Cartilage 7(1): 41-58.

Moyer, J. H., Lee-Tischler, M. J., Kwon, H. Y., Schrick, J. J., Avner, E. D., Sweeney, W. E., Godfrey, V. L., Cacheiro, N. L., Wilkinson, J. E. and Woychik, R. P. (1994). Candidate gene associated with a mutation causing recessive polycystic kidney disease in mice. Science 264(5163): 1329-1333.

Murphy, P. J., Morishima, Y., Kovacs, J. J., Yao, T. P. and Pratt, W. B. (2005). Regulation of the dynamics of hsp90 action on the glucocorticoid receptor by acetylation/deacetylation of the chaperone. J Biol Chem 280(40): 33792-33799.

Nachury, M. V., Loktev, A. V., Zhang, Q., Westlake, C. J., Peranen, J., Merdes, A., Slusarski, D. C., Scheller, R. H., Bazan, J. F., Sheffield, V. C. and Jackson, P. K. (2007). A core complex of BBS proteins cooperates with the GTPase Rab8 to promote ciliary membrane biogenesis. Cell 129(6): 1201-1213.

Nakano, Y., Kim, H. R., Kawakami, A., Roy, S., Schier, A. F. and Ingham, P. W. (2004). Inactivation of dispatched 1 by the chameleon mutation disrupts Hedgehog signalling in the zebrafish embryo. Dev Biol 269(2): 381-392.

Nauli, S. M., Alenghat, F. J., Luo, Y., Williams, E., Vassilev, P., Li, X., Elia, A. E., Lu, W., Brown, E. M., Quinn, S. J., Ingber, D. E. and Zhou, J. (2003). Polycystins 1 and 2 mediate mechanosensation in the primary cilium of kidney cells. Nat Genet 33(2): 129-137.

Nauli, S. M. and Zhou, J. (2004). Polycystins and mechanosensation in renal and nodal cilia. Bioessays 26(8): 844-856.

Naumanen, P., Lappalainen, P. and Hotulainen, P. (2008). Mechanisms of actin stress fibre assembly. Journal of Microscopy-Oxford 231(3): 446-454.

Neugebauer, J. M., Amack, J. D., Peterson, A. G., Bisgrove, B. W. and Yost, H. J. (2009). FGF signalling during embryo development regulates cilia length in diverse epithelia. Nature 458(7238): 651-654.

Newman, A. P. (1998). Articular cartilage repair. Am J Sports Med 26(2): 309-324.

Newman, P. and Watt, F. M. (1988). Influence of cytochalasin D-induced changes in cell-shape on proteoglycan synthesis by cultured articular chondrocytes. Experimental Cell Research 178(2): 199-210.

Ng, T. C., Chiu, K. W., Rabie, A. B. and Hagg, U. (2006). Repeated mechanical loading enhances the expression of Indian hedgehog in condylar cartilage. Front Biosci 11: 943-948.

Nimmanapalli, R., Fuino, L., Bali, P., Gasparetto, M., Glozak, M., Tao, J., Moscinski, L., Smith, C., Wu, J., Jove, R., Atadja, P. and Bhalla, K. (2003). Histone deacetylase inhibitor LAQ824 both lowers expression and promotes proteasomal degradation of Bcr-Abl and induces apoptosis of imatinib mesylate-sensitive or -refractory chronic myelogenous leukemia-blast crisis cells. Cancer Res 63(16): 5126-5135.

Nogales, E., Whittaker, M., Milligan, R. A. and Downing, K. H. (1999). High-resolution model of the microtubule. Cell 96(1): 79-88.

Nonaka, S., Tanaka, Y., Okada, Y., Takeda, S., Harada, A., Kanai, Y., Kido, M. and Hirokawa, N. (1998). Randomization of left-right asymmetry due to loss of nodal cilia generating leftward flow of extraembryonic fluid in mice lacking KIF3B motor protein. Cell 95(6): 829-837.

Nonaka, S., Yoshiba, S., Watanabe, D., Ikeuchi, S., Goto, T., Marshall, W. F. and Hamada, H. (2005). De novo formation of left-right asymmetry by posterior tilt of nodal cilia. PLoS Biol 3(8): e268.

North, B. J., Marshall, B. L., Borra, M. T., Denu, J. M. and Verdin, E. (2003). The human Sir2 ortholog, SIRT2, is an NAD+-dependent tubulin deacetylase. Mol Cell 11(2): 437-444.

Nowlan, N. C., Prendergast, P. J. and Murphy, P. (2008). Identification of mechanosensitive genes during embryonic bone formation. PLoS Comput Biol 4(12): e1000250.

Nusslein-Volhard, C. and Wieschaus, E. (1980). Mutations affecting segment number and polarity in Drosophila. Nature 287(5785): 795-801.

O'Connor, P., Orford, C. R. and Gardner, D. L. (1988). Differential response to compressive loads of zones of canine hyaline articular cartilage: micromechanical, light and electron microscopic studies. Ann Rheum Dis 47(5): 414-420.

Okayama, M., Pacifici, M. and Holtzer, H. (1976). Differences among sulfated proteoglycans synthesized in nonchondrogenic cells, presumptive chondroblasts, and chondroblasts. Proc Natl Acad Sci U S A 73(9): 3224-3228.

Olsen, B. R., Reginato, A. M. and Wang, W. (2000). Bone development. Annu Rev Cell Dev Biol 16: 191-220.

Ostrowski, L. E., Blackburn, K., Radde, K. M., Moyer, M. B., Schlatzer, D. M., Moseley, A. and Boucher, R. C. (2002). A proteomic analysis of human cilia: identification of novel components. Mol Cell Proteomics 1(6): 451-465.

Oswald, E. S., Chao, P. H., Bulinski, J. C., Ateshian, G. A. and Hung, C. T. (2008). Dependence of zonal chondrocyte water transport properties on osmotic environment. Cell Mol Bioeng 1(4): 339-348.

Otey, C. A. and Burridge, K. (1990). Patterning of the membrane cytoskeleton by the extracellular matrix. Semin Cell Biol 1(5): 391-399.

Ou, Y., Ruan, Y., Cheng, M., Moser, J. J., Rattner, J. B. and van der Hoorn, F. A. (2009). Adenylate cyclase regulates elongation of mammalian primary cilia. Exp Cell Res 315(16): 2802-2817.

Palmer, K. J., MacCarthy-Morrogh, L., Smyllie, N. and Stephens, D. J. (2011). A role for Tctex-1 (DYNLT1) in controlling primary cilium length. Eur J Cell Biol 90(10): 865-871.

Palmoski, M. J. and Brandt, K. D. (1982). Immobilization of the knee prevents osteoarthritis after anterior cruciate ligament transection. Arthritis Rheum 25(10): 1201-1208.

Pan, J. and Snell, W. (2007). The primary cilium: keeper of the key to cell division. Cell 129(7): 1255-1257.

Pan, J. and Snell, W. J. (2005). Chlamydomonas shortens its flagella by activating axonemal disassembly, stimulating IFT particle trafficking, and blocking anterograde cargo loading. Dev Cell 9(3): 431-438.

Parkkinen, J. J., Lammi, M. J., Inkinen, R., Jortikka, M., Tammi, M., Virtanen, I. and Helminen, H. J. (1995). Influence of short-term hydrostatic pressure on organization of stress fibers in cultured chondrocytes. J Orthop Res 13(4): 495-502.

Parnell, S. C., Magenheimer, B. S., Maser, R. L., Rankin, C. A., Smine, A., Okamoto, T. and Calvet, J. P. (1998). The polycystic kidney disease-1 protein, polycystin-1, binds and activates heterotrimeric G-proteins in vitro. Biochem Biophys Res Commun 251(2): 625-631.

Pawley, J., Ed. (2006). Handbook of Biological Confocal Microscopy, Springer Link.

Pazour, G. J., Dickert, B. L., Vucica, Y., Seeley, E. S., Rosenbaum, J. L., Witman, G. B. and Cole, D. G. (2000). Chlamydomonas IFT88 and its mouse homologue, polycystic kidney disease gene tg737, are required for assembly of cilia and flagella. J Cell Biol 151(3): 709-718.

Pazour, G. J., Dickert, B. L. and Witman, G. B. (1999). The DHC1b (DHC2) isoform of cytoplasmic dynein is required for flagellar assembly. J Cell Biol 144(3): 473-481.

Pazour, G. J., Wilkerson, C. G. and Witman, G. B. (1998). A dynein light chain is essential for the retrograde particle movement of intraflagellar transport (IFT). J Cell Biol 141(4): 979-992.

Pazour, G. J. and Witman, G. B. (2003). The vertebrate primary cilium is a sensory organelle. Curr Opin Cell Biol 15(1): 105-110.

Pearle, A. D., Warren, R. F. and Rodeo, S. A. (2005). Basic science of articular cartilage and osteoarthritis. Clin Sports Med 24(1): 1-12.

Pedersen, L. B. and Rosenbaum, J. L. (2008). Intraflagellar transport (IFT) role in ciliary assembly, resorption and signalling. Curr Top Dev Biol 85: 23-61.

Phan, M. N., Leddy, H. A., Votta, B. J., Kumar, S., Levy, D. S., Lipshutz, D. B., Lee, S. H., Liedtke, W. and Guilak, F. (2009). Functional characterization of TRPV4 as an osmotically sensitive ion channel in porcine articular chondrocytes. Arthritis Rheum 60(10): 3028-3037.

Pingguan-Murphy, B., El-Azzeh, M., Bader, D. L. and Knight, M. M. (2006). Cyclic compression of chondrocytes modulates a purinergic calcium signalling pathway in a strain rate- and frequency-dependent manner. J Cell Physiol 209(2): 389-397.

Pingguan-Murphy, B. and Knight, M. (2008). Mechanosensitive Purinergic Calcium Signalling in Articular Chondrocytes. Mechanosensitive Ion Channels. A. Kamkin and I. Kiseleva, Springer. **1:** 235-251.

Pingguan-Murphy, B., Lee, D. A., Bader, D. L. and Knight, M. M. (2005). Activation of chondrocytes calcium signalling by dynamic compression is independent of number of cycles. Arch Biochem Biophys 444(1): 45-51.

Piotrowska-Nitsche, K. and Caspary, T. (2012). Live imaging of individual cell divisions in mouse neuroepithelium shows asymmetry in cilium formation and Sonic hedgehog response. Cilia 1: 6.

Piperno, G., LeDizet, M. and Chang, X. J. (1987). Microtubules containing acetylated alpha-tubulin in mammalian cells in culture. J Cell Biol 104(2): 289-302.

Piperno, G., Siuda, E., Henderson, S., Segil, M., Vaananen, H. and Sassaroli, M. (1998). Distinct mutants of retrograde intraflagellar transport (IFT) share similar morphological and molecular defects. J Cell Biol 143(6): 1591-1601.

Pirkkala, L., Nykanen, P. and Sistonen, L. (2001). Roles of the heat shock transcription factors in regulation of the heat shock response and beyond. FASEB J 15(7): 1118-1131.

Pitaval, A., Tseng, Q., Bornens, M. and Thery, M. (2010). Cell shape and contractility regulate ciliogenesis in cell cycle-arrested cells. J Cell Biol 191(2): 303-312.

Plotnikova, O. V., Nikonova, A. S., Loskutov, Y. V., Kozyulina, P. Y., Pugacheva, E. N. and Golemis, E. A. (2012). Calmodulin activation of Aurora-A kinase (AURKA) is required during ciliary disassembly and in mitosis. Mol Biol Cell 23(14): 2658-2670.

Plotnikova, O. V., Pugacheva, E. N., Dunbrack, R. L. and Golemis, E. A. (2010). Rapid calcium-dependent activation of Aurora-A kinase. Nat Commun 1: 64.

Plotnikova, O. V., Pugacheva, E. N. and Golemis, E. A. (2011). Aurora A kinase activity influences calcium signaling in kidney cells. J Cell Biol 193(6): 1021-1032.

Polte, T. R., Eichler, G. S., Wang, N. and Ingber, D. E. (2004). Extracellular matrix controls myosin light chain phosphorylation and cell contractility through modulation of cell shape and cytoskeletal prestress. American Journal of Physiology-Cell Physiology 286(3): C518-C528.

Poole, C. A. (1997). Articular cartilage chondrons: form, function and failure. J Anat 191 ( Pt 1): 1-13.

Poole, C. A., Ayad, S. and Schofield, J. R. (1988). Chondrons from articular cartilage: I. Immunolocalization of type VI collagen in the pericellular capsule of isolated canine tibial chondrons. J Cell Sci 90 ( Pt 4): 635-643.

Poole, C. A., Flint, M. H. and Beaumont, B. W. (1984). Morphological and functional interrelationships of articular cartilage matrices. J Anat 138 ( Pt 1): 113-138.

Poole, C. A., Flint, M. H. and Beaumont, B. W. (1985). Analysis of the morphology and function of primary cilia in connective tissues: a cellular cybernetic probe? Cell Motil 5(3): 175-193.

Poole, C. A., Jensen, C. G., Snyder, J. A., Gray, C. G., Hermanutz, V. L. and Wheatley, D. N. (1997). Confocal analysis of primary cilia structure and colocalization with the Golgi apparatus in chondrocytes and aortic smooth muscle cells. Cell Biol Int 21(8): 483-494.

Poole, C. A., Zhang, Z. J. and Ross, J. M. (2001). The differential distribution of acetylated and detyrosinated alpha-tubulin in the microtubular cytoskeleton and primary cilia of hyaline cartilage chondrocytes. J Anat 199(Pt 4): 393-405.

Porter, J. A., Ekker, S. C., Park, W. J., von Kessler, D. P., Young, K. E., Chen, C. H., Ma, Y., Woods, A. S., Cotter, R. J., Koonin, E. V. and Beachy, P. A. (1996). Hedgehog patterning activity: role of a lipophilic modification mediated by the carboxy-terminal autoprocessing domain. Cell 86(1): 21-34.

Praetorius, H. A., Frokiaer, J., Nielsen, S. and Spring, K. R. (2003). Bending the primary cilium opens Ca2+-sensitive intermediate-conductance K+ channels in MDCK cells. J Membr Biol 191(3): 193-200.

Praetorius, H. A. and Spring, K. R. (2001). Bending the MDCK cell primary cilium increases intracellular calcium. J Membr Biol 184(1): 71-79.

Praetorius, H. A. and Spring, K. R. (2003). The renal cell primary cilium functions as a flow sensor. Curr Opin Nephrol Hypertens 12(5): 517-520.

Pugacheva, E. N. and Golemis, E. A. (2006). HEF1-aurora A interactions: points of dialog between the cell cycle and cell attachment signaling networks. Cell Cycle 5(4): 384-391.

Pugacheva, E. N., Jablonski, S. A., Hartman, T. R., Henske, E. P. and Golemis, E. A. (2007). HEF1-Dependent aurora a activation induces disassembly of the primary cilium. Cell 129(7): 1351-1363.

Qin, H., Diener, D. R., Geimer, S., Cole, D. G. and Rosenbaum, J. L. (2004). Intraflagellar transport (IFT) cargo: IFT transports flagellar precursors to the tip and turnover products to the cell body. J Cell Biol 164(2): 255-266.

Quarmby, L. M. and Hartzell, H. C. (1994). Two distinct, calcium-mediated, signal transduction pathways can trigger deflagellation in Chlamydomonas reinhardtii. J Cell Biol 124(5): 807-815.

Rabie, A. B. and Al-Kalaly, A. (2008). Does the degree of advancement during functional appliance therapy matter? Eur J Orthod 30(3): 274-282.

Ragan, P. M., Badger, A. M., Cook, M., Chin, V. I., Gowen, M., Grodzinsky, A. J. and Lark, M. W. (1999). Down-regulation of chondrocyte aggrecan and type-II collagen gene expression correlates with increases in static compression magnitude and duration. J Orthop Res 17(6): 836-842.

Ramage, L., Nuki, G. and Salter, D. M. (2009). Signalling cascades in mechanotransduction: cell-matrix interactions and mechanical loading. Scand J Med Sci Sports 19(4): 457-469.

Razzaque, M. S., Soegiarto, D. W., Chang, D., Long, F. and Lanske, B. (2005). Conditional deletion of Indian hedgehog from collagen type 2alpha1-expressing cells results in abnormal endochondral bone formation. J Pathol 207(4): 453-461.

Reed, N. A., Cai, D., Blasius, T. L., Jih, G. T., Meyhofer, E., Gaertig, J. and Verhey, K. J. (2006). Microtubule acetylation promotes kinesin-1 binding and transport. Curr Biol 16(21): 2166-2172.

Reilly, G. C., Haut, T. R., Yellowley, C. E., Donahue, H. J. and Jacobs, C. R. (2003). Fluid flow induced PGE(2) release by bone cells is reduced by glycocalyx degradation whereas calcium signals are not. Biorheology 40(6): 591-603.

Reiter, J. F., Blacque, O. E. and Leroux, M. R. (2012). The base of the cilium: roles for transition fibres and the transition zone in ciliary formation, maintenance and compartmentalization. EMBO Rep 13(7): 608-618.

Resnick, A. and Hopfer, U. (2007). Force-response considerations in ciliary mechanosensation. Biophys J 93(4): 1380-1390.

Resnick, A. and Hopfer, U. (2008). Mechanical stimulation of primary cilia. Front Biosci 13: 1665-1680.

Rich, D. R. and Clark, A. L. (2012). Chondrocyte primary cilia shorten in response to osmotic challenge and are sites for endocytosis. Osteoarthritis Cartilage 20(8): 923-930.

Rieder, C. L., Jensen, C. G. and Jensen, L. C. (1979). The resorption of primary cilia during mitosis in a vertebrate (PtK1) cell line. J Ultrastruct Res 68(2): 173-185.

Ringo, D. L. (1967). Flagellar motion and fine structure of the flagellar apparatus in Chlamydomonas. J Cell Biol 33(3): 543-571.

Roberts, S. R., Knight, M. M., Lee, D. A. and Bader, D. L. (2001). Mechanical compression influences intracellular Ca2+ signaling in chondrocytes seeded in agarose constructs. J Appl Physiol 90(4): 1385-1391.

Rochlin, M. W., Wickline, K. M. and Bridgman, P. C. (1996). Microtubule stability decreases axon elongation but not axoplasm production. J Neurosci 16(10): 3236-3246.

Rohatgi, R., Milenkovic, L. and Scott, M. P. (2007). Patched1 regulates hedgehog signaling at the primary cilium. Science 317(5836): 372-376.

Rohatgi, R. and Snell, W. J. (2010). The ciliary membrane. Curr Opin Cell Biol 22(4): 541-546.

Rondanino, C., Poland, P. A., Kinlough, C. L., Li, H., Rbaibi, Y., Myerburg, M. M., Al-bataineh, M. M., Kashlan, O. B., Pastor-Soler, N. M., Hallows, K. R., Weisz, O. A., Apodaca, G. and Hughey, R. P.

(2011). Galectin-7 modulates the length of the primary cilia and wound repair in polarized kidney epithelial cells. Am J Physiol Renal Physiol 301(3): F622-633.

Rosenbaum, J. L. and Witman, G. B. (2002). Intraflagellar transport. Nat Rev Mol Cell Biol 3(11): 813-825.

Rosenzweig, D. H., Matmati, M., Khayat, G., Chaudhry, S., Hinz, B. and Quinn, T. M. (2012). Culture of Primary Bovine Chondrocytes on a Continuously Expanding Surface Inhibits Dedifferentiation. Tissue Engineering Part A 18(23-24): 2466-2476.

Ross, A. J., May-Simera, H., Eichers, E. R., Kai, M., Hill, J., Jagger, D. J., Leitch, C. C., Chapple, J. P., Munro, P. M., Fisher, S., Tan, P. L., Phillips, H. M., Leroux, M. R., Henderson, D. J., Murdoch, J. N., Copp, A. J., Eliot, M. M., Lupski, J. R., Kemp, D. T., Dollfus, H., Tada, M., Katsanis, N., Forge, A. and Beales, P. L. (2005). Disruption of Bardet-Biedl syndrome ciliary proteins perturbs planar cell polarity in vertebrates. Nat Genet 37(10): 1135-1140.

Ruiz-Heiland, G., Horn, A., Zerr, P., Hofstetter, W., Baum, W., Stock, M., Distler, J. H., Nimmerjahn, F., Schett, G. and Zwerina, J. (2012). Blockade of the hedgehog pathway inhibits osteophyte formation in arthritis. Ann Rheum Dis 71(3): 400-407.

Ryan, K. E. and Chiang, C. (2012). Hedgehog secretion and signal transduction in vertebrates. J Biol Chem 287(22): 17905-17913.

Saamanen, A. M., Tammi, M., Jurvelin, J., Kiviranta, I. and Helminen, H. J. (1990). Proteoglycan alterations following immobilization and remobilization in the articular cartilage of young canine knee (stifle) joint. J Orthop Res 8(6): 863-873.

Saggese, T., Young, A. A., Huang, C., Braeckmans, K. and McGlashan, S. R. (2012). Development of a method for the measurement of primary cilia length in 3D. Cilia 1(1): 11-11.

Sah, R. L. Y., Grodzinsky, A. J., Plaas, A. H. K. and Sandy, J. D. (1992). Effects of Static and Dynamic Compression on Matrix Metabolism in Cartilage Explants. Articular Cartilage and Osteoarthritis: 373-392.

Saito, T., Nishida, K., Furumatsu, T., Yoshida, A., Ozawa, M. and Ozaki, T. (2013). Histone deacetylase inhibitors suppress mechanical stress-induced expression of RUNX-2 and ADAMTS-5 through the inhibition of the MAPK signaling pathway in cultured human chondrocytes. Osteoarthritis Cartilage 21(1): 165-174.

Salminen, A., Ojala, J., Kaarniranta, K., Hiltunen, M. and Soininen, H. (2011). Hsp90 regulates tau pathology through co-chaperone complexes in Alzheimer's disease. Prog Neurobiol 93(1): 99-110.

Sasaki, H., Nishizaki, Y., Hui, C., Nakafuku, M. and Kondoh, H. (1999). Regulation of Gli2 and Gli3 activities by an amino-terminal repression domain: implication of Gli2 and Gli3 as primary mediators of Shh signaling. Development 126(17): 3915-3924.

Schaller, M. D., Otey, C. A., Hildebrand, J. D. and Parsons, J. T. (1995). Focal adhesion kinase and paxillin bind to peptides mimicking beta integrin cytoplasmic domains. J Cell Biol 130(5): 1181-1187.

Schmal, H., Mehlhorn, A. T., Fehrenbach, M., Muller, C. A., Finkenzeller, G. and Sudkamp, N. P. (2006). Regulative mechanisms of chondrocyte adhesion. Tissue Engineering 12(4): 741-750.

Schneider, L., Cammer, M., Lehman, J., Nielsen, S. K., Guerra, C. F., Veland, I. R., Stock, C., Hoffmann, E. K., Yoder, B. K., Schwab, A., Satir, P. and Christensen, S. T. (2010). Directional cell migration and chemotaxis in wound healing response to PDGF-AA are coordinated by the primary cilium in fibroblasts. Cell Physiol Biochem 25(2-3): 279-292.

Schneider, L., Clement, C. A., Teilmann, S. C., Pazour, G. J., Hoffmann, E. K., Satir, P. and Christensen, S. T. (2005). PDGFR alpha alpha signaling is regulated through the primary cilium in fibroblasts. Current Biology 15(20): 1861-1866.

Schulze-Tanzil, G., de Souza, P., Castrejon, H. V., John, T., Merker, H. J., Scheid, A. and Shakibaei, M. (2002). Redifferentiation of dedifferentiated human chondrocytes in high-density cultures. Cell and Tissue Research 308(3): 371-379.

Schumacher, M. A., Donnelly, J. M., Engevik, A. C., Xiao, C., Yang, L., Kenny, S., Varro, A., Hollande, F., Samuelson, L. C. and Zavros, Y. (2012). Gastric Sonic Hedgehog acts as a macrophage chemoattractant during the immune response to Helicobacter pylori. Gastroenterology 142(5): 1150-1159 e1156.

Schwartz, E. A., Leonard, M. L., Bizios, R. and Bowser, S. S. (1997). Analysis and modeling of the primary cilium bending response to fluid shear. Am J Physiol 272(1 Pt 2): F132-138.

Seeley, E. S. and Nachury, M. V. (2010). The perennial organelle: assembly and disassembly of the primary cilium. J Cell Sci 123(Pt 4): 511-518.

Serrat, M. A., King, D. and Lovejoy, C. O. (2008). Temperature regulates limb length in homeotherms by directly modulating cartilage growth. Proc Natl Acad Sci U S A 105(49): 19348-19353.

Shao, Y. Y., Wang, L., Welter, J. F. and Ballock, R. T. (2011). Primary cilia modulate Ihh signal transduction in response to hydrostatic loading of growth plate chondrocytes. Bone 50(1): 79-84.

Sharma, N., Kosan, Z. A., Stallworth, J. E., Berbari, N. F. and Yoder, B. K. (2011). Soluble levels of cytosolic tubulin regulate ciliary length control. Mol Biol Cell 22(6): 806-816.

Shida, T., Cueva, J. G., Xu, Z., Goodman, M. B. and Nachury, M. V. (2010). The major alpha-tubulin K40 acetyltransferase alphaTAT1 promotes rapid ciliogenesis and efficient mechanosensation. Proc Natl Acad Sci U S A 107(50): 21517-21522.

Shyy, J. Y. and Chien, S. (1997). Role of integrins in cellular responses to mechanical stress and adhesion. Curr Opin Cell Biol 9(5): 707-713.

Signor, D., Wedaman, K. P., Orozco, J. T., Dwyer, N. D., Bargmann, C. I., Rose, L. S. and Scholey, J. M. (1999). Role of a class DHC1b dynein in retrograde transport of IFT motors and IFT raft particles along cilia, but not dendrites, in chemosensory neurons of living Caenorhabditis elegans. J Cell Biol 147(3): 519-530.

Simons, K. and Toomre, D. (2000). Lipid rafts and signal transduction. Nat Rev Mol Cell Biol 1(1): 31-39.

Simons, M., Gloy, J., Ganner, A., Bullerkotte, A., Bashkurov, M., Kronig, C., Schermer, B., Benzing, T., Cabello, O. A., Jenny, A., Mlodzik, M., Polok, B., Driever, W., Obara, T. and Walz, G. (2005). Inversin, the gene product mutated in nephronophthisis type II, functions as a molecular switch between Wnt signaling pathways. Nat Genet 37(5): 537-543.

Skerritt, P. W. (1987). Psoriatic arthritis during lithium therapy. Aust N Z J Psychiatry 21(4): 601-604.

Song, B., Haycraft, C. J., Seo, H. S., Yoder, B. K. and Serra, R. (2007). Development of the post-natal growth plate requires intraflagellar transport proteins. Dev Biol 305(1): 202-216.

Sorokin, S. (1962). Centrioles and the formation of rudimentary cilia by fibroblasts and smooth muscle cells. J Cell Biol 15: 363-377.

St-Jacques, B., Hammerschmidt, M. and McMahon, A. P. (1999). Indian hedgehog signaling regulates proliferation and differentiation of chondrocytes and is essential for bone formation. Genes Dev 13(16): 2072-2086.

Steigelman, K. A., Lelli, A., Wu, X., Gao, J., Lin, S., Piontek, K., Wodarczyk, C., Boletta, A., Kim, H., Qian, F., Germino, G., Geleoc, G. S., Holt, J. R. and Zuo, J. (2011). Polycystin-1 is required for stereocilia structure but not for mechanotransduction in inner ear hair cells. J Neurosci 31(34): 12241-12250.

Steinmeyer, J. and Knue, S. (1997). The proteoglycan metabolism of mature bovine articular cartilage explants superimposed to continuously applied cyclic mechanical loading. Biochem Biophys Res Commun 240(1): 216-221.

Stone, D. M., Hynes, M., Armanini, M., Swanson, T. A., Gu, Q., Johnson, R. L., Scott, M. P., Pennica, D., Goddard, A., Phillips, H., Noll, M., Hooper, J. E., de Sauvage, F. and Rosenthal, A. (1996). The tumour-suppressor gene patched encodes a candidate receptor for Sonic hedgehog. Nature 384(6605): 129-134.

Stout, C. E., Costantin, J. L., Naus, C. C. G. and Charles, A. C. (2002). Intercellular calcium signaling in astrocytes via ATP release through connexin hemichannels. Journal of Biological Chemistry 277(12): 10482-10488.

Sun, H. B. (2010). Mechanical loading, cartilage degradation, and arthritis. Ann N Y Acad Sci 1211: 37-50.

Taipale, J., Chen, J. K., Cooper, M. K., Wang, B., Mann, R. K., Milenkovic, L., Scott, M. P. and Beachy, P. A. (2000). Effects of oncogenic mutations in Smoothened and Patched can be reversed by cyclopamine. Nature 406(6799): 1005-1009.

Takaki, E., Fujimoto, M., Nakahari, T., Yonemura, S., Miyata, Y., Hayashida, N., Yamamoto, K., Vallee, R. B., Mikuriya, T., Sugahara, K., Yamashita, H., Inouye, S. and Nakai, A. (2007). Heat shock transcription factor 1 is required for maintenance of ciliary beating in mice. J Biol Chem 282(51): 37285-37292.

Tanaka, N., Ohno, S., Honda, K., Tanimoto, K., Doi, T., Ohno-Nakahara, M., Tafolla, E., Kapila, S. and Tanne, K. (2005). Cyclic mechanical strain regulates the PTHrP expression in cultured chondrocytes via activation of the Ca2+ channel. J Dent Res 84(1): 64-68.

Tchetina, E. V., Squires, G. and Poole, A. R. (2005). Increased type II collagen degradation and very early focal cartilage degeneration is associated with upregulation of chondrocyte differentiation related genes in early human articular cartilage lesions. J Rheumatol 32(5): 876-886.

Teilmann, S. C., Byskov, A. G., Pedersen, P. A., Wheatley, D. N., Pazour, G. J. and Christensen, S. T. (2005). Localization of transient receptor potential ion channels in primary and motile cilia of the female murine reproductive organs. Mol Reprod Dev 71(4): 444-452.

Teilmann, S. C. and Christensen, S. T. (2005). Localization of the angiopoietin receptors Tie-1 and Tie-2 on the primary cilia in the female reproductive organs. Cell Biol Int 29(5): 340-346.

Tetsunaga, T., Nishida, K., Furumatsu, T., Naruse, K., Hirohata, S., Yoshida, A., Saito, T. and Ozaki, T. (2011). Regulation of mechanical stress-induced MMP-13 and ADAMTS-5 expression by RUNX-2 transcriptional factor in SW1353 chondrocyte-like cells. Osteoarthritis Cartilage 19(2): 222-232.

Thiel, C., Kessler, K., Giessl, A., Dimmler, A., Shalev, S. A., von der Haar, S., Zenker, M., Zahnleiter, D., Stoss, H., Beinder, E., Abou Jamra, R., Ekici, A. B., Schroder-Kress, N., Aigner, T., Kirchner, T., Reis, A., Brandstatter, J. H. and Rauch, A. (2011). NEK1 mutations cause short-rib polydactyly syndrome type majewski. Am J Hum Genet 88(1): 106-114.

Thomas, R. S., Clarke, A. R., Duance, V. C. and Blain, E. J. (2011). Effects of Wnt3A and mechanical load on cartilage chondrocyte homeostasis. Arthritis Res Ther 13(6): R203.

Tickle, C. (2006). Making digit patterns in the vertebrate limb. Nat Rev Mol Cell Biol 7(1): 45-53.

Tobin, J. L. and Beales, P. L. (2009). The nonmotile ciliopathies. Genet Med 11(6): 386-402.

Torzilli, P. A., Deng, X. H. and Ramcharan, M. (2006). Effect of compressive strain on cell viability in statically loaded articular cartilage. Biomech Model Mechanobiol 5(2-3): 123-132.

Torzilli, P. A., Grigiene, R., Huang, C., Friedman, S. M., Doty, S. B., Boskey, A. L. and Lust, G. (1997). Characterization of cartilage metabolic response to static and dynamic stress using a mechanical explant test system. J Biomech 30(1): 1-9.

Traiffort, E., Dubourg, C., Faure, H., Rognan, D., Odent, S., Durou, M. R., David, V. and Ruat, M. (2004). Functional characterization of sonic hedgehog mutations associated with holoprosencephaly. J Biol Chem 279(41): 42889-42897.

Tran, P. V., Haycraft, C. J., Besschetnova, T. Y., Turbe-Doan, A., Stottmann, R. W., Herron, B. J., Chesebro, A. L., Qiu, H., Scherz, P. J., Shah, J. V., Yoder, B. K. and Beier, D. R. (2008). THM1 negatively modulates mouse sonic hedgehog signal transduction and affects retrograde intraflagellar transport in cilia. Nat Genet 40(4): 403-410.

Trickey, W. R., Vail, T. P. and Guilak, F. (2004). The role of the cytoskeleton in the viscoelastic properties of human articular chondrocytes. Journal of Orthopaedic Research 22(1): 131-139.

Tucker, R. W., Pardee, A. B. and Fujiwara, K. (1979). Centriole ciliation is related to quiescence and DNA synthesis in 3T3 cells. Cell 17(3): 527-535.

Tukachinsky, H., Kuzmickas, R. P., Jao, C. Y., Liu, J. and Salic, A. (2012). Dispatched and scube mediate the efficient secretion of the cholesterol-modified hedgehog ligand. Cell Rep 2(2): 308-320.

Tuson, M., He, M. and Anderson, K. V. (2011). Protein kinase A acts at the basal body of the primary cilium to prevent Gli2 activation and ventralization of the mouse neural tube. Development 138(22): 4921-4930.

Urban, J. P. (1994). The chondrocyte: a cell under pressure. Br J Rheumatol 33(10): 901-908.

Vande Geest, J. P., Di Martino, E. S. and Vorp, D. A. (2004). An analysis of the complete strain field within Flexercell membranes. J Biomech 37(12): 1923-1928.

Varjosalo, M. and Taipale, J. (2008). Hedgehog: functions and mechanisms. Genes Dev 22(18): 2454-2472.

Velleman, S. G. (2000). The role of the extracellular matrix in skeletal development. Poult Sci 79(7): 985-989.

Verghese, E., Ricardo, S. D., Weidenfeld, R., Zhuang, J., Hill, P. A., Langham, R. G. and Deane, J. A. (2009). Renal primary cilia lengthen after acute tubular necrosis. J Am Soc Nephrol 20(10): 2147-2153.

Verghese, E., Zhuang, J., Saiti, D., Ricardo, S. D. and Deane, J. A. (2011). In vitro investigation of renal epithelial injury suggests that primary cilium length is regulated by hypoxia-inducible mechanisms. Cell Biol Int 35(9): 909-913.

Verhey, K. J. and Gaertig, J. (2007). The tubulin code. Cell Cycle 6(17): 2152-2160.

Vortkamp, A., Lee, K., Lanske, B., Segre, G. V., Kronenberg, H. M. and Tabin, C. J. (1996). Regulation of rate of cartilage differentiation by Indian hedgehog and PTH-related protein. Science 273(5275): 613-622.

Vortkamp, A., Pathi, S., Peretti, G. M., Caruso, E. M., Zaleske, D. J. and Tabin, C. J. (1998). Recapitulation of signals regulating embryonic bone formation during postnatal growth and in fracture repair. Mech Dev 71(1-2): 65-76.

Wan, Q., Kim, S. J., Yokota, H. and Na, S. (2013). Differential Activation and Inhibition of RhoA by Fluid Flow Induced Shear Stress in Chondrocytes. Cell Biol Int.

Wang, B., Fallon, J. F. and Beachy, P. A. (2000). Hedgehog-regulated processing of Gli3 produces an anterior/posterior repressor gradient in the developing vertebrate limb. Cell 100(4): 423-434.

Wann, A. K. and Knight, M. M. (2012). Primary cilia elongation in response to interleukin-1 mediates the inflammatory response. Cell Mol Life Sci 69(17): 2967-2977.

Wann, A. K., Mistry, J., Blain, E. J., Michael-Titus, A. T. and Knight, M. M. (2010). Eicosapentaenoic acid and docosahexaenoic acid reduce interleukin-1beta-mediated cartilage degradation. Arthritis Res Ther 12(6): R207.

Wann, A. K., Zuo, N., Haycraft, C. J., Jensen, C. G., Poole, C. A., McGlashan, S. R. and Knight, M. M. (2012). Primary cilia mediate mechanotransduction through control of ATP-induced Ca2+ signaling in compressed chondrocytes. FASEB J 26(4): 1663-1671.

Waters, A. M. and Beales, P. L. (2011). Ciliopathies: an expanding disease spectrum. Pediatr Nephrol 26(7): 1039-1056.

Wei, F., Zhou, J., Wei, X., Zhang, J., Fleming, B. C., Terek, R., Pei, M., Chen, Q., Liu, T. and Wei, L. (2012). Activation of Indian Hedgehog Promotes Chondrocyte Hypertrophy and Upregulation of MMP-13 in Human Osteoarthritic Cartilage. Osteoarthritis Cartilage 20(7): 755-763.

Weightman, B. (1976). Tensile Fatigue of Human Articular-Cartilage. Journal of Biomechanics 9(4): 193-200.

Weimbs, T. (2007). Polycystic kidney disease and renal injury repair: common pathways, fluid flow, and the function of polycystin-1. Am J Physiol Renal Physiol 293(5): F1423-1432.
Weir, E. C., Philbrick, W. M., Amling, M., Neff, L. A., Baron, R. and Broadus, A. E. (1996). Targeted overexpression of parathyroid hormone-related peptide in chondrocytes causes chondrodysplasia and delayed endochondral bone formation. Proc Natl Acad Sci U S A 93(19): 10240-10245.
Weis, F., Moullintraffort, L., Heichette, C., Chretien, D. and Garnier, C. (2010). The 90-kDa heat shock protein Hsp90 protects tubulin against thermal denaturation. J Biol Chem 285(13): 9525-9534.
Wen, X., Lai, C. K., Evangelista, M., Hongo, J. A., de Sauvage, F. J. and Scales, S. J. (2010). Kinetics of hedgehog-dependent full-length Gli3 accumulation in primary cilia and subsequent degradation. Mol Cell Biol 30(8): 1910-1922.
Westendorf, J. J., Zaidi, S. K., Cascino, J. E., Kahler, R., van Wijnen, A. J., Lian, J. B., Yoshida, M., Stein, G. S. and Li, X. (2002). Runx2 (Cbfa1, AML-3) interacts with histone deacetylase 6 and represses the p21(CIP1/WAF1) promoter. Mol Cell Biol 22(22): 7982-7992.
Wheatley, D. N., Feilen, E. M., Yin, Z. and Wheatley, S. P. (1994). Primary cilia in cultured mammalian cells: detection with an antibody against detyrosinated alpha-tubulin (ID5) and by electron microscopy. J Submicrosc Cytol Pathol 26(1): 91-102.
Wheatley, D. N., Wang, A. M. and Strugnell, G. E. (1996). Expression of primary cilia in mammalian cells. Cell Biol Int 20(1): 73-81.
Wiesner, S., Legate, K. R. and Fassler, R. (2005). Integrin-actin interactions. Cell Mol Life Sci 62(10): 1081-1099.
Williams, C. L., Li, C., Kida, K., Inglis, P. N., Mohan, S., Semenec, L., Bialas, N. J., Stupay, R. M., Chen, N., Blacque, O. E., Yoder, B. K. and Leroux, M. R. (2011). MKS and NPHP modules cooperate to establish basal body/transition zone membrane associations and ciliary gate function during ciliogenesis. J Cell Biol 192(6): 1023-1041.
Williams, N. E. and Nelsen, E. M. (1997). HSP70 and HSP90 homologs are associated with tubulin in hetero-oligomeric complexes, cilia and the cortex of Tetrahymena. J Cell Sci 110 ( Pt 14): 1665-1672.
Williams, R., Khan, I. M., Richardson, K., Nelson, L., McCarthy, H. E., Analbelsi, T., Singhrao, S. K., Dowthwaite, G. P., Jones, R. E., Baird, D. M., Lewis, H., Roberts, S., Shaw, H. M., Dudhia, J., Fairclough, J., Briggs, T. and Archer, C. W. (2010). Identification and clonal characterisation of a progenitor cell sub-population in normal human articular cartilage. PLoS One 5(10): e13246.
Wilsman, N. J. (1978). Cilia of adult canine articular chondrocytes. J Ultrastruct Res 64(3): 270-281.
Wilson, C. W., Chen, M. H. and Chuang, P. T. (2009). Smoothened adopts multiple active and inactive conformations capable of trafficking to the primary cilium. PLoS One 4(4): e5182.
Wislman, N. J. and Fletcher, T. F. (1978). Cilia of neonatal articular chondrocytes: incidence and morphology. Anat Rec 190(4): 871-889.
Wong, M., Wuethrich, P., Buschmann, M. D., Eggli, P. and Hunziker, E. (1997). Chondrocyte biosynthesis correlates with local tissue strain in statically compressed adult articular cartilage. J Orthop Res 15(2): 189-196.
Wong, M., Wuethrich, P., Eggli, P. and Hunziker, E. (1996). Zone-specific cell biosynthetic activity in mature bovine articular cartilage: a new method using confocal microscopic stereology and quantitative autoradiography. J Orthop Res 14(3): 424-432.
Woolley, D. E. and Evanson, J. M. (1977). Collagenase and its natural inhibitors in relation to the rheumatoid joint. Connect Tissue Res 5(1): 31-35.
Wright, M., Jobanputra, P., Bavington, C., Salter, D. M. and Nuki, G. (1996). Effects of intermittent pressure-induced strain on the electrophysiology of cultured human chondrocytes: evidence for the presence of stretch-activated membrane ion channels. Clin Sci (Lond) 90(1): 61-71.

Wright, M. O., Nishida, K., Bavington, C., Godolphin, J. L., Dunne, E., Walmsley, S., Jobanputra, P., Nuki, G. and Salter, D. M. (1997). Hyperpolarisation of cultured human chondrocytes following cyclical pressure-induced strain: evidence of a role for alpha 5 beta 1 integrin as a chondrocyte mechanoreceptor. J Orthop Res 15(5): 742-747.

Wu, Q., Zhang, Y. and Chen, Q. (2001). Indian hedgehog is an essential component of mechanotransduction complex to stimulate chondrocyte proliferation. J Biol Chem 276(38): 35290-35296.

Wu, W., Billinghurst, R. C., Pidoux, I., Antoniou, J., Zukor, D., Tanzer, M. and Poole, A. R. (2002). Sites of collagenase cleavage and denaturation of type II collagen in aging and osteoarthritic articular cartilage and their relationship to the distribution of matrix metalloproteinase 1 and matrix metalloproteinase 13. Arthritis Rheum 46(8): 2087-2094.

Wuelling, M. and Vortkamp, A. (2010). Transcriptional networks controlling chondrocyte proliferation and differentiation during endochondral ossification. Pediatr Nephrol 25(4): 625-631.

Xiao, Z., Zhang, S., Mahlios, J., Zhou, G., Magenheimer, B. S., Guo, D., Dallas, S. L., Maser, R., Calvet, J. P., Bonewald, L. and Quarles, L. D. (2006). Cilia-like structures and polycystin-1 in osteoblasts/osteocytes and associated abnormalities in skeletogenesis and Runx2 expression. J Biol Chem 281(41): 30884-30895.

Yang, C., Chen, W., Chen, Y. and Jiang, J. (2012). Smoothened transduces Hedgehog signal by forming a complex with Evc/Evc2. Cell Res.

Yang, J., Liu, X., Yue, G., Adamian, M., Bulgakov, O. and Li, T. (2002). Rootletin, a novel coiled-coil protein, is a structural component of the ciliary rootlet. J Cell Biol 159(3): 431-440.

Yellowley, C. E., Jacobs, C. R., Li, Z., Zhou, Z. and Donahue, H. J. (1997). Effects of fluid flow on intracellular calcium in bovine articular chondrocytes. Am J Physiol 273(1 Pt 1): C30-36.

Yoder, B. K., Richards, W. G., Sommardahl, C., Sweeney, W. E., Michaud, E. J., Wilkinson, J. E., Avner, E. D. and Woychik, R. P. (1997). Differential rescue of the renal and hepatic disease in an autosomal recessive polycystic kidney disease mouse mutant. A new model to study the liver lesion. Am J Pathol 150(6): 2231-2241.

Yoder, B. K., Tousson, A., Millican, L., Wu, J. H., Bugg, C. E., Jr., Schafer, J. A. and Balkovetz, D. F. (2002). Polaris, a protein disrupted in orpk mutant mice, is required for assembly of renal cilium. Am J Physiol Renal Physiol 282(3): F541-552.

You, J., Reilly, G. C., Zhen, X. C., Yellowley, C. E., Chen, Q., Donahue, H. J. and Jacobs, C. R. (2001). Osteopontin gene regulation by oscillatory fluid flow via intracellular calcium mobilization and activation of mitogen-activated protein kinase in MC3T3-E1 osteoblasts. Journal of Biological Chemistry 276(16): 13365-13371.

Youn, I., Choi, J. B., Cao, L., Setton, L. A. and Guilak, F. (2006). Zonal variations in the three-dimensional morphology of the chondron measured in situ using confocal microscopy. Osteoarthritis Cartilage 14(9): 889-897.

Zhang, Q., Murcia, N. S., Chittenden, L. R., Richards, W. G., Michaud, E. J., Woychik, R. P. and Yoder, B. K. (2003). Loss of the Tg737 protein results in skeletal patterning defects. Dev Dyn 227(1): 78-90.

Zhang, X., Yuan, Z., Zhang, Y., Yong, S., Salas-Burgos, A., Koomen, J., Olashaw, N., Parsons, J. T., Yang, X. J., Dent, S. R., Yao, T. P., Lane, W. S. and Seto, E. (2007). HDAC6 modulates cell motility by altering the acetylation level of cortactin. Mol Cell 27(2): 197-213.

Zhou, X. Y., Liu, Z. Q., Jang, F., Xiang, C. N., Li, Y. and He, Y. Z. (2012). Autocrine Sonic Hedgehog Attenuates Inflammation in Cerulein-Induced Acute Pancreatitis in Mice via Upregulation of IL-10. PLoS One 7(8).

Zhu, D., Shi, S., Wang, H. and Liao, K. (2009). Growth arrest induces primary-cilium formation and sensitizes IGF-1-receptor signaling during differentiation induction of 3T3-L1 preadipocytes. J Cell Sci 122(Pt 15): 2760-2768.

# List of publications arising from this thesis

## Journal papers

- N.V. Prodromou*, C.L. Thompson*, D.P. Osborn, K.F. Cogger, R. Ashworth, M.M. Knight, P.L. Beales, J.P. Chapple (2012). Heat shock induces rapid resorption of primary cilia. *J Cell Sci.125(Pt 18):4297-305.*

  **Joint first author*

- C.L. Thompson, J.P. Chapple, M.M. Knight (2013). Primary cilia disassembly down regulates mechanosensitive hedgehog signalling: a feedback mechanism controlling ADAMTS-5 expression in chondrocytes. *Osteoarthritis and Cartilage* (submitted)

## Book chapters

- A. K. T. Wann, C. L. Thompson and M. M. Knight (2012). The Role of the Primary Cilium in Chondrocyte Response to Mechanical Loading. *Mechanically Gated Channels and their Regulation: Mechanosensitivity in Cells and Tissue. Volume 6, Chapter 15, pp 405-426*

## Conference abstracts

- C.L. Thompson, J.P. Chapple, M.M. Knight. Mechanical strain reduces primary cilia length and stimulates hedgehog signalling in adult chondrocytes

  Autumn Meeting of the British-Society-for-Matrix-Biology (BSMB), Newcastle University, UK, Sept 2011

- Mechanical strain stimulates hedgehog signalling in adult articular chondrocytes and reduces primary cilia length

  World Congress on Osteoarthritis, Osteoarthritis Research society international (OARSI), Barcelona, Spain April 2012

# Appendix

# Heat shock induces rapid resorption of primary cilia

**Natalia V. Prodromou[1,*], Clare L. Thompson[1,2,*], Daniel P. S. Osborn[3], Kathryn F. Cogger[1], Rachel Ashworth[4], Martin M. Knight[2], Philip L. Beales[3] and J. Paul Chapple[1,‡]**

[1]Centre for Endocrinology, William Harvey Research Institute, Barts and the London School of Medicine and Dentistry, Queen Mary University of London, London EC1M 6BQ, UK
[2]Institute of Bioengineering, School of Engineering and Material Sciences, Queen Mary University of London, London E1 4NS, UK
[3]Molecular Medicine Unit, University College London Institute of Child Health, London WC1N 1EH, UK
[4]School of Biological and Chemical Sciences, Queen Mary University of London, London E1 4NS, UK

*These authors contributed equally to this work
‡Author for correspondence (j.p.chapple@qmul.ac.uk)

*Accepted 20 May 2012*
*Journal of Cell Science 125, 4297–4305*

*doi: 10.1242/jcs.100545*

## Summary

Primary cilia are involved in important developmental and disease pathways, such as the regulation of neurogenesis and tumorigenesis. They function as sensory antennae and are essential in the regulation of key extracellular signalling systems. We have investigated the effects of cell stress on primary cilia. Exposure of mammalian cells in vitro, and zebrafish cells in vivo, to elevated temperature resulted in the rapid loss of cilia by resorption. In mammalian cells loss of cilia correlated with a reduction in hedgehog signalling. Heat-shock-dependent loss of cilia was decreased in cells where histone deacetylases (HDACs) were inhibited, suggesting resorption is mediated by the axoneme-localised tubulin deacetylase HDAC6. In thermotolerant cells the rate of ciliary resorption was reduced. This implies a role for molecular chaperones in the maintenance of primary cilia. The cytosolic chaperone Hsp90 localises to the ciliary axoneme and its inhibition resulted in cilia loss. In the cytoplasm of unstressed cells, Hsp90 is known to exist in a complex with HDAC6. Moreover, immediately after heat shock Hsp90 levels were reduced in the remaining cilia. We hypothesise that ciliary resorption serves to attenuate cilia-mediated signalling pathways in response to extracellular stress, and that this mechanism is regulated in part by HDAC6 and Hsp90.

**Key words:** Heat shock, Molecular chaperone, Primary cilia

## Introduction

The cellular response to environmental stress is complex and encompasses mechanisms to regulate cell cycle checkpoints, modulate energy metabolism and maintain macromolecular integrity (Kültz, 2005). Key to this response is the synthesis of cytoprotective heat shock proteins (Hsps) and a decrease in the translation of components of the normal proteome. Hsp expression is primarily regulated by heat shock transcription factors and is required for the development of thermotolerance (Cotto and Morimoto, 1999; Anckar and Sistonen, 2007).

Although elevated temperature affects multiple cellular compartments, the consequences for the primary cilium have not been well analysed. The majority of mammalian cells have a single primary cilium protruding from their surface. Primary cilia function as sensory antennae in the signal transduction of extracellular stimuli from the environment and other cells (Davenport and Yoder, 2005; Singla and Reiter, 2006; Berbari et al., 2009). They play an important role in the normal function of key intercellular signalling pathways. In particular they are essential for ligand-dependent sonic hedgehog (Shh) signalling (Corbit et al., 2005; Haycraft et al., 2005; Rohatgi et al., 2009) and platelet-derived growth factor-α signalling (Schneider et al., 2005). Primary cilia also have cell-type-specific roles, dependent on the receptors localised to them. This includes acting as mechanosensors in kidney epithelial cells where polycystin-2, a member of the transient receptor potential family of ion channels, monitors urine flow (Nauli et al., 2003). Unsurprisingly, abnormal primary cilium function is linked to both monogenic disorders and complex diseases (Fliegauf et al., 2007; Baker and Beales, 2009; Nigg and Raff, 2009).

The structure of the primary cilium is closely related to that of motile cilia and flagella. These are all microtubule-based organelles that consist of a basal body and an axoneme of nine microtubule doublets covered by a ciliary membrane. Microtubules are dynamic and maintenance of a constant cilium length is dependent on the balance between rates of assembly and disassembly at the axoneme tip. The elongation of the axoneme from the basal body is dependent on intraflagellar transport (IFT), a bidirectional process that facilitates axonemal turnover (Rosenbaum and Witman, 2002; Pedersen et al., 2008). Kinesin-2 motor complexes mediate the anterograde transport of axonemal precursors and other cargos to the site of assembly at the distal tip of the cilium. Concurrently, IFT particles are returned to the cell body by cytoplasmic dynein-2 motors. In addition to IFT proteins a number of other proteins have been identified as necessary for normal ciliogenesis and maintenance.

Assembly and disassembly of the primary cilium is a dynamic process that is regulated through the cell cycle. Although there is evidence that primary cilia are present on some proliferating cells, resorption generally occurs at mitotic entry followed by re-emergence after cell division (Seeley and Nachury, 2010). In



Journal of Cell Science

addition to the loss of primary cilia by resorption, observed in mammalian cells as part of their normal function, unicellular flagellates (e.g. *Clamydomonas*) also exhibit deflagellation. Flagellar excision occurs at the transition zone between the axoneme and the basal body and is dependent on microtubule severing. Deflagellation occurs in response to environmental stresses, including heat shock. It is a conserved cellular process, with deciliation of motile cilia from epithelia, such as the upper respiratory tract, reported to occur by this mechanism (Quarmby, 2004).

In mammalian cells, primary cilia disassemble in response to addition of serum. This is dependent on an Aurora-A kinase pathway (Pugacheva et al., 2007). In this pathway the pro-metastatic scaffolding protein HEF-1 (NEDD9) activates Aurora-A kinase. This is sufficient to induce rapid ciliary resorption through phosphorylation of histone deacetylase 6 (HDAC6), which then deacetylates ciliary tubulin and destabilises the axonemal microtubules (Pugacheva et al., 2007).

Intriguingly, heat shock factor-1 (HSF-1), the key mammalian HSF, has been shown to be necessary for the maintenance of beating of motile (9+2) cilia in murine respiratory epithelium. This is most likely because HSF-1 regulates the expression of constitutively expressed Hsp90, a molecular chaperone protein that plays a role in tubulin polymerisation (Takaki et al., 2007). Moreover, HDAC6 is an Hsp90 deacetylase and has been reported to trigger the disassociation of an HDAC6/Hsp90/HSF-1 complex in response to the accumulation of ubiquitinated protein (Boyault et al., 2007). This allows activation of HSF-1 and subsequent expression of stress inducible molecular chaperones.

Recent evidence demonstrates that primary cilia are lost from mammalian cells in response to chemical agents such as chloral hydrate by deciliation (Overgaard et al., 2009). Cilia have also been observed to exhibit altered frequency and length in response to mechanical stimuli (McGlashan et al., 2010). However, little is known of how these sensory organelles respond to extracellular stress. We report that primary cilia are highly sensitive to sub-lethal elevated temperature and are quickly lost from many cells by resorption. Importantly, heat-shock-induced loss of primary cilia reduced cilium-mediated signalling. This heat-shock-induced cilium resorption is dependent on HDAC activation. Hsp90 function was found to be required for normal ciliary maintenance. Moreover heat shock reduced levels of Hsp90 in cilia. HDAC6 and Hsp90 are known to form a complex in the cytosol (Boyault et al., 2007), and we demonstrate partial colocalisation of these proteins within ciliary axonemes. We hypothesise that this complex may exist in the axoneme and that it potentially disassembles upon heat-shock-promoting HDAC6-mediated ciliary resorption.

## Results

### Heat shock causes a loss of primary cilia and decreases hedgehog signalling in mammalian cells

We hypothesised that primary cilia would be responsive to extracellular stress. To test this we exposed ciliated NIH3T3 (mouse embryonic fibroblast) cells to a sub-lethal heat shock. NIH3T3 cells were cultured for 24 hours after seeding, until 70–80% confluent, and then transferred to serum-free conditions for 20 hours to promote cilia formation. Cells were then maintained at 37℃ or exposed to a 42℃ heat shock for up to 30 minutes. After fixation, cells were then processed for immunofluorescent detection of acetylated tubulin and pericentrin (Fig. 1A). The frequency of primary cilia was quantified in cells exposed to control and heat shock conditions (Fig. 1B). Primary cilia were detected on 85±9% of the cells maintained at 37℃. Remarkably, exposure to a 42℃ heat shock resulted in a significant reduction in the number of cells that exhibited primary cilia after only 5 minutes ($P<0.01$). Furthermore, after 30 minutes at the elevated temperature just 34±5% cells had a detectable primary cilium. Western analyses revealed that levels of acetylated tubulin and pericentrin were not altered by the heat shock (Fig. 1C). To confirm the heat shock conditions used were sufficient to rapidly activate stress response associated signalling cascades, we immunoblotted for the phosphorylated forms of extracellular signal-regulated kinases (Erk1/2) (Ng and Bogoyevitch, 2000) (Fig. 1C). Like the ciliary axoneme, the cytoplasmic bridges connecting daughter cells in cytokinesis are highly enriched in acetylated tubulin in many cell types. The number of these structures was not altered in populations of cells exposed to a 42℃ heat shock for 30 minutes (data not shown).

To confirm that the observed loss of primary cilia was due to their absence and not a lack of acetylated tubulin staining in the ciliary axoneme we stained cells with an additional marker (supplementary material Fig. S1). ADP-ribosylation factor-like protein 13B (Arl13b) is a small GTPase that has previously been reported to localise to primary cilia (Caspary et al., 2007). NIH3T3 cells maintained at 37℃ or exposed to 42℃ were processed for dual-immunofluorescence. We observed colocalisation of acetylated tubulin and Arl13b in the primary cilia of control cells and cells exposed to elevated temperature (supplementary material Fig. S1). In all cilia examined acetylated tubulin and Arl13b staining overlapped along the entire axoneme. Moreover, in control and heat shocked cells we were unable to identify any putative ciliary structures that did not label with both markers. These data further support a loss of primary cilia.

To test if the loss of primary cilia in response to heat shock was a general phenomenon we investigated their frequency in IMCD3 (murine inner medullary collecting duct) and ARPE19 (human retinal pigment epithelial) cells maintained at 37℃ or exposed to elevated temperature. For these cell types we also observed a rapid loss of primary cilia in response to heat shock (supplementary material Fig. S2).

The functional consequences of heat-induced resorption on primary-cilium-mediated signal transduction, were tested by analysing Shh signalling. NIH3T3 cells, which contain all of the components required to activate target gene transcription when exposed to ligand (Taipale et al., 2000; Rohatgi et al., 2009), were transfected with a Gli-dependent luciferase reporter and a constitutively active Renilla reporter. 16 hours post-transfection cells were heat shocked at 42℃ for up to 30 minutes, allowed to recover for 4 hours, and then treated with a pathway agonist for 12 hours before measurement of luciferase activity. Luciferase activity was significantly reduced in cells exposed to a 30 minute heat shock (Fig. 1D).

### Heat shock causes loss of cilia by resorption

Having established that the number of primary cilia are reduced in populations of mammalian cells in response to heat shock, we next investigated the mechanism of their disappearance. Measurement of mean axonemal length revealed that on average cilia were becoming progressively shorter with increased exposure to elevated temperature (Fig. 2A,B). This was suggestive of ciliary resorption rather than excision at the

transition zone. In support of this, ultracentrifugation and subsequent western analyses did not detect elevated levels of acetylated tubulin in cell culture supernatants from cells exposed to heat shock (not shown).

### Cells reassemble primary cilia following heat shock

The reduction in Shh signalling observed after heat shock suggested that primary cilia were not reassembled immediately. In NIH3T3 cells exposed to a 30 minute heat shock we observed no significant increase in cilia incidence or length up to 4 hours after heat shock (Fig. 2C,D). Although the percentage of NIH3T3 cells possessing primary cilia recovered to pre-heat-shock levels by 16 hours, they were significantly shorter up to 24 hours after exposure to elevated temperature ($P<0.05$). After the 24 hour time point, the serum-free conditions required for cilium formation began to impact on NIH3T3 cell survival. Therefore to investigate reassembly of primary cilia over a longer period we utilised IMCD3 cells. A high incidence of cilia occur on confluent IMCD3 cells in the presence of serum, making them more suitable than NIH3T3 cells for longer time course experiments. Exposure to 42℃ for 30 minutes reduced the frequency of primary cilia in populations of IMCD3 cells from 77±2% to 33±2% (Fig. 2E). 6 hours after heat shock the percentage of cells possessing primary cilia had not significantly increased. 24 hours after heat shock there was evidence of ciliary reassembly as the organelle was present on 56±2% of cells. The frequency of cilia remained slightly lower than before the heat shock for up to 4 days later ($P<0.05$). 24 hours after heat shock the average axoneme length was also less than in control cells (Fig. 2F). Together these data suggest that cells that have lost primary cilia in response to elevated temperature do not reassemble them immediately.

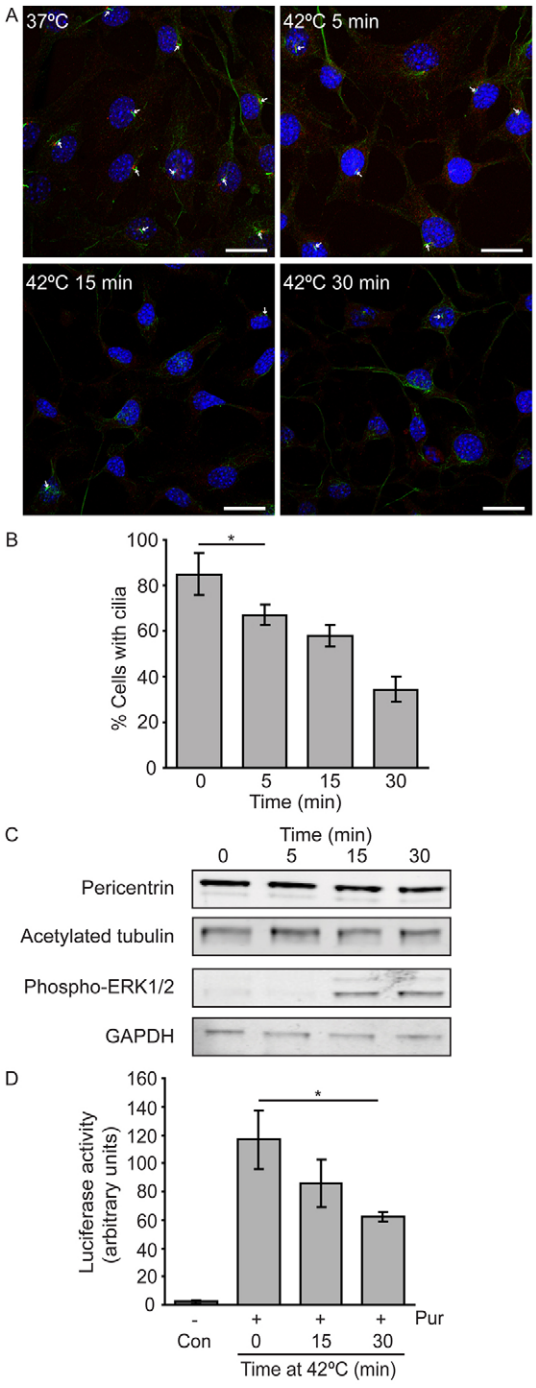


### Primary cilia are sensitive to heat shock in vivo

Primary cilia are essential for the normal function of signalling pathways in vertebrates, with zebrafish (*Danio rerio*) widely used as a model system to study their function in vivo. To investigate the effect of elevated temperature on cilia in vivo we established a 5 minute 42℃ heat shock was non-lethal for zebrafish embryos at the 24 hours post-fertilisation (hpf) stage. In 42℃ exposed fish and control fish, maintained at 28.5℃, we detected ciliary axonemes by staining for acetylated tubulin. Confocal analyses of the caudal region of embryos, using the tip of the tail as a reference for orientation, was performed (Fig. 3A,B) and the number of cilia within a defined region quantified from a Z-series of images. Both the number of ciliated cells (Fig. 3C) and the length of cilia (Fig. 3D) were reduced in the tails of heat-shocked fish. We also observed a reduction in acetylated tubulin staining in the pronephric duct of heat-shocked fish, which predominantly contains motile cilia, along a dense brush border (Fig. 3E). Gaps in the acetylated tubulin staining of the pronephric duct were not observed in fish maintained at 28.5℃ but were seen in fish exposed to 42℃, indicating a reduction in the frequency of motile cilia in these embryos. Thus heat shock triggered the rapid onset of cilia loss in zebrafish embryos analogous to the disassembly of primary cilia seen in cultured mammalian cells. Although cilium

**Fig. 1. Primary cilia are lost and hedgehog signalling reduced in mammalian cells exposed to elevated temperature.** (**A**) NIH3T3 cells stained to detect the ciliary axoneme with anti-acetylated tubulin (green), basal body with anti-pericentrin (red) and nuclei with DAPI (blue). Cells were maintained at 37℃ or exposed to 42℃ for 5, 15 or 30 minutes. Scale bars: 20 μm. (**B**) The percentage of cells with primary cilia was quantified. The number of cilia, defined by both acetylated tubulin and pericentrin labelling, and the number of nuclei (to give the total number of cells) were counted in 10 randomly selected fields from three replicates for each experimental condition. (**C**) Western blot analyses of levels of pericentrin, acetylated tubulin, phospho-Erk1/2 and GAPDH in NIH3T3 cells exposed to 42℃ for the indicated times. (**D**) Luciferase activity was measured in NIH3T3 cells transfected with a Gli-dependent reporter and normalised to the activity of a constitutively active renilla reporter. 16 hours post-transfection cells were exposed to 42℃ for the indicated times, cells were then allowed to recover for 4 hours prior to the addition of medium containing purmorphamine or vehicle (DMSO) for 12 hours. Error bars indicate 2× s.e.m. *$P<0.05$.

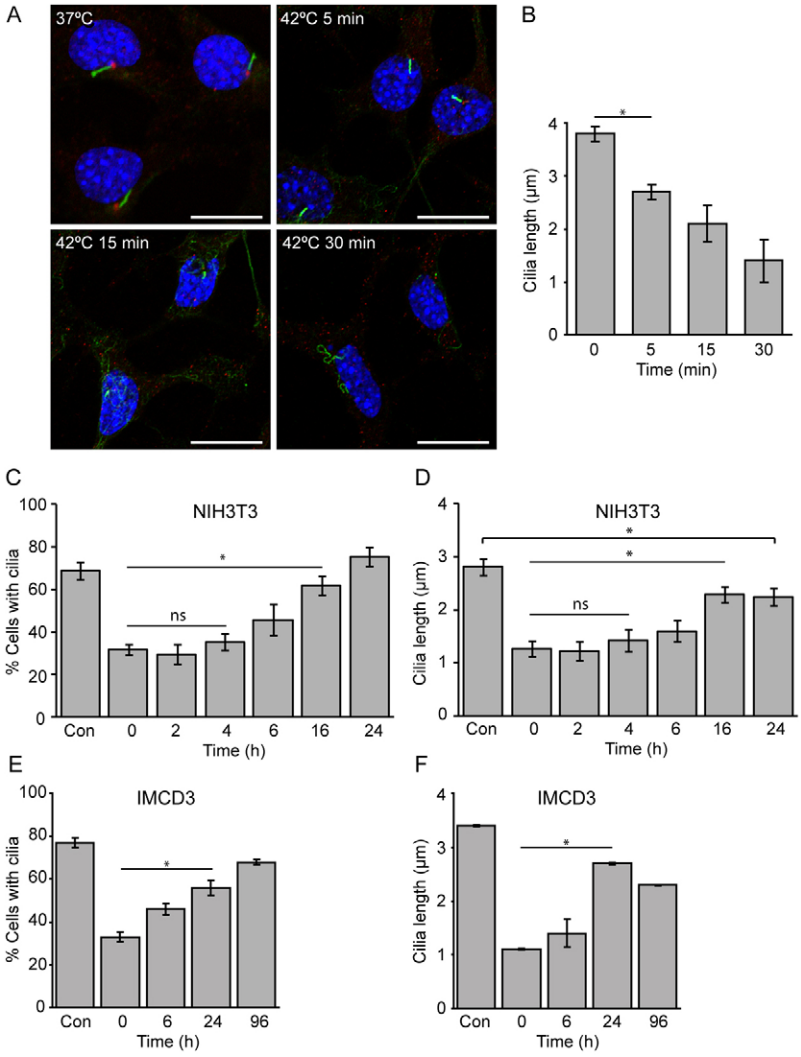


**Fig. 2. Primary cilia rapidly shorten upon heat shock and do not immediately reassemble.** (**A**) Cilium shortening in NIH3T3 cells, revealed by staining with anti-acetylated tubulin (green) and anti-pericentrin (red). Nuclei were labelled with DAPI (blue). Cells were maintained at 37℃ or exposed to 42℃ for 5, 15 or 30 minutes. Scale bars: 20 μm. (**B**) Mean axoneme length was quantified from confocal images of at least 50 randomly selected ciliated cells for each experimental condition. (**C–F**) To investigate the dynamics of cilium reassembly after heat shock NIH3T3 (C,D) cells were exposed to 42℃ for 30 minutes and then returned to 37℃ for up to 24 hours . (E,F) Cilium recovery was also quantified in IMCD3 cells cultured for up to 96 hours. Controls (Con) were not heat shocked. (C,E) The percentage of cells with primary cilia was quantified. The numbers of cilia and nuclei were counted in 10 randomly selected fields for each experimental condition in three biological replicates. (D,F) Mean axoneme length was quantified from confocal images of at least 50 randomly selected ciliated cells for each experimental condition. Error bars indicate 2× s.e.m. *$P<0.05$.

loss was observed, the heat shock conditions were sub-lethal, as assessed by examining the gross development and head/trunk angle up to 8 hours after the 42℃ heat shock (supplementary material Fig. S3).

### Heat-shock-induced cilium loss is dependent on a HDAC-mediated pathway

The resorption of primary cilia, in mammalian cells, in response to serum has previously been shown to be dependent on an Aurora-A/HDAC6 pathway (Pugacheva et al., 2007) (Fig. 4A). We used inhibitors to test if this pathway was implicated in heat-shock-induced cilium resorption. Inhibition with 0.5 μM PHA-680632, which specifically targets Aurora-A (Pugacheva et al., 2007), did not inhibit thermally induced cilium resorption (Fig. 4B,C). The effectiveness of this inhibitor in NIH3T3 cells was confirmed by testing its ability to prevent serum-induced cilium resorption (supplementary material Fig. S4). In contrast, after 30 minutes heat shock ciliary resorption was significantly reduced in cells treated with the mammalian class I and II HDAC inhibitor trichostatin A (TSA; $P<0.01$; Fig. 4D). In TSA-treated heat-shocked cells, remaining primary cilia were also longer than in untreated cells (Fig. 4E). HDAC6 has previously been localized to the ciliary axoneme (Pugacheva et al., 2007). HDAC6 staining was often punctuate along the length of the cilium and commonly localised to the distal end of the axoneme (supplementary material Fig. S5). Immunofluorescent staining identified that HDAC6 still localised to remaining primary cilia in cells exposed to heat shock. No significant differences were observed in the number of HDAC6-positive cilia or the intensity of HDAC6 staining in axonemes (Fig. 4F; quantification not shown). These data are consistent with heat-shock-induced primary cilium resorption involving HDAC6. They also further confirm that primary cilia are lost from heat-shocked cells by resorption.

### Primary cilium resorption in response to heat shock is reduced in thermotolerant cells

The cellular response to sub-lethal heat shock involves the synthesis of Hsps and the development of thermotolerance. We hypothesised that primary cilia would be less sensitive to elevated temperature in thermotolerant cells. To make NIH3T3 cells thermotolerant we exposed them to a 30 min priming heat shock (42℃) 4 hours prior to passage. After seeding, these cells were cultured for 24 hours and then transferred to serum-free medium for 16 hours to promote cilium formation. Western analyses confirmed these cells expressed Hsp70, indicating the cellular stress response had been induced (Fig. 5A). Resorption of primary cilia in response to heat shock, was significantly

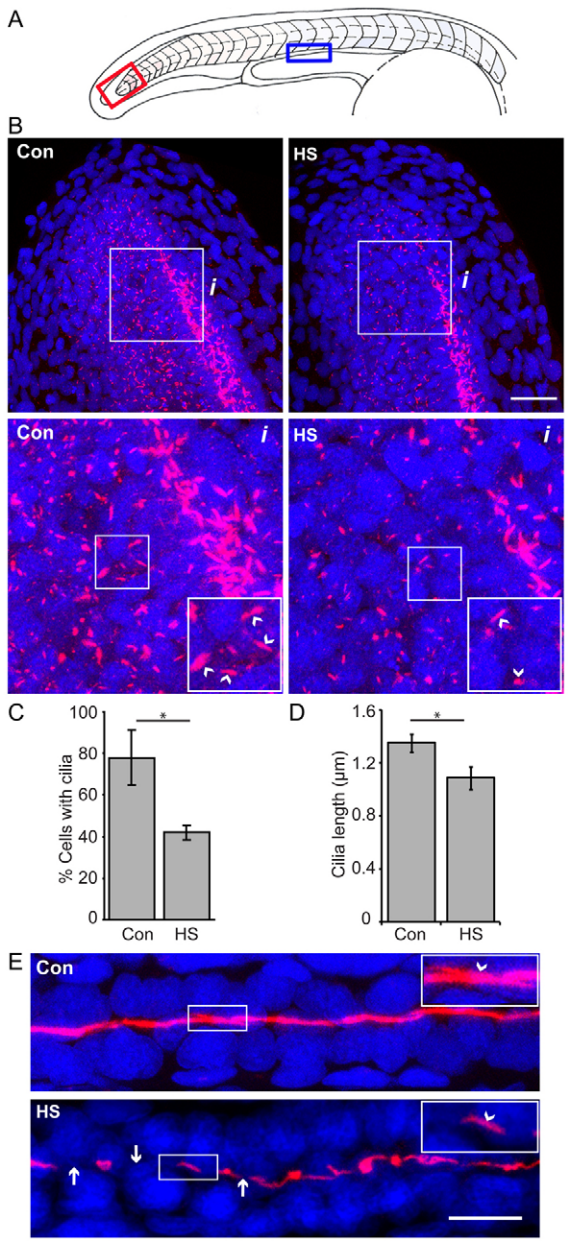


**Fig. 3. Heat-shock-induced resorption of cilia occurs in vivo.** (**A**) In zebrafish embryos we investigated the effects of exposure to elevated temperature on primary cilia in the area of the tip of the tail (red box) and motile cilia in the pronephric duct (blue box). 24 hour post-fertilisation embryos were either maintained at the normal growth temperature (28.5℃) or transferred to 42℃ for 5 minutes. Immediately after this non-lethal heat shock fish were fixed and ciliary axonemes stained with anti-acetylated tubulin (red) and nuclei with DAPI (blue). (**B**) Imaging of fish tails was performed to generate confocal z-stacks. Maximum intensity projections of these z-stacks are presented. Scale bars: 20 μm. Boxed regions indicated by *i* in the top panel are shown enlarged in the lower panel with a further enlarged insert, where individual cilia are indicated by arrowheads. (**C**) From this confocal data the percentage of cells with primary cilia was quantified. The numbers of primary cilia and nuclei were counted in a defined region at the tip of the tail of five fish per treatment. (**D**) Mean axoneme length was quantified from confocal images of at least 30 randomly selected ciliated cells from five fish for each experimental condition. Error bars indicate 2× s.e.m. *$P$<0.05. (**E**) A representative confocal imaging of the pronephric ducts. Arrows indicate areas of motile cilia loss. In the enlarged insert arrowheads indicate individual cilia.

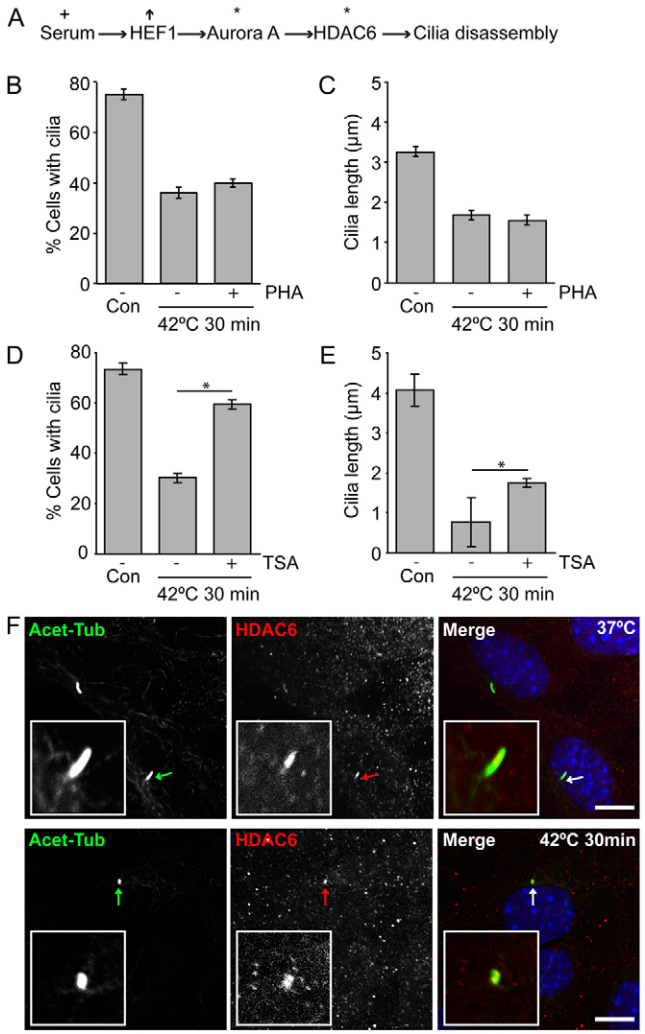


**Fig. 4. Heat-shock-induced cilium resorption is HDAC6 dependent.** (**A**) Schematic of the Aurora-A–HDAC6 cilium resorption pathway (Pugacheva et al., 2007). Upward arrow indicates increased expression and asterisks indicate activation. To test whether Aurora-A (**B**,**C**) and HDAC6 (**D**,**E**) activities are required for heat-induced cilium resorption, NIH3T3 cells were cultured in medium containing the Aurora-A inhibitor PHA-680632 (PHA), the HDAC inhibitor trichostatin A (TSA), or DMSO vehicle for 4 hours, prior to exposure to 42℃ for 30 minutes or continued maintenance at 37℃ (Con). (B,D) The percentage of cells with primary cilia was quantified. The numbers of cilia and nuclei were counted in 10 randomly selected fields for each experimental condition. (C,E) Mean axoneme length was quantified from confocal images of at least 50 randomly selected ciliated cells for each experimental condition. (**F**) HDAC6 localises to primary cilia in NIH3T3 cells maintained at 37℃ or exposed to 42℃ for 30 minutes. Cells were stained to detect the ciliary axoneme with anti-acetylated tubulin (green) and HDAC6 (red). Nuclei were detected with DAPI (blue). Enlarged images of the cilia indicated by arrows are shown in the insets. Scale bars: 10 μm.

reduced in these thermotolerant cells ($P$<0.01; Fig. 5B), furthermore remaining cilia were longer than in non-thermotolerant cells ($P$<0.01; Fig. 5C).

### Hsp90 plays a role in primary cilium maintenance

The observation that the primary cilia of thermotolerant cells are more resistant to heat shock suggested a possible role for Hsps in ciliary maintenance. One candidate protein for such a role is

Hsp90. This molecular chaperone has been reported to be associated with ciliary microtubules in a protozoan (Williams and Nelsen, 1997) and is implicated in the normal function of motile cilia in mice (Takaki et al., 2007). Moreover, the constitutive (HSP90AB) and inducible (HSP90AA) cytosolic Hsp90 proteins, as well as the ER resident Grp94 (HSP90B) have been identified as being in the ciliary proteome (Gherman et al., 2006). Inhibition of Hsp90s with the benzoquinone ansamycin geldanamycin (GA) resulted in a reduction in the frequency (Fig. 5D) and average length (Fig. 5E) of primary cilia in a

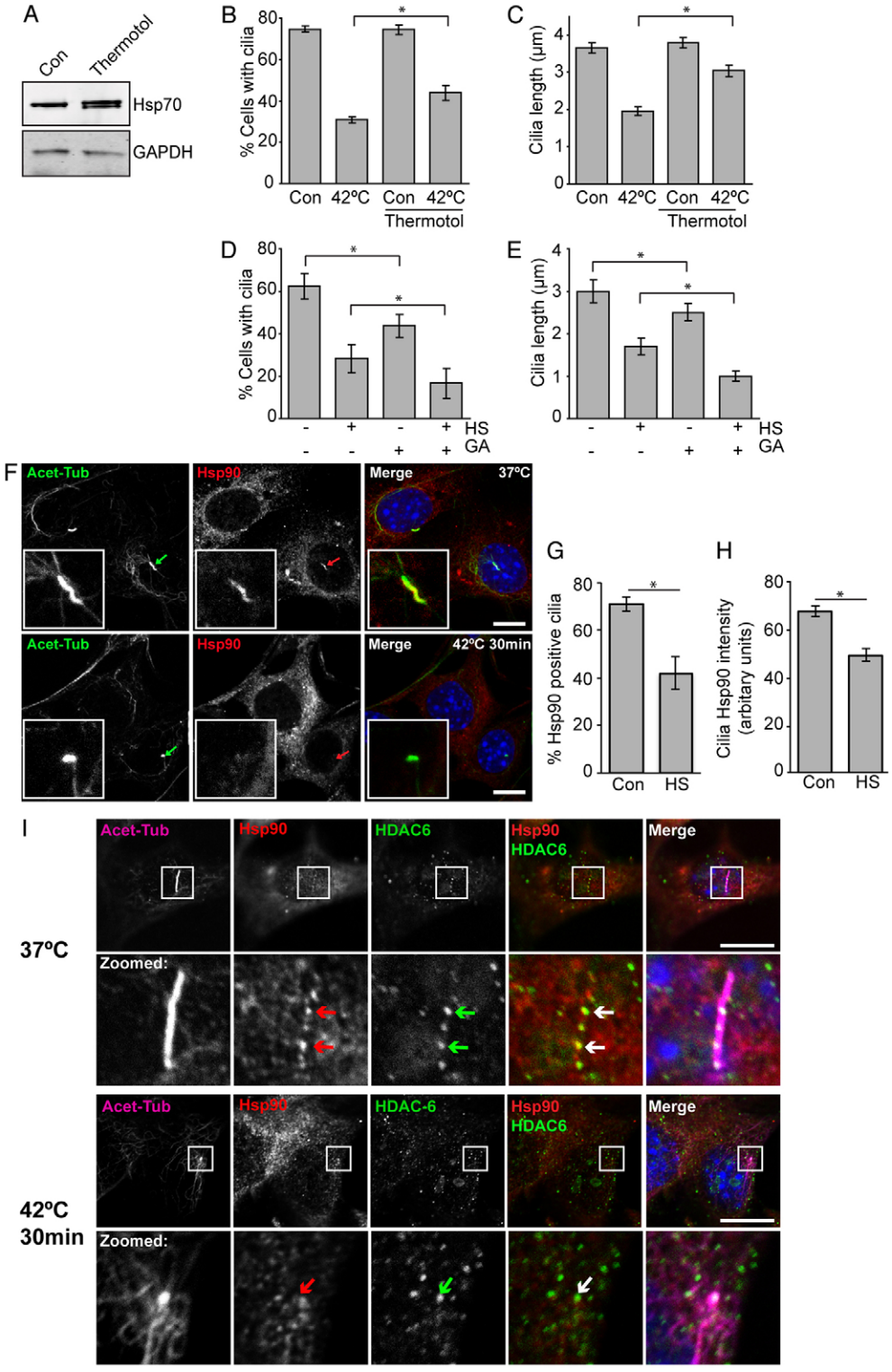


**Fig. 5.** See next page for legend.

population of NIH3T3 cells maintained at 37℃. In cells exposed to 42℃, GA treatment further reduced cilia frequency and length relative to the heat shock alone. These data indicate a possible role for Hsp90 in the maintenance of primary cilia.

### Localisation of Hsp90 to primary cilia is reduced by heat shock

To further investigate the association between primary cilia and Hsp90 we performed immunofluorescent staining, using an antibody that detects both the constitutively expressed and inducible cytosolic Hsp90s (Fig. 5F; supplementary material Fig. S5). Hsp90 has previously been reported to be present in the nucleus and cytoplasm with some enrichment at centrosomes (Lange et al., 2000). In 71±3% of ciliated NIH3T3s Hsp90 staining was detected in axonemes (Fig. 5F,G). For cells that retained primary cilia after 30 minutes of heat shock, the incidence of cilia with an Hsp90-positive axoneme was reduced to 42±7%. Therefore, heat shock resulted in a significant decrease ($P<0.01$) in the percentage of primary cilia that were positive for Hsp90. Cells that retained primary cilia also had significantly less intense Hsp90 staining in the organelle ($P<0.01$; Fig. 5H). This was quantified by measuring the Hsp90 immunofluorescent signal that colocalised with acetylated tubulin in individual primary cilium. Together these data suggest that Hsp90 levels are decreased in cilia upon heat shock. They could also indicate that cilia that are positive for Hsp90 are more readily lost upon heat shock, however given that GA treatment reduces cilia frequency this seems unlikely.

**Fig. 5. Hsp90 is required for maintenance of primary cilia and is lost from the axoneme upon heat shock.** (**A–C**) Thermotolerant cells are resistant to heat-induced resorption of primary cilia. NIH3T3 cells, which had received a 20 minute priming heat shock 4 hours before passage (Thermortol), and control cells where seeded and cultured for 24 hours prior to a further 16 hours culture in serum-free conditions, to promote cilium formation. Cells were then maintained at 37℃ (Con) or exposed to 42℃ for 30 minutes. Induction of a heat-shock response in thermotolerant cells was confirmed by immunoblot of Hsp70 (A). The prevalence (B) and length (C) of cilia were quantified in control and thermotolerant cells. (**D–E**) To examine whether Hsp90 was involved in maintenance of cilia under normal and heat-shock conditions NIH3T3 cells were treated for 3 hours with the inhibitor geldanamycin (GA) or vehicle (DMSO) alone. Cells were then either maintained at 37℃ or exposed to 42℃ for 30 minutes. The prevalence (D) and length (E) of cilia were then quantified. The numbers of cilia and nuclei were counted in 10 randomly selected fields for each experimental condition (B,D). Mean axoneme length was quantified from confocal images of at least 50 randomly selected ciliated cells for each experimental condition (C,E). (**F–H**) Hsp90 is lost from the axoneme upon heat shock. NIH3T3 cells were maintained at 37℃ or exposed to 42℃ for 30 minutes. (F) NIH3T3 cells were stained to detect the ciliary axoneme with anti-acetylated tubulin (green) and Hsp90 (red). Nuclei were detected with DAPI (blue). Enlarged images of the cilia indicated by arrows are shown in the insets. Scale bars: 10 μm. The incidence of primary cilia with detectable levels of Hsp90 (G) and the intensity of Hsp90 staining in axonemes, relative to acetylated tubulin levels (H), were quantified. 100 primary cilia were assessed for Hsp90 staining in three separate experiments and fluorescence intensities quantified in 50 randomly selected axonemes. Error bars indicate s.e.m. *$P<0.05$. (**I**) NIH3T3 cells maintained at 37℃ or exposed to 42℃ for 30 minutes were stained with anti-acetylated tubulin (magenta) to detect the ciliary axoneme. They were co-stained for HDAC (green), Hsp90 (red) and with DAPI. Boxed regions in the top panel are shown enlarged in the lower panel (zoom). Arrows indicate areas where HDAC6 and Hsp90 stainings overlap. Scale bars: 10 μm.

As HDAC6 and Hsp90 have previously been reported to interact we investigated if they colocalised in the ciliary axoneme by triple immunofluorescent staining (Fig. 5I; supplementary material Fig. S6). Cells were stained for acetylated tubulin to reveal cilia as well as HDAC6 and Hsp90. This triple staining required the use of a different HDAC6 antibody that needed an additional methanol fixation step. This fixation gave a more punctate cilia staining for both Hsp90 and HDAC6 (alone and in combination). We observed partial colocalisation of Hsp90 and HDAC6 in cilia of cells maintained at 37℃. This was particularly evident in puncta along longer cilia. In cells exposed to 42℃ for 30 minutes it was difficult to identify Hsp90 staining in the remaining shortened ciliary axonemes. This data further supports that, in contrast to HDAC6, Hsp90 levels are reduced in cilia upon heat shock.

## Discussion

Understanding the assembly and disassembly of primary cilia is important because of the role of this organelle in human development and disease. For example, primary cilia are critical in processes such as neurogenesis (Breunig et al., 2008) and Shh driven oncogenesis (Han et al., 2009).

We demonstrate here that primary cilia undergo rapid resorption in response to heat shock. After heat-induced loss, primary cilia eventually reappear in mammalian cells, however this takes significantly longer than their resorption. This is consistent with attenuation of the cilium-mediated Shh signalling pathway in cells exposed to heat shock. Data from zebrafish experiments indicated that cilia are also sensitive to non-lethal exposure to elevated temperature in vivo. This was the case for primary cilia in the fish tail and motile cilia in the pronephric duct. It has been suggested that the regulated disassembly or shortening of cilia may serve as a rheostat to limit the cellular response to overly persistent or abnormal growth cues in the extracellular environment (Pugacheva et al., 2007). Similarly, we speculate that ciliary resorption may also play a role in regulating gene expression under conditions of extracellular stress. The cellular response to heat shock includes downregulating expression of non-essential proteins and it is possible that resorption of primary cilia, leading to signalling downregulation, would represent another component of this cellular survival mechanism. That both mammalian and zebrafish primary cilia are reduced in response to elevated temperature indicates that rapid resorption is likely to be an evolutionarily conserved phenomenon amongst vertebrates. Interestingly not all cells in the population lost primary cilia after a 30 minute heat shock, indicating variability in this response. Multiple factors are known to regulate biogenesis and resorption of primary cilia and it seems possible that in some cells ciliogenesis pathways could counteract heat-induced loss. Alternately, some cells may be more stress tolerant and thus resistant to the effects of elevated temperature on cilia.

Previously it has been demonstrated that resorption of cilia is dependent on an Aurora-A/HDAC6 pathway that regulates deacetylation of microtubules (Pugacheva et al., 2007). Our data is consistent with resorption under heat shock conditions being, at least in part, HDAC modulated yet downstream of Aurora-A. Importantly, the finding that HDAC inhibition reduced heat-shock-induced resorption, in addition to the rapidity of cilia loss, also implies that cilium resorption is a signalling response, as opposed to the result of an inability of the cell to maintain the

organelle. We localised Hsp90 and HDAC6 to the ciliary axoneme. These proteins have previously been reported to exist in a complex that disassociates as part of the cellular stress response, activated by cytotoxic protein aggregate formation. We propose a model where cilium resorption in response to heat shock is mediated by the deactylase activity of HDAC6 and loss of axoneme Hsp90 function, possibly after disassembly of an HDAC6/Hsp90 complex.

Although our data supports resorption as part of a regulated response to heat shock, it is also likely that heat shock may reduce the pool of dimeric soluble tubulin available for IFT and subsequent incorporation into ciliary microtubules. Indeed, it has recently been demonstrated in vitro that dimeric soluble tubulin is prone to aggregation even at physiological temperatures and furthermore that Hsp90 has been shown to protect tubulin against thermal denaturation (Weis et al., 2010). Consistent with this, we observed that inhibition of Hsp90 reduced the frequency of ciliated cells and cilium length under both control and heat shock conditions. We also observed that in thermotolerant cells where relative levels of Hsp90 and Hsp70 proteins are elevated, primary cilia are more resistant to heat-shock-induced resorption.

In conclusion, the cellular stress response is multifaceted and adaptive and we hypothesise the loss of cilia may be a normal cellular mechanism that downregulates non-essential signalling pathways during stress conditions.

## Materials and Methods

### Cell culture

All cell lines where from the American Type Culture Collection. NIH3T3 cells were grown in Dulbecco's modified Eagle's medium (DMEM). IMCD3 and ARPE19 cells were grown in DMEM at a 1:1 ratio with Ham's F12 medium. Cells were maintained in medium supplemented with 10% fetal calf serum (FCS) containing 100 U/ml penicillin and 100 mg/ml streptomycin. To promote the appearance of primary cilia on NIH3T3 cells serum was withdrawn for 20 hours, as previously described (Pugacheva et al., 2007).

### Heat shock, recovery, thermotolerance and drug inhibition

Cells were grown in 35 mm cell culture dishes that contained a 10 mm coverslip. For heat shock experiments 37℃ medium was rapidly exchanged for 42℃ medium and dishes immediately transferred to a 42℃ water bath. For experiments with a recovery period after heat shock cells were returned to a 37℃ incubator. To generate thermotolerant cells a 42℃ 30 minute heat shock was administered 4 hours before passaging into cell culture dishes. For Hsp90 inhibition NIH3T3 cells were treated for 3 hours with 2 μM geldanamycin (Sigma) For Aurora-A inhibition cells were treated with PHA-680632 (Selleck Chemicals, Houston) at a concentration of 0.5 μM for 4 hours. For HDAC inhibition cells were treated for 4 hours with trichostatin A (Sigma) at final concentration of 10 nM. Vehicle only (DMSO treated) controls were also performed. These inhibitors have been used previously to establish the Aurora-A cilium resorption pathway (Pugacheva et al., 2007). After treatments coverslips were processed for immunofluorescent staining and the remaining cells in each dish collected for western analyses.

### Immunofluorescence detection and quantification of primary cilia

For detection of cilia using immunofluorescence, cells grown on coverslips were fixed in 4% (v/v) formaldehyde followed by detergent permeabilization with 0.05% Triton X-100. For triple staining, a 5 minute additional methanol fix was included immediately after the formaldehyde fixation (Pugacheva et al., 2007). Monoclonal anti-acetylated tubulin, clone 611 B-1, mouse ascites 1:1000 (Sigma), and rabbit polyclonal anti-pericentrin, 1:2000 (Abcam), were used for detection of the ciliary axoneme and basal body respectively. Rabbit polyclonal anti-HDAC6 (phosphor-22; Abcam) and goat polyclonal anti-HDAC6 (Santa Cruz) were used at titers of 1:200 and 1:50 and anti-Hsp90 (Abcam) was used at a titer of 1:500. Appropriate Alexa-Fluor-488- and Alexa-Fluor-568-conjugated secondary antibodies (Molecular probes) were used and nuclei were detected with DAPI (4′,6-diamidino-2-phenylindole). Imaging and quantification of the percentage of ciliated cells and cilium length was performed using a Zeiss LSM510 laser scanning confocal microscope and the Zeiss ZEN software. For quantification both acetylated tubulin and pericentrin labelling were used to define cilia. The proportion of ciliated cells in a given field was determined by counting the number of cilia and the number of nuclei present and is expressed as % of the total cell population. Cilium prevalence was measured for 10 fields (>20 cells/field) in three separate experiments giving a total of approximately 600 cells. Sequential 0.5 μm thick z-stacked sections were imaged through the entirety of the cellular profile using a 63× objective lens and were used to create maximum intensity projections (MIPs). Zen analysis software (Zeiss) was used to trace and measure the length of cilia in MIPs. Due to the differences in the z resolution of the microscope compared with the x and y planes, only cilia that were approximately 90° to the incident light were selected. Z-stacks were carefully examined prior to measurement to ensure vertical cilia were excluded. Axonemal length of at least 30 cilia were measured from five fields for each experimental condition. Experiments were conducted in triplicate. Measurements were made blind to experimental status and statistical significance determined by unpaired *t*-test or one-way ANOVA as appropriate.

### Hedgehog signalling assay

NIH3T3 cells were transfected, using Lipofectamine Plus (Invitrogen), with a Gli-binding site luciferase reporter plasmid (pGBS-luc) and a constitutive expressing vector for Renilla (pRL, from Promega). Cells were allowed to recover from transfection and then serum starved for 16 hours to promote cilium formation. Heat shock for the specified times was then performed and cells were allowed to recover for 4 hours prior to addition of 2 μM purmorphamine. 16 hours later a Dual-Luciferase Reporter Assay (Promega) was performed and luciferase activity normalized to renilla values.

### Western blot analyses

For western blot analyses of levels of acetylated tubulin and pericentrin in cell lysates the same antibodies as for immunofluorescence were used, Hsp70 proteins and GAPDH were detected using anti-Hsp70 clone BRM-22 and rabbit anti-GAPDH (Santa Cruz Biotechnology). Infrared-dye-conjugated secondary antibodies were used for detection of bands with an Odyssey Infrared Imaging System (LI-COR). Cell lysates were prepared for western analyses as described previously (Meimaridou et al., 2011).

### Heat shock and detection of cilia using immunofluorescence in zebrafish

24 hour post-fertilization zebrafish (*Danio rerio*) were heat shocked at 42℃ for 5 minutes. Immediately after heat shock whole fish were fixed in 4% paraformaldehyde overnight prior to processing for immunofluorescent detection of primary cilia, as described above. Cilium frequency and length were quantified from z-series through the full thickness of the tail in a region up to 100 μm from the tip. The number of cells with cilia was determined by counterstaining nuclei with DAPI. Z-stacks were generated from five fish for each treatment. The lengths of at least 30 randomly selected cilia were quantified for each fish using Zen software giving a total of at least 150 cilia. Head–trunk angle measurements were made between a line drawn through the middle of the ear and eye, and a second line parallel to the notochord in the mid-trunk region (myotomes 5–10).

## Funding

This work was supported by the Biotechnology and Biological Sciences Research Council [grant number BB/E009824/1 to J.P.C.]; and the Wellcome Trust [grant number 084717 to M.M.K.]. Deposited in PMC for immediate release.

Supplementary material available online at
http://jcs.biologists.org/lookup/suppl/doi:10.1242/jcs.100545/-/DC1

## References

**Anckar, J. and Sistonen, L.** (2007). Heat shock factor 1 as a coordinator of stress and developmental pathways. *Adv. Exp. Med. Biol.* **594**, 78-88.

**Baker, K. and Beales, P. L.** (2009). Making sense of cilia in disease: the human ciliopathies. *Am. J. Med. Genet. C. Semin. Med. Genet.* **151C**, 281-295.

**Berbari, N. F., O'Connor, A. K., Haycraft, C. J. and Yoder, B. K.** (2009). The primary cilium as a complex signaling center. *Curr. Biol.* **19**, R526-R535.

**Boyault, C., Zhang, Y., Fritah, S., Caron, C., Gilquin, B., Kwon, S. H., Garrido, C., Yao, T. P., Vourc'h, C., Matthias, P. et al.** (2007). HDAC6 controls major cell response pathways to cytotoxic accumulation of protein aggregates. *Genes Dev.* **21**, 2172-2181.

**Breunig, J. J., Sarkisian, M. R., Arellano, J. I., Morozov, Y. M., Ayoub, A. E., Sojitra, S., Wang, B., Flavell, R. A., Rakic, P. and Town, T.** (2008). Primary cilia regulate hippocampal neurogenesis by mediating sonic hedgehog signaling. *Proc. Natl. Acad. Sci. USA* **105**, 13127-13132.

**Caspary, T., Larkins, C. E. and Anderson, K. V.** (2007). The graded response to Sonic Hedgehog depends on cilia architecture. *Dev. Cell* **12**, 767-778.

**Corbit, K. C., Aanstad, P., Singla, V., Norman, A. R., Stainier, D. Y. and Reiter, J. F.** (2005). Vertebrate Smoothened functions at the primary cilium. *Nature* **437**, 1018-1021.

**Cotto, J. J. and Morimoto, R. I.** (1999). Stress-induced activation of the heat-shock response: cell and molecular biology of heat-shock factors. *Biochem. Soc. Symp.* **64**, 105-118.
**Davenport, J. R. and Yoder, B. K.** (2005). An incredible decade for the primary cilium: a look at a once-forgotten organelle. *Am. J. Physiol.* **289**, F1159-F1169.
**Fliegauf, M., Benzing, T. and Omran, H.** (2007). When cilia go bad: cilia defects and ciliopathies. *Nat. Rev. Mol. Cell Biol.* **8**, 880-893.
**Gherman, A., Davis, E. E. and Katsanis, N.** (2006). The ciliary proteome database: an integrated community resource for the genetic and functional dissection of cilia. *Nat. Genet.* **38**, 961-962.
**Han, Y. G., Kim, H. J., Dlugosz, A. A., Ellison, D. W., Gilbertson, R. J. and Alvarez-Buylla, A.** (2009). Dual and opposing roles of primary cilia in medulloblastoma development. *Nat. Med.* **15**, 1062-1065.
**Haycraft, C. J., Banizs, B., Aydin-Son, Y., Zhang, Q., Michaud, E. J. and Yoder, B. K.** (2005). Gli2 and Gli3 localize to cilia and require the intraflagellar transport protein polaris for processing and function. *PLoS Genet.* **1**, e53.
**Kültz, D.** (2005). Molecular and evolutionary basis of the cellular stress response. *Annu. Rev. Physiol.* **67**, 225-257.
**Lange, B. M., Bachi, A., Wilm, M. and González, C.** (2000). Hsp90 is a core centrosomal component and is required at different stages of the centrosome cycle in Drosophila and vertebrates. *EMBO J.* **19**, 1252-1262.
**McGlashan, S. R., Knight, M. M., Chowdhury, T. T., Joshi, P., Jensen, C. G., Kennedy, S. and Poole, C. A.** (2010). Mechanical loading modulates chondrocyte primary cilia incidence and length. *Cell Biol. Int.* **34**, 441-446.
**Meimaridou, E., Gooljar, S. B., Ramnarace, N., Anthonypillai, L., Clark, A. J. and Chapple, J. P.** (2011). The cytosolic chaperone Hsc70 promotes traffic to the cell surface of intracellular retained melanocortin-4 receptor mutants. *Mol. Endocrinol.* **25**, 1650-1660.
**Nauli, S. M., Alenghat, F. J., Luo, Y., Williams, E., Vassilev, P., Li, X., Elia, A. E., Lu, W., Brown, E. M., Quinn, S. J. et al.** (2003). Polycystins 1 and 2 mediate mechanosensation in the primary cilium of kidney cells. *Nat. Genet.* **33**, 129-137.
**Ng, D. C. and Bogoyevitch, M. A.** (2000). The mechanism of heat shock activation of ERK mitogen-activated protein kinases in the interleukin 3-dependent ProB cell line BaF3. *J. Biol. Chem.* **275**, 40856-40866.
**Nigg, E. A. and Raff, J. W.** (2009). Centrioles, centrosomes, and cilia in health and disease. *Cell* **139**, 663-678.
**Overgaard, C. E., Sanzone, K. M., Spiczka, K. S., Sheff, D. R., Sandra, A. and Yeaman, C.** (2009). Deciliation is associated with dramatic remodeling of epithelial cell junctions and surface domains. *Mol. Biol. Cell* **20**, 102-113.
**Pedersen, L. B., Veland, I. R., Schrøder, J. M. and Christensen, S. T.** (2008). Assembly of primary cilia. *Dev. Dyn.* **237**, 1993-2006.
**Pugacheva, E. N., Jablonski, S. A., Hartman, T. R., Henske, E. P. and Golemis, E. A.** (2007). HEF1-dependent Aurora A activation induces disassembly of the primary cilium. *Cell* **129**, 1351-1363.
**Quarmby, L. M.** (2004). Cellular deflagellation. *Int. Rev. Cytol.* **233**, 47-91.
**Rohatgi, R., Milenkovic, L., Corcoran, R. B. and Scott, M. P.** (2009). Hedgehog signal transduction by Smoothened: pharmacologic evidence for a 2-step activation process. *Proc. Natl. Acad. Sci. USA* **106**, 3196-3201.
**Rosenbaum, J. L. and Witman, G. B.** (2002). Intraflagellar transport. *Nat. Rev. Mol. Cell Biol.* **3**, 813-825.
**Schneider, L., Clement, C. A., Teilmann, S. C., Pazour, G. J., Hoffmann, E. K., Satir, P. and Christensen, S. T.** (2005). PDGFRalphaalpha signaling is regulated through the primary cilium in fibroblasts. *Curr. Biol.* **15**, 1861-1866.
**Seeley, E. S. and Nachury, M. V.** (2010). The perennial organelle: assembly and disassembly of the primary cilium. *J. Cell Sci.* **123**, 511-518.
**Singla, V. and Reiter, J. F.** (2006). The primary cilium as the cell's antenna: signaling at a sensory organelle. *Science* **313**, 629-633.
**Taipale, J., Chen, J. K., Cooper, M. K., Wang, B., Mann, R. K., Milenkovic, L., Scott, M. P. and Beachy, P. A.** (2000). Effects of oncogenic mutations in Smoothened and Patched can be reversed by cyclopamine. *Nature* **406**, 1005-1009.
**Takaki, E., Fujimoto, M., Nakahari, T., Yonemura, S., Miyata, Y., Hayashida, N., Yamamoto, K., Vallee, R. B., Mikuriya, T., Sugahara, K. et al.** (2007). Heat shock transcription factor 1 is required for maintenance of ciliary beating in mice. *J. Biol. Chem.* **282**, 37285-37292.
**Weis, F., Moullintraffort, L., Heichette, C., Chrétien, D. and Garnier, C.** (2010). The 90-kDa heat shock protein Hsp90 protects tubulin against thermal denaturation. *J. Biol. Chem.* **285**, 9525-9534.
**Williams, N. E. and Nelsen, E. M.** (1997). HSP70 and HSP90 homologs are associated with tubulin in hetero-oligomeric complexes, cilia and the cortex of Tetrahymena. *J. Cell Sci.* **110**, 1665-1672.

Journal of Cell Science